Emergent Dynamics from the Complex Interplay Between Ecology and Evolutionary Game Dilemmas

Thesis
submitted for the Degree of

Doctor of Philosophy

in Science

by

Sourav Roy
(PhD Index No: 140/18/Maths./26)

Department of Mathematics
Jadavpur University
Kolkata - 700032, India
August, 2025

Jointly worked in the

Physics and Applied Mathematics Unit
Indian Statistical Institute
Kolkata - 700108, India

Emergent Dynamics from the Complex Interplay Between Ecology and Evolutionary Game Dilemmas

Sourav Roy

This thesis is dedicated to my parents, my brother, and all the teachers of my life starting from my existence!

CERTIFICATE FROM THE SUPERVISOR

This is to certify that the thesis entitled "Emergent Dynamics from the Complex Interplay Between Ecology and Evolutionary Game Dilemmas" submitted by Sri Sourav Roy, who got his name registered on 05.09.2018 for the award of Ph. D. (Science) Degree of Jadavpur University, is absolutely based upon his own work under the supervision of Prof. Prakash Chandra Mali, and that neither this thesis nor any part of it has been submitted for either any degree / diploma or any other academic award anywhere before.

13.8.2025

(Signature of the Supervisor, date with official seal)

INDIAN STATISTICAL INSTITUTE
203 B. T. ROAD, KOLKATA 700108

Telephone : (+91) 9830334136
(033) 2575-3024
Fax : (+91) (33) 2577-3026

Dr. Dibakar Ghosh,
Professor,
Physics and Applied Mathematics Unit,
Indian Statistical Institute,
Kolkata-700108, India.
Email: dibakar@isical.ac.in;
dghosh.nld@gmail.com

Certificate from the co-supervisor

This is to certify that the thesis entitled "Emergent Dynamics from the Complex Interplay Between Ecology and Evolutionary Game Dilemmas" submitted by Sri Sourav Roy, who got his name registered on July 5, 2018, for the award of Ph. D. (Science) degree from Jadavpur University is absolutely based upon his own work under the co-supervision of Prof. Dibakar Ghosh, Physics and Applied Mathematics Unit, Indian Statistical Institute, Kolkata, and that neither this thesis nor any part of it has been submitted for either any degree/diploma or any other academic award anywhere before.

With best wishes from ISI, Kolkata!

Sincerely Yours,

Dibakar Ghosh 13/08/25

Dr. Dibakar Ghosh
Professor
Physics and Applied Mathematics Unit,
Indian Statistical Institute, Kolkata,
203 B. T. Road, Baranagar,
Kolkata-700108, West Bengal, India.

Dr. Dibakar Ghosh
Professor of Applied Mathematics
Physics and Applied Mathematics Unit
भारतीय सांख्यिकी संस्थान / INDIAN STATISTICAL INSTITUTE
203 बी. टी. रोड, कोलकता / 203 B. T. Road, Kolkata - 700108

Declaration

I certify that

1. The works contained in this thesis are original and have been done by me under the guidance of my supervisors.
2. The works have not been submitted to any other university/institute for any degree or diploma.
3. I have followed the guidelines provided by the university/institute in preparing the thesis.
4. I have conformed to the norms and guidelines given in the Ethical Code of Conduct of the university/institute.
5. Whenever I have used materials (data, theoretical analysis, figures, and text) from other sources, I have given due credit to them by citing them in the text of the thesis and giving their details in the references. Further, I have taken permission from the copyright owners of the sources, whenever necessary.

Sourav Roy

Sourav Roy

Kolkata

August, 2025

Abstract

This thesis delves into the emergent behaviors arising from the dynamical coupling between ecological processes and evolutionary game dilemmas. Motivated by a growing body of empirical and theoretical evidence that evolution can operate on ecological timescales, the work constructs and analyzes a suite of nonlinear dynamical models to explore how feedback between strategic behavior and ecological context shape population dynamics, cooperation, and biodiversity.

The research builds upon the foundational framework of evolutionary game theory, particularly the Prisoner's Dilemma (PD) and Snowdrift (SD) games, and systematically extends it to incorporate multigame environments, stochastic strategy mutation, ecological feedback through density-dependent variables, and time-delayed interactions. These modifications reflect the heterogeneity and complexity observed in real-world systems, where individuals encounter varying interaction contexts, behave non-deterministically, and respond to both current and past ecological pressures. A central theme is the incorporation of ecological free space as a dynamical variable influencing reproduction and dispersal, which allows the models to reflect realistic environmental constraints and resource limitations.

The first part of the thesis investigates eco-evolutionary dynamics under multigame conditions, where individuals probabilistically engage in either PD or SD games. The inclusion of mutation enables the persistence of strategy diversity, and the coupling with ecological free space reveals rich dynamical regimes, including multiple stable states and coexistence zones. Building upon this, the second part introduces time delays in ecological feedback, showing that temporal lags in payoff realization can induce Hopf bifurcations and oscillatory dynamics, significantly altering cooperation patterns. These analyses demonstrate how the timing of ecological responses is as critical as their magnitude in determining system stability.

In the third section, the thesis examines systems governed by cyclic dominance, particularly inspired by the rock-paper-scissors (RPS) dilemma, modeling the eco-evolutionary interactions of strategic species. This approach uncovers the conditions under which biodiversity is maintained via interior attractors and planar coexistence states, supported by bifurcation analysis and sensitivity computations such as the Sobol indices. The complex basin structures and parameter-driven phase transitions illustrate how eco-evolutionary feedbacks can dynamically select among multiple attractors.

The final part of the thesis generalizes the framework to include hierarchical interactions between species, transitioning from symmetric cyclic games to asymmetric dominance scenarios, including predator-prey systems and models mimicking

rumor spreading phenomena. These systems exhibit a variety of dynamical behaviors, including extinction, strategy exclusion, coexistence, and chaotic oscillations, all modulated by ecological constraints and interaction asymmetries.

Together, these contributions offer a unified theoretical framework for understanding cooperation and coexistence through the lens of eco-evolutionary dynamics. The models developed capture a spectrum of biological phenomena and reveal mechanisms by which cooperative behavior, often fragile in traditional models, can emerge and stabilize through ecological mediation. By bridging mathematical analysis with ecological realism, the thesis advances both the conceptual and practical understanding of evolutionary dynamics in complex adaptive systems, with implications spanning conservation biology, epidemiology, and social dynamics.

Keywords: Nonlinear dynamics, Eco-evolutionary dynamics, Game theory, Ecology & Evolution, Cooperation, Cyclic dominance.

Sourav Roy 13.8.2025

Signature of Student

13.8.2025

Signature of Supervisor

Dibakar Ghosh 13/08/25

Signature of Co-Supervisor

Dr. Dibakar Ghosh
Professor of Applied Mathematics
Physics and Applied Mathematics Unit
भारतीय सांख्यिकी संस्थान / INDIAN STATISTICAL INSTITUTE
203 बी. टी. रोड, कोलकाता / 203 B. T. Road, Kolkata - 700108

ACKNOWLEDGEMENT

The journey of my PhD has been immense and transformative. Looking back to the moment when I first registered at Jadavpur University, and now arriving at the point of finally writing this thesis, it feels both surreal and deeply fulfilling. So much has changed within me and around me—and the path has been marked by countless memories, challenges, and quiet moments of growth. There are many people to acknowledge, and even more moments, some joyous, others difficult, that have shaped this journey. Through it all, I have felt an inner evolution, a constant urge to grow and adapt. I may fall short in expressing it all fully through words, but the depth of this experience lives on beyond what any sentence can capture.

First and foremost, I would like to express my deepest and most sincere gratitude to my supervisor, Prof. Prakash Chandra Mali of the Department of Mathematics, Jadavpur University, Kolkata – 700032 (Retired), for extending his support when I had very little to hold on to. His unwavering belief in me, steadfast support, and encouragement have been a pillar of strength throughout my PhD journey. Equally heartfelt thanks go to my co-supervisor, Prof. Dibakar Ghosh of the Physics and Applied Mathematics Unit, Indian Statistical Institute, Kolkata – 700108, whom I regard as the guiding force, the true captain of the ship of my academic existence. His mentorship, insight into the field of Nonlinear Science and Network Theory, and relentless encouragement have not only shaped me as a researcher but have also deeply influenced my personal growth. The countless days I spent under his guidance at the Physics and Applied Mathematics Unit were profoundly transformative, instilling in me the spirit to venture into the unknown with curiosity and confidence. I feel incredibly fortunate to have had both these exceptional mentors on my side. His guidance, wisdom and unwavering support have been instrumental in every step of my research journey.

The journey of my PhD as a researcher has been nothing short of overwhelming, a path filled with challenges, learning, and growth. It would be deeply unjust not to acknowledge those whose constant encouragement, unwavering support, and helping hands have carried me through. First of all, my deepest gratitude goes to my family. I would like to start by recalling my late grandfathers (both maternal and paternal), my late paternal grandmother, and my maternal grandmother, "Mrs" Krishna Rani Das. To all of you eternally, I owe my life. My parents, Mrs. Pramila Das (Roy) and Mr. Surash Chandra Roy, have been a divine force in my life since the very beginning, standing beside me as an unshakeable pillar of strength and motivation. Their belief in me has never wavered, and unconditional support has been the backbone of this entire journey. To my brother, Mr. Sourjya Roy, my closest friend, my partner in crime, and my silent cheerleader, thank you for always being there, often behind the scenes, but never unnoticed in my heart. I am equally grateful to all my extended family members, all my uncles and aunts, whose encouragement and helping hands often arrived just when I needed them the most several times. A special mention goes to my aunt (masi), "Mrs." Swapna Paul, who has been, in every sense, my first mathematics teacher, and Mrs. Sandhya Talukder for standing beside me as a true guardian, second only to my mother. However, I also would like

to lovingly mention my maternal uncles and aunts, Mr. Prabir Kumar Das, Mrs. Rina Das, Mr. Debabrata Das, and Mrs. Pialy Das, for always cheering me through every situation in life, offering their unwavering support and encouragement. To my maternal uncle and aunt (Mama and Mami), Dr. Goutam Das, and Dr. Chitra Sarkar, thank you for inspiring me to pursue a Ph.D., even when the path ahead felt uncertain. Your faith in me planted the seed of perseverance.I would also like to fondly remember my late uncle-in-law, Mr. Subhasish Paul, whose unwavering support, though brief in the time we shared, left a lasting impact on me. I am equally grateful to my paternal elder brothers and sisters, whose steady hands of support and heartfelt blessings have always guided me forward. To all my younger brothers and sisters in my family, thank you for your patience, love, and for always seeing and considering me as your elder brother, even in my worst. I always carry your warmth with me. I love you all.

My journey in research has expanded and matured through the unwavering support of several individuals, each of whom I deeply acknowledge and sincerely thank. I am grateful to all my teachers, starting from my early education at Sri Ramkrishna Vidyasram, to my teachers at Dum Dum Subhas Nagar High School and Dum Dum Kishore Bharati High School. I extend heartfelt thanks to my coaching teachers, whose blessings and encouragement have always lifted me whenever I have had the opportunity to meet them. I also convey my sincere appreciation to my professors at Scottish Church College, Kolkata, where I completed my undergraduate studies, and to the esteemed faculty at the Indian Institute of Technology (Indian School of Mines), Dhanbad, Jharkhand, where I pursued my M.Sc. A special note of gratitude goes to Prof. Matjaž Perc, Prof. Timoteo Carletti, Prof. Syamal Kumar Dana, Prof. Kamrul Hassan Mamun, Prof. Sarika Jalan, Prof. Sagar Chakraborty, Prof. Abhijit Lahiri, and Dr. Chittaranjan Hens for their motivation and consistent support throughout this academic journey. I am also thankful to all my collaborators, who have contributed to the research work that shaped my PhD experience. I am profoundly indebted to Dr. Sayantan Nag Chowdhury (my academic father), who mentored me during my very first research project. It is because of him that I learned how to transform an idea into a meaningful research problem. Words fall short to express how much I owe you. My heartfelt thanks also go to Dr. Subrata Ghosh for standing by me during some of the most difficult times and for being not only a research collaborator but a trusted companion in many adventures. I wish to extend my sincere gratitude to my collaborators: Dr. Srilena Kundu, Dr. Soumen Majhi, Dr. Gourab Kumar Sar, Dr. Md Sayeed Anwar, Ms. Sagarika Dutta, Dr. Biswambhar Rakshit, Dr. Jeet Banerjee, Dr. Arindam Saha, Atefeh Ahmadi, Mahtab Mehrabbeik, Prof. Sourav Kumar Sasmal, Prof. Helen M. Byrne, and Prof. Sajad Jafari. I would particularly like to thank Dr. Gourab Kumar Sar once again for being a pillar of inspiration throughout my research life—your trust in me has played a vital role in shaping my confidence and character. A very personal note of affection is reserved for Dr. Arnob Ray (my spiritual sequence), who has been so many things to me—friend, mirror, and motivator. It is difficult to capture it all in words. Let's just say: I hope we collaborate someday! Another token of deep appreciation goes to my friend and true technical expert, Dr. Md

Sayeed Anwar—thank you for always being there during the most critical moments. Your presence and support have meant more than words could ever convey. I would like to express my heartfelt gratitude to my senior, friend, and collaborator, Dr. Soumen Majhi, whose unwavering support during challenging times has meant a great deal to me. His companionship and shared spirit of exploration made our journey through the PNLD 2025 conference in Italy not only intellectually enriching but also full of memorable, if occasionally anonymous, adventures. My PhD journey would be incomplete without acknowledging the steadfast presence of my labmates and friends of ISI, Kolkata, who have been my constants through every up and down: Dr. Sarbendu Rakshit, Mr. Dhiman Das, Mr. Sayan Acharya, Mr. Tapas Kumar Pal, Mr. Palash Kumar Pal, Dr. S. Sudharsan Hari, Mr. Suvam Pal, Ms. Samali Ghosh, Mr. Abhijeet Kumar, Dr. Krishnendu Pal, Dr. Naresh Saha, Mrs. Antara Dey, Dr. Saswati Biswas, Mr. Debarun Pal, Mr. Sourav Kumar Pal, Mr. Sourav Karmakar, Mr. Mosedul Sarkar, Mr. Biswadip Saha, Mr. Angshuman Mahata, Mr. Md Kausar Sk, Dr. Satwik Mukherjee, and Mr. Sourin Chatterjee; I love you all deeply. Maintaining a work-life balance has been crucial for me, and this wouldn't have been possible without the love and presence of friends outside the academic world. A special mention must go to my friend Mr. Usnish Mukherjee; all that I am today has been shaped in many subtle yet profound ways by you. You have refined me, pushed me, and helped me envision the version of myself I aspire to become. I love you, man! To Dr. Sandipan Sen, thank you for being the one who always challenged me to push harder with your signature mantra: "If not die, then just do it!" Cheers, bro! Finally, to my constants— Mr. Swagata Sasmal (for bearing my daily burden and constantly assuring me of my worth as family), Mr. Swapnadeep Sen, Mr. Prayas Kumar Mitra, Mr. Swarnadeep Bakshi, Mr. Arnab Majhi, Mr. Biplab Lohar, Mr. Arijit Nandy, Mrs. Dipanjana Sarkar, Dr. Srinanda Majumder, Mr. Abhik Roy Chowdhury, Mrs. Debasmita Datta, Mr. Kumar Roy, Mrs. Shreyoshi Das, Mrs. Sujata Roy, Mrs. Anasuya Dey, Mr. Aranya Biswas, Ms. Shreya Choudhury, Mrs. Megha Sinha, Mr. Tamal Saha, Mrs. Sinjini Dasgupta, Mrs. Deborpita Biswas, Mrs. Poulomi Chakraborty, Mr. Soumya Ghosh, Mrs. Snigdha Bardhan, Dr. Debajyoti Kumar, Mr. Anirban Patra, Dr. Sourav Kumar Panja, Mrs. Amrita Singha, Mr. Prasenjit Pal, Mr. Jyotirmoy Moshan, Mr. Sanjay Kumar Jena, Mr. Anirban Chakraborty, Dr. Diya Bhattacharya, Mr. Ankur Chatterjee, Dr. Subhasanket Dutta, Mr. Debargha Mukherjee and so many others—I owe you more than I can express. You have all touched my life in ways that go beyond words. As a student during my graduation and post-graduation years, I often found myself wishing that certain peers had pursued a PhD and entered the world of research. I have told them this many times, and I genuinely meant it. I have spiritually missed my friends from academia, Kumar Roy, Abhik Roychowdhury, and Usnish Mukherjee, as co-workers in my field of research. I often imagine how inspiring it would have been to work together. I sincerely hope that one day, we will have the opportunity to work scientifically. To all my students, I have had the opportunity to teach; you guys have nurtured the academic configuration inside me in wholehearted ways.

My heartfelt acknowledgements also extend to all the esteemed faculty members

of the Department of Mathematics at Jadavpur University, with special gratitude to the Head of the Department for their continued guidance and support. I would also like to acknowledge the many people who have always worked quietly behind the scenes. My heartfelt thanks go to all the respected office members in the Ph.D. sections of Jadavpur University and the departmental employees of the Indian Statistical Institute, Kolkata, whose support and helping hands have benefited me and many other research scholars year after year. I am especially grateful to Mr. Monojit Dey for meticulously managing my funding, even while I resided far from Jadavpur University, and to Mr. Azizur Rahaman, who has been a constant support since the very beginning of my registration at the university. Their prompt responses and careful attention to every inconsistency have been immensely helpful and reassuring. I also want to toast my beloved students for a short span of my life and for fleshing out a teacher-like soul inside me.

Lastly, I must proudly confess—I am a die-hard movie buff! If I were to describe my PhD journey cinematically, it has been nothing short of a spectacular saga—filled with moments of thrill, drama, and profound slices of life. Looking back, it feels like a script shaped not just by equations, but by the many people, emotions, and turning points that continuously rewrote the narrative. Just like in every great film, some scenes were rewritten, some dialogues improvised, and some characters became irreplaceable. Equations evolved, ideas collided, and collaborations brought plot twists I never saw coming. And so, borrowing from the spirit of cinema and the soul of science, I always find myself saying with a smile:

Till the left-hand side and the right-hand side are not equated, *"Picture abhi baaki hain, mere dost! (The show must go on...)"*

Sourav Roy

Sourav Roy

Kolkata - 700032
August, 2025

List of publications

Publications included in the thesis:

1. **Sourav Roy**, Sayantan Nag Chowdhury, Prakash Chandra Mali, Matjaž Perc and Dibakar Ghosh (2022): **Eco-evolutionary dynamics of multigames with mutations**, Plos One, 17(8): e0272719, 2022, https://doi.org/10.1371/journal.pone.0272719.
(SCI Journal, Impact Factor: 2.6).

2. **Sourav Roy**, Sayantan Nag Chowdhury, Srilena Kundu, Gourab Kumar Sar, Jeet Banerjee, Biswambhar Rakshit, Prakash Chandra Mali, Matjaž Perc and Dibakar Ghosh (2023): **Time delays shape the eco-evolutionary dynamics of cooperation**, Scientific Reports, 13(1), p.14331. https://doi.org/10.1038/s41598-023-41519-1.
(SCI Journal, Impact Factor: 3.9).

3. **Sourav Roy**, Subrata Ghosh, Arindam Saha, Prakash Chandra Mali, Matjaž Perc and Dibakar Ghosh (2024): **The eco-evolutionary dynamics of strategic species**, Proceedings of the Royal Society A, 480(2288), p.20240127, https://doi.org/10.1098/rspa.2024.0127.
(SCI Journal, Impact Factor: 3.0).

4. Subrata Ghosh, **Sourav Roy**, Matjaž Perc and Dibakar Ghosh (2024): **The eco-evolutionary dynamics of two strategic species: From the predator-prey to the innocent-spreader rumor model**, Journal of Theoretical Biology, 595, p.111955, https://doi.org/10.1016/j.jtbi.2024.111955.
(SCI Journal, Impact Factor: 2.691).

Other publications (not included in the thesis):

1. Atefeh Ahmadi, **Sourav Roy**, Mahtab Mehrabbeik, Dibakar Ghosh, Sajad Jafari and Matjaž Perc (2023): **The dynamics of a duopoly Stackelberg game with marginal costs among heterogeneous players**, Plos One, 18(4), p.e0283757, https://doi.org/10.1371/journal.pone.0283757.
   (SCI Journal, Impact Factor: 2.6).

2. **Sourav Roy**, Soumen Majhi, Matjaž Perc and Dibakar Ghosh (2025): **Transitive to cyclic dominance in eco-evolutionary dynamics of strategic species**, Proceedings of the Royal Society A,481: 20240734, http://doi.org/10.1098/rspa.2024.0734.
   (SCI Journal, Impact Factor: 3.0).

Papers presented in national/international conference/seminar/school:

1. Name of the conference: 13th Conference on Nonlinear Systems and Dynamics (CNSD 2021)
   Venue: SASTRA Deemed University, Thanjavur, India. 17th - 22nd December, 2021
   Title of presentation: *"Eco Evolutionary Dynamics Under Mutation"*.

2. Name of the conference: 14th Conference on Nonlinear Systems and Dynamics (CNSD 2022)
   Venue: IISER Pune, India. 15th - 18th December, 2022
   Title of presentation: *"Eco-evolutionary dynamics of multigames with mutations"*.

3. Name of the conference: Nonlinear Data Analysis and Modeling: Advances, Applications, Perspectives (NDA23)
   Venue: Potsdam Institute for Climate Impact Research , PIK, Germany. 15th to 17th March, 2023
   Title of presentation: *"Eco-evolutionary dynamics with multi-games under mutation"*.

4. Name of the conference: Perspectives in Nonlinear Dynamics 2023 (PNLD 2023)
   Venue: IIT Madras, Chennai, India. August 1 to 4, 2023
   Title of presentation: *"Uncovering the role of time delays in shaping eco-evolutionary dynamics of cooperative behavior"*.

5. Name of the conference: 7th International Conference on Complex Dynamical Systems and Applications (CDSA 2024)
   Venue: Digha Science Centre & National Science Camp, Digha organised by Indian Statistical Institute, Kolkata. January 25-27, 2024
   Title of presentation: *"The dynamics of a duopoly Stackelberg game with marginal costs among heterogeneous players"*.

6. Name of the conference: 8th India Biodiversity Meet 2025 (IBM 2025)
   Venue: Agricultural and Ecological Research Unit & Biological Anthropology Unit, Indian Statistical Institute, Kolkata. January 24-26, 2025
   Title of presentation: *"The Eco-Evolutionary dynamics of Strategic Species"*.

7. Name of the conference: Perspectives in Nonlinear Dynamics 2025 (PNLD 2025)
   Venue: IMT School for Advanced Studies Lucca, Italy. 21st - 24th July, 2025
   Title of presentation: *"Transitive to cyclic dominance in eco-evolutionary dynamics of strategic species"*.

8. Name of the event: Winter School on Games in Evolutionary Dynamics
   Venue: Shiv Nadar Institution of Eminence (Deemed to be University), 18th to 23rd December, 2023
   Participant.

Contents

Chapter 1

Introduction

"*The interaction of organisms with their environment is the central theme of biology.*"

This seminal assertion by Ernst Mayr (1961) [1] distills the essence of ecology and evolution as intrinsically linked disciplines. The conceptual unification of these fields, however, followed a centuries-long intellectual journey that began with Darwin's revolutionary insights. In *On the Origin of Species* (1859) [2], Charles Darwin established the fundamental principle of natural selection as the mechanism of evolutionary change, while simultaneously laying ecological foundations through his observations of species interactions and biogeography. His concept of the "struggle for existence" explicitly connected evolutionary adaptation to ecological pressures, though the temporal scales he envisioned were geological in magnitude.

The early 20th century saw these disciplines diverge as ecology emerged as a distinct field through the works of Warming [3] and Clements [4], who focused on community structure and succession, while evolutionary biology became increasingly genetic-centric following the Modern Synthesis [5, 6]. This theoretical schism persisted through mid-century, with ecologists like Lotka [7] and Volterra [8] developing population models that treated species traits as fixed parameters, and evolutionary biologists like Fisher [9] and Wright [10] modeling genetic change without explicit ecological feedbacks.

The intellectual groundwork for reconciliation was laid by G. Evelyn Hutchinson, whose seminal metaphor of *The Ecological Theater and the Evolutionary Play* (1965) [11] reimagined ecosystems as dynamic stages where evolutionary actors continuously adapt to shifting ecological scripts. Hutchinson's niche concept and his work on competitive exclusion [12] bridged the gap between ecological interactions and evolutionary consequences. His student, Robert MacArthur, further advanced this synthesis through theoretical ecology [13], demonstrating how evolutionary principles could explain ecological patterns of species distribution and abundance.

This conceptual shift gained empirical support through groundbreaking studies demonstrating rapid evolution in natural populations. Grants' work on Darwin's finches [14] provided the first compelling evidence that ecological changes could drive measurable evolutionary responses within observable timescales, exactly in the system that originally inspired Darwin's theory [15]. Concurrently, theoretical developments in evolutionary ecology [16] and coevolution [17] demonstrated how

reciprocal selection pressures could generate complex ecological dynamics.

The resulting paradigm of *eco-evolutionary dynamics* [18, 19] represents the maturation of this synthesis, recognizing that ecological and evolutionary processes operate on overlapping timescales with continuous feedback. Modern research has revealed how anthropogenic changes can accelerate these dynamics, creating evolutionary consequences within years or decades [20], thus validating Darwin's original insight about the environmental basis of evolutionary change while dramatically compressing his envisioned timescales.

1.1 Empirical evidence of eco-evolutionary feedbacks

The past half century has produced overwhelming evidence that evolutionary change can unfold on ecological timescales, reshaping population dynamics and ecosystem processes in ways that challenge the classical view of evolution as a slow backdrop to rapid ecological dynamics. This reciprocal interplay, termed eco-evolutionary feedback, reveals a continuous dialogue that shapes biodiversity, community structure, and ecosystem function.

1.1.1 Case studies in rapid adaptation

One of the most iconic demonstrations of rapid evolutionary change comes from the long-term studies of Darwin's finches (*Geospiza* spp.) by Peter and Rosemary Grant on the Galápagos Islands. Their work revealed that drought-induced changes in seed size and availability triggered strong selection on beak morphology, leading to measurable changes in beak size and shape within just a few years [14]. These morphological changes, in turn, altered the efficiency of bird feeding and competitive hierarchies, influencing which species and individuals thrived under new environmental conditions. Such feedback loops illustrate how ecological changes can drive rapid evolutionary shifts that then reshape ecological interactions in a dynamic and ongoing process.

In aquatic systems, predator-prey dynamics between rotifers (*Brachionus calyciflorus*) and algae (*Chlorella vulgaris*) have provided some of the clearest evidence of eco-evolutionary feedbacks. Yoshida et al. (2003) showed that prey populations evolved anti-grazing defenses that fundamentally altered the population cycles of both predators and prey, stabilizing the system and preventing classic predator-driven extinctions [21]. This evolutionary feedback also affected nutrient dynamics, illustrating how trait evolution can reverberate through multiple levels of ecological organization.

Trinidadian guppies (*Poecilia reticulata*) have also emerged as a model system for understanding rapid evolution in response to predation. In high-predation environments, guppies evolved earlier reproductive maturity and increased fecundity compared to populations in low-predation environments [22]. These changes in life history not only altered the dynamics of the guppy population but also influenced the nutrient dynamics of the entire stream ecosystem by changing feeding behaviors

and excretion rates [23]. This example highlights how evolutionary changes in life history traits can cascade through both biotic and abiotic components of ecosystems.

In terrestrial systems, evening primroses (*Oenothera biennis*) have evolved increased chemical defenses in response to herbivory by specialist moths. Agrawal et al. (2012) demonstrated that these evolutionary changes in plant defense can shift herbivore abundance and indirectly affect pollinator communities by altering floral traits and nectar rewards [24]. Such tri-trophic interactions underscore how evolutionary responses to one selective pressure can restructure entire ecological networks.

1.1.2 Anthropogenic accelerators of eco-evolutionary change

Human activities now represent some of the most powerful drivers of rapid evolution, often generating feedback loops that reshape ecological dynamics in ways that pose challenges for biodiversity conservation and resource management. For example, urbanization has forced many bird species to adapt their acoustic signals to cope with anthropogenic noise. The great tit (*Parus major*) adjusts its song frequencies in urban environments to avoid being filtered by traffic noise, which in turn affects mate choice, reproductive success, and potential gene flow within and between populations [25–28]. Such behavioral adaptations illustrate how anthropogenic stressors can rapidly drive evolutionary change, reshaping ecological interactions and species distributions.

In agricultural systems, the extensive use of pesticides and herbicides has led to the rapid evolution of resistance in insect pests and weeds, profoundly altering trophic interactions and ecosystem stability [29, 30]. This evolutionary feedback loop not only diminishes the effectiveness of chemical controls but also reshapes predator-prey interactions, pest population dynamics, and crop yields, creating complex challenges for sustainable agriculture.

In fisheries, size-selective harvesting has driven rapid evolutionary changes in fish growth rates and age at maturation, particularly in heavily fished species such as Atlantic cod (*Gadus morhua*) [31, 32]. These shifts can reduce population resilience, complicate stock management, and even destabilize marine food webs by altering trophic interactions and reproductive output.

Recent studies have also revealed that urbanization and habitat fragmentation can accelerate evolutionary changes in dispersal traits, reproductive strategies, and anti-predator behaviors across a wide range of taxa, from insects to mammals [33]. These rapid changes affect not only local species interactions but also have broader implications for community composition, disease dynamics, and ecosystem services.

1.1.3 Integrating empirical insights into eco-evolutionary models

These diverse case studies collectively demonstrate that eco-evolutionary feedbacks are not isolated phenomena but are widespread across natural and human-altered

ecosystems. They underscore the need for theoretical frameworks that can integrate both ecological and evolutionary processes, capturing the reciprocal interactions that shape system dynamics. Mathematical models incorporating evolutionary game theory, replicator dynamics, and nonlinear feedback mechanisms have proven particularly valuable for analyzing these complex interactions [34]. For example, the study of cyclic dominance in rock-paper-scissors systems has revealed how strategic interactions among species can maintain biodiversity and drive community-level oscillations, as observed in side-blotched lizards (*Uta stansburiana*) where alternative male mating strategies cycle over time [35].

Moreover, models incorporating spatial structure, dispersal, and stochasticity have highlighted how local adaptation and gene flow can interact with ecological dynamics to shape the resilience and stability of communities [36]. These theoretical advances provide essential insights into how eco-evolutionary feedbacks can promote or hinder cooperation, competition, and coexistence in natural systems.

Together, these empirical and theoretical insights lay the groundwork for the subsequent chapters of this thesis, which aim to develop and analyze eco-evolutionary models that incorporate key factors such as multigames, behavioral mutation, ecological feedback, and time delays. By combining empirical realism with mathematical rigor, this thesis seeks to deepen our understanding of how the complex interplay between ecology and evolutionary game dilemmas shapes the dynamics of biodiversity and cooperation in real-world ecosystems.

1.2 Theoretical foundations and unresolved questions

Mathematical models have played a central role in formalizing the principles of eco-evolutionary dynamics. By bridging individual behaviors and population-level consequences, these models help us understand how evolutionary and ecological processes shape complex natural systems. Foundational tools like evolutionary game theory, replicator dynamics, and spatially explicit frameworks provide powerful lenses through which to study these interactions [34].

For example, the study of cyclic dominance—most notably illustrated in the rock-paper-scissors dynamics of side-blotched lizards (*Uta stansburiana*)—has revealed how frequency-dependent selection can sustain biodiversity within a population. Here, alternative male strategies (territorial, sneaker, and satellite) cycle over time in response to selective pressures from each other, maintaining genetic diversity and preventing competitive exclusion [35]. This dynamic interplay demonstrates how even simple strategic interactions can lead to complex and stable ecological patterns.

Incorporating spatial structure has been another major advance. Metapopulation models show how dispersal between subpopulations, combined with local adaptation, can influence the evolution of cooperation, competition, and community structure [36]. For example, patchy environments and migration rates can determine whether cooperative strategies persist or are outcompeted by defectors, highlighting the importance of connectivity and landscape heterogeneity in eco-evolutionary

outcomes. Despite these advances, critical gaps remain that demand further exploration:

- **Social interaction heterogeneity:** Most models assume homogeneous interactions, yet real-world populations often navigate diverse social and ecological contexts [37]. How do multigame environments—where individuals switch between different game structures, such as Prisoner's Dilemma (PD) and Snowdrift (SD)—affect the evolution of cooperation? Understanding how these dynamic interaction contexts modulate strategy frequencies is essential for predicting the emergence of cooperation in complex systems.

- **Behavioral mutation and time delays:** Evolutionary models typically assume immediate responses to selection pressures [38]. However, behaviors can shift through learning, cultural transmission, or genetic mutation, introducing stochasticity into population dynamics. Furthermore, time delays in feedbacks—such as reproduction rates depending on past environmental conditions—can destabilize or stabilize populations. How do these factors interact to influence the long-term coexistence of competing strategies and the resilience of eco-evolutionary systems?

- **Ecological constraints and resource limitation:** Natural populations often face ecological limitations, such as resource availability and habitat space. The inclusion of free space as an ecological variable mediating reproduction and dispersal highlights how spatial constraints shape fitness landscapes. How do these constraints influence strategy success, especially in structured populations where resource competition is intense? Integrating ecological variables like free space into evolutionary models can reveal new insights into the dynamics of cooperation and biodiversity maintenance [39].

Moreover, these theoretical questions are not purely academic. They have profound implications for applied challenges in conservation biology, ecosystem management, and disease ecology. For instance, understanding how multi-game dynamics affect cooperation could inform the design of interventions to promote beneficial behaviors in social species or control the spread of pathogens in human and wildlife populations. Likewise, elucidating how time delays and behavioral mutations affect eco-evolutionary stability can improve our predictions of species persistence under rapid environmental change.

These unresolved questions form the backbone of this thesis, motivating the development of nonlinear, dynamical models that incorporate multi-game frameworks, stochastic behavioral mutation, ecological variables like free space, and time-delayed feedback. Through this integration, this work seeks to uncover the mechanisms that govern the emergence, persistence, and resilience of cooperation in eco-evolutionary systems, ultimately contributing to a deeper understanding of the complex interplay between ecology and evolutionary game dilemmas.

1.3 Literature review

The concept of eco-evolutionary dynamics gained further traction with the work of scientists like Peter Grant and Rosemary Grant [14], whose decades-long study of Darwin's finches in the Galápagos Islands provided empirical evidence of rapid evolutionary change in response to ecological pressures. Their research demonstrated how droughts and food scarcity could lead to measurable shifts in beak size and shape within just a few generations, illustrating the intimate link between ecological conditions and evolutionary adaptation. As Grants noted, "Evolution is not a remote process; it is an ongoing, observable phenomenon."

In parallel, theoretical advances by researchers such as David Reznick and Joseph Travis underscored the importance of feedback loops between ecological and evolutionary processes [40]. Reznick's work on guppies in Trinidadian streams, for example, revealed how predator-induced mortality could drive evolutionary changes in life history traits, altering population dynamics and ecosystem structure. These studies collectively demonstrated that evolution is not only a historical force, but a contemporary driver of ecological change [41]. The recognition of anthropogenic impacts on natural systems further catalyzed the emergence of eco-evolutionary dynamics as a distinct field. Human activities, from habitat destruction to climate change, alter ecological conditions at unprecedented rates, forcing species to adapt or face extinction. As Thompson (1998) aptly observed, "The rate of environmental change is now outpacing the ability of many species to evolve in response" [42]. This realization has imbued the study of eco-evolutionary dynamics with both urgency and relevance, as understanding these processes is critical for predicting and mitigating the impacts of global change.

Against this rich historical and intellectual backdrop, this thesis seeks to contribute to the growing body of knowledge on eco-evolutionary dynamics. By synthesizing insights from four published studies, this work explores how ecological and evolutionary processes interact across different scales and contexts, shedding light on the mechanisms that underpin these dynamic relationships. In doing so, it builds on the foundational ideas of Hutchinson, the empirical rigor of the Grants, and the theoretical frameworks of Reznick and others, while also addressing contemporary challenges in a rapidly changing world.

As we embark on this exploration, it is worth reflecting on Theodosius Dobzhansky's (1973) words: "Nothing in biology makes sense except in the light of evolution" [43]. We might add that nothing in evolution makes sense except in the light of ecology. This interplay between ecological and evolutionary science lies at the heart of this thesis and the future of biological science. As environmental and evolutionary processes interact over contemporary timescales, they form feedback loops that shape species survival, community structures, and ecosystem stability. Unlike classical ecological models, which often assume that species traits remain static, the eco-evolutionary approach acknowledges that organisms are not only shaped by their environments but also actively modify them, creating dynamic feedback loops between natural selection and ecological change [44]. The reluctance to accept rapid evolutionary change as an ecological driver persisted for much of the twentieth century, largely due to the dominance of classical evolutionary thought,

which emphasized slow genetic shifts over millennia. However, empirical studies have increasingly demonstrated that evolutionary changes can occur on timescales comparable to ecological processes. The long-term studies of Darwin's finches (Geospiza spp.) on the Galápagos Islands provide one of the most compelling examples of such rapid adaptation. Over several decades, shifts in beak morphology driven by fluctuations in seed availability during periods of drought led to strong selection pressures favoring individuals with particular beak sizes [45]. Similarly, populations of guppies (Poecilia reticulata) in Trinidadian streams exposed to high predation pressures evolved different life-history traits, such as earlier reproduction and increased offspring numbers, compared to those in predator-free environments [46].

Such findings necessitate a re-evaluation of traditional ecological theories. The integration of eco-evolutionary perspectives into ecological modeling has demonstrated that evolving traits, such as predator avoidance strategies, resource exploitation efficiencies, and competitive interactions, can drive significant shifts in species abundances and even lead to emergent ecosystem properties [47]. This dynamic perspective has been particularly influential in areas such as predator-prey systems, mutualistic networks, and social dilemmas in structured populations, where evolutionary shifts in strategy alter the stability and resilience of entire communities [48].

A crucial aspect of eco-evolutionary dynamics is the presence of feedback loops, wherein evolutionary processes alter ecological interactions, which in turn shape subsequent evolutionary pressures. One striking example is seen in the case of stickleback fish (Gasterosteus aculeatus), where shifts in armor plating, driven by predator presence, not only affect individual survival but also influence habitat selection and competition for resources [49]. Similarly, the interplay between plant-pollinator interactions provides another example, where the evolution of floral traits in response to pollinator behavior feeds back into pollinator foraging patterns, creating a reciprocal selective pressure that drives rapid diversification [50].

Beyond empirical studies, theoretical frameworks have played a vital role in formalizing the principles of eco-evolutionary feedback. Mathematical models incorporating evolutionary game theory, replicator dynamics, and nonlinear ecological interactions have provided deep insights into how evolving strategies influence cooperation, competition, and species coexistence [34]. In particular, the study of cyclic dominance in rock-paper-scissors-type interactions has revealed how strategic decision-making among species can generate sustained ecological oscillations, preventing competitive exclusion and fostering biodiversity [51].

As research in this field advances, new questions continue to emerge, particularly regarding the role of higher-order interactions, spatial structure, and stochastic effects in shaping eco-evolutionary trajectories [36]. The realization that evolution can operate on ecological timescales has profound implications for conservation biology, ecosystem management, and our understanding of resilience in natural systems [52]. Recognizing that adaptive responses can buffer or amplify ecological disturbances forces a reconsideration of how we model species persistence in rapidly changing environments. This perspective becomes particularly relevant in the face of climate change, habitat fragmentation, and species invasions, where eco-evolutionary insights may offer critical strategies for predicting and mitigating biodiversity loss

[53].

The exploration of eco-evolutionary dynamics thus represents a fundamental shift in how we perceive the relationship between ecological and evolutionary forces. By acknowledging that organisms do not merely respond to their environments but actively shape them through evolutionary processes, this framework offers a richer, more dynamic understanding of biological systems. As this thesis will demonstrate, the application of nonlinear dynamics to eco-evolutionary models provides powerful tools for unraveling the complexity of species interactions, strategic behaviors, and emergent ecological patterns.

The generality of the interplay between ecological and evolutionary processes becomes even more compelling when examined through the lens of real biological systems. Empirical studies across a wide array of taxa—from microbes to vertebrates—have demonstrated how changes in environmental parameters can rapidly reshape evolutionary trajectories, and vice versa. In microbial systems, for example, nutrient availability not only dictates growth dynamics but also selects for metabolic efficiency and competitive strategies. In long-term evolution experiments with *Escherichia coli*, Lenski and colleagues revealed that populations exposed to constant glucose limitation evolved diverse adaptive traits, including increased fitness, metabolic specialization, and altered cell morphology, within only a few thousand generations. These adaptations subsequently restructured ecological interactions within the populations, illustrating the recursive nature of eco-evolutionary feedbacks.

Similar patterns are evident in aquatic ecosystems. In rotifer-algae systems, prey species such as *Chlorella vulgaris* evolve anti-grazing defenses in response to rotifer predation, leading to oscillatory population dynamics that differ significantly from those predicted by purely ecological models. Here, the evolution of defense traits in the prey modifies both the abundance and feeding behavior of the predator, underscoring how even subtle evolutionary shifts can alter trophic interactions and system-level dynamics. In terrestrial ecosystems, rapid evolutionary changes in flowering time among plant species subjected to climate fluctuations have been shown to disrupt plant-pollinator synchrony, with cascading effects on community stability. Such findings reinforce the idea that adaptive evolution can occur swiftly enough to influence—and be influenced by—ecological conditions, challenging the outdated dichotomy between "fast" ecology and "slow" evolution.

Crucially, these feedbacks are not restricted to natural settings. Anthropogenic environmental changes, including urbanization, pollution, and habitat fragmentation, are now exerting intense selective pressures on species, prompting real-time adaptive responses. For instance, urban bird populations have evolved altered song frequencies to avoid acoustic masking by traffic noise, which in turn influences mate choice and reproductive success. In agricultural contexts, the widespread use of pesticides has led to the rapid evolution of resistance in numerous insect species, which feeds back into pest population dynamics, crop yields, and management strategies. Such examples emphasize the importance of incorporating evolutionary change into ecological forecasting and policy-making frameworks. While these biological systems illustrate the empirical richness of eco-evolutionary feedbacks, theoretical models have played a central role in generalizing and predicting their consequences. Among

the most powerful conceptual tools in this domain is evolutionary game theory, which provides a formal framework to analyze the strategic interactions of individuals whose behaviors evolve over time. In this context, evolution is shaped not only by external ecological conditions but also by the behaviors and strategies of other individuals within the population.

Traditionally, evolutionary game theory has been employed to study dilemmas of cooperation, wherein individuals must choose between self-interest and collective benefit. A classic example is the Prisoner's Dilemma (PD), where defection yields a higher individual payoff regardless of the partner's action, leading to mutual defection as the dominant outcome. However, natural populations often exhibit persistent cooperative behaviors that contradict this prediction. This discrepancy has motivated the introduction of alternative game structures, such as the Snowdrift Game (SD), where cooperation can coexist with defection under certain conditions, thereby capturing more realistic aspects of strategic interactions.

Importantly, real-world social and ecological systems are rarely governed by a single type of strategic dilemma. Rather, individuals often navigate multiple interaction contexts—sometimes resembling PD, other times SD—depending on environmental conditions, social norms, or cultural background. This heterogeneity in social context is effectively captured by the concept of multigames, where individuals probabilistically choose among different game types. Such models allow for a richer representation of strategic diversity and provide insights into how behavioral heterogeneity influences macro-level outcomes. Incorporating mutation into these frameworks further enhances their biological realism. In nature, strategic decisions are not always perfectly rational, and behavior can shift due to errors, learning, or genetic drift. Mutation allows individuals to occasionally switch between strategies, introducing stochasticity into the system. This mechanism also permits the reintroduction of rare strategies, preventing premature convergence to suboptimal equilibria and fostering the long-term coexistence of competing behaviors. In multigame environments, mutation ensures that the strategy space remains dynamically accessible, reflecting the ongoing exploration and adaptation that characterize real populations.

However, behavioral strategy alone does not fully determine evolutionary outcomes. The ecological context—particularly the availability of resources and reproductive opportunities—plays an equally crucial role. To capture this, we introduce the notion of free space as an ecological variable that mediates reproduction and dispersal. In our model, free space acts as a shared environmental resource that influences individuals' fitness by enabling successful reproduction. An individual's reproductive rate is assumed to depend not only on the payoff accrued from strategic interactions but also on the availability of this spatial resource. This dual dependency reflects the idea that fitness is both interaction- and environment-dependent—a central theme in eco-evolutionary systems.

Interestingly, the role of free space resembles that of a social good: it contributes selflessly to the reproductive potential of others without demanding any return. Though free space itself is not a strategic agent, its dynamics shape and are shaped by the evolving population. In this sense, it behaves analogously to public goods in microbial communities, where secreted enzymes benefit all nearby cells, including

non-producers. The altruistic character of such resources fosters cooperation under certain ecological conditions, creating opportunities for evolutionary stability even in the absence of formal enforcement mechanisms.

By embedding ecological constraints directly into the structure of our evolutionary model, this thesis bridges the gap between strategic behavior and environmental limitation. In doing so, we explore a richer set of dynamics, including bistability, coexistence, and oscillatory behaviors, that emerge from the interaction between game-theoretic payoffs and ecological feedbacks. This approach aligns with a growing body of literature that recognizes eco-evolutionary dynamics as not merely an intersection of ecology and evolution, but as a distinct framework that reveals emergent properties inaccessible to purely ecological or evolutionary analysis alone.

In contrast to conventional models that assume ecological change occurs on faster timescales than evolutionary adaptation, our model assumes that both operate concurrently. This assumption allows us to investigate scenarios where behavioral and environmental changes unfold hand in hand, as observed in numerous empirical systems. For instance, in cooperative breeding species such as meerkats and African wild dogs, social structure and ecological resource distribution co-evolve, shaping reproductive strategies and group dynamics in tandem. Similarly, in microbial biofilms, spatial structure, diffusion dynamics, and social interactions evolve simultaneously, resulting in complex pattern formation and functional specialization.

In the chapters that follow, we develop and analyze a suite of mathematical models, each serving as a conceptual 'toy model' that systematically synthesizes key elements of eco-evolutionary dynamics. These models capture diverse situational dilemmas by incorporating strategic interactions, behavioral mutations, time-delayed feedback, and ecological variables such as free space. Our investigation addresses fundamental questions surrounding the existence, persistence, uniqueness, and dynamical properties of the resulting systems under a range of ecological and evolutionary parameters. By leveraging both rigorous theoretical analysis and extensive numerical simulations, we identify the conditions under which cooperative behaviors can persist, explore the emergence of oscillatory regimes, and elucidate the critical role of ecological feedback in shaping strategic dynamics. Collectively, this thesis unites insights from four published studies, each examining different facets of these complex interactions—from multigame frameworks and mutation-driven strategy switching to time delays and species interactions. Ultimately, this work deepens our understanding of how the intricate interplay between ecology and evolutionary game dilemmas drives the diversity, stability, and resilience of natural systems.

1.4 Motivation and objective

The central objective of this thesis is to investigate how such coupled eco-evolutionary dynamics influence the emergence, maintenance, and diversity of cooperation. Specifically, we aim to understand how multigame environments, behavioral mutation, and ecological variables such as free space collectively shape evolutionary outcomes. By extending classical game-theoretic models into a nonlinear dynamical framework that incorporates these features, we uncover novel mechanisms that support the coexistence of cooperation and defection—even in the absence of external

enforcement like punishment or reputation systems.

Despite significant advances in eco-evolutionary theory, many crucial questions remain regarding the conditions under which cooperation can both emerge and persist amidst a backdrop of competing strategies, environmental complexity, and human-induced disturbances. For instance, how does the inherent heterogeneity of social interactions—captured through frameworks such as multigame dynamics—shape the evolutionary trajectories of cooperation in structured populations where spatial and temporal factors intertwine? Real-world systems—from microbial biofilms to social insect colonies—exhibit a mosaic of interaction types and intensities, suggesting that a single-game approach may be insufficient to capture the richness of natural social dilemmas [54, 55].

Furthermore, to what extent does behavioral mutation—representing errors, spontaneous shifts in strategy, learning, or genetic variability—impact the long-term coexistence of competing strategies, especially when ecological conditions fluctuate due to environmental change, predation, or anthropogenic impacts? For example, studies on Trinidadian guppies (*Poecilia reticulata*) have demonstrated that predator-induced evolutionary shifts in life-history traits can cascade through the ecosystem, affecting resource distribution and competitive dynamics [40, 56]. Similarly, research on Darwin's finches in the Galápagos has highlighted the importance of rapid trait evolution in response to drought and resource scarcity, influencing both ecological and evolutionary feedbacks [57].

Additionally, how do time delays, feedback loops, and higher-order interactions shape the resilience and stability of these coupled eco-evolutionary systems? Empirical studies have revealed that delays in feedback between ecological interactions and evolutionary responses can generate oscillatory dynamics and even chaotic patterns, as demonstrated in rotifer-algae systems where anti-grazing defenses evolve in response to predation [21]. The challenge of capturing such complexities underscores the need for a holistic approach that integrates strategic decision-making with dynamic ecological variables.

Motivated by these pressing questions, the objective of this thesis is to construct a comprehensive, nonlinear dynamical framework that integrates evolutionary game theory with ecological feedbacks, explicitly incorporating multigame dynamics, behavioral mutation, and ecological variables such as free space. This approach extends traditional game-theoretic frameworks to account for the multiple social dilemmas faced by real organisms—where individuals do not simply confront a single payoff matrix but navigate a landscape of interaction contexts determined by environmental conditions, social norms, or historical contingencies [58, 59]. By modeling behavioral mutation as a continuous stochastic process, this work captures the inherent unpredictability and adaptability that characterize natural populations. Moreover, by introducing free space as an ecological variable that mediates reproduction and dispersal, the model reflects how resource availability shapes fitness and evolutionary outcomes—analogous to public goods in microbial systems where secreted enzymes benefit all individuals in the local environment [60, 61].

Beyond its theoretical contributions, this thesis seeks to bridge the gap between abstract models and empirical systems by exploring how eco-evolutionary dynamics operate across multiple timescales and levels of biological organization. For example,

in cooperative breeding species such as meerkats and African wild dogs, social structure and ecological resource distribution co-evolve, shaping reproductive strategies and group dynamics in tandem [62]. In microbial communities, biofilms demonstrate how spatial structure, diffusion, and social interactions evolve simultaneously, generating complex pattern formation and functional specialization [63]. Such examples underscore the importance of linking micro-level interactions to macro-level patterns to understand biodiversity maintenance, ecosystem functioning, and the resilience of natural systems under rapid environmental change.

Ultimately, this research aims to contribute a robust and flexible framework for understanding how the complex interplay between ecology and evolution shapes the emergence, maintenance, and diversity of cooperation. By synthesizing insights from multigame frameworks, mutation dynamics, ecological variables, and empirical systems, this thesis aspires to reveal new mechanisms of eco-evolutionary feedback and to guide future empirical and theoretical research in this rapidly evolving field.

1.5 Outline of the thesis

The thesis is organized into several chapters, each addressing a specific aspect of eco-evolutionary dynamics while building upon the previous chapters' insights. Following this introductory chapter, Chapter 2 presents the foundational concepts of evolutionary game theory, including Nash equilibria, evolutionary stable strategies, and replicator dynamics, which provide the mathematical underpinnings for the subsequent analyses.

Chapter 3 introduces the concept of multi-games and social heterogeneity, focusing on my first research paper [64] published in the journal Plos One. This chapter examines how probabilistic interactions between the Prisoner's dilemma and the Snowdrift game can promote cooperative behavior under specific ecological constraints. This chapter also extends the analysis by incorporating the role of mutation and behavioral switching.

Chapter 4 delves into the impact of time delays on eco-evolutionary dynamics, informed by my second research paper [65] published in the Scientific Reports journal. This chapter examines how feedback delays can generate complex dynamical behaviors, including oscillations, multi-stability, and transitions between cooperative and defective states, using an additional policing strategy, named Punishment.

Chapter 5 and Chapter 6 extend the investigation into eco-evolutionary dynamics by exploring how strategic species interactions shape complex feedback between ecology and evolution. These chapters draw directly on insights from the third and fourth research papers [66, 67], published in the Proceedings of the Royal Society A and the Journal of Theoretical Biology (JTB), respectively. Chapter 5 focuses on the dynamics of three interacting species that engage in direct, cyclical dominance relationships within their environment. This model illuminates how cyclic interactions can foster biodiversity and drive emergent ecological patterns through evolutionary adaptations. This chapter also deals with the sensitivity analysis of the model's parameters used as payoff values. In contrast, Chapter 6 examines a system where two species interact asymmetrically, with one species exerting a dominant influence on the other. This hierarchical interaction introduces novel eco-evolutionary

feedback that differ from those in cyclic systems. In both cases, the evolutionary scenarios considered shape the eco-evolutionary dynamics in distinct ways, offering valuable insights into how diverse species interactions can mediate community structure, stability, and evolutionary trajectories.

Finally, Chapter 7 synthesizes the findings from the entire thesis, discussing broader implications, limitations, and potential avenues for future research. Through this structured progression, the thesis aims to provide a comprehensive understanding of the complex interplay between ecology and evolutionary game dilemmas.

Chapter 2

Basic definitions and model

This chapter lays the theoretical foundation for the models explored throughout this thesis. It begins with classical concepts from evolutionary game theory and gradually expands to encompass more complex formulations, including multigames, ecological feedback mechanisms, time delays, cyclic dominance among strategic species, and the interpretation of evolutionary tactics within various spreading phenomena. The unified framework presented here underpins all subsequent analyses of eco-evolutionary dynamics.

2.1 Basics of evolutionary game theory

2.1.1 Classical game theory and Nash Equilibrium

Game theory, pioneered by von Neumann and Morgenstern in 1944 [68], provides a mathematical framework to understand strategic interactions among rational decision-makers. Originally applied to economic behaviors, it soon found relevance in evolutionary biology, where the payoff from an interaction is analogous to reproductive fitness.

A fundamental solution concept in game theory is the Nash equilibrium, introduced by John Nash in 1950. In a two-player game, a strategy profile is called a Nash equilibrium if no player can increase their payoff by unilaterally deviating from their current strategy. Let s^* be a strategy and $f(s, s')$ denote the payoff to a player playing strategy s against an opponent using s'. Then s^* is a Nash equilibrium if:

$$f(s^*, s^*) \geq f(s, s^*) \quad \forall s \in S,$$

where S is the set of all available strategies.

Nash equilibria describe steady states in which no individual has an incentive to change their behavior. However, in biological systems, where populations evolve over time due to differential reproduction, static equilibrium concepts need to be expanded to capture dynamic stability.

2.1.2 Evolutionarily stable strategy (ESS)

Maynard Smith and Price (1973) extended game theory to evolutionary biology by introducing the concept of an evolutionarily stable strategy (ESS) [69]. An ESS is a strategy that, if adopted by the majority of a population, cannot be invaded by a small number of individuals using an alternative strategy. This concept is critical for understanding the stability of observed behaviors in animal populations, such as aggression, mating systems, and foraging strategies.

Mathematically, a strategy s^* is evolutionarily stable if it satisfies the following conditions for all $s \neq s^*$:

$$f(s^*, s^*) > f(s, s^*) \quad \text{or} \quad f(s^*, s^*) = f(s, s^*) \text{ and } f(s^*, s) > f(s, s).$$

The ESS concept refines Nash equilibrium by introducing robustness against invasion, thus making it particularly suitable for evolutionary contexts. It has been used to explain the distribution of behavioral traits in nature, such as the Hawk-Dove game, where a mixture of aggressive and passive behaviors leads to a stable equilibrium in the population.

2.1.3 Replicator dynamics

While ESS describes static stability, the dynamics of strategy change in populations are captured by the replicator equations, originally formalized by Taylor and Jonker (1978) [70]. These equations describe how the frequency x_i of a strategy i changes over time based on its relative performance compared to the population average.

Let f_i denote the expected payoff of strategy i, and $\bar{f} = \sum_j x_j f_j$ be the average payoff in the population. Then the replicator equation is:

$$\dot{x}_i = x_i(f_i - \bar{f}).$$

This dynamic embodies natural selection: strategies that perform better than average increase in frequency, while poorly performing strategies decline. The set of fixed points of this system includes Nash equilibria, and stable fixed points often correspond to evolutionarily stable strategies.

Replicator dynamics have broad applicability across fields. In biology, they describe the spread of genetic traits and behavioral strategies. In economics and sociology, they model the adoption of norms or technologies. In this thesis, replicator dynamics are extended to incorporate mutation, ecological feedback, and strategic complexity through multigames and structured interactions.

2.2 Modeling cooperation: PD and SD Games

2.2.1 The Prisoner's Dilemma

The Prisoner's Dilemma (PD) is the canonical model for studying social dilemmas and is central to the field of cooperation theory. It was first formalized by Flood and Dresher in the 1950s [71] and gained popularity through Axelrod's evolutionary tournaments in the 1980s [72]. In its evolutionary form, it models interactions

between individuals who can choose to cooperate or defect. The payoff matrix is defined by four parameters:

$$\begin{bmatrix} R & S \\ T & P \end{bmatrix}, \quad \text{where } T > R > P > S.$$

Here, R is the reward for mutual cooperation, P is the punishment for mutual defection, T is the temptation to defect against a cooperator, and S is the sucker's payoff. Despite the higher mutual payoff R, rational agents in a single encounter will defect, as defection strictly dominates cooperation. Thus, in well-mixed populations governed by the PD, defection typically evolves and prevails, leading to a socially suboptimal outcome.

This paradox—why cooperation persists in nature despite individual incentives to defect—lies at the heart of eco-evolutionary modeling and is a key motivation behind the development of more sophisticated models throughout this thesis.

2.2.2 The Snowdrift Game

The Snowdrift Game (SD), also known as the Chicken Game or Hawk-Dove Game in specific contexts, offers an alternative to the Prisoner's Dilemma in which cooperation can coexist with defection [73]. The payoff ranking here is:

$$T > R > S > P.$$

In this configuration, a player's best response depends on their opponent's strategy. If the opponent defects, it is beneficial to cooperate; if the opponent cooperates, it is tempting to defect. This interplay leads to a stable mixed equilibrium, where both cooperators and defectors are maintained in the population. This balance captures the realistic dynamics often observed in nature, where pure cooperation or pure defection are rarely stable over evolutionary timescales.

The SD game has been instrumental in explaining the coexistence of strategies in microbial communities, such as the production of public goods like siderophores in bacteria. Cooperators bear the cost of production, but all individuals benefit, creating a scenario where defectors can exploit cooperators. However, cooperators can persist because, when rare, they reap higher payoffs than common defectors. This dynamic is mirrored in social animals, where cooperation may be conditionally adopted depending on group structure, social reputation, or environmental factors. In evolutionary theory, the SD game has illuminated the mechanisms by which conditional cooperation emerges in diverse taxa, from bacteria and plants to vertebrates and even humans, emphasizing the context-dependent nature of social behaviors.

Beyond its explanatory power in single-game settings, the SD game provides a foundation for understanding the interplay of multiple strategic contexts, where individuals do not face a single type of dilemma, but instead encounter a mix of cooperative and competitive situations throughout their lives.

2.2.3 From payoff matrices to replicator dynamics

The payoff matrices of the PD and SD games provide the essential foundation for modeling evolutionary interactions among individuals in a population. To connect these strategic interactions to population-level outcomes, we utilize the replicator equation, a fundamental concept in evolutionary game theory that describes how strategies evolve based on their relative payoffs.

In a well-mixed population where x_C and x_D denote the frequencies of cooperators and defectors, respectively (with $x_C + x_D = 1$), the average payoffs Π_C and Π_D for each strategy are determined directly from the payoff matrix of the selected game (either PD or SD). The replicator equations governing the dynamics of these strategies are given by:

$$\dot{x}_C = x_C(\Pi_C - \bar{\Pi}), \quad \dot{x}_D = x_D(\Pi_D - \bar{\Pi}),$$

where the average payoff in the population is:

$$\bar{\Pi} = x_C\Pi_C + x_D\Pi_D.$$

These equations formalize the principle that strategies performing better than the average increase in frequency over time, while less successful strategies decline.

2.2.4 Linking game matrices to dynamics

To compute Π_C and Π_D, we use the payoff matrices from the PD or SD games, for example, in the PD game. If both players cooperate, they each receive the reward R, whereas if both defect, they each receive the punishment P. If one cooperates and the other defects, the defector receives the temptation payoff T and the cooperator gets the sucker's payoff S.

Therefore, the average payoffs in a population with fractions x_C and x_D are:

$$\Pi_C = Rx_C + Sx_D,$$

$$\Pi_D = Tx_C + Px_D.$$

Similarly, in the SD game, the payoffs follow the ranking $T > R > S > P$, but with different strategic implications that influence the population dynamics.

The replicator equation can also accommodate scenarios where individuals may face different games at different times (i.e., multi-games) or where mutation allows for occasional strategy switching. These extensions are crucial for capturing the richness of real-world interactions and will be introduced in subsequent sections.

2.2.5 Cooperation in eco-evolutionary systems

The evolution and maintenance of cooperation represent one of the most profound and enduring puzzles in both biological and social sciences. In the traditional Darwinian sense, natural selection favors individuals that maximize their own fitness. Cooperative behavior, which often involves a cost to the actor and a benefit to

others, seems paradoxical under this framework. Nevertheless, cooperation is ubiquitous in nature, from the coordinated behavior of microbial colonies to complex social institutions among humans. Understanding the mechanisms that allow cooperation to evolve and persist has thus become a central question in evolutionary theory, ecology, sociology, and even economics.

In eco-evolutionary systems, cooperation is not static—it evolves under dynamic feedback between ecological conditions and evolutionary pressures. Unlike classical models, which isolate ecological or evolutionary processes, eco-evolutionary models recognize that the environment can influence evolutionary outcomes, while evolving traits can, in turn, modify the environment. This reciprocal relationship is particularly important in systems where cooperation affects not only direct payoffs but also resource distribution, population structure, and ecosystem stability.

Biologically, cooperation has been observed in various forms:

- **Microbial cooperation**: In bacterial communities, individual cells secrete enzymes or siderophores that scavenge essential nutrients (like iron) for the group at a personal cost. These substances act as public goods, enhancing collective survival. However, cheater strains that don't produce siderophores can exploit the benefits without contributing, creating a classic public goods dilemma. Recent experimental work highlights how siderophore-mediated iron partitioning fosters dynamic coexistence between cooperators and cheaters across spatially structured environments [74]. This empirical evidence aligns closely with evolutionary game theoretical models and underscores the importance of incorporating ecological feedback and spatial context in cooperation studies.

- **Animal cooperation**: In animal societies, cooperation manifests in behaviors such as sentinel duty in meerkats, coordinated hunting by wolves or orcas, and alloparenting in elephants and some bird species. These behaviors impose immediate costs on individuals but provide long-term benefits through increased inclusive fitness, either by helping relatives or establishing reciprocal social contracts. Evolutionary game theory, rooted in Maynard Smith, and Price's framework, effectively models these behaviors, suggesting that reciprocity and kin selection strategies evolved to support cooperation despite short-term costs [75]. Such models have been invaluable in quantifying the balance between costs, benefits, and social structure influencing animal cooperative behaviors.

- **Human cooperation**: Human cooperation underpins the success of families, institutions, and societies, relying on mechanisms like reputation, punishment, and institutional design to stabilize collective action in the face of free-riders. A recent experimental study using repeated public goods games with real participants demonstrated that integrating punishment incentives and heterogeneous contributions (reflecting reputation effects) significantly enhances cooperation levels [76]. These findings parallel theoretical work showing how reputation- and punishment-based mechanisms can offset defection in repeated strategic interactions, highlighting the power of social norms in fostering cooperation.

From an ecological perspective, cooperation can impact the availability of shared resources, affect competition dynamics, and enhance group survival under adverse conditions. For instance, plants may share nutrients via mycorrhizal networks; coral reefs depend on mutualistic relationships between coral and algae; and ecosystems often contain keystone species whose cooperative roles sustain community structure.

In this thesis, cooperation is modeled using the formalism of evolutionary game theory, with special attention given to the Prisoner's dilemma and the Snowdrift games, which typify the strategic conflict between self-interest and collective benefit. The models developed herein go beyond static strategic settings by incorporating mechanisms such as:

- **Multigames**: In real-world settings, individuals may encounter varying social dilemmas (e.g., PD or SD), which we model by allowing players to randomly experience different payoff matrices. Recent work using structured-population models with stochastic game assignments supports how multigame heterogeneity can stabilize cooperation [77].

- **Mutation**: To capture behavioral errors or experimentation, our model includes spontaneous strategy mutations. This mechanism builds on findings by Roy et al. (2022), showing that mutation coupled with ecological dynamics can stabilize cooperation [64].

- **Ecological feedback**: Payoffs are modulated by ecological variables such as population density or free space, linking reproductive success to environmental context. A 2024 analysis confirmed that incorporating density-dependent ecological feedback yields qualitatively different cooperation equilibria in evolutionary games [78].

- **Time delay**: Recognizing that biological and social processes often have delayed effects, we include lagged strategy updating and feedback mechanisms. Recent work on dynamic public goods games demonstrated that introducing temporal delays can generate richer dynamics, such as oscillations and stability switches [79].

- **Structured populations and diffusion**: Individuals are embedded in limited networks or spatial environments, and we allow for movement across these structures. This mirrors the recent advances in structured-feedback coevolutionary models, showing how spatially embedded networks alter eco-evolutionary outcomes compared to well-mixed systems.

These modeling tools allow us to study cooperation as a dynamic process influenced by both individual-level interactions and system-level constraints. One of the core findings, supported by simulations and analytical results across the four papers included in this thesis, is that cooperation can emerge and be sustained not despite, but because of, eco-evolutionary feedbacks. In particular, the inclusion of ecological variables such as free space and dynamic environmental conditions reveals novel pathways through which cooperation is favored—especially when traditional game-theoretic predictions would suggest its collapse.

Thus, the eco-evolutionary approach offers a unifying lens through which to study cooperation: not as a fragile exception to self-interest, but as a robust and adaptive outcome of complex interactions between strategy, structure, and environment. This framework will be systematically explored in the chapters that follow, each focusing on specific extensions and applications of evolutionary game dynamics to cooperative behavior in evolving ecological landscapes. In real-world ecosystems and social systems, individuals rarely face a single, consistent type of social dilemma. Instead, their interactions are shaped by multiple, context-dependent factors that introduce heterogeneity into their strategic environments. This diversity is effectively captured by the concept of *multigames*, an extension of classical evolutionary game theory that allows individuals to probabilistically engage in different games during each encounter.

2.3 Multigames and social heterogeneity

In this thesis, we primarily consider multi-games involving the PD and SD, two canonical games that represent distinct types of social dilemmas [59]. Let p denote the probability that an individual plays the PD game and $(1-p)$ the probability of playing the SD game in a given interaction. The effective payoff π for an individual is then given by

$$\pi = p\pi_{\mathrm{PD}} + (1-p)\pi_{\mathrm{SD}}.$$

This probabilistic mixing captures the heterogeneity in individual perceptions and environmental contexts. Such models reflect real biological systems, where fluctuating conditions—such as resource abundance, predation pressure, or habitat heterogeneity—can shift the relative costs and benefits of cooperative behaviors, effectively altering the underlying game being played. For example, in microbial systems, stress-induced environments can transform interactions from cooperative (e.g., public goods sharing) to competitive (e.g., toxin production). Similarly, in social mammals, group composition, kin structure, and territory defense can influence whether cooperation or defection is favored in a given scenario [80].

Multi-game frameworks thus provide a powerful lens to understand the persistence of cooperation under social heterogeneity. They reveal that populations can sustain mixed strategies under a broader range of conditions than predicted by single-game models, offering insight into why cooperation is so widespread in nature [81]. For instance, in bird societies, feeding interactions may resemble a Snowdrift Game when resources are abundant but shift towards a Prisoner's Dilemma under scarcity or conflict.

Importantly, multi-games are particularly relevant for studying eco-evolutionary dynamics because they integrate seamlessly with ecological feedback. By allowing the probability of playing a particular game to be influenced by environmental conditions, such as population density, predation risk, or spatial structure, multigames can capture feedback loops where ecology shapes strategy and strategy, in turn, influences ecology. For example, increased predation risk might elevate the frequency of risk-averse (PD-like) interactions, which can then alter group cohesion, vigilance

behavior, and even the structure of community interactions.

Incorporating multigames into our models enables the exploration of how behavioral heterogeneity interacts with key ecological factors. When combined with mechanisms like mutation (introducing stochastic strategy shifts) and time delays (reflecting generational or behavioral lags), multigames produce rich dynamics, including oscillations, bistability, and even chaotic regimes. These complex dynamics can reveal conditions under which cooperation persists, collapses, or re-emerges depending on the interplay between game frequencies and ecological feedbacks.

Overall, integrating multigames into eco-evolutionary frameworks offers a more realistic and nuanced approach to understanding the emergence and maintenance of cooperation in complex systems. It highlights the importance of considering not only the strategic decisions of individuals but also the broader ecological and social contexts that shape those decisions over time.

2.4 Mutation and strategy switching

In both natural and artificial systems, individuals are not perfectly rational or genetically fixed in their strategies. Errors, learning, exploration, and genetic mutations introduce variability in behavior, allowing for occasional strategy switching. This process is modeled using a fixed, symmetric mutation rate μ, which allows cooperators to become defectors and vice versa, regardless of their immediate fitness.

Mathematically, the replicator-mutator dynamics can be expressed as:

$$\dot{x}_C = x_C(f_C - \bar{f}) + \mu(x_D - x_C),$$

$$\dot{x}_D = x_D(f_D - \bar{f}) + \mu(x_C - x_D).$$

These equations incorporate the idea that while selection favors strategies with higher payoffs, random switching maintains strategic diversity within the population. Mutation plays a crucial role in preventing fixation to suboptimal strategies, enabling the reintroduction of cooperative behaviors even in predominantly defective populations.

Biologically, mutation encapsulates a range of real-world phenomena. In microbial populations, gene regulation, horizontal gene transfer, and stochastic gene expression can produce phenotypic switching between cooperative and competitive states [82, 83]. For example, bacteria can switch between producing public goods like siderophores (cooperative) and non-producing phenotypes (defective) depending on local conditions and mutations. In animal behavior, learning errors, exploration, and cultural transmission can lead individuals to shift strategies, even in the absence of direct fitness advantages [84]. In human societies, social learning, experimentation, and imitation similarly generate strategic variability, contributing to the dynamic evolution of cooperation and defection norms [48, 85].

From a theoretical perspective, mutation serves several crucial roles in eco-evolutionary systems. First, it prevents the population from becoming trapped in suboptimal equilibria by reintroducing rare or previously outcompeted strategies,

thereby promoting long-term coexistence and resilience [86]. Second, it enables populations to respond to fluctuating environments by maintaining a flexible strategic pool, which is essential for adapting to changing ecological contexts [87]. Third, mutation contributes to the maintenance of biodiversity by balancing selection pressures and preventing the dominance of a single strategy, especially in systems characterized by frequency-dependent selection, such as the rock-paper-scissors game.

By incorporating mutation into our models, we bridge the gap between purely deterministic dynamics and the stochastic realities of natural and social systems. This approach enhances the realism of eco-evolutionary models by capturing the inherent uncertainty and adaptability observed in living systems, providing insights into how cooperation can persist and re-emerge even in the face of defection-dominated dynamics.

2.5 Ecological feedback and free space

Traditional game-theoretic models often neglect the ecological context in which interactions occur. However, in eco-evolutionary systems, the environment itself is a dynamic player, influencing and being influenced by strategic behaviors. In our models, we introduce an ecological variable called *free space*, denoted by $z = 1-x-y$, representing unoccupied or available resources in the system.

Reproductive success is not solely determined by payoffs from social interactions but also by the availability of free space. Each strategy's effective fitness is thus modulated by:

$$f_i = \sigma_i \cdot \Pi_i \cdot z,$$

where σ_i reflects the ecological contribution of strategy i (e.g., cooperators may benefit more from free space than defectors due to synergistic interactions). Free space behaves as an altruistic, non-strategic ecological variable, donating reproductive opportunities to all players without receiving direct feedback. This concept aligns with empirical observations where unclaimed resources (e.g., habitat patches, breeding sites) enable population growth and facilitate the spread of cooperative traits.

Examples include forest gaps that enable the establishment of new seedlings, open microbial niches that allow colonization, and social systems where demographic turnover provides opportunities for strategy renewal. Incorporating free space in our models captures the dynamic interplay between ecological opportunities and evolutionary processes, highlighting how environmental constraints shape the evolutionary viability of cooperation.

2.6 Time-delayed feedback

In many biological and social systems, the impact of strategic interactions on reproductive success is not instantaneous. Gestation periods, resource regeneration times, and social learning processes can introduce delays between the cause (e.g.,

an individual's behavior) and its ecological or evolutionary effect (e.g., changes in population density or payoff structures).

To capture these processes, our models incorporate *time-delayed feedback*, where the reproduction rate at time t depends on the payoffs experienced at an earlier time $t - \tau$, with τ representing the delay. The delayed replicator dynamics can be expressed as:

$$\dot{x}(t) = x(t) \left[f_C(x(t-\tau), y(t-\tau)) - \bar{f}(t-\tau) \right].$$

Time delays can profoundly affect the dynamics of eco-evolutionary systems. They can stabilize otherwise unstable equilibria, induce sustained oscillations, or even lead to chaotic dynamics, depending on parameter values and feedback strengths. In ecological contexts, such delays are evident in predator-prey cycles, host-parasite dynamics, and cooperative breeding systems where helper contributions affect reproductive success with a temporal lag.

Our models demonstrate that time delays in eco-evolutionary feedback can sustain cooperation through dynamic mechanisms, even when static analysis would predict its extinction. This insight is particularly relevant for conservation strategies and management of social-ecological systems.

2.7 Strategic species and multi-species systems

In complex ecosystems, species often interact not only with conspecifics but also with individuals from other species. These interactions can be competitive, mutualistic, or exploitative, and each species may adopt different strategies that co-evolve with the strategies of others. To model such systems, we extend the replicator framework to include multiple species, each with its own strategic and ecological parameters.

Let x_i denote the density of a strategy in species i, with fitness $f_i(x, y, z, \ldots)$ depending on the densities of all interacting species. The multi-species replicator dynamics are given by:

$$\dot{x}_i = x_i \left[f_i(x, y, z, \ldots) - \bar{f} \right].$$

This formulation allows us to model cross-species interactions where, for example, the cooperative behavior of one species can enhance the ecological opportunities for another, creating positive feedback loops. Conversely, defection or exploitation in one species can reduce the resources or habitat availability for others, potentially leading to cascading extinctions or shifts in community structure.

Empirical examples abound: pollinators and flowering plants engage in mutualistic interactions that affect each other's population dynamics; predators can influence prey evolution, which in turn shapes the predator's own ecological niche; and human-induced changes, such as habitat fragmentation, can differentially affect species with different life-history strategies.

In this thesis, the inclusion of strategic species interactions enriches the modeling of eco-evolutionary dynamics, highlighting the interconnectedness of ecological communities and the role of strategy evolution in shaping biodiversity.

2.8 Cyclic dominance: Rock-Paper-Scissors

A special and fascinating case of evolutionary dynamics arises in systems of cyclic dominance, often modeled using the Rock-Paper-Scissors (RPS) game. Here, each strategy defeats one and is defeated by another, forming a closed loop:

$$A \to B \to C \to A.$$

The dynamics of such systems are governed by:

$$\dot{x}_i = x_i(f_i - \bar{f}), \quad f_i = \sum_j a_{ij} x_j,$$

where a_{ij} represents the payoff of strategy i against strategy j. Cyclic dominance is prevalent in many biological systems: microbial communities where antibiotic production and resistance form feedback loops; mating systems in lizards where different male strategies cyclically dominate; and even in social systems where competing norms or ideologies vie for dominance.

These systems can exhibit a rich variety of dynamical behaviors, including stable coexistence of all strategies, limit cycles, or heteroclinic orbits where the system cycles between near-extinction states of each strategy. Such dynamics highlight the importance of nonlinear interactions in maintaining biodiversity and the emergence of complex ecological patterns.

In the context of this thesis, RPS dynamics provide a natural extension of the eco-evolutionary framework, illustrating how strategic interactions can generate persistent oscillations and stabilize diversity through dynamic feedbacks. By coupling cyclic dominance with ecological variables and time delays, we reveal new mechanisms through which cooperative and competitive behaviors shape the structure and function of ecological communities.

2.9 Spreading phenomena and social dilemmas in evolutionary game theory

In addition to biological and ecological contexts, evolutionary game theory has found profound applications in understanding the dynamics of social systems, particularly in modeling the spread of behaviors, beliefs, and information. Phenomena such as epidemic outbreaks, rumor diffusion, opinion formation, and technology adoption all involve individuals making decisions that affect both their own well-being and that of the broader population. These decisions often entail social dilemmas, where individual incentives conflict with collective welfare—making them natural candidates for evolutionary game-theoretic modeling.

At the heart of such models lies the conflict between spreading and suppression, which can be framed using classical strategy pairs like spreaders vs. ignorants, informed vs. uninformed, or infected vs. susceptible. These behavioral roles resemble the classic game-theoretic structure of cooperators and defectors, especially when viewed through the lens of information as a public good or a social burden.

2.9.1 Basic spreading model and strategic interpretation

Let us consider a simplified setting where individuals adopt one of two strategies:

- **S**: Spreader (e.g., someone who shares information or a rumor)
- **R**: Refrainer (someone who does not spread or counters misinformation)

In a well-mixed population, the densities of spreaders and refrainers at time t are denoted by $x_S(t)$ and $x_R(t)$, respectively. Assuming no births or deaths, the total population remains conserved:

$$x_S + x_R = 1.$$

A basic payoff structure, capturing the benefit of virality and the cost of being misinformed or ignored, can be expressed through a 2×2 payoff matrix:

$$\begin{bmatrix} R & S \\ T & P \end{bmatrix}, \quad \text{where } T > R > P > S,$$

similar to the structure of the Prisoner's Dilemma. Here, a spreader gains a higher payoff when interacting with a refrainer (temptation T), while mutual spreading or refraining may result in lower gains due to saturation or redundancy.

The evolution of strategy frequencies over time can be described using the replicator equation:

$$\dot{x_i} = x_i(f_i - \bar{f}),$$

where f_i is the fitness (or effective payoff) of strategy $i \in \{S, R\}$, and $\bar{f}$ is the average payoff of the population. The payoffs f_i are computed as:

$$f_i = \sum_j a_{ij} x_j,$$

with a_{ij} denoting the entry in the payoff matrix when strategy i meets strategy j.

In this framework, one can study the spread of behavior like rumor or misinformation as an evolutionary competition between spreading and refraining behaviors, especially when combined with environmental or network factors.

2.9.2 Link with social dilemma

In many cases, the decision to refrain from spreading a harmful message (such as a rumor or fake news) is altruistic, offering a benefit to the community while possibly imposing a personal cost (e.g., social exclusion or reduced attention). Thus, refrainers can be viewed as cooperators, while spreaders resemble defectors who exploit attention dynamics. This situates the spreading dynamics within a social dilemma structure.

Moreover, introducing additional strategies—such as informed spreaders, skeptics, or fact checkers- can expand the system into richer game-theoretic classes, such as public goods games,the volunteer's dilemma of volunteers, or cyclic dominance systems, depending on the payoffs and strategic transitions.

2.9.3 Relevance to real-world phenomena

Evolutionary models of rumor and epidemic spreading offer valuable insights into:

- **Behavioral response to pandemics** (e.g., mask-wearing, vaccine uptake)
- **Misinformation dynamics on networks** (e.g., Twitter, Facebook)
- **Adoption of social norms and practices**
- **Cultural and ideological competition**

These applications highlight the universality of evolutionary game theory in modeling a wide class of spatially extended, socially informed, and temporally dynamic phenomena.

The concept of strategic species, introduced in earlier chapters in the context of ecological interactions, can be translated into social settings by interpreting strategies such as spreading or refraining as traits competing for dominance. By leveraging the eco-evolutionary modeling framework—where strategies evolve under ecological constraints and social incentives—one can analyze the conditions under which harmful behaviors are suppressed or proliferate. In this way, rumor spreading dynamics become a compelling social analogue of predator-prey or parasite-host systems, driven by similar mathematical and conceptual tools.

Chapter 3

The eco-evolutionary muti-game framework with the presence and absence of ecological free space and the ability to mutation †

The persistence of biodiversity and the emergence of cooperation among species have long intrigued researchers, particularly given the competitive advantages often enjoyed by defectors. Darwinian evolution [2] challenges the spontaneous rise of cooperation, as cooperative behavior typically incurs costs while providing benefits to others [54]. Defectors, by exploiting these investments, undermine the stability of cooperation. This paradox raises a fundamental question: If natural selection favors the fittest, why does cooperation persist across diverse biological and social systems?

To address this question, this chapter adopts an evolutionary game-theoretic framework using a 2×2 payoff matrix, a robust method for analyzing rational decision-making in competitive environments [88]. Evolutionary game theory has proven invaluable for understanding the mechanisms sustaining cooperation [89, 61, 34], leading to key theoretical and empirical advances [90–92, 55, 93, 94, 48, 95].

This chapter constructs a mathematical model of evolutionary multigames [81, 59, 96–106], extending classical frameworks by integrating two fundamental games: the prisoner's dilemma [107] and the snowdrift game [108, 109]. This combination reflects the reality that individuals rarely encounter uniform strategic scenarios; rather, they navigate heterogeneous social landscapes. The multigame framework allows individuals to engage in different games probabilistically, capturing the diversity of strategic contexts encountered in real systems [58].

In the PD, defection dominates, leading to the erosion of cooperation. In contrast, the SD allows cooperators and defectors to coexist, as optimal strategies depend on opponents' choices. Probabilistic game selection introduces behavioral diversity into the system. This chapter also includes mutation, modeling the ca-

†A considerable part of this chapter has been published in **Plos One**, Volume 17, Page 08, Article ID: Roy, S., Nag Chowdhury, S., Mali, P.C., Perc, M. and Ghosh, D., 2022. Eco-evolutionary dynamics of multigames with mutations. PLoS one, 17(8), p.e0272719.

pacity of individuals to switch strategies over time [110, 111, 86, 112–117, 87, 118]. This captures real-world phenomena such as genetic mutations, learning errors, or behavioral flexibility, essential for maintaining strategic diversity.

Beyond strategic interactions, ecological constraints are introduced via free space—a key ecological variable affecting population dynamics and collective behavior [119–125]. Here, an individual's birth rate depends on both its average payoff and the availability of free space, which provides reproductive opportunities. Free space also acts altruistically, benefiting all individuals without direct compensation. This concept reflects real-world situations where resources like habitat or nutrients shape survival and competition, as seen in microbial communities [126] and animal populations [127].

This ecological dimension aligns with empirical observations of altruism, from eusocial insects to cooperative vertebrates and human societies, highlighting how shared resources shape evolutionary trajectories. By integrating free space, this chapter bridges ecological and evolutionary perspectives, enriching the multigame framework.

Unlike conventional models assuming rapid ecological processes relative to evolution [128], this chapter explicitly examines ecological and evolutionary dynamics on comparable timescales. This allows an exploration of how ecological factors, game-theoretic interactions, and mutation collectively shape population stability. Earlier studies by Nag Chowdhury et al. [91, 59] examined eco-evolutionary dynamics using punishment as a supporting mechanism for cooperation. However, this chapter demonstrates that cooperation can persist even without such enforcement mechanisms. Moreover, it innovates by linking birth rates not only to payoffs but also to shared ecological factors.

The remainder of this chapter is structured as follows: Section (3.1) details the model's formulation, underlying assumptions, and key variables. Section (3.2) explores the theoretical properties—including existence, uniqueness, and boundedness—and presents extensive numerical simulations and discussions.

3.1 Mathematical model

To start with, we consider a simplistic assumption that each individual has two distinct choices, viz. (i) cooperation (**C**) and (ii) defection (**D**). Even they can play any of the two possible games (a) PD game and (b) SD game. They can adopt the PD game with probability p, and alternatively, they interact with other individuals by playing the SD game with the complimentary probability $(1-p)$. Both of these two-person games can be given by the following two payoff matrices A and B respectively, where

$$A = \begin{array}{c} \\ \mathbf{C} \\ \mathbf{D} \end{array} \begin{array}{c} \begin{array}{cc} \mathbf{C} & \mathbf{D} \end{array} \\ \begin{pmatrix} R_{PD} & S_{PD} \\ T_{PD} & P_{PD} \end{pmatrix} \end{array} \text{and } B = \begin{array}{c} \\ \mathbf{C} \\ \mathbf{D} \end{array} \begin{array}{c} \begin{array}{cc} \mathbf{C} & \mathbf{D} \end{array} \\ \begin{pmatrix} R_{SD} & S_{SD} \\ T_{SD} & P_{SD} \end{pmatrix} \end{array},$$

in which the entries portray the payoff accumulated by the players in the left.

Here, R_{PD} and R_{SD} contemplate the reward for mutual cooperation among two players in the respective PD and SD games. Similarly, both unrelated players receive the punishment P_{PD} and P_{SD} for mutual defection in the games PD and SD, respectively. An exploited cooperator gains the sucker's payoff S_{PD} and S_{SD}, respectively in the PD and SD games when confronted by a defector. The mixed choice yields the defector temptations T_{PD} and T_{SD} to exploit a cooperator in the PD and SD games, respectively. The payoff ranking of these four-game parameters determines the two-person games. The conventional relative ordering for the PD game is $T_{PD} > R_{PD} > P_{PD} > S_{PD}$ [91, 59, 58] and $2R_{PD} > S_{PD} + T_{PD}$ [129]. Without loss of any generality, we choose $T_{PD} = \beta > 1$, $R_{PD} = 1$, $P_{PD} = \eta \in (0, 1)$, and $S_{PD} = 0$. Similarly, we choose $T_{SD} = \beta > 1$, $R_{SD} = 1$, $S_{SD} = 0$, and $P_{SD} = -\eta \in (-1, 0)$, maintaining the relative ordering $T_{SD} > R_{SD} > S_{SD} > P_{SD}$ for the standard SD game [91, 59, 58]. Thus, the payoff matrices A and B become

$$A = \begin{array}{c} \\ \mathbf{C} \\ \mathbf{D} \end{array} \begin{array}{c} \begin{array}{cc} \mathbf{C} & \mathbf{D} \end{array} \\ \begin{pmatrix} 1 & 0 \\ \beta & \eta \end{pmatrix} \end{array} \text{and } B = \begin{array}{c} \\ \mathbf{C} \\ \mathbf{D} \end{array} \begin{array}{c} \begin{array}{cc} \mathbf{C} & \mathbf{D} \end{array} \\ \begin{pmatrix} 1 & 0 \\ \beta & -\eta \end{pmatrix} \end{array}.$$

Note that, in both of these games, mutual cooperation leads to the payoff R_{PD} and R_{SD}, which is relatively higher than P_{PD} and P_{SD}, which one defector receives when playing with a defector. Thus, cooperation always promises higher income than defection if both the rational players choose the same strategy. The difference between these two games' relative ordering leads to a contrasting scenario. In the SD game, the interaction between the cooperator and defector always promises a better income in terms of payoff than the interaction between two defectors. A reverse reflection is observed in the case of the PD game thanks to the choice of such relative ranking of game parameters in the PD game. The interaction between two defectors in the PD game allows them to earn more than a cooperator encountering a defector. The switching between P and S in the relative ordering of both games thus produces noticeable unexpected consequences on the evolution of cooperation.

Since a player can decide which game they want to play, thus the final payoff matrix for the multigame looks like

$$E = pA + (1-p)B = \begin{array}{c} \\ \mathbf{C} \\ \mathbf{D} \end{array} \begin{array}{c} \begin{array}{cc} \mathbf{C} & \mathbf{D} \end{array} \\ \begin{pmatrix} 1 & 0 \\ \beta & (2p-1)\eta \end{pmatrix} \end{array}.$$

Here, $p \in [0, 1]$ is the probability of playing the PD game. Moreover, we consider free space $\mathbf{F}$ as an ecological variable, which contributes altruistically by helping others. Nevertheless, free space does not get any benefits by giving them reproductive opportunities. We incorporate this charitable role of free space by extending the 2×2 payoff matrix E to the 3×3 payoff matrix G as follows

$$G = \begin{array}{c} \\ \mathbf{C} \\ \mathbf{D} \\ \mathbf{F} \end{array} \begin{array}{c} \begin{array}{ccc} \mathbf{C} & \mathbf{D} & \mathbf{F} \end{array} \\ \begin{pmatrix} 1 & 0 & \sigma_1 \\ \beta & (2p-1)\eta & \sigma_2 \\ 0 & 0 & 0 \end{pmatrix} \end{array}.$$

The matrix G clearly reveals that the free space never earns any payoff for their selfless charitable act; however, it contributes a positive payoff σ_1 and σ_2 to the cooperators and the defectors, respectively. Since most of the game parameters (not all) lies within the closed interval $[0, 1]$, we assume, for the sake of feasible comparison, σ_1 and σ_2 both lies within the interval $[0, 1]$. When σ_1 and σ_2 are equal to zero, free space will not contribute anything to anyone. However, whenever σ_1 and σ_2 attain positive values, individuals gain an additional payoff from free space.

Inspired by the Malthusianism, we consider the following set of differential equations governing the changes in frequencies of cooperators and defectors as a function of time t

$$\begin{aligned} \dot{x} &= x\left[b_{\mathbf{C}} - d_{\mathbf{C}}\right], \\ \dot{y} &= y\left[b_{\mathbf{D}} - d_{\mathbf{D}}\right], \end{aligned} \tag{3.1}$$

where

$$\begin{cases} b_{\mathbf{C}} = \text{birth rate of cooperators}, \\ b_{\mathbf{D}} = \text{birth rate of defectors}, \\ d_{\mathbf{C}} = \text{death rate of cooperators}, \quad \text{and} \\ d_{\mathbf{D}} = \text{death rate of defectors}. \end{cases}$$

Here, x and y are the normalized densities of cooperators and defectors, respectively. Let z be the available free space. Thus, we have

$$x + y + z = 1. \tag{3.2}$$

Relation (3.2) assures that by studying x and y alone, one can easily capture the dynamics of the two strategies. We assume the birth rates of each individual depends crucially on the available free space as well as on their respective average fitnesses. Thus, we consider

$$\begin{aligned} b_{\mathbf{C}} &= z f_{\mathbf{C}} = (1 - x - y) f_{\mathbf{C}}, \\ b_{\mathbf{D}} &= z f_{\mathbf{D}} = (1 - x - y) f_{\mathbf{D}}, \end{aligned} \tag{3.3}$$

where $f_{\mathbf{C}}$ and $f_{\mathbf{D}}$ are average fitness of the cooperators and the defectors, respectively. The average payoff of cooperators and defectors can be determined using the payoff matrix G of the multigame, and the relation (3.2) as follows,

$$\begin{aligned} f_{\mathbf{C}} &= x.1 + y.0 + z.\sigma_1 = (1 - \sigma_1)x - \sigma_1 y + \sigma_1, \\ f_{\mathbf{D}} &= x.\beta + y.(2p-1)\eta + z.\sigma_2 \\ &= (\beta - \sigma_2)x + [(2p-1)\eta - \sigma_2]y + \sigma_2. \end{aligned} \tag{3.4}$$

Note that the average fitness of free space is

$$f_{\mathbf{F}} = x.0 + y.0 + z.0 = 0. \tag{3.5}$$

Table 3.1: Parameters with their physical significances and domains

Parameters	**Physical Significance**	**Domain**
ξ	Death Rate	$(0, 1]$
β	The gain of a defector while interacting with a cooperator	$(1, 2)$
η	The payoff for mutual defection	$(0, 1)$
p	Probability of playing the PD game	$[0, 1]$
μ	Mutation probability	$[0, 1]$
σ_1	The altruistic incentive of free space towards the cooperators	$[0, 1]$
σ_2	The altruistic incentive of free space towards the defectors	$[0, 1]$

This is expected as free space does not gain anything for its benevolent nature. For simplicity, we further assume that all individuals die at a uniform and constant mortality rate $\xi \in (0, 1]$. Hence using the relations (3.3) and (3.4), our constructed model (3.1) transforms into

$$\begin{aligned} \dot{x} &= x\left[(1-x-y)\{(1-\sigma_1)x - \sigma_1 y + \sigma_1\} - \xi\right], \\ \dot{y} &= y[(1-x-y)\{(\beta-\sigma_2)x + ((2p-1)\eta - \sigma_2)y + \sigma_2\} - \xi]. \end{aligned} \tag{3.6}$$

Now, we introduce a constant probability μ as a rate with which each individual mutates from one strategy to the others, in a continuous manner,

$$x \underset{\mu}{\overset{\mu}{\rightleftarrows}} y. \tag{3.7}$$

Relation (3.7) reflects that the mutation probability μ from the cooperators to the defectors is identical to the mutation rate from the defectors to the cooperators. So using the system (3.6), the well-mixed population under the influence of bidirectional mutation gives rise to the differential equations

$$\begin{aligned} \dot{x} &= x\left[(1-x-y)\{(1-\sigma_1)x - \sigma_1 y + \sigma_1\} - \xi\right] + \mu(y-x), \\ \dot{y} &= y[(1-x-y)\{(\beta-\sigma_2)x + ((2p-1)\eta - \sigma_2)y + \sigma_2\} - \xi] + \mu(x-y). \end{aligned} \tag{3.8}$$

The system (3.8) contains seven different parameters. We summarize the necessary information about these parameters in Table (3.1).

3.2 Results and discussions

3.2.1 Existence, uniqueness and positive invariance

Before investigating the model (3.8) using numerical simulations, we first prove the positive invariance of the proposed system (3.8). Clearly, the functions on the right-hand side of the differential equations (3.8) are continuously differentiable and at the same time, locally Lipschitz in the first quadrant of $\mathbb{R} \times \mathbb{R}$. This ensures the existence and uniqueness of solutions for the model (3.8) with suitable initial values. Note that the initial conditions (x_0, y_0) must lie within the domain $[0,1] \times [0,1]$ maintaining the inequality $0 \leq x_0 + y_0 \leq 1$, as they represent the frequencies of the two strategies. To determine the positivity of the proposed model (3.8), we write the system as follows,

$$\begin{aligned} \dot{x} &= x\psi_1, \\ \dot{y} &= y\psi_2, \end{aligned} \tag{3.9}$$

where $\psi_1 = b_{\mathbf{C}} - d_{\mathbf{C}} - \mu + \dfrac{\mu y}{x}$ and $\psi_2 = b_{\mathbf{D}} - d_{\mathbf{D}} - \mu + \dfrac{\mu x}{y}$ are two integrable functions in the Riemannian sense. Solving equations (3.9), we get

$$\begin{aligned} x &= c_1 \exp(\textstyle\int \psi_1 dt), \\ y &= c_2 \exp(\textstyle\int \psi_2 dt), \end{aligned} \tag{3.10}$$

where c_1 and c_2 are the integrating constants depending on the initial densities x_0 and y_0. This proves that both x and y are non-negative. Now, to calculate the upper bound of $x + y$, we proceed as follows. The dynamical equations (3.8) yield

$$\frac{d}{dt}(x+y) = (1-x-y)[xf_{\mathbf{C}} + yf_{\mathbf{D}}] - \xi(x+y). \tag{3.11}$$

Since as per our previous analysis, $x + y \geq 0$ and the mortality rate ξ is always positive, we have $\xi(x + y) \geq 0$. Thus, (3.11) reduces to

$$\frac{d}{dt}(x+y) \leq (1-x-y)[xf_{\mathbf{C}} + yf_{\mathbf{D}}]. \tag{3.12}$$

Integrating both sides, we get

$$(x+y) \leq 1 - c_3 \exp\big[-\textstyle\int [xf_{\mathbf{C}} + yf_{\mathbf{D}}]dt\big] \leq 1, \tag{3.13}$$

where c_3 is the initial density dependent constant. Hence, we find that

$$0 \leq x + y \leq 1, \tag{3.14}$$

i.e., the overall species density $x + y$ eventually remains bounded within the region $[0, 1]$. This boundedness within the closed interval $[0, 1]$ allows us to relate the possible emerging dynamics of the system (3.8) to physically implementable scenarios with biological relevance. When the sum of the population density $(x+y)$ is precisely one, the available free space is zero, as $z = 1 - (x + y)$. i.e., there is no reproductive opportunity accessible to any individual in that situation with $z = 0$. When $(x+y) = 0$, then individually $x = 0$ and $y = 0$. Hence, all individuals die, and

z is equal to one. Thus despite the presence of ample free space, all the individuals are extinct under that circumstances.

3.2.2 Coexistence of different stationary points depending on the initial conditions

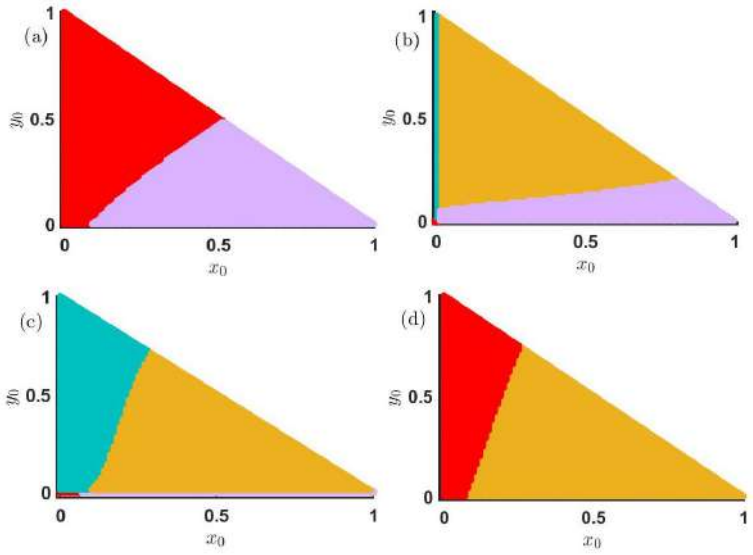

Figure 3.1: **Alternations between multiple co-existing steady states depending on initial conditions**: The coexistence of various stable states is portrayed here by varying the initial conditions, maintaining $0 \leq (x_0 + y_0) \leq 1$. Red points signify the extinction equilibrium E_0. Violet points represent the defector-free steady state E_1. The cooperator-free stationary points E_2 are shown by sea blue points, and the coexistence equilibrium E_3 is plotted using yellow points. The mutation-free model in subfigures (a-c) allows four stable steady states to coexist. However, subfigure (d) supports only bistability for the chosen parameters' values. The parameter values for each of these subfigures are (a) $\xi = 0.38$, $\beta = 1.1$, $p = 0.30$, $\sigma_1 = 0.36$, $\sigma_2 = 0.25$, and $\mu = 0$. (b) $\xi = 0.15$, $\beta = 1.06$, $p = 0.69$, $\sigma_1 = 0.75$, $\sigma_2 = 0.25$, and $\mu = 0$. (c) $\xi = 0.15$, $\beta = 1.1$, $p = 0.10$, $\sigma_1 = 0.10$, $\sigma_2 = 0.25$, and $\mu = 0$. (d) $\xi = 0.30$, $p = 0.30$, $\beta = 1.1$, $\mu = 0.02$, $\sigma_1 = 0.30$, and $\sigma_2 = 0.20$. The other parameter is $\eta = 0.85$.

Next, we point out the multistable dynamics of our model (3.8), resulting in the system's vulnerability to small perturbations. Initially, we set the parameter values at $\xi = 0.38$, $\beta = 1.1$, $\eta = 0.85$, $p = 0.30$, $\sigma_1 = 0.36$, $\sigma_2 = 0.25$ and $\mu = 0$ in Fig. 3.1 (a). We vary the initial conditions (x_0, y_0) within the interval $[0, 1] \times [0, 1]$ maintaining the inequality $(x_0 + y_0) \in [0, 1]$. We find that the dynamics switching between two stationary points, viz. $E_0 = (0, 0)$ and $E_1 = (x^*, 0)$. We analytically calculate the stationary points of the system (3.8) in the absence of the mutation, i.e., with $\mu = 0$. We trace out four different stationary points,

1. $E_0 = (0, 0)$ reveals all individuals die. This point is locally stable when

$$\begin{cases} \sigma_1 < \xi, & \text{and} \\ \sigma_2 < \xi. \end{cases}$$

2. $E_1 = (x^*, 0)$ exhibits a society free from any defectors. Here,

$$x^* = \frac{(1 - 2\sigma_1) \pm \sqrt{(1 - 2\sigma_1)^2 - 4(\xi - \sigma_1)(1 - \sigma_1)}}{2(1 - \sigma_1)},$$

and $x^* \in (0, 1]$. The stability criteria is given by

$$\begin{cases} \xi > (1 - \sigma_1)(2x^* - 3x^{*2}) + \sigma_1(1 - 2x^*) & \text{and} \\ \xi > (\beta - \sigma_2)(x^* - x^{*2}) + \sigma_2(1 - x^*). \end{cases}$$

3. $E_2 = (0, y^*)$ represents that we have only left with defectors. Here, $y^* = \frac{(2p\eta - \eta - 2\sigma_2)}{2(2p\eta - \eta - \sigma_2)} \pm \frac{\sqrt{(2p\eta - \eta - 2\sigma_2)^2 - 4(2p\eta - \eta - \sigma_2)(\xi - \sigma_2)}}{2(2p\eta - \eta - \sigma_2)}$, and $y^* \in (0, 1]$. This stationary state is stable if

$$\begin{cases} \xi > \sigma_1(1 - y^*) - \sigma_1(y^* - y^{*2}) & \text{and} \\ \xi > \sigma_2(1 - 2y^*) + (2p\eta - \eta - \sigma_2)(2y^* - 3y^{*2}). \end{cases}$$

4. $E_3 = (x^{**}, y^{**})$ indicates the coexistence equilibrium offering the survival of cooperation and defection simultaneously. Here, $y^{**} = \frac{(1 - \beta - \sigma_1 + \sigma_2)x^{**} + \sigma_1 - \sigma_2}{2p\eta - \eta + \sigma_1 - \sigma_2}$, and x^{**} satisfies the equation, $(1 - \sigma_1)\tau x^{**} - \sigma_1\left(\frac{(1 - \beta - \sigma_1 + \sigma_2)x^{**} + \sigma_1 - \sigma_2}{2p\eta - \eta + \sigma_1 - \sigma_2}\right)\tau + \sigma_1\tau - \xi = 0$, where, $\tau = \frac{(2p\eta - \eta + \sigma_1 - \sigma_2)(1 - x^{**}) - (1 - \beta - \sigma_1 + \sigma_2)x^{**} + \sigma_2 - \sigma_1}{(2p\eta - \eta + \sigma_1 - \sigma_2)}$. x^{**} and y^{**} both should lie within the interval $(0, 1)$. The local stability yields the conditions for the stability of (x^*, y^*) are

$$\begin{cases} 2\xi > (\beta - \sigma_2)(x^{**} - x^{**2} - 2x^{**}y^{**}) + (1 - \sigma_1)(2x^{**} - 3x^{**2} - 2x^{**}y^{**}) \\ -\sigma_1(y^{**} - y^{**2} - 2x^{**}y^{**}) + (2p\eta - \eta - \sigma_2)(2y^{**} - 3y^{**2} - 2x^{**}y^{**}) \\ +\sigma_1(1 - 2x^{**} - y^{**}) + \sigma_2(1 - 2y^{**} - x^{**}), \quad \text{and} \\ [(\beta - \sigma_2)(x^{**} - x^{**2} - 2x^{**}y^{**}) + (2p\eta - \eta - \sigma_2)(2y^{**} - 3y^{**2} - 2x^{**}y^{**}) \\ +\sigma_2(1 - x^{**} - 2y^{**}) - \xi][(1 - \sigma_1)(2x^{**} - 3x^{**2} - 2x^{**}y^{**}) \\ -\sigma_1(y^{**} - y^{**2} - 2x^{**}y^{**}) + \sigma_1(1 - 2x^{**} - y^{**}) - \xi] > \\ [(\sigma_1 - 1)x^{**2} - \sigma_1(x^{**} - x^{**2} - 2x^{**}y^{**}) - \sigma_1 x^{**}][(\beta - \sigma_2)(y^{**} \\ -y^{**2} - 2x^{**}y^{**}) - (2p\eta - \eta - \sigma_2)y^{**2} - \sigma_2 y^{**}]. \end{cases}$$

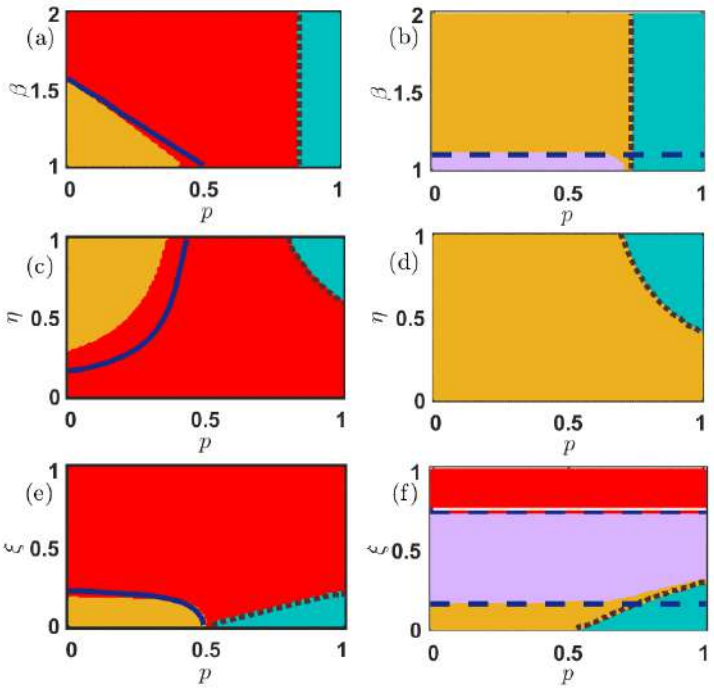

Figure 3.2: **Interplay of Parameters in the Mutation-Free Model** (3.8): The parameter p denotes the probability of playing the PD game. We examine its role in model (3.8) without mutation. Figs. (a), (c), and (e) on the left-hand side depict $\sigma_1 = \sigma_2 = 0$, while the right-hand figures include non-zero σ_1 and σ_2. Free space advantages support cooperation, shown by the broad yellow and violet regions in (b), (d), and (f). Red, sea blue, violet, and yellow represent the stable extinct, cooperator-free, defector-free, and coexistence states, respectively. White, blue, brown dotted, and blue dashed lines correspond to stability curves for E_0, E_3, E_2, and E_1. Minor mismatches arise from model multistability. Other parameters: (a-d) $\xi = 0.15$, (c-f) $\beta = 1.1$, (a,b,e,f) $\eta = 0.85$, (b,d,f) $\sigma_1 = 0.75$, $\sigma_2 = 0.25$, and $\mu = 0$.

Clearly, the chosen parameters satisfy the local stability criteria of both stationary points E_0 and E_1. Note that E_1 leads to two different values for the selected values of the parameters, out of which $(0.34751, 0)$ always remains locally stable, and $(0.0899, 0)$ is unstable. Thus, we see the appearance of two different stationary points E_0 (shown by red points) and E_1 (displayed by violet points) in the basin of attraction portrayed in Fig. 3.1 (a). Such toggling between alternate stable stationary points is one of the generic features in some biological systems involving the fundamental processes of life [130–132] and in a few nonlinear dynamical systems [133–136]. The initial condition $(x_0, y_0) = (0, 0)$ always helps the system (3.8) to converge to the stationary point E_0. The system is never able to give rise to the survival of any cooperators and defectors without the presence of any individual at the beginning. Since the chosen initial point $(0, 0)$ itself is the stationary state, the system always stabilizes in the $(0, 0)$ stationary point irrespective of the parameter values. Figure 3.1 (b) is drawn with $\xi = 0.15$, $\beta = 1.06$, $\eta = 0.85$, $p = 0.69$, $\sigma_1 = 0.75$, $\sigma_2 = 0.25$, and $\mu = 0$. Similarly, we find the system (3.8) in the absence of mutation (i.e., $\mu = 0$) converges to E_0 for the single initial condition $(x_0, y_0) = (0, 0)$. It is anticipated that the choice of $x_0 = 0$ always leads to the cooperator-free steady

state. The initial absence of cooperators in the mutation-free model will not entertain any exposure for the cooperators in the long run. The line of initial conditions $x_0 = 0$ and $y_0 \neq 0$ produces the stationary state E_2 (sea blue points in Fig. 3.1 (b)). Apart from these two steady states, the mutation-free system also switches between E_1 (violet points) and E_3 (yellow points) depending on the suitable choice of initial conditions (See Fig. 3.1 (b)). Thus, for the same choices of parameters' values, the system flips between four alternate steady states depending on the initial densities of cooperators and defectors. Similarly, we find the system (3.8) with the parameters' values $\xi = 0.15$, $\beta = 1.1$, $\eta = 0.85$, $p = 0.10$, $\sigma_1 = 0.10$, $\sigma_2 = 0.25$ and $\mu = 0$ converges to all these four stationary points. All population extincts for the initial conditions ranging from $(0, 0)$ to $(0.06, 0)$ (See red points in Fig. 3.1 (c)). The system (3.8) can be solved analytically with $\sigma_1 = \sigma_2 = \mu = 0$ in the absence of defectors (i.e., $y = 0$) as follows,

$x(t) =$

$$\begin{cases} 0, \\ \dfrac{1}{2} \pm \dfrac{(1-4\xi)^{\frac{1}{2}}}{2}, \\ c_4 - t = \dfrac{1}{2\xi}\Bigg[-\log(\xi + x(x-1)) + 2\log x + \dfrac{2\tan^{-1}\left(\dfrac{2x-1}{\sqrt{4\xi-1}}\right)}{\sqrt{4\xi-1}}\Bigg], \end{cases}$$

where c_4 is the integrating constant.
Similarly, the system (3.8) can be solved analytically with $\sigma_1 = \sigma_2 = \mu = 0$ in the absence of cooperators (i.e., $x = 0$) as follows

$y(t) =$

$$\begin{cases} 0, \\ \dfrac{1}{2} \pm \dfrac{[-\eta(2p-1)(\eta+4\xi-2\eta p)]^{\frac{1}{2}}}{2\eta(2p-1)}, \\ c_5 - t = \dfrac{1}{2\xi}\Bigg[-\log(\xi + (2p-1)\eta(y-1)y) \\ \qquad +2\log y + \dfrac{2\sqrt{(2p-1)\eta}\tan^{-1}\dfrac{\sqrt{(2p-1)\eta}(2y-1)}{\sqrt{4\xi-(2p-1)\eta}}}{\sqrt{4\xi-(2p-1)\eta}}\Bigg], \end{cases}$$

where c_5 is the integrating constant.

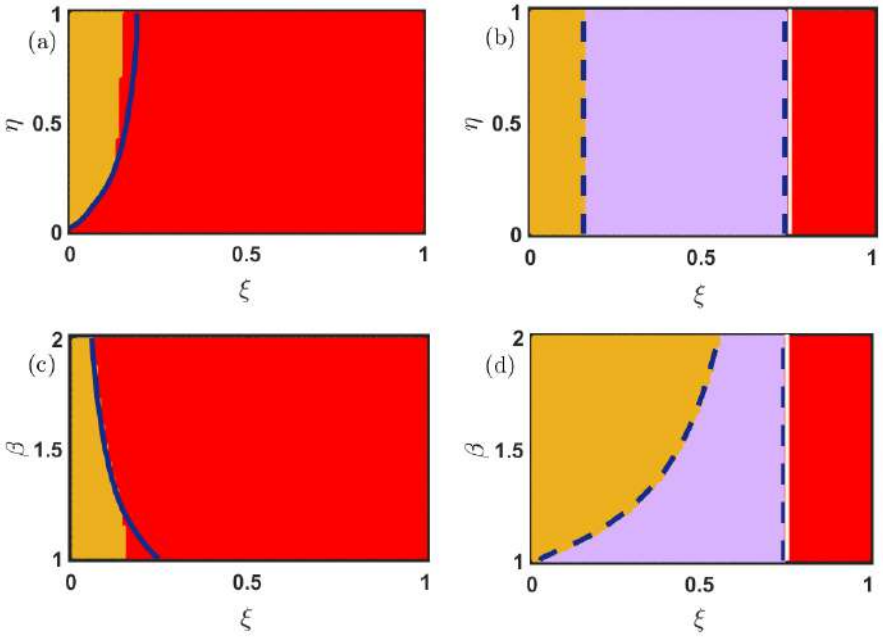

Figure 3.3: **Influence of death rate ξ in the mutation-free model** (3.8): The influence of game parameters β and η and the mortality rate ξ on the emergent dynamics of the model (3.8) in the absence of mutation is examined here. Subfigures (a) and (c) are drawn with $\sigma_1 = \sigma_2 = 0$. While subfigures (b) and (d) are generated with $\sigma_1 = 0.75$ and $\sigma_2 = 0.25$. Since, $\sigma_1 > \sigma_2$, we notice a fair portion of defector-free region (violet points) in subfigures (b) and (d). In the absence of free space induced benefits, we are unable to trace such defector-free regions in subfigures (a) and (c). The red region reflects the disappearance of all individuals for relatively high values of death rate ξ. Note that we keep the value of p fixed at 0.3. Thus, the system gets more opportunities to play the SD game, which generally encourages stabilizing the coexistence equilibrium. Therefore, we notice lower values of ξ will lead to the convergence towards the coexistence equilibrium E_3 (yellow points). β is kept fixed at 1.1 for the subfigures (a-b) and η is set at 0.85 for subfigures (c-d). We iterate the system (3.8) with $\mu = 0$ for 20×10^5 iterations with fixed integration step size $\delta t = 0.01$ and fixed initial condition $(x_0, y_0) = (0.35, 0.35)$.

Figure 3.1 is plotted by solving the differential equations (3.8) by varying the initial conditions within $[0, 1] \times [0, 1]$ with fixed step-length $\delta x_0 = \delta y_0 = 0.01$ and maintaining $0 \leq x_0 + y_0 \leq 1$. To solve our proposed system (3.8) numerically, we use the 4th order Runge-Kutta (RK4) method with 20×10^5 iterations with fixed integration step length $\delta t = 0.01$. The final point (x, y) is stored to decide the asymptotic dynamics of the system. Other initial conditions with $y_0 = 0$ stabilize the dynamics in the defector-free state E_1 (violet points). We also track a fair portion of the basin in Fig. 3.1 (c), where the system (3.8) with $\mu = 0$ converges to either E_2 (sea blue points) or E_3 (yellow points) depending on the choice of initial conditions.

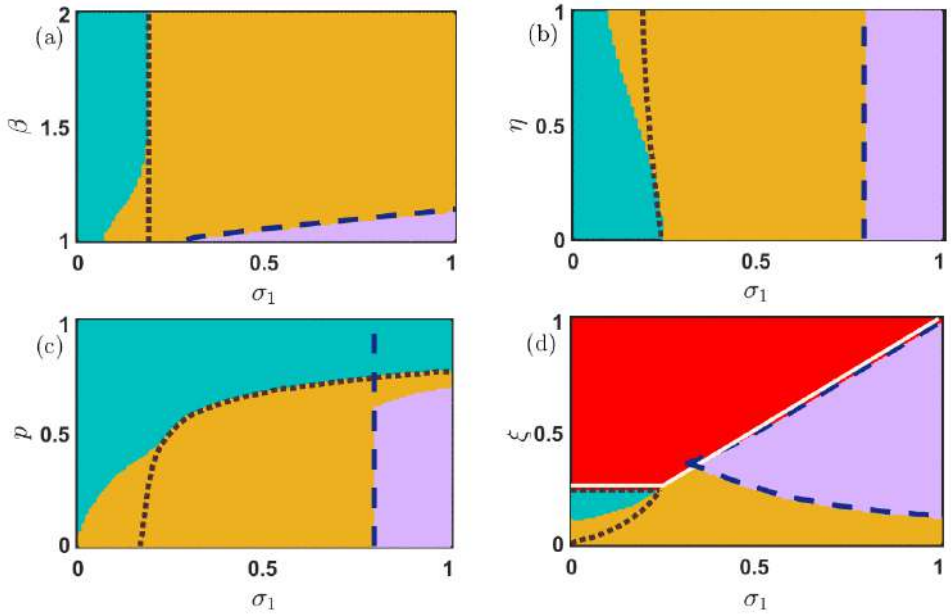

Figure 3.4: **Importance of σ_1 in the enhancement of cooperation**: Four different parameter spaces (a) $\sigma_1 - \beta$, (b) $\sigma_1 - \eta$, (c) $\sigma_1 - p$, and (d) $\sigma_1 - \xi$ are contemplated here with fixed initial condition $x_0 = 0.35$ and $y_0 = 0.35$. σ_1 is varied within $[0, 1]$, and the other parameters' values are for the subfigures (a) $\xi = 0.15$, $\eta = 0.85$, $p = 0.30$, $\sigma_2 = 0.25$, and $\mu = 0$. β is varied within the open interval $(1, 2)$, (b) $\xi = 0.15$, $\beta = 1.1$, $p = 0.30$, $\sigma_2 = 0.25$ and $\mu = 0$. η is varied within $(0, 1)$, (c) $\xi = 0.15$, $\beta = 1.1$, $\eta = 0.85$, $\sigma_2 = 0.25$, and $\mu = 0$. p is varied within the closed interval $[0, 1]$, and (d) $\beta = 1.1$, $\eta = 0.85$, $p = 0.30$, $\sigma_2 = 0.25$ and $\mu = 0$. ξ is varied within the interval (0,1]. The color code represents the following: (i) red represents the extinct state, (ii) yellow portrays the co-existence state, (iii) violet displays the defector-free state, and (iv) sea blue depicts cooperator-free state, respectively. We have run the numerical simulations for 20×10^5 iterations for each point and store the final value for determining the final asymptotic state. Increment of σ_1 contributes more to the cooperators' payoff, and hence, we observe a defector-free region for higher values of σ_1 depending on the other parameters. We draw the stability curves for E_0 (the brown dotted line), E_1 (the blue dashed line), E_2 (the brown dotted line), and E_3 (the solid blue line).

Although we choose the mutation-free model for the Figs. 3.1 (a-c), we consider the contribution of μ in Fig. 3.1 (d). We generate Fig. 3.1 (d) with $\xi = 0.30$, $p = 0.30$, $\beta = 1.1$, $\eta = 0.85$, $\mu = 0.02$, $\sigma_1 = 0.30$, and $\sigma_2 = 0.20$. This non-zero μ leads to the disappearance of two stationary points, (i) the defector-free steady state E_1, and (ii) the cooperator-free steady state E_2. The symmetric mutation from one species to another species always gives them two feasible opportunities. Either both strategies survive or all the individuals perish for $\mu \neq 0$. We also mathematically derive two possible stationary points as follows,

1. The extinction equilibrium $E_0 = (0, 0)$, which is stable under the conditions,

$$\begin{cases} 2(\xi + \mu) > \sigma_1 + \sigma_2, \\ \mu^2 < (\xi + \mu - \sigma_1)(\xi + \mu - \sigma_2). \end{cases}$$

2. The interior equilibriun $E_3 = (x^*, y^*)$ becomes stable, if

$$\begin{cases} 2(\mu + \xi) > (1 - \sigma_1)(2x^* - 3x^{*2} - 2x^*y^*) \\ +(2p\eta - \eta - \sigma_2)(2y^* - 3y^{*2} - 2x^*y^*) \\ -\sigma_1(y^* - y^{*2} - 2x^*y^*) \\ +(\beta - \sigma_2)(x^* - x^{*2} - 2x^*y^*) \\ +\sigma_1(1 - 2x^* - y^*) + \sigma_2(1 - x^* - 2y^*), \\ \text{and,} \\ [(1 - \sigma_1)(2x^* - 3x^{*2} - 2x^*y^*) \\ -\sigma_1(y^* - y^{*2} - 2x^*y^*) \\ +\sigma_1(1 - 2x^* - y^*) - \xi - \mu][(\beta - \sigma_2)(x^* - x^{*2} \\ -2x^*y^*) + (2p\eta - \eta - \sigma_2)(2y^* - 3y^{*2} \\ -2x^*y^*) + \sigma_2(1 - x^* - 2y^*) - \xi - \mu] > [(\sigma_1 - 1)x^{*2} \\ -\sigma_1(x^* - x^{*2} - 2x^*y^*) - \sigma_1 x + \mu][(\beta \\ -\sigma_2)(y^* - y^{*2} - 2x^*y^*) - (2p\eta - \eta \\ -\sigma_2)y^{*2} - \sigma_2 y^* + \mu], \\ \text{where } x^* \text{ and } y^* \text{ satisfy the equations :} \\ x^*[(1 - \sigma_1)x^*(1 - x^* - y^*) - \sigma_1 y^*(1 - x^* \\ -y^*) + \sigma_1(1 - x^* - y^*) - \mu - \xi] + \mu y^* = 0, \\ \text{and} \\ y^*[(\beta - \sigma_2)x^*(1 - x^* - y^*) \\ +(2p\eta - \eta - \sigma_2)y^*(1 - x^* - y^*) \\ +\sigma_2(1 - x^* - y^*) - \mu - \xi] + \mu x^* = 0. \end{cases}$$

The compelling evidence of bistability under the same choice of parameters' values is recognized in Fig. 3.1 (d).

3.2.3 Emergent dynamics in absence of mutation

We examine the impact of the parameters p, β, η, and ξ on the system (3.8) with $\mu = 0$ in Fig. 3.2. For the comparability, we choose $\sigma_1 = \sigma_2 = 0$ in subfigures (a), (c) and (e). Also, we set $\sigma_1 \neq 0$ and $\sigma_2 \neq 0$ for the subfigures (b), (d) and (f). In the absence of mutation ($\mu = 0$) and free space induced benefits ($\sigma_1 = \sigma_2 = 0$), the defector-free $E_1 = \left(x^* = \dfrac{1 \pm \sqrt{1 - 4\xi}}{2}, 0\right)$ is unable to stabilize. Although E_1 exists for $0 < \xi \leq \dfrac{1}{4}$, but two eigen values of the Jacobian of the linearized system are

$$\begin{cases} \lambda_1 = 2x^* - 3x^{*2} - \xi, \\ \lambda_2 = \beta x^* - \beta x^{*2} - \xi = \xi(\beta - 1). \end{cases}$$

Since $\beta > 1$ and $\xi > 0$, λ_2 is always positive. Consequently, E_1 is always unstable. This result is physically meaningful, as both the chosen games (PD and SD) do not encourage a defection-free society without any supporting mechanism. However, we find three different steady states in Fig. 3.2 (a), (c) and (e). These stationary points and their corresponding stability analysis are given below,

1. The extinction equilibrium $E_0 = (0, 0)$ (red points in subfigures (a), (c) and (e) of Fig. 3.2) always exists and is always locally stable.

2. $E_2 = (0, y^{**})$ is the cooperator-free stationary point (sea blue points in subfigures (a), (c) and (e) of Fig. 3.2), where $y^{**} = \frac{1}{2} \pm \frac{\sqrt{\eta^2(2p-1)^2 - 4\eta\xi(2p-1)}}{2\eta(2p-1)}$. This state exists under the condition $0 \leq 4\xi\eta(2p-1) \leq \eta^2(2p-1)^2$, and becomes stable if $\xi > \eta(2p-1)(2y^{**} - 3y^{**2})$.

3. $E_3 = (x^*, y^*)$ allows the coexistence of both cooperators and defectors (yellow points in subfigures (a), (c) and (e) of Fig. 3.2), where $x^* = \frac{1 \pm \sqrt{1 - 4\kappa\xi}}{2\kappa}$, and $y^* = \frac{1-\beta}{2p\eta - \eta} x^*$, with $\kappa = \frac{1 - \beta + 2p\eta - \eta}{2p\eta - \eta}$. The stationary state is stable under the following conditions,

$$\begin{cases} 2\xi > (2+\beta)x^* - (3+\beta)x^{*2} - 2(\beta+1)x^*y^* \\ +(2p\eta - \eta)(2y^* - 3y^{*2} - 2x^*y^*), \\ (2x^* - 3x^{*2} - 2x^*y^* - \xi)(\beta x^* - \\ \beta x^{*2} - 2\beta x^*y^* + (2p\eta - \eta)(2y^* - 3y^{*2} - 2x^*y^*) \\ -\xi) + x^{*2}(\beta y^* - \beta y^{*2} - 2\beta x^*y^* - (2p\eta - \eta)y^{*2}) > 0. \end{cases}$$

With increasing p, players are prone to play the PD game. Hence, we can not anticipate the survival of cooperators for large p. Thus, for large p, either the extinction equilibrium E_0 or the cooperator-free stationary point E_2 stabilizes in Figs. 3.2 (a), (c) and (e). However, the free-space induced benefits in Figs. 3.2 (b), (d) and (f) facilate the emergence of cooperation and stabilize the interior equilibrium E_3. Even, Fig. 3.2 (f) provides a range in the $p - \xi$ parameter space, where the defector-free stationary point E_1 stabilizes. The comparative study between the left and right column of Fig. 3.2 ensures the encouraging role of free space in the promotion of cooperation under suitable circumstances.

With increasing β, the defectors are getting extra aid, and thus, we get the stabilization of the extinction equilibrium E_0 (red zone) in Fig. 3.2 (a). However, the presence of free space assistance converts that area into a coexistence zone (yellow zone) in Fig. 3.2 (b). The increment of p in both subfigures (a-b) permits only the existence of defectors, as people are playing mostly the PD game in such circumstances. Defectors are getting a favorable atmosphere in the PD game for our

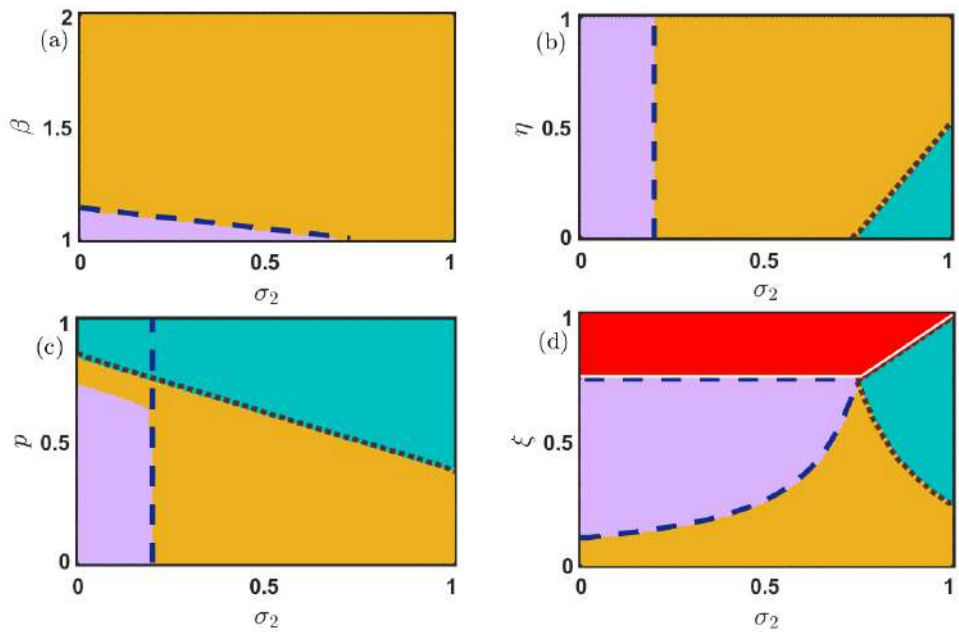

Figure 3.5: **Impact of σ_2 on Cooperation Evolution**: In the mutation-free system, low σ_2 favors defector-free societies (violet), while higher σ_2 stabilizes the cooperator-free state E_2 (sea blue). Appropriate parameters support co-existence of cooperators and defectors. At higher mortality rates ξ, all individuals die (red region in subfigure (d)). Parameters: $\xi = 0.15$, $\eta = 0.85$, $\beta = 1.1$, $p = 0.30$, $\sigma_1 = 0.75$, $\mu = 0$ unless varied. Simulations run for 20×10^5 iterations from initial $(x_0, y_0) = (0.35, 0.35)$. Color codes: (i) red—extinct state E_0, (ii) yellow—coexistence state E_3, (iii) violet—defector-free state E_1, (iv) sea blue—cooperator-free state E_2. Stability curves are plotted for each stationary point in each subfigure.

chosen PD game parameters' values. A similar sort of stabilization of cooperator-free steady state (sea blue area) is observed in subfigures (c-d) for larger values of p. However, lower values of p provide the opportunity for playing the SD game. Hence, coexistence equilibrium (yellow region) stabilizes in figs. 3.2 (c-d) for smaller p. Nevertheless, the inclusion of free space induced benefits helps to broaden the region of coexistence in the $p-\eta$ parameter plane, as shown in Fig. 3.2 (d). The comparison between the Figs. 3.2 (e) and (f) suggests that appropriate non-zero values of σ_1 and σ_2 entertain the stabilization of a defector-free steady state (violet region). Hence, we can trace a fair portion of violet points in the $p-\xi$ parameter space of the subfigure (f). However, too large a mortality rate reduces the opportunity of survivability of any individual, resulting in the stabilization of the extinction equilibrium E_0. We focus on the effect of mortality rate ξ more elaborately in Fig. 3.3.

As expected, higher values of ξ constantly enlarge the chances of extinction. Thus, we observe a fair portion of the red region in Fig. 3.3. Nevertheless, the amount of this red area is considerably lesser in the right column of Fig. 3.3 compared to the left column. We introduce the non-zero values of σ_1 and σ_2 in the right column of this figure. These free space induced benefits encourage maintaining a defector-free society, as shown in Figs. 3.3 (b) and 3.3 (d). We choose $\sigma_1 = 0.75 > 0.25 = \sigma_2$ for

Figs. 3.3 (b) and 3.3 (d). i.e., the free space will provide an additional advantage for the cooperators, and thus depending on the other parameters, the defectors are vanished in the long run, as shown in Figs. 3.3 (b) and 3.3 (d). In all of these subfigures of Fig. 3.3, we trace a portion of yellow points depicting the survival of both cooperators as well as defectors simultaneously. We choose $p = 0.3$ in Fig. 3.3. Thus, people get more chances to play the SD game, which facilitates the concurrence of both cooperation and defection. Thus, smaller values of ξ provide an opportunity to coexist for all strategies, which is observed in Fig. 3.3 with initial condition $(x_0, y_0) = (0.35, 0.35)$. We plot the stability curve of all stationary points in Figs. (3.2,3.3,3.4,3.5) as follows,
(i) The brown dotted line for the cooperator-free steady state E_2,
(ii) the blue dashed line for the defector-free steady state E_1,
(iii) the solid blue line for the interior equilibrium E_3, and
(iv) the solid white line for the extinction equilibrium E_0.

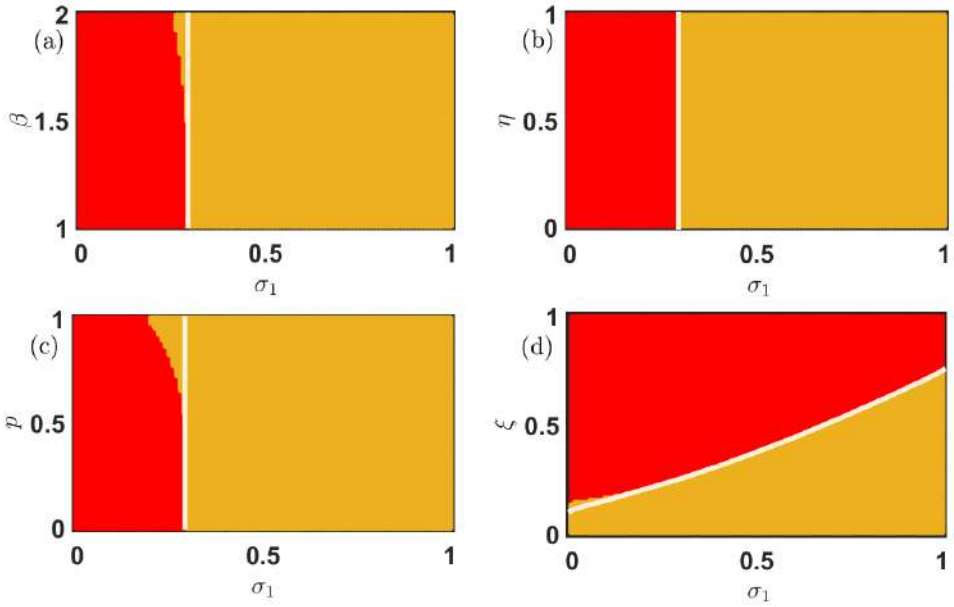

Figure 3.6: **The effect of altruist free space on the nonlinear dynamics of multigame with mutation**: The influence of free space-induced benefits by varying σ_1 within the closed interval $[0, 1]$ is established. The whole population goes extinct in the red region, and the yellow area reflects the system's stable interior point, corresponding to the coexistence of all two strategies. All the parameters are kept fixed at $\xi = 0.25$, $\eta = 0.85$, $p = 0.30$, $\sigma_2 = 0.20$, $\beta = 1.1$, $\mu = 0.5$, unless it is varied. The initial condition is kept fixed at $(0.35, 0.35)$. A notable difference is observed from Fig. (3.4), which is drawn in the absence of mutation. Larger values of σ_1 always facilitate the maintenance of cooperation, and the bidirectional mutation reinforces the system's inherent tendency to flow from cooperators to defectors. The solid white line in each figure is the analytically computed stability curve corresponding to the extinction equilibrium.

In Fig. 3.4, we fix the value of σ_2 at 0.25 and examine the role of σ_1. Since σ_1 represents the free space induced benefits towards the cooperators, thus enhance-

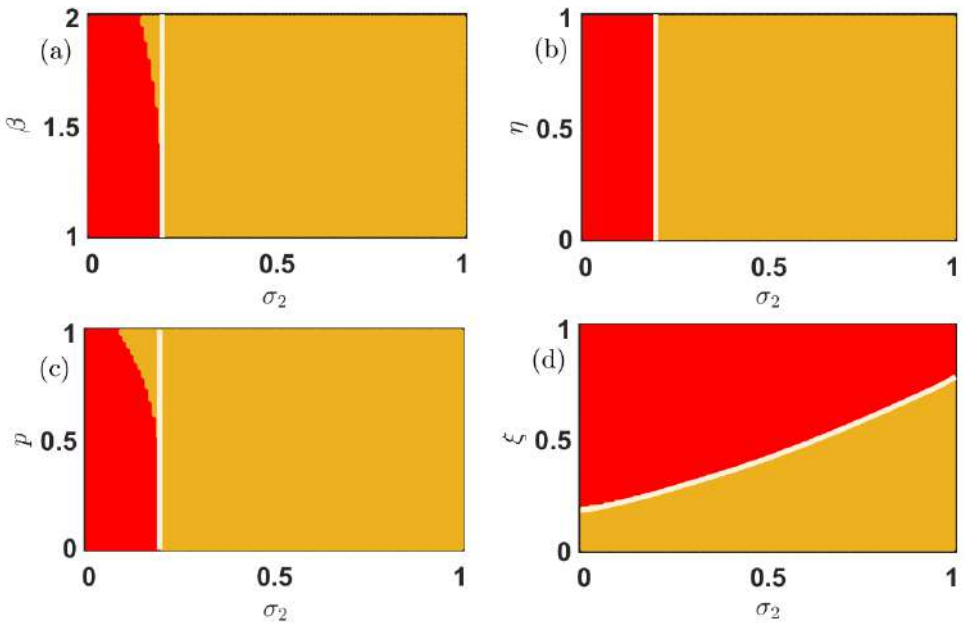

Figure 3.7: **Impact of free space-induced benefits on defectors with mutation**: Either extinction (red) or symmetric mutation preserves coexistence (yellow) across subfigures. Beyond a critical σ_2, mutations enable coexistence of both strategies. Solid white lines show analytically derived stability curves for the extinction equilibrium. Parameters: $\xi = 0.25$, $\eta = 0.85$, $p = 0.30$, $\sigma_1 = 0.30$, $\mu = 0.5$, $\beta = 1.1$ unless varied; initial condition $(0.35, 0.35)$. Small mismatches in extinction stability in (a) and (c) arise from multistability in model (3.8).

ment of its (σ_1) value will help in promoting cooperation in the society. Figure 3.4 reflects the same scenario. A defector-free society (violet region) is noticed in all these subfigures. The increment of temptation parameter β's value challenges the prevalence of cooperation. Thus, for a small σ_1, we find a defector dominated society (the sea blue region in Fig. 3.4 (a)). σ_1 proves to be a cooperator facilitating parameter as we detect a wide range of yellow regions in Fig. 3.4 (a), where both cooperators and defectors can coexist. Similarly, irrespective of the choice of η in Fig. 3.4 (b), higher values of σ_1 provide all cooperators an extra benefit for survival, and thus, the stationary point E_1 (violet points) stabilizes. For the intermediate choice of σ_1, the stationary point E_3 (yellow) yields the stable coexistence of both strategies. However, cooperators strive to keep in existence for the lower values of σ_1, and we find the sea blue region of cooperator-free steady state. The parameter p indicates the probability of playing the PD game. Thus, $p \to 1-$ always gives defectors a more favorable environment to survive. That's why we spot a sea blue portion in Fig. 3.4 (c) for higher values of p and σ_1. When p is small, people are prone to play the SD game; and thus, we get the coexistence of both strategies (the yellow region in Fig. 3.4 (c)) for smaller p and σ_1. Nevertheless, a larger value of σ_1 with a moderate value of p always provides a reasonable scope for the cooperators to survive, and we discover a healthy portion of the stationary point E_1 (the violet region) in Fig. 3.4 (c). A higher mortality rate ξ always results in the extinction

of both cooperators and defectors, and we locate a huge red region in the $\sigma_1 - \xi$ parameter plane of Fig. 3.4 (d). We find a very tiny sea blue region in Fig. 3.4 (d), where defectors are only able to survive. But, as expected, a higher value of σ_1 always promotes the cooperation strategy, and we obtain a violet zone of defector-free stationary point and a yellow region of interior equilibrium E_3 in Fig. 3.4 (d).

Figure 3.5 (a) shows that except for a smaller portion of the defector-free region (violet zone), the whole $\sigma_2 - \beta$ parameter space produces the coexistence of both cooperators and defectors depending on other parameters' values. Despite the increment of σ_2 and β, the cooperators are able to survive along with the defectors due to our choice of other parameters' values. The $\sigma_2 - \eta$ parameter space portrays that smaller values of σ_2 can not provide any benefit to the defectors, and stabilize the defector-free stationary point E_1 (violet region) irrespective of η's value. However, if σ_2 increases, it will yield a window of opportunity for the defectors to thrive. We observe a wide coexistence region (yellow region) and a small area of cooperator-free stationary point (sea blue region)in Fig. 3.5 (b). σ_2 indicates the free-space induced benefits towards the defectors. So, it is expected that larger values of σ_2 always enhance the chances of defectors' survivability. Thus, we notice a cooperator-free region (sea blue zone) in both Figs. 3.5 (c-d). Nevertheless, larger values of p enhance the chances of playing the PD game, where defectors get a favorable environment to survive. Thus, the cooperator-free sea blue region is found in Fig. 3.5 (c). We are also able to detect a small violet region of a defector-free environment in the $\sigma_2 - p$ parameter space. However, we trace a healthy portion of coexistence (yellow) too in Fig. 3.5 (c) due to our chosen parameters' values.

3.2.4 The influence of bidirectional mutation

Now we investigate the influence of bidirectional mutation on the long-term behavior of the nonlinear differential equations (3.8). Since every species can mutate into the other at a specific uniform rate $\mu \in (0, 1]$, thus cooperators and defectors can not remain alive alone. Either all populations will die; otherwise, the dynamics will lead to the coexistence of all two species. Figure 3.4 already portrays the influence of free space-induced benefits on the cooperators in the absence of mutation. We scrutinize the impact of σ_1 under the influence of 50% mutation (i.e., $\mu = 0.5$) in Fig. 3.6. As σ_1 increases, the cooperators are getting a better environment for survival. We find a portion of stable coexistence equilibrium in each two-dimensional parameter space for large σ_1 in Fig. 3.6. Thanks to the mutation, the cooperators can not live alone. The white line in Fig. 3.6 is the stability curve corresponding to the extinction equilibrium. The local stability analysis fits almost exactly with the numerical simulations in Fig. 3.6 with fixed initial condition $(x_0, y_0) = (0.35, 0.35)$. There are a few places where the stability analysis fails to predict the stabilization of the extinction stationary point $(0, 0)$. This is mainly due to the multistable behavior of the proposed model 3.8.

As discussed, the increasing values of the parameters β, η, and p always provide the defectors a favorable environment to dominate the cooperators. However, beyond a critical value of σ_1, both the cooperators and defectors can coexist, as shown in Figs. 3.6 (a-c). The larger values of ξ always hinder the evolution of cooperators

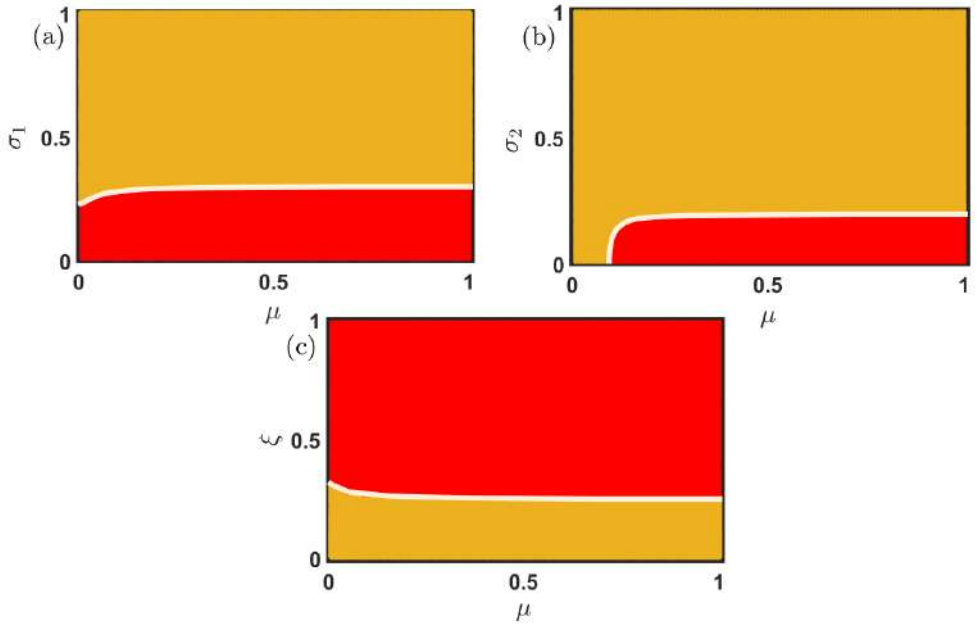

Figure 3.8: **Effect of bidirectional mutation on the emergent dynamics**: The positive mutation rate $\mu \in (0, 1]$ allows the system (3.8) to settle into two stationary points depending on the choice of other parameters' values. When the free space-induced benefits are small, all species are extinct, as depicted through subfigures (a-b). However, all strategies can coexist for suitable choices of other parameters. The red region reflects the extinction equilibrium, and the yellow region indicates the stable coexistence of cooperators and defectors. The solid white line represents the analytically derived stability curve below which the extinction equilibrium $(0, 0)$ is locally stable in subfigures (a-b). The initial condition is chosen here as $(x_0, y_0) = (0.35, 0.35)$. Other parameters' values are kept fixed at $\xi = 0.25$, $\beta = 1.1$, $\eta = 0.85$, $p = 0.30$, $\sigma_2 = 0.20$, $\sigma_1 = 0.30$, unless they are varied. The moderate choice of mortality rate $\xi \in (0, 1]$ allows the species' coexistence in subfigure (c). Beyond a critical value of ξ, both the cooperators as well as the defectors die, as reflected through the red region of subfigure (c).

as well as of defectors. However, an intermediate choice of $\sigma_1 - \xi$ favors the successful evolution of both strategies, as portrayed through Fig. 3.6 (d). The same feature is also noticeable in Fig. 3.7. The complex evolutionary dynamics switch between two stationary points depending on the choices of parameters' values in Fig. 3.7. For smaller values of σ_2, the defectors are not getting enough advantages to survive, and thus the extinction equilibrium $(0, 0)$ stabilizes in the red region of all subfigures of Fig. 3.7. The choice of other parameters' values is also crucial for obtaining these stationary states. The parameter σ_2 benefits the defectors; hence the defectors can survive beyond a certain threshold of σ_2. The employed 50% mutation rate helps to flow a certain fraction of defectors into cooperators, and we have a moderate portion of coexistence state (yellow region) in Fig. 3.7. The observed results may vary for different choices of initial conditions, as the system is multistable. We plot the boundary separating solid white lines in all subfigures by analyzing the local

stability analysis of the extinction equilibrium. Clearly, this stability curve agrees well with our numerical simulations, and the places, where they don't agree with the numerical simulations, is due to the multistable behavior of our proposed model 3.8. All the simulations are done by iterating for 20×10^5 times with fixed integrating step length $\delta t = 0.01$. The last point is gathered to finalize the asymptotic state.

Figure 3.8 demonstrates the importance of the parameters σ_1, σ_2 and ξ for the enhancement of cooperation under the presence of mutation. The larger values of σ_1 and σ_2 facilitate the evolution of at least one species, and the positive mutation rate $\mu \in (0, 1]$ assures that species should mutate into the other. This mechanism will lead to the species' coexistence in a major portion (yellow region) of the two-dimensional parameter spaces represented in Figs. 3.8 (a-b). The results are further validated by plotting the stability curve (white solid lines) below which the stationary point $(0, 0)$ is locally stable. A higher mortality rate never entertains the evolution of both strategies; thus, we obtain the red region in Fig. 3.8 (c). This red region indicates the extinction equilibrium $(0, 0)$. Once again, we plot the stability curve (solid white line) in Fig. 3.8 (c), above which both the species should be extinct as per our local stability analysis. All the subfigures are drawn with fixed initial condition $(0.35, 0.35)$.

We inspect the influence of different parameters on the constructed model (3.8) in Fig. 3.9. We keep fixed all parameters' values at $\xi = 0.25$, $\beta = 1.1$, $\mu = 0.5$, $p = 0.65$, $\eta = 0.85$, $\sigma_1 = 0.75$ and $\sigma_2 = 0.25$, unless they are varied. Since free space provides additional advantage to the cooperators compared to the defectors as we choose $\sigma_1 = 0.75 > \sigma_2 = 0.25$, we have a defector-free society at least initially with $\mu = 0$ in Fig. 3.9 (a). However, whenever the mutation rate μ becomes positive, each strategy can mutate into other. In this way, the density of the cooperators (red line) decreases, and the defectors' density (blue line) increases. Eventually, both densities almost become identical for $\mu \to 1-$. In of Fig. 3.9 (b), the vital role of p is investigated in the one-dimensional bifurcation diagram. As $p \to 1-$, the defectors are getting the upper hand over the cooperators as p indicates the probability of playing the PD game. PD game always provides additional assistance to the defectors. All these results obtained in Fig. 3.9 are consistent with the social dilemmas considered for constructing the model (3.8). Figure 3.9 (b) points out that lower values of p are always better for the maintenance of cooperation as small values of p indicate more rational people are playing the SD game and the SD game always favors the coexistence of both strategies. Increasing the temptation parameter β always uplifts the defectors' fraction y (blue line). Thus, one needs to choose the value of β wisely so that we obtain a moderate range of β in Fig. 3.9 (c) allowing the coexistence of both strategies. When β is small, we found the cooperators' density x (red line) dominates the defectors' fraction y (blue line). However for $\beta > 1.45$, y is larger than x. Note that the results may alter for a different choice of initial condition as the system 3.8 is multistable. We plot Fig. 3.9 with fixed initial condition $(0.35, 0.35)$ and the code to generate this figure is freely available at [**?**]. Increasing the parameter $\eta \in (0, 1)$ can provide extra benefits to the defectors. Thus, the rate of increment of y is slightly better than that of x in subfigure (d) of Fig. 3.9. However, other parameters' values are also crucial for stabilizing the competitive communities. Hence, y (blue line) remains always lower than x (red

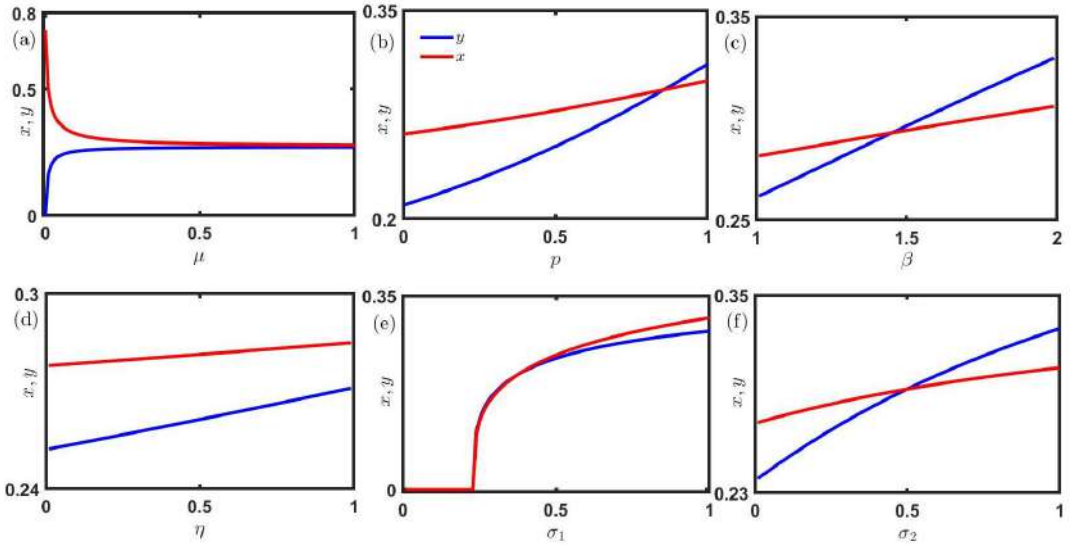

Figure 3.9: **Effects of various parameters in spreading of cooperative behavior**: Subfigure (a) shows that as the mutation rate μ increases, cooperators decline while defectors rise. In the absence of mutation ($\mu = 0$), defectors vanish due to the higher cooperator benefit from free space ($\sigma_1 = 0.75 > \sigma_2 = 0.25$). In subfigure (b), both densities increase with the probability p of playing the PD game, but defectors surpass cooperators after $p = 0.85$, reflecting the PD game's bias toward defection. Subfigure (c) shows similar trends with the temptation payoff β; both fractions increase, with defectors overtaking cooperators beyond $\beta = 1.45$. Subfigure (d) highlights the effect of increasing punishment parameter η: both strategies grow, but cooperators remain dominant due to stronger ecological support. In subfigure (e), both strategies go extinct for low σ_1, where mortality ξ outweighs ecological benefit, but higher σ_1 favors cooperators. Finally, subfigure (f) illustrates that increasing σ_2 boosts both fractions, but cooperators dominate until $\sigma_2 = 0.5$, after which defectors prevail. All results are based on long-term integration of system (3.8) with 2×10^6 iterations, fixed step size $\delta t = 0.01$, and initial condition $(x_0, y_0) = (0.35, 0.35)$. Unless varied, parameters are fixed at $\xi = 0.25$, $\beta = 1.1$, $\mu = 0.5$, $p = 0.65$, $\eta = 0.85$, $\sigma_1 = 0.75$, and $\sigma_2 = 0.25$.

line) in Fig. 3.9 (d) for our chosen parameters' values.

Since the mutation rate μ is 50%, we can obtain only two stationary points of the model (3.8). Thus, initially, for a smaller choice of σ_1, extinction of both species prevails in Fig. 3.9 (e). Nevertheless, with an increment of σ_1, cooperators are getting further assistance from free space, and hence x becomes positive beyond $\sigma_1 = 0.25$. Since $\mu = 0.5$, 50% of these cooperators mutate bidirectionally into the defectors, and thus, we have positive y too in that range of σ_1. Since $\sigma_2 = \xi = 0.25$, thus we get the stabilization of $(0, 0)$ within the interval $\sigma_1 \in [0, 0.25]$. In fact, the cooperators' density x is slightly better than that of y for the higher values of σ_1 in Fig. 3.9 (e). The choice of the initial condition and other parameters' values are vital in obtaining all these results. Similar observation can be found in Fig. 3.9 (f), where we examine the role of σ_2 in our proposed model (3.8). With increasing σ_2, the defectors will be benefited from free space, and hence, y (blue line) dominates

x (red line) for larger values of σ_2. But since σ_1 is taken sufficiently large in this Fig. 3.9 (f), we initially have a small portion for smaller values of σ_2 where $x > y$. Figure 3.9 discloses suitable choices of all parameters' values not only entertain the coexistence of both strategies but also may promote the evolution of cooperation.

3.3 Conclusion

The mutation-induced model in this chapter provides widespread coexistence of both strategies under suitable choices of parameters' values. This stable persistence of ecological communities strengthens the theory of concurrency. Our thorough analysis with several numerical simulations enhances our understanding of the mechanisms that drive the survival of cooperative behavior in the multigame consisting of both the Prisoner's Dilemma and the Snowdrift games. The inclusion of altruistic behavior of free space along with the mutation in our proposed evolutionary model seems to be a natural course of action as observed in many realistic settings. Our findings clearly demonstrate that there exists an optimal probability of playing each game so that people are more likely to cooperate in such circumstances. Throughout the chapter, we have pointed out the positive impact of diverse factors (parameters) on significant improvement of cooperation. We have shown that the selfless contribution of free space promotes the coexistence of all strategies efficiently, even in the absence of mutation.

In summary, our research indicates the proposed model (3.8) may possess four different stationary points in the absence of mutation. The exciting feature of this model is that the system never allows settling into a cooperator-free state in the lack of free space-induced benefits and mutation rate. This precise result is consistent with the chosen games as both the PD and SD games never encourage a cooperator-free society in the usual scenario. The merging of two games with different outcomes provides a more realistic representation of the concept of opinion formation. However, the numerical results presented here are highly sensitive to the variation of initial conditions. The positive invariance and boundedness of the model are analyzed too in this article. We have shown the viable choice of bidirectional mutation allows the system to switch between only two stationary states. Either all people will die, or both the strategies coexist in the eco-evolutionary model with mutation. This is an interesting angle of our research as our model brings forth stable biodiversity in the form of a heterogeneous population (mixed cooperator-defector state). Note that we have only focused on the equilibria of the corresponding dynamical system (3.8) throughout the article so that we can relate those stationary states from the game-theoretical point of view. Our simple model with mutation sheds light on how cooperation emerges in a complex society. The presented results are insightful, attesting that altruistic behavior and mutation are advantageous for the spontaneous maintenance of biodiversity. We believe the presented results may help us understand the mechanism behind the coexistence of competing species through the co-evolution of both strategies. 7

In the next chapter of this thesis, we study the interplay between ecological and evolutionary processes through the lens of the weak PD game with an additional strategy of policing in it. Although previous studies often assumed instantaneous

interactions, we incorporated time delays to examine their impact on cooperation. Through analytical calculations and numerical simulations, we demonstrate that delays can induce oscillations and, by including ecological free space and the strategy of punishment, explore how these factors shape population and community dynamics. Our eco-evolutionary model can also mimic cyclic dominance and even chaotic behavior, underscoring the role of complex dynamics in managing and conserving ecological communities. The following chapter thus contributes to understanding the emergence of moral behavior in multidimensional social systems.

Chapter 4

Uncovering the temporal roots of cooperation incorporating the concept of time delay *

The PD game [137, 89] is a foundational model for analyzing the conflict between individual and collective interests among selfish individuals. Defection always yields a higher payoff than cooperation, leading to a tragedy of the commons [138]. This raises a fundamental question in evolutionary dynamics: if natural selection favors the fittest, why does cooperation persist across biological and social systems?

Cooperation has shaped evolutionary progress—from the genome's formation to multicellular organisms and social structures [139]. Despite the vulnerability of cooperation to exploitation, human societies thrive on cooperation, facilitating complex social structures. Research has identified several mechanisms promoting cooperation in PD games, including spatial structure [140–142], network topology [143–145], mobility [99], kin selection [146], reproduction restrictions [147], aging [148], and direct and indirect reciprocity [149, 107]. Strategies like tit-for-tat [116] and punishment [150–158] further sustain cooperation.

Nag Chowdhury et al. [91] examined punishment in the PD game alongside altruistic free space—an ecological variable enabling others' reproduction at no benefit to itself—capturing the simultaneous operation of ecological and evolutionary dynamics, relaxing Slobodkin's assumption [159] that evolution is slower than ecology. Studies on eco-evolutionary feedbacks [160, 64, 18, 161, 19, 162] now reveal that evolution and ecology shape each other on similar timescales [60, 163, 59, 164–166].

This chapter investigates the influence of time delays on cooperation in the PD game, integrating punishment and free space. Time delays are ubiquitous in nature—from echoes [167] to crickets [168], neural information flow [169], and digestion [170]. They also influence collective behaviors in coupled systems [171–178]. Recent studies highlight delays in cooperation: delayed multigames with environmental space [179], time delays in spatial public goods games [180], fractional-order systems

*A considerable part of this chapter has been published in **Scientific Reports**, Volume 32, No. 01, Article ID: Roy, S., Nag Chowdhury, S., Kundu, S., Sar, G.K., Banerjee, J., Rakshit, B., Mali, P.C., Perc, M. and Ghosh, D., 2023. Time delays shape the eco-evolutionary dynamics of cooperation. Scientific reports, 13(1), p.14331.

with delay feedback [181], and replicator dynamics with random delays [182]. Hu et al. [183] showed that delays affect convergence time but not equilibrium stability, while delays in intraspecific interactions can induce oscillations.

Inspired by these findings, this chapter examines delayed eco-evolutionary dynamics in the PD game with punishment and free space. We show how time delays shape cooperation, addressing a key gap in the literature and offering insights into sustaining cooperation among rational individuals.

4.1 Mathematical model

We start with the evolutionary two-strategy PD game, where players can decide whether to cooperate (**C**) or defect (**D**). For mutual cooperation, they both can earn a reward R. The mutual defection yields both the player punishment P. The dealing between a cooperator and a defector gives the sucker's payoff S to the cooperator, while the defector receives the temptation to defect T. Throughout our investigation, we maintain the ranking between the payoff as $T > R > P \geq S$ and adopt the same parameter values $T = \beta > 1$, $R = 1$, and $P = S = 0$ from Refs. [91, 143]. This inequality of the weak PD game indicates that mutual defection always promises less payoff, as $0 = P < R = 1$. However, from the individual standpoint, defection serves as the intelligent strategy between the two competing strategies. If the player chooses cooperation, the defector earns more as $\beta = T > R = 1$. If the opponent also decides to defect, still the defector can not earn more by cooperating due to our choice of parameter values. The 2×2 payoff matrix looks like

$$\begin{array}{c} \\ \mathbf{C} \\ \mathbf{D} \end{array} \begin{array}{c} \begin{array}{cc} \mathbf{C} & \mathbf{D} \end{array} \\ \begin{pmatrix} R & S \\ T & P \end{pmatrix} \end{array} = \begin{array}{c} \\ \mathbf{C} \\ \mathbf{D} \end{array} \begin{array}{c} \begin{array}{cc} \mathbf{C} & \mathbf{D} \end{array} \\ \begin{pmatrix} 1 & 0 \\ \beta & 0 \end{pmatrix} \end{array} \tag{4.1}$$

in which the entries represent the payoff accumulated by the player in the left. We consider an additional strategy, the 'punisher' who acts like a cooperator and receives the same payoff $R = 1$ if the other player decides to cooperate. However, if the opponent player defects, the punisher will use their own resources to punish them and earn a payoff value of $S - \delta = -\delta$. In return, the defector makes $T - \delta = \beta - \delta$ with $\delta > 0$. Note that a defector earns more if they interact with a cooperator. This inclusion of punishers will extend our payoff matrix (4.1) to the following matrix

$$\begin{array}{c} \\ \mathbf{C} \\ \mathbf{P} \\ \mathbf{D} \end{array} \begin{array}{c} \begin{array}{ccc} \mathbf{C} & \mathbf{P} & \mathbf{D} \end{array} \\ \begin{pmatrix} 1 & 1 & 0 \\ 1 & 1 & -\delta \\ \beta & \beta - \delta & 0 \end{pmatrix} \end{array} \tag{4.2}$$

We further incorporate the ecological contribution of free space in the payoff matrix. Free space allows others to replicate and provide others ample opportunity to survive. Interestingly, free space never anticipates anything in return, and this selfless contribution of free space motivates us to update our payoff matrix (4.2) in the following way,

$$\begin{array}{c} \\ \mathbf{C} \\ \mathbf{P} \\ \mathbf{D} \\ \mathbf{F} \end{array} \begin{array}{c} \begin{array}{cccc} \mathbf{C} & \mathbf{P} & \mathbf{D} & \mathbf{F} \end{array} \\ \begin{pmatrix} 1 & 1 & 0 & \sigma_1 \\ 1 & 1 & -\delta & \sigma_2 \\ \beta & \beta-\delta & 0 & \sigma_3 \\ 0 & 0 & 0 & 0 \end{pmatrix} \end{array} \tag{4.3}$$

Here, all these parameters σ_1, σ_2, and σ_3 are strictly positive quantities, as free space contributes altruistically to all the rational individuals. Free space earns only zero in return as it never expects any benefits for its generous acts. Now we calculate each strategy's fitness and determine the evolution of populations by assuming that an individual's reproduction rate depends solely on their average fitness. Let us assume x, y, z, and w be the respective fraction of cooperators, punishers, defectors, and free space, respectively. Hence, $x, y, z, w \in [0, 1]$ and $x + y + z + w = 1$. Interestingly, the process of learning takes time and effort. It takes a considerable amount of time for people to adapt strategies based on the information they learn. The players need to gather the information at each round of the game and then assess the effectiveness of the methods. Based on their understanding, they spread that information which helps others to recognize which strategy is the most successful in society. Thus individuals select a strategy at time t based on the fitness before $\tau \geq 0$ time instance. We introduce the variables $x_\tau = x(t-\tau)$, $y_\tau = y(t-\tau)$, $z_\tau = z(t-\tau)$ and $w_\tau = w(t-\tau)$. Since we are interested in inferring the obtained results using fundamental principles of biological systems, we maintain the constraint $x_\tau + y_\tau + z_\tau + w_\tau = 1$ along with $x_\tau, y_\tau, z_\tau, w_\tau \in [0, 1]$ throughout the article. This constraint helps us to eliminate one independent variable and construct a simple eco-evolutionary model. The respective average fitness of cooperators, punishers, defectors and free space is given by

$$\begin{aligned} f_{\mathbf{C}} &= x_\tau + y_\tau + \sigma_1 w_\tau = (1-\sigma_1)x_\tau + (1-\sigma_1)y_\tau - \sigma_1 z_\tau + \sigma_1, \\ f_{\mathbf{P}} &= x_\tau + y_\tau - \delta z_\tau + \sigma_2 w_\tau = (1-\sigma_2)x_\tau + (1-\sigma_2)y_\tau - (\delta+\sigma_2) z_\tau + \sigma_2, \\ f_{\mathbf{D}} &= \beta x_\tau + (\beta-\delta) y_\tau + \sigma_3 w_\tau = (\beta-\sigma_3)x_\tau + (\beta-\delta-\sigma_3)y_\tau - \sigma_3 z_\tau + \sigma_3, \text{and}, \\ f_{\mathbf{F}} &= 0. \end{aligned} \tag{4.4}$$

We assume all players die with a uniform rate $\xi > 0$. Thus, our proposed delayed system looks like

$$\begin{aligned} \dot{x} &= x[f_{\mathbf{C}} - \xi], \\ \dot{y} &= y[f_{\mathbf{P}} - \xi], \\ \dot{z} &= z[f_{\mathbf{D}} - \xi]. \end{aligned} \tag{4.5}$$

Thus substituting Eq. (4.4) in Eq. (4.5), we obtain

$$\begin{aligned} \dot{x} &= x[(1-\sigma_1)x_\tau + (1-\sigma_1)y_\tau - \sigma_1 z_\tau + (\sigma_1 - \xi)], \\ \dot{y} &= y[(1-\sigma_2)x_\tau + (1-\sigma_2)y_\tau - (\delta+\sigma_2) z_\tau + (\sigma_2 - \xi)], \\ \dot{z} &= z[(\beta-\sigma_3)x_\tau + (\beta-\delta-\sigma_3)y_\tau - \sigma_3 z_\tau + (\sigma_3 - \xi)]. \end{aligned} \tag{4.6}$$

Note that $\tau = 0$ gives the non-delayed system. In the subsequent section, we

comprehensively discuss the difference between the outcomes in delayed and non-delayed systems.

4.2 Numerical Results

4.2.1 Comparison between delayed and non-delayed model

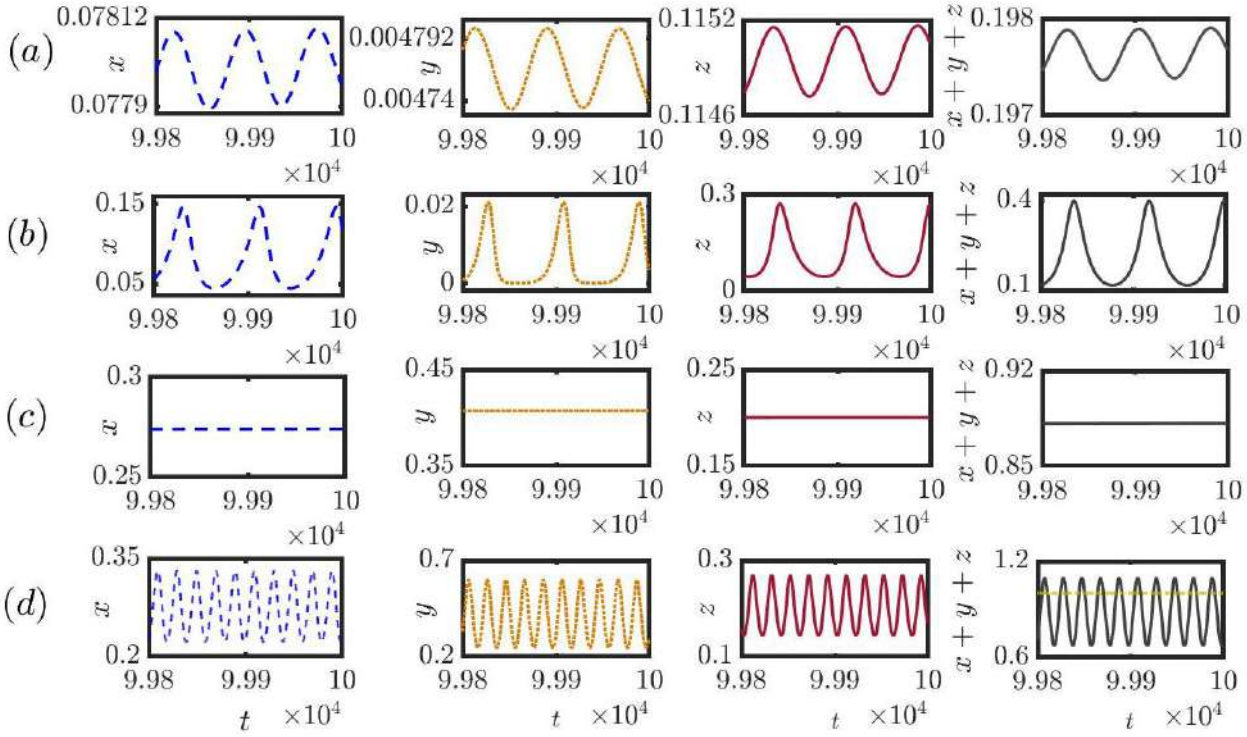

Figure 4.1: **Time series comparison: delay-free vs. delayed systems**: Panels (a) and (c) show dynamics of the system (4.6) without delay ($\tau = 0$), exhibiting small oscillations or convergence to equilibrium. Panels (b) and (d) introduce delay ($\tau = 0.24,\ 1.5$), amplifying oscillations and, in some cases, causing overcrowding ($x + y + z > 1$). Columns represent the time evolution of cooperators, punishers, defectors, and total population. Initial states: $(0.3, 0.3, 0.3)$ (no delay), $(0.25, 0.25, 0.25)$ (delay). Parameters: (a-b) $\xi = 0.50$, $\beta = 2.15$, $\delta = 1.4$, $\sigma_1 = 0.52$, $\sigma_2 = 0.72$, $\sigma_3 = 0.41$; (c-d) $\xi = 0.80$, $\beta = 1.25$, $\delta = 0.30$, $\sigma_1 = 1.00$, $\sigma_2 = 1.50$, $\sigma_3 = 0.60$.

To understand the impact of time delay in population dynamics, specifically in the context of a prisoner's dilemma game, we present the comparative temporal behavior of variables in the presence and absence of delay in Fig. (4.1). To start with, we consider the values of the parameters as $\xi = 0.50$, $\beta = 2.15$, $\delta = 1.4$, $\sigma_1 = 0.52$, $\sigma_2 = 0.72$ and $\sigma_3 = 0.41$ in the subfigures (a-b). Subfigures of (a) demonstrate small amplitude oscillations of all variables without delay. Clearly,

the chosen parameter values help the defectors to dominate others as we identify the inequality $z > x > y$. It should be noted that our observation may alter for a different set of initial conditions, as the system (4.6) is multistable. Later, we will examine the role of initial conditions in our model in detail. We fix the initial conditions at $(x_0, y_0, z_0) = (0.3, 0.3, 0.3)$. We further set the initial conditions for the delay variables as $x_\tau(0) = 0.25, y_\tau(0) = 0.25$, and $z_\tau(0) = 0.25$ for the subfigures in the presence of delay. The chosen parameter values and initial conditions provide an opportunity to maintain biodiversity by allowing the coexistence of all strategies in subfigures (a-b). The range of oscillations for $x \in [0.0775, 0.0779]$, $y \in [0.004732, 0.00477]$, and $z \in [0.1145, 0.1148]$ is petite in subfigures (a), where the sum of the population lies within the range $[0.197, 0.1975]$. Since the punishment parameter's value ($\delta = 1.4$) is high enough, punishers can not afford to survive in the long run, despite the free space-induced benefits towards the punishers being higher as per our chosen parameter values ($\sigma_2 > \sigma_1 > \sigma_3$). Since the temptation to defect is high for the defectors as $\beta = 2.15$, defectors are able to overcome the hurdle in the long run in our model. We further analytically calculate the interior equilibrium point $(0.0777, 0.0047, 0.1147))$ for this set of parameter values, which is found to be an unstable focus node as the eigenvalues of the Jacobian at this point are $\lambda_1 = 0.1236$, and $\lambda_{2,3} = -0.004 \pm 0.0785i$ where $i = \sqrt{-1}$. To investigate the delay effect, we allow a small amount of delay $\tau = 0.24$ in the state variables in subfigures (b) by keeping fixed all the parameters' values and initial conditions of subfigures (a). This inclusion of delay will not alter the inequality $z > x > y$ observed in subfigures (a); however, the amplitude of oscillations amplifies. We find $x \in [0.0447, 0.1462]$, $y \in [0.0001126, 0.02117]$, and $z \in [0.04503, 0.2736]$ in subfigures (b) and their overall sum remains bounded in $[0, 1]$.

A striking difference is also observed for the subfigures (c-d) with the fixed parameter values $\xi = 0.80$, $\beta = 1.25$, $\delta = 0.30$, $\sigma_1 = 1.00$, $\sigma_2 = 1.50$, and $\sigma_3 = 0.60$ and fixed initial conditions $x_0 = 0.3$, $y_0 = 0.3$ and, $z_0 = 0.3$. The subfigure is drawn additionally with the delay parameter $\tau = 1.5$ with fixed initial condition $x_\tau(0) = 0.25, y_\tau(0) = 0.25$, and $z_\tau(0) = 0.25$. Subfigure (c) reveals the coexistence of all strategies, and we analytically calculate the interior equilibrium $(0.274, 0.407, 0.2)$ for the chosen parameter values. We find this steady state is a locally stable focus node as the eigenvalues of the Jacobian at this steady state are $\lambda_1 = -0.0208$, $\lambda_{2,3} = -0.3327 \pm 0.2251i$. Interestingly, the punishers' population is the dominant in this case as we identify the inequality $y > x > z$. The lower abundance of defectors is due to the choice of insufficient temptation to defect ($\beta = 1.25$) and free space-induced benefits towards defectors $\sigma_3 = 0.60$ is lower. Punishers overcome the fierce struggle as punishment parameter value $\delta = 0.30$ is chosen sufficiently low. Punishers use their own resources to penalize the defectors, and since δ is chosen low here, punishers' resources are not overly utilized. Furthermore, our selected parameter values suggest free space-induced benefits toward punishers are higher compared to others ($\sigma_2 > \sigma_1 > \sigma_3$). The addition of a time delay of suitable strength not only destroys the stability of this interior point but also yields an overcrowded solution as $x + y + z$ exceeds 1. This introduction of time delay leads to an instantaneous change in the system's dynamics.

The emergence of these oscillations hints us the spontaneous emergence of cyclic

dominance among those strategies. In the following subsection, we discuss this occurrence in more detail.

4.2.2 Cyclic dominance

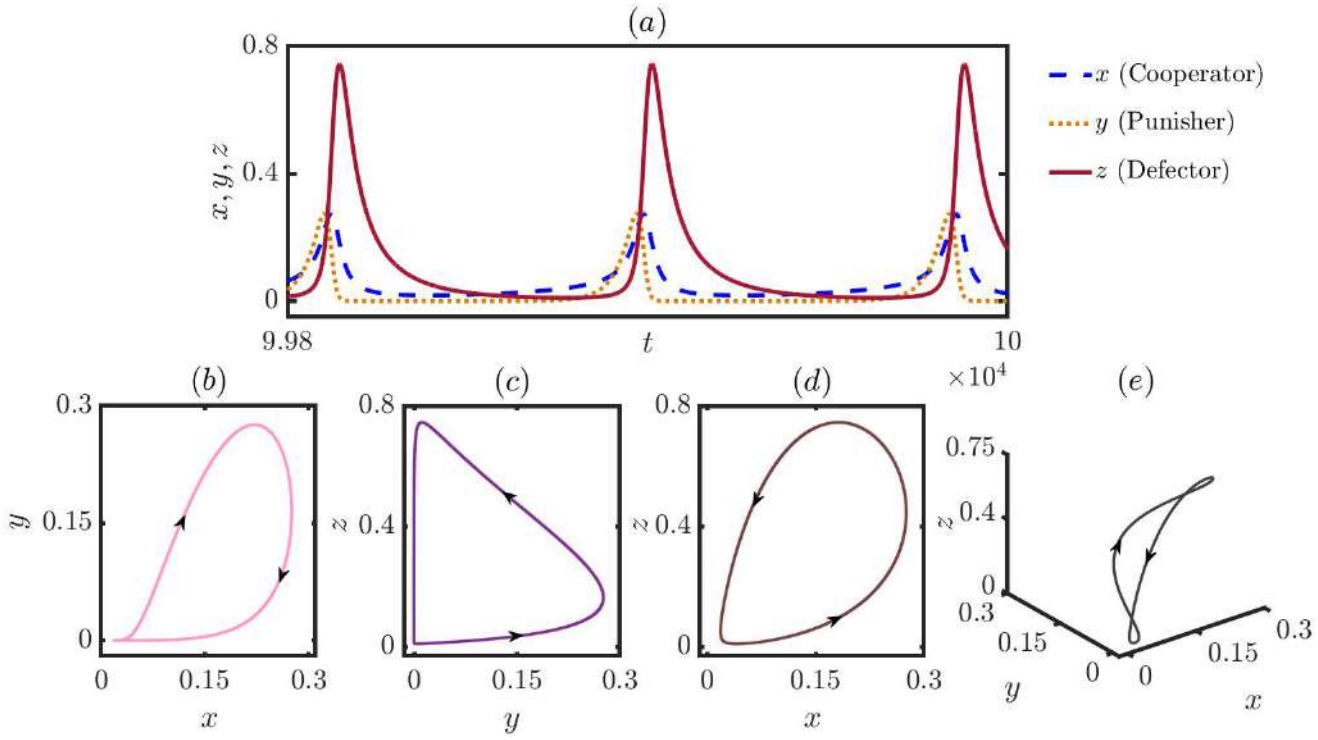

Figure 4.2: **Cyclic dominance among three competing strategies**: (a) Temporal dynamics of the oscillatory coexistence of all three strategies exhibiting the emergence of cyclic dominance among the species that allows each speices to dominate others. The following parameter values are chosen for numerical simulation: $\xi = 0.5$, $\beta = 2.5$, $\delta = 1.39$, $\sigma_1 = 0.52$, $\sigma_2 = 0.72$, $\sigma_3 = 0.41$ and, $\tau = 0.019$. Higher value of the temptation parameter β facilitates the defectors although the punishment parameter δ helps controlling their population by penalizing them. On the other hand cooperators get more benefit from the altruistic free space compared to the defectors due to our chosen parameter values, which helps in maintaining the coexistence of all three strategies. Phase portraits of the periodic attractor along with the direction of the flow in (b-d) two dimensions and in (e) three dimension. The initial values for the state variables associated with the player strategies are considered to be, $(x_0, y_0, z_0) = (0.3, 0.3, 0.3)$ and those for the delayed variables, are considered to be, $(x_\tau(0), y_\tau(0), z_\tau(0)) = (0.25, 0.25, 0.25)$.

We consider the same parameter values $\xi = 0.50$, $\beta = 2.5$, $\delta = 1.39$, $\sigma_1 = 0.52$, $\sigma_2 = 0.72$, $\sigma_3 = 0.41$ and $\tau = 0.019$ and integrate our model (4.6) using Huen's method [184] with 10^7 number of iterations. After discarding a sufficiently long transient of length 9.9×10^6 iterations, we present their delayed eco-evolutionary dynamics in Fig. (4.2). We maintain the same initial conditions as in Fig. (4.1) (b).

Interestingly, the delay parameter helps the system maintain oscillatory dynamics that attest to the emergence of cyclic dominance in our model. Cyclic dominance [185] allows each strategy to dominate others for a specific time window, which is impossible if we attain steady-state dynamics. The periodic dynamics of each variable portray the coexistence of competing strategies. The maxima of each variable in the first row in Fig. (4.2) unveils $z_{max} > x_{max} > y_{max}$. Since our chosen value of the temptation parameter, $\beta = 2.50$ is higher than the payoffs of a cooperator and punisher, z_{max} can attain such larger values in its temporal dynamics. On the other hand, the punishment parameter, δ, is fixed at 1.39, which helps to control the defection by penalizing them; however, the punisher also loses this amount while punishing the defectors. This makes punishers vulnerable in society for our specific choices of initial conditions and parameter values. Furthermore, the interplay between all parameters is more pronounced in this figure, as despite altruistic free space contributing more towards the punishers and lesser towards the defectors ($\sigma_2 > \sigma_1 > \sigma_3$), punishers are still unable to take over the defectors. The temptation to defect is so high that it helps to ignore the selfless contribution of free space, and thus defectors can gain a higher density in the long run. Nevertheless, periodic oscillation allows a window of opportunity for the cooperators to invade the defectors, who in turn can invade the punishers and, ultimately, punishers are able to overrun the cooperators. In this way, cyclic dominance emerges spontaneously and captures the beauty of governing eco-evolutionary dynamics. We further confirm that the obtained solution and their sum remain bounded within $[0, 1]$, providing a biologically feasible solution.The two and three-dimensional projections of the attractor, along with the direction of the flow, are plotted in the second row of Fig. (4.2).

In the next subsection, we will scrutinize the underlying mechanism that drives the system toward an oscillatory behavior.

4.2.3 Exploring the role of delay in the eco-evolutionary dynamics

To further study the effect of delay in our model (4.6), we keep all parameter values fixed at $\xi = 1.2$, $\beta = 1.6$, $\delta = 0.30$, $\sigma_1 = 1.35$, $\sigma_2 = 1.50$, $\sigma_3 = 1.35$ and vary the delay parameter τ within the closed interval $[8, 12]$ with a fixed step length 0.005 and plot the bifurcation diagrams in Fig. (4.3). We find out the cooperators extinct in the long run throughout the interval, as x remains at zero in Fig. (4.3) (b). Nevertheless, the dynamics of the punishers and defectors offer a great variety of dynamical behaviors. Our system experiences a series of transitions from a periodic to a chaotic state as τ is varied in Fig. (4.3). All these figures provide valuable insight into how our system responds to changes in the delay parameter.

We identify punishers overrule the defectors in the steady state regime for the chosen initial conditions and parameter values. Assuming an initial condition of $(0.1, 0.2, 0.5)$ for the state variables and $(0.3, 0.3, 0.3)$ for the delayed variables, we performed 10^7 iterations of the system (4.6). We discarded the first 9.8×10^6 iterations to ensure that our analysis focuses only on the system's long-term behavior. However, this steady state loses its stability and gives rise to a periodic solution

beyond a specific value of τ. We will provide a thorough analysis later to detect the point of this Hopf bifurcation analytically. Interestingly, the range of y is vast compared to that of z (c.f. subfigures (c-d) of Fig. (4.3)). This indicates the punishers gain some kind of opportunity through our setup and can dominate the defectors. Notably, the free space-induced benefits towards the punishers are slightly larger than others ($\sigma_2 > \sigma_1 = \sigma_3$) in this figure. Interestingly, we observe this periodic solution loses its stability and gives rise to a new periodic solution with twice the period of the original one as the delay parameter value is increased. As τ is further increased, the system goes through additional period-doubling bifurcations, giving rise to periodic solutions with four times, eight times, and so on, the period of the original periodic attractor. Eventually, the system enters a chaotic regime, where the dynamics are unpredictable and sensitive to small perturbations. To further validate our findings, we use the Lyapunov exponent to measure the sensitivity of our eco-evolutionary model (4.6) to small perturbations in its initial conditions. The calculation of Lyapunov exponents for delayed systems is generally more complicated than that of non-delayed systems due to the need to consider the effect of time delay on the system's dynamics. We calculate the Lyapunov exponents of the system for $\tau \in [8, 12]$ by increasing τ with a fixed step length 0.04. Since our system (4.6) contains only one delay parameter, the number of Lyapunov exponents is equal to the dimensionality of the non-delayed system (i.e., the number of variables in the system). We plot each of these Lyapunov exponents in Fig. (4.3) (a).

The first and the second largest Lyapunov exponents reveal valuable information about our system. The largest Lyapunov exponent λ_1, shown in deep purple, remains negative up to a certain value of τ, indicating stable steady states. For a suitable range of the delay parameter τ, it converges to zero, which reflects a standard signature of having a periodic solution in our system (4.6). In both of these stable states, nearby trajectories converge towards each other, meaning that small perturbations in the system's initial conditions lead to similar outcomes. Beyond this range of τ, it offers only the positive value describing the rate of exponential divergence of nearby trajectories. This positive Lyapunov exponent λ_1 identifies the onset of chaos and validates our bifurcation diagram, which reflects the period doubling route to chaos. Interestingly, most of the previous studies on Lyapunov exponents only concentrate on the largest Lyapunov exponent and ignore the possibility of extracting invaluable information from the other Lyapunov exponents. The second-largest Lyapunov exponent λ_2, shown in cyan color dashed line in Fig. (4.3) (a), discloses fascinating details on the bifurcation point in our study in this chapter. It initially remains at negative values when the system's behavior remains constant over time. As the system experiences Hopf bifurcation, it attains a value of zero and again provides only negative values for a range of τ. At the Hopf bifurcation point, the system changes from having a stable steady state to a stable periodic orbit, as observed in y and z variables in subfigures (c-d) of Fig. (4.3). The second-largest Lyapunov exponent λ_2 again takes the zero value while the system undergoes a period-doubling bifurcation. Furthermore, it acquires the value of zero during the appearance of a new stable periodic solution with twice the period of the original periodic attractor. In this way, the second-largest Lyapunov exponent helps to validate the points where period-doubling bifurcation occurs. It assumes

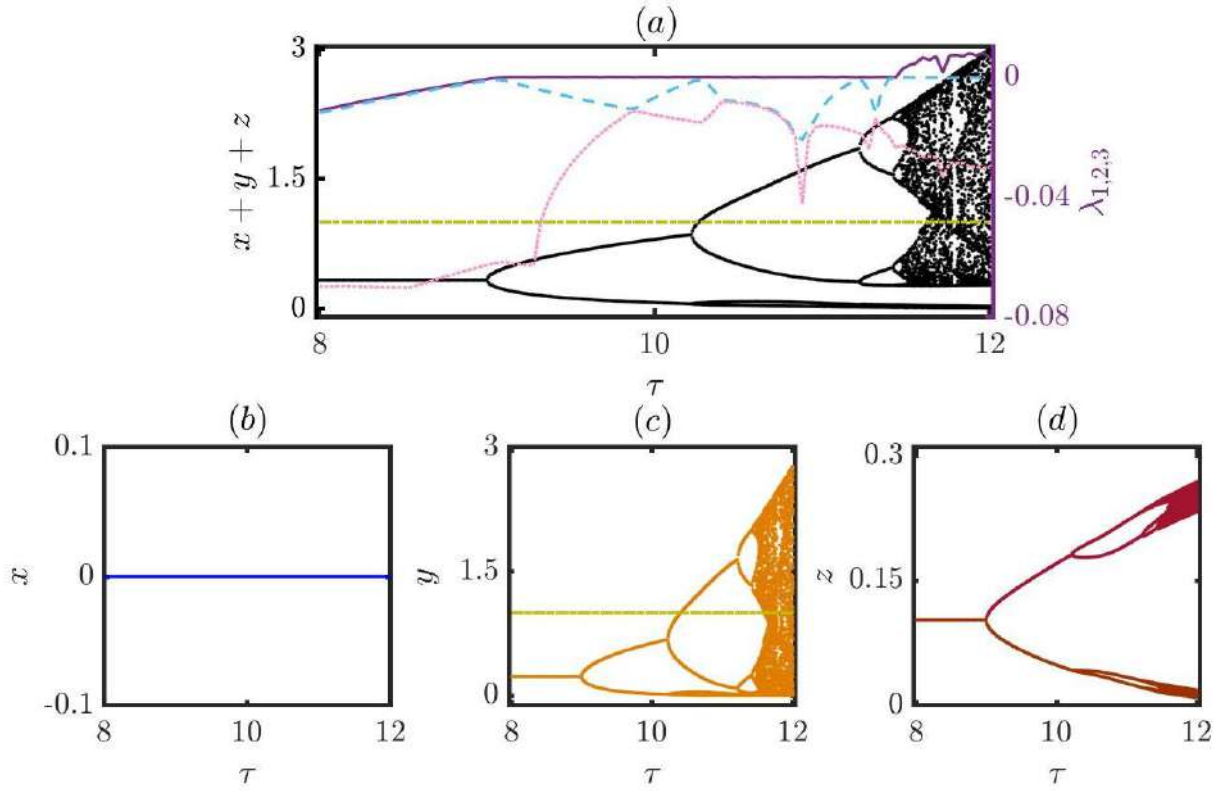

Figure 4.3: **Bifurcation and Lyapunov exponents of the delayed system**: (a) Bifurcation diagram of total population $x + y + z$ with increasing delay τ, showing Hopf bifurcation at $\tau = 8.99$, followed by period-doubling and eventual chaos. Lyapunov exponents λ_1 (solid purple), λ_2 (cyan dashed), and λ_3 (pink dotted) confirm transitions: λ_1 distinguishes steady (< 0), periodic ($= 0$), and chaotic (> 0) states; λ_2 stays negative except at bifurcations; λ_3 remains negative throughout. Panels (b–d) show corresponding bifurcations for x, y, and z, respectively, confirming coexistence of punishers and defectors with punisher dominance. Parameters: $\xi = 1.20$, $\beta = 1.60$, $\delta = 0.30$, $\sigma_1 = 1.35$, $\sigma_2 = 1.50$, $\sigma_3 = 1.35$; initial states: $(0.1, 0.2, 0.5)$ (non-delayed), $(0.3, 0.3, 0.3)$ (delayed). Step sizes: $\Delta\tau = 0.005$ (bifurcation), 0.04 (Lyapunov) over $\tau \in [8, 12]$.

a value of zero when τ is larger and close to 12, as the system experiences a series of period-doubling bifurcations. The third Lyapunov exponent λ_3 shown in light pink dotted line in Fig. (4.3) (a) always remains negative throughout the interval of investigation. All these Lyapunov exponents help characterize the system's dynamics and provide a better understanding of its sensitivity to initial conditions and predictability.

In spite of obtaining such captivating dynamics, we can not infer a few of these results from the biological viewpoint. The dynamics must be bounded within $[0, 1]$; otherwise when the total population exceeds the maximum value 1, we obtain an overcrowded solution. We plot a dash-dotted horizontal line in subfigures (a) and (c) of Fig. (4.3), below which the dynamics remain bounded within $[0, 1]$. Within the feasible range, we observe steady states as well as periodic oscillations in this figure. Apart from this dynamical behavior, our system (4.6) may depict quasiperiodic

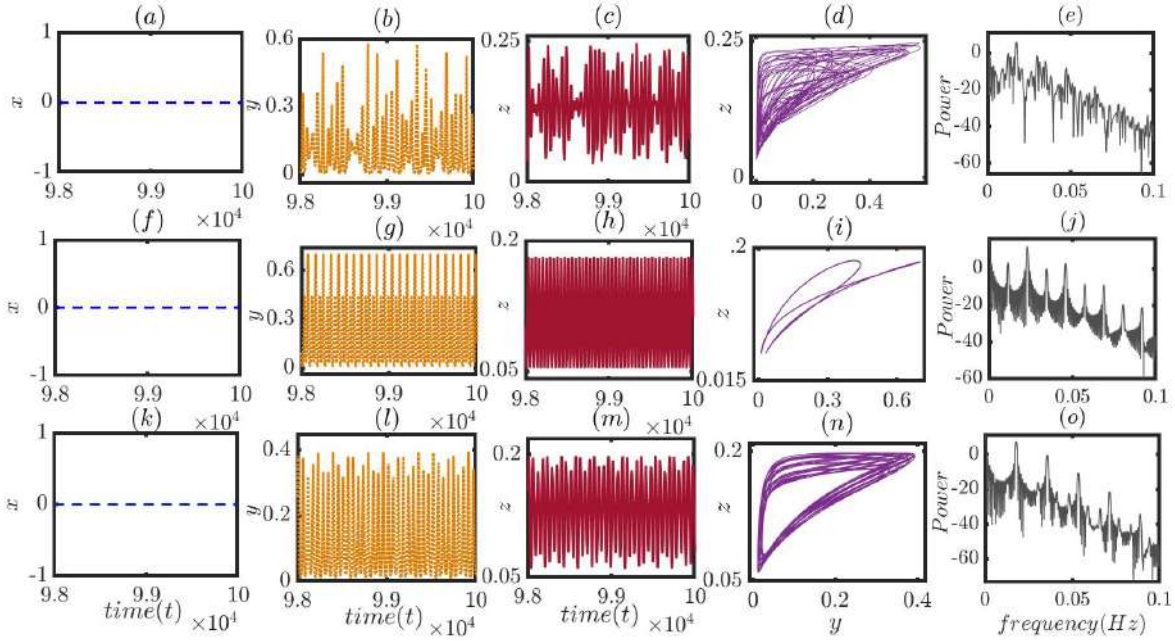

Figure 4.4: **Dynamical regimes and power spectra of player populations**: Temporal dynamics and spectral properties are shown for three parameter sets (β, τ), illustrating the effect of temptation and delay. Time series of cooperators (x), punishers (y), and defectors (z) are in columns 1–3; the y-z phase portrait appears in column 4; power spectra via FFT in column 5. Panels (a–e): chaotic dynamics in y and z for $(1.93, 11.64)$; (f–j): two-period oscillations for $(1.64, 10.73)$; (k–o): quasi-periodicity with irregular patterns for $(1.90, 10.50)$. Cooperators remain extinct in all cases due to fixed parameters: $\xi = 1.2$, $\delta = 0.3$, $\sigma_1 = 1.35$, $\sigma_2 = 1.5$, $\sigma_3 = 1.35$. Spectral peaks confirm dynamical types. Initial conditions: non-delayed $(0.1, 0.2, 0.5)$; delayed $(0.3, 0.3, 0.3)$. Final dynamics shown after discarding first 98×10^5 of 10^7 iterations.

oscillation too, under a suitable choice of parameter values and initial conditions. The temptation parameter always plays a crucial role in determining the fate of defectors. If it is very large, defectors gain massive benefits that are too large to overcome. Under that circumstances, defectors are the unbeatable winners. If the temptation parameter is moderate, one can think about any approach to overcome the natural selfish instinct. To understand the effect of the temptation parameter in our study, we keep fixed all the parameter values and initial conditions as in Fig. (4.3) and choose three different pairs of values of (β, τ). The dynamics offer a plethora of new behavior depending on these choices. We present all these observations in Fig. (4.4). Clearly, the temptation to defect can not help cooperators survive and evolve. Thus, we are never able to observe the survival of cooperators in Fig. (4.4) for the chosen parameter values and initial conditions. The cooperators' fraction x always remains at zero. However, the dynamics of y and z again offer a wide variety. The chaotic dynamics observed in Fig. (4.3) is an overcrowded solution as $x + y + z > 1$; hence we can not offer any biological interpretations for such an attractor. The upper panel of Fig. (4.4) shows a chaotic oscillation in y and z for $\beta = 1.93$ and

$\tau = 11.64$; where $x + y + z \in [0, 1]$. We plot the power spectrum corresponding to this temporal dynamics, which exhibits a broad range of frequencies in their power spectra, with no single dominant frequency. To avoid repetition, we chose not to display the Lyapunov exponent plot in this instance, but we have confirmed the validity of our results through its inclusion. Here for this set of parameter values, there is no ultimate winner among punishers and defectors, as they dominate one another in an unordered way, as revealed in subfigure (d). The chaotic oscillation never allows strict dominance over one another. Nevertheless, this scenario may alter for a different choice of (β, τ), and one may dominate another in the long run. We choose $\beta = 1.64$ and $\tau = 10.73$ for the middle panel of this figure. The change in two parameter values does not alter the fortune of the cooperators, and they remain extinct in the long run, as shown in subfigure (f). However, maximum values of punishers' density can dominate the defectors' density for this set of parameter values (see subfigures (g-i)). We identify the oscillations that portray two-periodic dynamics. We plot the power spectrum of the time series in subfigure (j) and find these dominant frequencies correspond to the frequencies at which the signal repeats itself. All these subfigures confirm that the system (4.6) spends some time oscillating with one amplitude or frequency, then switching to the other amplitude or frequency, and continue oscillating in this way for these parameter values and initial conditions. The phase portrait in the yz plane in subfigure (i) of Fig. (4.4) also confirms this behavior.

The dynamical behavior is much more complex in the bottom panel of Fig. (4.4) where we choose $\beta = 1.9$ and $\tau = 10.5$. Cooperators are still unable to overcome the fierce struggle for resources and end up saturating in zero density, as shown in Fig. (4.4) (k). Punishers and defectors keep oscillating at two or more incommensurate frequencies, meaning that their ratio is irrational. The oscillation frequencies of these two populations exhibit a pattern that repeats itself over time, but the repetition is not strictly periodic (see subfigures (l-n)). The power spectrum of this attractor in of Fig. (4.4) (o) confirms the appearance of a broad band of frequency components rather than distinct peaks at specific frequencies. And the width of these bands indicates the degree of incommensurability between the frequencies. This non-periodic and non-chaotic temporal behavior is a subject of deeper investigation and can provide insights into the behavior of complex systems. We would like to investigate the underlying mechanisms driving the system's quasiperiodic dynamics and identify the key factors influencing its behavior in the future.

Figure (4.4) highlights the importance of these two parameters β and τ. In the following subsection, we will investigate the interplay of these two parameters in much more detail.

4.2.4 Investigating the complex relationship between the temptation parameter and delay parameter

Our proposed eco-evolutionary delay model explores various scenarios and player population diversities in society by changing the parameters in the model. The time delay parameter, τ, is critical in altering the population dynamics, while the

payoff parameters determine the viability of competing strategies in society. We analyze the survivability of different strategies and their dynamical behaviors by simultaneously varying two parameters: the temptation payoff parameter, β, and the time delay parameter, τ, in a two-dimensional parameter space. We investigate the behavior of our model (4.6) by varying $\beta \in (1, 2]$ and $\tau \in [8, 12]$ with fixed step length 0.01, while keeping other parameters fixed at $\xi = 1.20$, $\delta = 0.30$, $\sigma_1 = 1.35$, $\sigma_2 = 1.50$, and $\sigma_3 = 1.35$. The initial fractions for the non-delayed state variables are $(0.1, 0.2, 0.5)$, while the initial fractions of the delayed variables are $(0.3, 0.3, 0.3)$. This two-dimensional parameter space in Fig. (4.5) provides plenty of information about our proposed delayed system (4.6). In the classical PD game, defectors have a primary advantage over cooperators. We consider the chosen advantages from the free space as attributes to be equal for both the cooperator and defector populations ($\sigma_1 = \sigma_3 = 1.35$). Moreover, the initial fraction of the population of cooperators is much lesser than others. Consequently, we end up with a society free from cooperators for any choice of temptation and delay parameters.

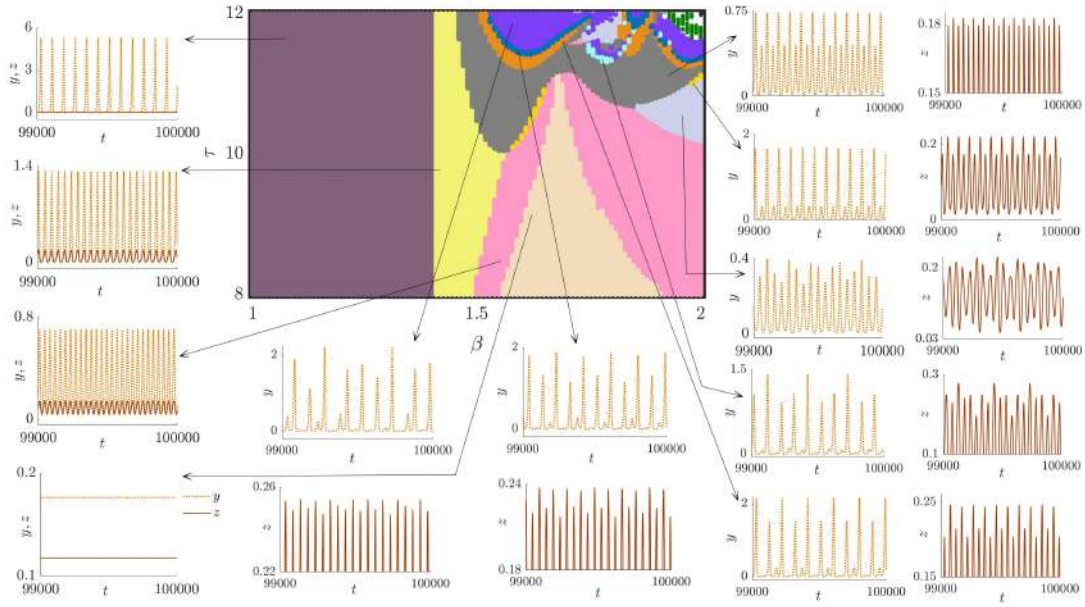

Figure 4.5: **Parameter space of β and τ showing diverse dynamics**: The β–τ space ($\beta \in [1, 2]$, $\tau \in [8, 12]$) reveals rich dynamics of punishers (y) and defectors (z), with cooperators extinct due to initial advantage of defectors, despite $\sigma_1 = \sigma_3$. Other parameters: $\xi = 1.20$, $\delta = 0.30$, $\sigma_{1,3} = 1.35$, $\sigma_2 = 1.50$; initial conditions $(0.1, 0.2, 0.5)$ (non-delayed) and $(0.3, 0.3, 0.3)$ (delayed). Mauve: periodic y-only dynamics; lime yellow and light pink: periodic coexistence ($y + z > 1$ and bounded, respectively); beige: steady coexistence; grey and yellow: period-2 (bounded and overcrowded); orange and deep blue: period-4 and period-8 (overcrowded); violet: chaos (bounded/unbounded); cyan and light purple: period-6 and quasiperiodicity; deep green: extinction; white: unbounded or defector-only states. Time series shown accordingly.

Since punishers receive significantly higher benefits ($\sigma_2 = 1.50$) from the free space compared to others, only the punishers are observed to survive periodically

(indicated by mauve colored region in Fig. (4.5)) while cooperators and defectors can not compete. In this regard, the fraction of the punisher population exceeds the threshold 1. When we vary the time delay by keeping the value of β fixed, we observe an increase in the amplitude of oscillation but no change in the behavior of the competing strategies. However, an increment of β always helps the defectors back in the contest. We locate a small area highlighted by lime yellow in Fig. (4.5) where defectors can coexist with the punishers. Beyond $\beta = 1.4$, the punishers and defectors begin to dominate one another depending on the time window and yield a periodic attractor here. This periodic oscillation occurs due to the Hopf bifurcation, and the value of τ, where the Hopf bifurcation occurs, gradually decreases as the value of β increases. Notably, Ref. [99] also found this critical value of $\beta = 1.40$, beyond which defectors are very hard to defeat. As we further increase the temptation to defect, we observe an attractor with period-2 emerges at $\beta = 1.46$ (See the deep grey area of Fig. (4.5)). We further add the temporal behavior of different regions of the parameter space in Fig. (4.5). We observe the z_{max} increases as β increases. In other words, the progressive growth of β facilitates the growth of the defector populations. However, the solution remains overcrowded as $y + z$ exceeds the upper bound of unity.

Noticably, we are able to detect a fair portion, shown by light pink in Fig. (4.5), where the overall population remains bounded within $[0, 1]$. The punishers and defectors oscillate periodically, allowing each to dominate the other depending on the time window. Even we are able to detect a very narrow yellow region in the parameter space, where the dynamics of y and z variables exhibit periodic oscillations with period-2. In this region the overall population density $x + y + z$ remains within 1. Note that although society lacks the cooperators, punishers are also special kind of cooperators with some additional power to punish the defectors using their own resources. The absence of cooperators in the community is thus somehow controlled. More importantly, neither the punishers nor the defectors emerge as a dominant winner in this parameter space. Either of them can enjoy being dominant for a time window. However, their fate alters, and the other strategy dominates society for a different time course. Increasing the delay parameter τ leads to an amplification of oscillation amplitudes, which undergo period-doubling bifurcation as explained earlier. This results in oscillations with a period of 4, as highlighted in the orange section of Fig. 4.5. Further increment of τ results in the appearance of eight periodic dynamics in the deep blue region of Fig. 4.5, where the proportion of punishers and defectors oscillate. However, these orange and deep blue regions occur only in overcrowded solutions, where the sum of $x + y + z$ exceeds 1. As we continue to increase the value of τ, our model (4.6) may exhibit chaotic behavior, as indicated by the violet area in the $\beta - \tau$ parameter space. In this region, the sum of $x+y+z$ may or may not be bounded within 1. Our findings are supported by power spectrum analysis, but these results are not presented here to avoid redundancy.

Figure (4.5) also displays a beige colored region where the system (4.6) converges to a steady state with no cooperators. Furthermore, the system (4.6) may converge to the extinction equilibrium $(0, 0, 0)$, shown by deep green in Fig. (4.5), resulting in a population-free state (time series not shown). In the next section, we will perform an analytical calculation for each of these steady states. The white region

in the parameter space is identified as a region where the solution may become unbounded or converge to the steady state $\left(0, 0, 1 - \frac{\xi}{\sigma_3}\right)$. This disappearance of attractors is similar to what is discussed in Ref. [59]. In the future, we aim to investigate the underlying cause of this disappearance of attractors in our model. It is worth noting from an ecological perspective that the steady-state solution is now bounded within the range of $[0, 1]$. Interestingly, the cooperator's survivability cannot be facilitated by either the temptation or delay parameter in the entire domain of analysis. Increasing the value of β only helps to promote the density of defectors depending on the initial conditions and other parameter values. The delay parameter leads to the emergence of periodic behavior, allowing the populations to dominate each other regularly. However, periodic and chaotic attractors are not the only possible outcomes that can be obtained by varying the parameters. In Fig. 4.5, we identify a light purple region where the density of punishers and defectors display quasiperiodic oscillations that remain bounded within the range of $[0, 1]$. We additionally identify a regime, shown by cyan in Fig. (4.5), where both y and z variables oscillate with six periodic dynamics.

In the upcoming subsection, we will shed light on the impact of additional system parameters on our model. Specifically, we will investigate the effects by varying two different parameters while keeping the others fixed. By doing so, we aim to uncover valuable insights into the influence of these specific parameters on our model's behavior.

4.2.5 System parameters and eco-evolutionary dynamics: unveiling the hidden connections

In the context of our study in this chapter, it becomes evident that when free space presents a more favorable opportunity for defectors, while keeping other parameter values constant, their survival becomes highly likely. In such scenarios, if the benefit induced by free space towards defectors, denoted as σ_3, reaches a sufficiently large value, the other strategies face intense competition and may eventually disappear from the societal dynamics. This observation is depicted in Fig. (4.6) (a), where we observe that an increase in the mortality rate ξ leads to an equilibrium of extinction, rendering no viable survivors. Conversely, when the mortality rate is moderate, the system exhibits the potential to sustain a society solely composed of cooperators, contingent upon other parameter considerations. Further reducing the mortality rate enables the coexistence of cooperators and defectors. However, an amplification of the free space-induced benefit toward defectors favors their dominance, ultimately eliminating cooperators from the competition. Consequently, under such circumstances, defectors emerge as the sole surviving strategy.

An analogous observation is evident when examining Fig. (4.6) (b), which further accentuates this phenomenon of interest. Once again, we observe that as mortality rate escalates, no strategies are able to evolve, ultimately leading to their eventual extinction over extended time period. However, within the expansive $\beta - \xi$ parameter space, a distinct region emerges where the survival of solely cooperators becomes feasible. It is important to note, however, that this region diminishes in size as

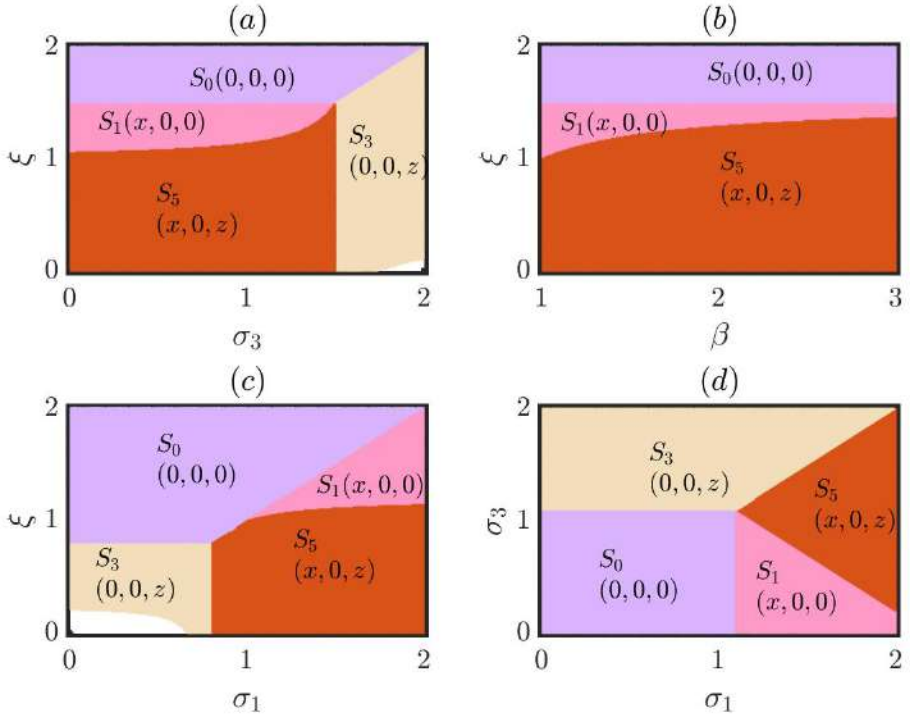

Figure 4.6: **Exploring system parameters in eco-evolutionary dynamics**: (a) Increased mortality ξ causes extinction, unless defectors gain high free space benefit, enabling their survival. Coexistence and cooperator-only states also emerge. (b) Higher ξ again drives extinction, with a diminishing cooperator-only region as temptation β increases; coexistence remains possible. (c) Boosting cooperator benefit σ_1 increases their density, helping survival despite high ξ; white area indicates unbounded dynamics. (d) Balance between σ_1 and σ_3 shows defectors dominate if their advantage exceeds ξ; cooperators thrive if their benefit surpasses both ξ and σ_3. Punishers are absent due to the chosen parameters and initial states. Fixed values: $\sigma_1 = 1.2$, $\sigma_2 = 1.5$, $\sigma_3 = 1.4$, $\xi = 1.1$, $\beta = 1.5$, $\delta = 0.5$, $\tau = 0.2$ (unless varied); initial conditions: delayed $(0.25, 0.25, 0.25)$, non-delayed $(0.3, 0.3, 0.3)$.

the temptation parameter β increases. This correlation arises from the fact that defectors receive an augmented advantage with a higher β, thereby reducing the space where the sole coexistence of cooperators can only occur. In fact, it is within the moderate range of mortality rate that the majority of the parameter space allows for the coexistence of defectors and cooperators.

In a similar vein, if we delve into the intricate interplay of free space-induced benefits towards cooperators, specifically σ_1, while keeping σ_3 and other parameters fixed, we anticipate a noticeable surge in the density of cooperators, denoted by x, with each incremental value of σ_1. The exquisite subfigure (4.6) (c) illuminates the captivating dynamics that unfold within the system. For lower values of σ_1, the system may initially lack any cooperators. However, as we venture beyond a critical threshold of σ_1, contingent upon the values of other parameters, cooperators reveal their resilience, persisting in the system over extended temporal horizons.

While a higher mortality rate poses a formidable barrier to the survival of any individual, the enhanced free space-induced benefits bestowed upon cooperators hold the potential for their sustenance, even under such adversities. Moreover, within the expanse of the $\sigma_1 - \xi$ parameter space, a significant portion emerges where only defectors can endure due to the relatively diminished contribution of free space towards cooperators. Nevertheless, as the value of σ_1 rises, cooperators resurge, reentering the competitive landscape and forging a coexistence alongside defectors. However, it is crucial to acknowledge the existence of a small region within this parameter space where the dynamics become unbounded over sufficiently long timeframes. The intriguing phenomenon of unboundedness manifests itself in a similar fashion within Fig. (4.6) (a) as well. In the near future, we aspire to delve deeper into this enthralling phenomenon, unveiling the precise mechanisms underlying this unboundedness.

Figure (4.6) (d) vividly illustrates the intricate interplay between the parameters σ_1 and σ_3. Notably, when both of these parameters are lesser than the mortality rate $\xi = 1.10$, the system reaches an equilibrium of extinction, effectively stabilizing the dynamics in an unwanted scenario. When free space provides defectors with a more favorable opportunity compared to cooperators (indicated by $\sigma_3 > \sigma_1$) and σ_3 surpasses the mortality rate ξ, defectors gain substantial advantages, thereby emerging as the sole surviving strategy within that specific parameter space. On the other hand, if σ_1 exceeds both ξ and σ_3, two distinct scenarios unfold, favoring the survivability of cooperators. In one scenario, the parameter choices allow for the coexistence of cooperators and defectors, contingent upon the specific values of σ_3. In the second scenario, cooperators thrive as the sole surviving strategy in the societal dynamics, while all others face extinction. It is worth noting that, due to our chosen parameter values and initial conditions, Fig. (4.6) remains devoid of any punishers, underscoring the fascinating dynamics at play within the system.

Intriguing insights into the behavior of our proposed model iawait us as we explore the captivating Fig. (4.7). Remarkably, we discover that the dynamics remain almost unaffected by variations in the delay parameter, despite we have found a profound effect of τ in this chapter through several earlier discussions (e.g., see Fig. (4.5)). Within Fig. (4.7) (a), we embark on a journey to explore the system's response when simultaneously varying two parameters, namely δ and τ, while maintaining fixed values for other parameters at $\sigma_1 = 1.2$, $\sigma_2 = 1.5$, $\sigma_3 = 1.4$, $\xi = 1.1$, and $\beta = 1.5$. A discernible pattern emerges from our investigation, shedding light on the interplay between fine imposition and the survival prospects of different strategies. At minimal fine levels, coexistence between punishers and defectors prevails within the societal landscape. However, as we escalate the fine magnitude, defectors too succumb to their inability to thrive, leaving behind a society solely populated by punishers. It is worth noting that these outcomes may exhibit variations when other parameter values are chosen differently. Our selection of parameter values deliberately maintains a moderate temptation to defect ($\beta = 1.5$) while endowing punishers with a more advantageous position in the free space hierarchy ($\sigma_2 > \sigma_3 > \sigma_1$). Consequently, cooperators, receiving the least support from free space, struggle to sustain themselves and ultimately face extinction in the long run. Furthermore, this subfigure, Fig. (4.7) (a), stands devoid of cooperators, underscoring the inhospitable

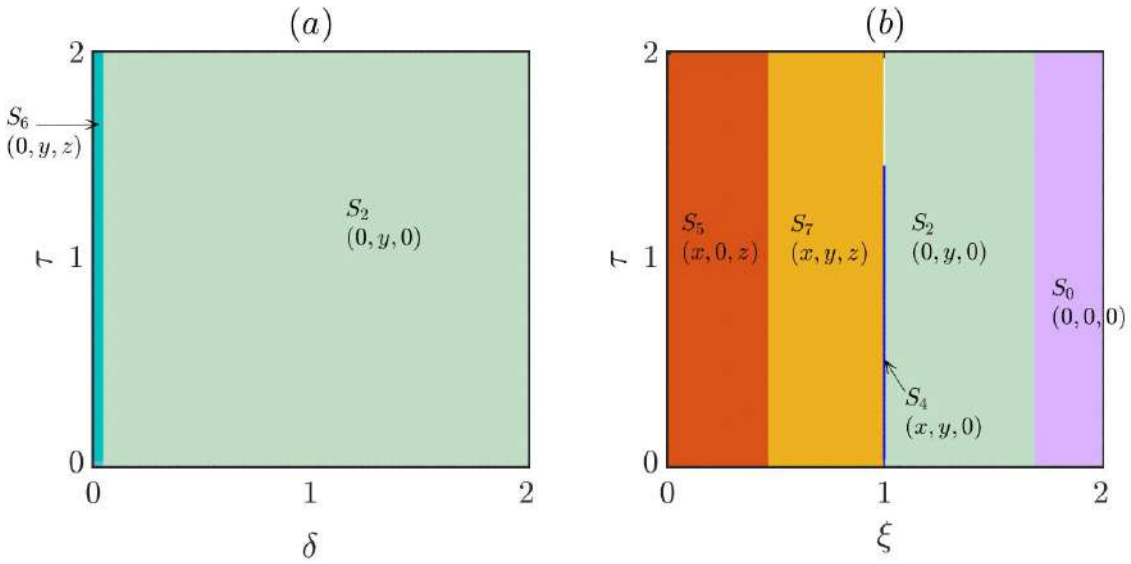

Figure 4.7: **Interplay of delay, mortality, and punishment in suppressing defection**: (a) Varying δ and τ reveals that low punishment allows coexistence of punishers and defectors, while stronger punishment leads to punisher dominance and defector extinction. Outcomes depend on specific parameters, highlighting the balance among temptation, hierarchy, and strategy survival. (b) Varying ξ and τ shows high mortality eliminates all strategies; lower ξ supports sole punishers, then narrow coexistence of cooperators and punishers (defector-free), and eventually full coexistence or cooperator-defector societies. Delay τ has limited impact except in a thin unbounded white region. Fixed parameters: $\sigma_1 = 1.2$, $\sigma_2 = 1.5$, $\sigma_3 = 1.4$, $\beta = 1.5$, $\delta = 0.5$, $\tau = 0.2$ (unless varied). Initial conditions: delayed $(0.25, 0.25, 0.25)$, non-delayed $(0.3, 0.3, 0.3)$.

environment created by the combined influence of fine imposition and delay on their survival prospects. The aforementioned exploration illuminates the intricate dynamics at play, deepening our understanding of the complex interactions within the proposed model.

The captivating subfigure (4.7) (b) unravels the intricate behavior of our model as we simultaneously vary the parameters ξ and τ, while holding the remaining parameters constant at the same values as in subfigure (4.7) (a) with $\delta = 0.5$. Within this visual exploration, we witness the system's remarkable response to these parameter variations, elucidating the delicate balance that governs the survival and coexistence of different strategies. As the mortality rate ξ escalates towards high values, approaching 2, a disheartening scenario unfolds where no strategies manage to endure in the long run. This highlights the adverse consequences of an excessively high mortality rate within the system. However, by reducing the strength of the mortality rate ξ, a fascinating transformation occurs, leading to the emergence of a society comprised solely of punishers. This finding aligns with the insights gleaned from subfigure (4.7) (a), highlighting the intricate relationship between mortality rate and strategy dynamics. It is noteworthy to mention that in our proposed model, punishers themselves embody a distinct form of cooperation. Intriguingly,

within the two-dimensional parameter space with $\xi = 1.0$, we discover a region where cooperators and punishers coexist harmoniously, while defectors remain absent from the societal landscape. This coexistence phenomenon further emphasizes the complex interplay between the investigated parameters. However, as we examine the intricacies portrayed in subfigure (4.7) (b), we observe that the delay parameter τ exhibits limited influence on the emerging state within the investigated range. Notably, a thin white portion in the parameter space for $\xi = 1.0$ unveils the emergence of unbounded dynamics, warranting further investigation into the precise mechanisms behind this intriguing phenomenon. By decreasing the value of the mortality rate ξ even further, we uncover a substantial portion within the parameter space that facilitates the coexistence of all three strategies, fostering biodiversity within the system. As the mortality rate ξ continues to decrease, we witness a captivating transformation where punishers struggle to survive, ultimately leading to a society where cooperators and defectors coexist in delicate harmony. This profound exploration offers invaluable insights into the complex dynamics of our model, unraveling the delicate relationships between mortality rate, delay parameter, and the survival prospects of different strategies.

Both Fig. (4.6) and Fig. (4.7) showcase numerical simulations based on a fixed initial condition. Specifically, the non-delayed variables are initialized with values of $(0.3, 0.3, 0.3)$, while the delayed variables begin with values of $(0.25, 0.25, 0.25)$. These initial conditions serve as the starting point for investigating the intriguing interplay of parameters in our proposed model and their influence on the emergence of eco-evolutionary dynamics. In the subsequent subsection, we will delve into the pivotal role of initial conditions in our model, analyzing how they shape and contribute to the complex dynamics observed within the system. By examining the impact of different initial conditions, we aim to gain a deeper understanding of the intricate relationships between system parameters, initial states, and the resulting eco-evolutionary dynamics.

4.2.6 Uncovering multistability: insights into eco-evolutionary dynamics

We retain the parameter values at $\sigma_1 = 1.2$, $\sigma_2 = 1.5$, $\sigma_3 = 1.4$, $\xi = 1.1$, $\beta = 1.5$, $\delta = 0.5$, and $\tau = 0.2$, consistent with the settings used in our earlier analyses presented in Figs. (4.6) and (4.7). In this subsection, however, we shift our focus to an equally crucial yet often overlooked factor in dynamical models: the role of initial conditions. Unlike parameter sensitivity, which has been extensively studied, the dependency of outcomes on initial population densities unveils another layer of complexity in eco-evolutionary dynamics.

To systematically explore the diversity of dynamical regimes, we vary the initial conditions (x_0, y_0, z_0) while enforcing the biologically motivated constraint $x_0 + y_0 + z_0 = 0.9$. This constraint ensures that the total initial population remains within a realistic and ecologically interpretable range, as the sum of strategic species densities must lie within $[0, 1]$. For comparison, and in alignment with our prior studies, we adopt the baseline configuration $(x_0, y_0, z_0) = (0.25, 0.25, 0.25)$ for the non-delayed

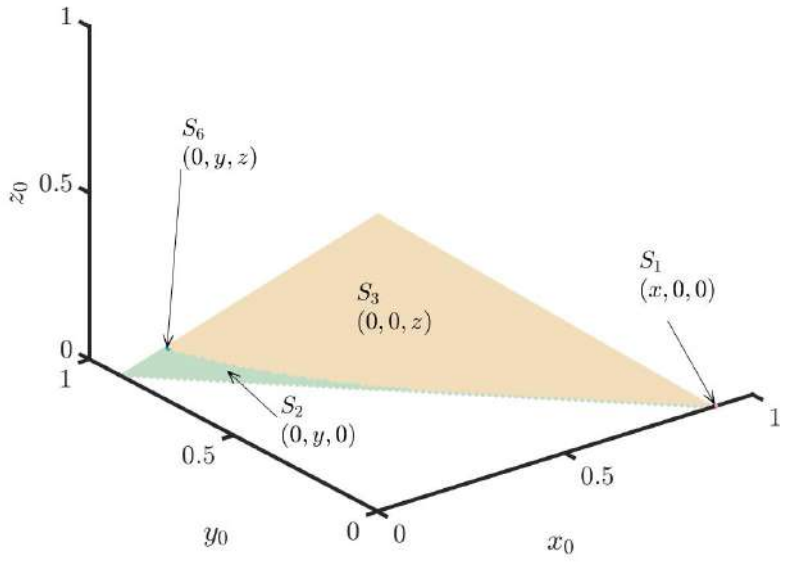

Figure 4.8: **Exploring the impact of initial conditions on eco-evolutionary dynamics**: Varying initial conditions within the constraint $x_0 + y_0 + z_0 = 0.9$, we uncover diverse steady states, highlighting the profound influence of initial conditions on emergent dynamics. This multistability provides valuable insights into system stability, robustness, and regime shifts. Notably, our findings reveal four distinct attractors representing different stable strategies, including coexistence of punishers and defectors. Depending on the chosen initial conditions, the system can exhibit stable states with cooperators, punishers, or defectors alone. These discoveries deepen our comprehension of the intricate dynamics and potential outcomes in our eco-evolutionary model, underscoring the critical interplay between initial conditions and steady states. Parameter values: $\sigma_1 = 1.2$, $\sigma_2 = 1.5$, $\sigma_3 = 1.4$, $\xi = 1.1$, $\beta = 1.5$, $\delta = 0.5$, and $\tau = 0.2$. Initial conditions for delayed variables: $(0.25, 0.25, 0.25)$.

variables, serving as a control against which we assess deviations in the system's response.

Strikingly, our numerical simulations reveal that different initial conditions lead to fundamentally different long-term outcomes. Depending on the specific composition of the initial population, the system settles into qualitatively distinct steady states. This outcome reaffirms and deepens our earlier conclusion: the dynamical evolution of our system is highly sensitive to initial states. In other words, the model exhibits multistability—a hallmark of complex systems where multiple attractors coexist and the final state is not uniquely determined by system parameters but also by initial configurations.

The discovery of multiple coexisting attractors holds profound implications for understanding the stability and resilience of eco-evolutionary systems. As illustrated in Fig. (4.9), we identify the presence of four distinct attractors, each corresponding

to a stable strategic outcome that the system can adopt. These attractors are not mere numerical artifacts but represent ecologically meaningful scenarios, including coexistence states and single-strategy dominance. Specifically, under certain initial conditions, the system supports the stable coexistence of punishers and defectors, highlighting a delicate balance between enforcement and exploitation. Under alternative initial conditions, the system may converge exclusively to cooperators, punishers, or defectors—each representing a qualitatively different ecological regime.

The identification of these attractors underscores the model's capacity to exhibit regime shifts—sudden transitions from one stable state to another triggered not by changes in parameters but by perturbations in initial states. This sensitivity to initial conditions enhances our understanding of ecological tipping points and evolutionary resilience, as real-world systems may undergo abrupt transformations due to minor initial differences.

Hence, the interplay between initial conditions and system parameters shapes a rich dynamical landscape in which multiple long-term outcomes are possible. This insight is vital for interpreting observed patterns in natural and social systems where history and context often dictate evolutionary outcomes.

In the upcoming section, we build on these findings by deriving the steady states of our model analytically and identifying the precise conditions under which Hopf bifurcation occurs. Through a combination of rigorous mathematical analysis and high-resolution numerical simulations, we validate the existence and stability of the bifurcating solutions, thereby offering a deeper theoretical foundation for the emergent dynamics observed in our eco-evolutionary framework.

4.3 Mathematical analyis

4.3.1 Various steady states and their biological relevance

The proposed model (4.6) results in eight steady states. They are briefly discussed in the following,

- **The extinction state** S_0: The state of extinction, denoted as S_0, corresponds to the equilibrium point $(0, 0, 0)$ in the dynamical system. At this state, each of the player populations eventually die out due to intense competition over long periods of time.

- **Punisher and Defector-free state** S_1: In this steady state, only individuals with cooperative strategy have the opportunity to survive, leading to the extinction of all other types of players in the game. The stationary point associated with this state is given by $\left(\frac{\sigma_1 - \xi}{\sigma_1 - 1}, 0, 0\right)$. Under these circumstances, cooperators have the ability to survive and ultimately dominate the entire game.

- **Cooperator and defector-free state** S_2: This state exclusively enables the survival of punishers, resulting in the eventual extinction of all other

populations in the game. The stationary point associated with this state is $\left(0, \frac{\sigma_2 - \xi}{\sigma_2 - 1}, 0\right)$. In this scenario, punishers gain the most significant advantage and can solely dominate the entire game. However, in an interactive context, if a society consists of exclusively punishers, they would act as cooperators because there would be no defectors to punish.

- **Cooperator and punisher-free state** S_3: This state allows only defectors to survive in a society, which supports the fundamental theory of the PD game, as defectors receive the greatest benefit compared to all other population strategies. The equilibrium point associated with this state is $\left(0, 0, 1 - \frac{\xi}{\sigma_3}\right)$. In such scenario, where only one population strategy can survive in the long run, there will be no interactive action between different player populations with different strategies.

- **Defector-free state** S_4: In this steady state, cooperators and punishers get the chance to survive side by side, with no defectors in the interaction. The equilibrium point gets the form $(x_*, y_*, 0)$, where, $x_* + y_* = \frac{\sigma_1 - \xi}{\sigma_1 - 1}$. Here, the defectors are unable to survive, whereas, the cooperators and the punishers jointly survive. Punishers also behave like cooperators in such state.

- **Punisher-free state** S_5: This state in the proposed model represents the basic scenario of the prisoner's dilemma game. In the long run, only the cooperators and defectors interact with each other, with no punishers present in the society. In such a scenario, the chances of implementing cooperation in different ways are reduced because the defector is not constrained in dealing with cooperators in the absence of punishers. The stationary point can be expressed as $(x_*, 0, z_*)$, where $x_* = \frac{\xi(\sigma_1 - \sigma_3)}{\beta\sigma_1 - \sigma_3}$, and $z_* = 1 - x_* + \frac{\xi(1-\beta)}{\beta\sigma_1 - \sigma_3}$.

- **Cooperator-free state** S_6**:** This steady state operates similarly to the previous state, S_5, where, in the long run of the dilemma, the punishers and the defectors can interact with each other. However, unlike state S_5, the defectors in this state face a slight constraint when interacting with the punishers. There would be a slight reduction in their payoffs when interacting with punishers than the cooperators. On the other hand, the punishers also behave like cooperators, but when interacting with the defectors, they face a loss of the fine δ to punish the defectors. The equilibrium point is given by $(0, y_*, z_*)$, where $y_* = \frac{\xi(\sigma_2 - \sigma_3) + \delta(\xi - \sigma_3)}{(\beta\sigma_2 - \sigma_3) + \delta(\beta - \delta - \sigma_2 - \sigma_3)}$, and $z_* = 1 - y_* + \frac{\xi(1 - \beta + 2\delta) - \delta(\beta - \delta)}{(\beta\sigma_2 - \sigma_3) + \delta(\beta - \delta - \sigma_2 - \sigma_3)}$.

- **State of co-existence** S_7: This steady state allows all three types of player populations to coexist and interact with each other simultaneously. It is considered the most biologically significant among all eight states as no player population goes extinct in the long run. The equilibrium point

for this state is (x_*, y_*, z_*), where $x_* = -\gamma_1 - \alpha_1 - z_* + \delta_1$, $y_* = \alpha_1 + \gamma_1$, and $z_* = \dfrac{(\xi-1)(\sigma_2-\sigma_1)}{\sigma_1-\sigma_2-\delta+\sigma_1\delta}$. Here, $\gamma_1 = \dfrac{(\beta-1)[\xi(\sigma_1-\sigma_2-\delta)+\sigma_1\delta]}{\sigma_1-\sigma_2-\delta+\sigma_1\delta}$, $\alpha_1 = \dfrac{(1-\xi)(\sigma_1-\sigma_3)}{\sigma_1-\sigma_2-\delta+\sigma_1\delta}$, $\delta_1 = 1+\dfrac{\delta(1-\xi)}{\sigma_1-\sigma_2-\delta+\sigma_1\delta}$, and $\sigma_1-\sigma_2-\delta+\sigma_1\delta \neq 0$.

4.3.2 Tracking the point of occurrence of Hopf bifurcation

Assuming (x_*, y_*, z_*) as the coordinates of a specific steady state, we explore the occurrence of the Hopf bifurcation by progressively increasing the time delay variable τ imposed on the system from this stable steady state. We refer to the value of τ at which the steady states begin to lose stability as the critical value of τ or τ_c. The linearization form of the proposed system (4.6) is presented below.

$$\begin{aligned}
&\dot{x} - [(1-\sigma_1)xx_\tau + (1-\sigma_1)xy_\tau - \sigma_1 xz_\tau + (\sigma_1-\xi)x] = 0,\\
&\dot{y} - [(1-\sigma_2)yx_\tau + (1-\sigma_2)yy_\tau - (\delta+\sigma_2)yz_\tau + (\sigma_2-\xi)y] = 0,\\
&\dot{z} - [(\beta-\sigma_3)zx_\tau + (\beta-\delta-\sigma_3)zy_\tau - \sigma_3 zz_\tau + (\sigma_3-\xi)z] = 0.
\end{aligned}$$

By calculating the linearized version of the above system about the general steady state (x_*, y_*, z_*), we obtain

$$\begin{aligned}
\dot{x} &= \psi_{11}x + \psi_{12}x_\tau + \psi_{13}y_\tau + \psi_{14}z_\tau,\\
\dot{y} &= \psi_{21}y + \psi_{22}x_\tau + \psi_{23}y_\tau + \psi_{24}z_\tau,\\
\dot{z} &= \psi_{31}z + \psi_{32}x_\tau + \psi_{33}y_\tau + \psi_{34}z_\tau,
\end{aligned} \tag{4.7}$$

where

$$\begin{aligned}
\psi_{11} &= (1-\sigma_1)(x_*+y_*) - \sigma_1 z_* + (\sigma_1-\xi),\\
\psi_{12} &= (1-\sigma_1)x_* = \psi_{13},\\
\psi_{14} &= -\sigma_1 x_*,\\
\psi_{21} &= (1-\sigma_2)(x_*+y_*) - (\delta+\sigma_2)z_* + (\sigma_2-\xi),\\
\psi_{22} &= (1-\sigma_2)y_* = \psi_{23},\\
\psi_{24} &= -(\delta+\sigma_2)y_*,\\
\psi_{31} &= (\beta-\sigma_3)x_* + (\beta-\delta-\sigma_3)y_* - \sigma_3 z_* + (\sigma_3-\xi),\\
\psi_{32} &= (\beta-\sigma_3)z_*,\\
\psi_{33} &= (\beta-\delta-\sigma_3)z_*,\\
\psi_{34} &= -\sigma_3 z_*.
\end{aligned} \tag{4.8}$$

The characteristic equations of the linearized system (4.7) are obtained as $\dot{S} = JX$, where

$$\dot{S} = \begin{bmatrix} sx(s)\\ sy(s)\\ sz(s)\end{bmatrix}, \quad J = \begin{bmatrix} \psi_{11}+\psi_{12}e^{-s\tau} & \psi_{13}e^{-s\tau} & \psi_{14}e^{-s\tau}\\ \psi_{22}e^{-s\tau} & \psi_{21}+\psi_{23}e^{-s\tau} & \psi_{24}e^{-s\tau}\\ \psi_{32}e^{-s\tau} & \psi_{33}e^{-s\tau} & \psi_{31}+\psi_{34}e^{-s\tau}\end{bmatrix}, \quad \text{and} \quad X = \begin{bmatrix} x(s)\\ y(s)\\ z(s)\end{bmatrix}.$$

In this case, J represents the Jacobian of the linearized system of equations. To obtain its characteristic equation, we set $det(J - \lambda I) = 0$, where λ is an eigenvalue of the Jacobian matrix J. From the resulting eigenvalues, we can deduce the critical value of τ. Therefore, we have the following transcendental equation from $det(J - \lambda I) = 0$:

$$\lambda^3 + \nu_1\lambda^2 + \nu_2\lambda + (\nu_3\lambda^2 + \nu_4\lambda + \nu_5)e^{-\lambda\tau} + (\nu_6\lambda + \nu_7)e^{-2\lambda\tau} + \nu_8 e^{-3\lambda\tau} + \nu_9 = 0, \tag{4.9}$$

where

$$\begin{aligned}
\nu_1 &= -(\psi_{11} + \psi_{21} + \psi_{31}),\\
\nu_2 &= \psi_{11}\psi_{21} + \psi_{11}\psi_{31} + \psi_{21}\psi_{31},\\
\nu_3 &= -(\psi_{12} + \psi_{23} + \psi_{34}),\\
\nu_4 &= \psi_{11}\psi_{23} + \psi_{11}\psi_{34} + \psi_{12}\psi_{21} + \psi_{12}\psi_{31} + \psi_{21}\psi_{34} + \psi_{23}\psi_{31},\\
\nu_5 &= -(\psi_{11}\psi_{21}\psi_{34} + \psi_{11}\psi_{23}\psi_{31} + \psi_{12}\psi_{21}\psi_{31}),\\
\nu_6 &= -(\psi_{24}\psi_{33} - \psi_{12}\psi_{23} - \psi_{12}\psi_{34} - \psi_{23}\psi_{34} + \psi_{13}\psi_{22} + \psi_{14}\psi_{32}),\\
\nu_7 &= -(\psi_{11}\psi_{23}\psi_{34} - \psi_{11}\psi_{24}\psi_{33} + \psi_{12}\psi_{21}\psi_{34} + \psi_{12}\psi_{23}\psi_{31} - \psi_{13}\psi_{22}\psi_{31} - \psi_{14}\psi_{21}\psi_{32}),\\
\nu_8 &= -(\psi_{12}\psi_{23}\psi_{34} - \psi_{12}\psi_{24}\psi_{33} - \psi_{13}\psi_{22}\psi_{34} + \psi_{13}\psi_{24}\psi_{32} + \psi_{14}\psi_{22}\psi_{33} - \psi_{14}\psi_{32}\psi_{23}),\\
\nu_9 &= -\psi_{11}\psi_{21}\psi_{31}.
\end{aligned} \tag{4.10}$$

To simplify the transcendental equation, we make the following substitution: $\lambda(\tau) = a(\tau) + ib(\tau)$ and $\lambda(\tau_c) = a(\tau_c) + ib(\tau_c)$. We then separate the real and imaginary parts of the equation by using the transformation $e^{a\pm ib} = e^a(\cos(b) \pm i\sin(b))$ on Eq. (4.9). This yields

$$\begin{aligned}
&a^3 - 3ab^2 + \nu_1(a^2 - b^2) + a\nu_2 + (\nu_3(a^2 - b^2) + a\nu_4 + \nu_5)e^{-a\tau}\cos(a\tau) +\\
&\{2\nu_3 ab + \nu_4 b\}e^{-a\tau}\sin(b\tau) + (a\nu_6 + \nu_7)e^{-2a\tau}\cos(2b\tau) +\\
&b\nu_6 e^{-2a\tau}\sin(2b\tau) + \nu_8 e^{-3a\tau}\cos(3b\tau) + \nu_9 = 0,\\
&\text{and,}\\
&3a^2 b - b^3 + 2\nu_1 ab + b\nu_2 - a\sin(b\tau) - \{\nu_3(a^2 - b^2) + a\nu_4 + \nu_5\}e^{-a\tau}\sin(b\tau) + \{2\nu_3 ab + b\nu_4\}\\
&e^{-a\tau}\cos(b\tau) - (a\nu_6 + \nu_7)e^{-2a\tau}\sin(2b\tau) + b\nu_6 e^{-2a\tau}\cos(2b\tau) - \nu_8 e^{-3a\tau}\sin(3b\tau) = 0.
\end{aligned} \tag{4.11}$$

Using the relation in Eq. (4.11), we can determine the value of the delay time variable τ_c at which the Hopf bifurcation occurs. At this value of τ, the eigenvalues of the Jacobian become purely imaginary. Therefore, we set $a(\tau_c) = 0$. This provides the following form of Eq. (4.11):

$$\begin{aligned}
&(b^{*2}\nu_3 - \nu_5)\cos(b^*\tau_c) - b^*\nu_4\sin(b^*\tau_c) = \nu_7\cos(2b^*\tau_c) + \nu_6 b^*\sin(2b^*\tau_c)\\
&+\nu_8\cos(3b^*\tau_c) + \nu_9 - b^{*2}\nu_1,\\
&\text{and,}\\
&b^*\nu_4\cos(b^*\tau_c) + (b^{*2}\nu_3 - \nu_5)\sin(b^*\tau_c) = \nu_7\sin(2b^*\tau_c) - b^*\nu_6\cos(2b^*\tau_c) +\\
&\nu_8\sin(3b^*\tau_c) + b^{*3} - b^*\nu_2.
\end{aligned} \tag{4.12}$$

Let us consider that

$A = (b^{*2}\nu_3 - \nu_5)\cos(b^*\tau_c) - b^*\nu_4 \sin(b^*\tau_c)$,
$B = \nu_7 \cos(2b^*\tau_c) + \nu_6 b^* \sin(2b^*\tau_c) + \nu_8 \cos(3b^*\tau_c)$,
$C = b^*\nu_4 \cos(b^*\tau_c) + (b^{*2}\nu_3 - \nu_5)\sin(b^*\tau_c)$, and
$D = \nu_7 \sin(2b^*\tau_c) - b^*\nu_6 \cos(2b^*\tau_c) + \nu_8 \sin(3b^*\tau_c)$.

Consequently, we find the following relations,

$$\begin{aligned} A - B &= \nu_9 - b^{*2}\nu_1, \\ C - D &= b^{*3} - b^*\nu_2, \end{aligned}$$

Using these two relations, we can easily conclude

$$(A^2 + C^2) + (B^2 + D^2) - 2(AB + CD) = b^{*6} + (\nu_1^2 - 2\nu_2)b^{*4} - (2\nu_1\nu_9 - \nu_2^2)b^{*2} + \nu_9^2 \tag{4.13}$$

Since the left-hand side of Eq. (4.13) includes the terms $(A-B)^2$ and $(C-D)^2$, and considering the assumptions we have made about these values, we can substitute them and rewrite Eq. (4.13) as follows:

$$\begin{aligned} &b^{*4}\nu_3^2 + \nu_5^2 - 2\nu_3\nu_5 b^{*2} + b^{*2}\nu_4^2 + \nu_7^2 + b^{*2}\nu_6^2 + \nu_8^2 + 2\nu_7\nu_8 \cos(b^*\tau_c) - 2\nu_6\nu_8 b^* \sin(b^*\tau_c) \\ &-2(\nu_3\nu_7 b^{*2}\cos(2b^*\tau_c) + \nu_3\nu_6 b^{*3}\sin(b^*\tau_c) + \nu_3\nu_8 b^{*2}\cos(2b^*\tau_c) - \nu_5\nu_7\cos(b^*\tau_c) - \nu_5\nu_8 b^*\sin(b^*\tau_c) \\ &-\nu_5\nu_8\cos(2b^*\tau_c) + \nu_4\nu_7 b^*\sin(b^*\tau_c) - \nu_4\nu_6 b^{*2} cos(b^*\tau_c) + \nu_4\nu_8 b^*\sin(2b^*\tau_c)) = \\ &b^{*6} + (\nu_1^2 - 2\nu_2)b^{*4} - (2\nu_1\nu_9 - \nu_2^2)b^{*2} + \nu_9^2. \end{aligned} \tag{4.14}$$

After performing extensive calculations, we can derive the following relationship by multiplying $\cos(2b^*\tau_c)$ with the first equation of system (4.12) and $\sin(2b^*\tau_c)$ with the second equation of the same system.

$$\begin{aligned} \sin(b^*\tau_c) &= \frac{c + d\cos(b^*\tau_c) + e\cos(2b^*\tau_c) - a\cos(b^*\tau_c)}{b - 2f\cos(b^*\tau_c)} \\ &= \frac{a\cos(b^*\tau_c) - c\cos(2b^*\tau_c) - d\cos(3b^*\tau_c) - e}{2g\cos(b^*\tau_c) + b}, \end{aligned} \tag{4.15}$$

where $a = \nu_3 b^{*2} - \nu_5$, $b = \nu_4 b^*$, $c = \nu_7$, $d = \nu_8$, $e = \nu_9 - \nu_1 b^{*2}$, and $f = b^{*3} - \nu_2 b^*$. Then, by comparing the calculated value of $\sin(b^*\tau_c)$, we arrive at the following result

$$\begin{aligned} &\cos(b^*\tau_c)[8m_1\cos^3(b^*\tau_c) - (4q_1 + 2t_1)\cos^2(b^*\tau_c) - \\ &(6m_1 + 2p_1 + s_1)\cos(b^*\tau_c) - (r_1 - t_1 - 3q_1)] = 0. \end{aligned} \tag{4.16}$$

where,

$m_1 = d_1 f_1$, $r_1 = 2c_1 g_1 + b_1 d_1 - 2a_1 b_1 - 2e_1 f_1$, $s_1 = 2d_1 g_1 - 2a_1 g_1 + 2a_1 f_1$,
$t_1 = 2e_1 g_1 - 2c_1 f_1$, $p_1 = b_1 e_1 + b_1 c_1$, $q_1 = b_1 d_1$,
with
$a_1 = b^{*2}\nu_3 - \nu_5$, $b_1 = b^*\nu_4$, $c_1 = \nu_7$,
$d_1 = \nu_8$, $e_1 = \nu_9 - b^{*2}\nu_1$, $f_1 = b^{*3} - b^*\nu_2$.

After substituting all the relevant terms as mentioned above, the above equation can be rewritten as:

$$cos(b^*\tau_c)[\xi_1 cos^3(b^*\tau_c) - \xi_2 cos^2(b^*\tau_c) - \xi_3 cos(b^*\tau_c) + \xi_4] = 0,$$

where

$\xi_1 = 8b^*\nu_8(b^{*2} - \nu_2)$,
$\xi_2 = -4b^*[(\nu_1\nu_6 + \nu_7)b^{*2} - (\nu_2\nu_7 + \nu_4\nu_8 + \nu_6\nu_9)]$,
$\xi_3 =$
$2b^*[b^{*4}\nu_3 + (3\nu_3 - \nu_1\nu_4 - \nu_2\nu_3 - \nu_3\nu_6 - \nu_5)b^{*2} + (\nu_2\nu_5 + \nu_4\nu_7 + \nu_4\nu_3 + \nu_5\nu_6 + \nu_6\nu_8 - 3\nu_2\nu_8)]$,
$\xi_4 = -b^*[2b^{*4}\nu_1 - 2(\nu_1\nu_2 + \nu_3\nu_4 + \nu_9 - \nu_1\nu_6 - \nu_7)b^{*2} - (2\nu_2\nu_7 + 3\nu_4\nu_8 + 2\nu_6\nu_9 - 2\nu_2\nu_9 - \nu_4\nu_8 - 2\nu_4\nu_5 - 2\nu_6\nu_7)]$.

Equation (4.16) brings forth one of the solutions as $\cos(b^*\tau_c) = 0$. Therefore, we need to determine the value of b^* for which the relation $\cos(b^*\tau_c) = 0$ holds true. We can use this relationship to calculate the critical value τ_c, at which Hopf bifurcation occurs. Therefore, the value of τ obtained from this relationship can be considered as the value of τ_c.

By modifying Eq. (4.14), we can obtain a sixth-degree polynomial in terms of b^*. Substituting the value of $\sin(b^*\tau_c)|_{\cos(b^*\tau_c)=0}$ from Eq. (4.15), we can derive an equation in terms of b^*, which is sufficient to calculate τ_c. The resulting sixth-degree equation is

$$b^{*6} + \eta_1 b^{*4} + \eta_2 b^{*2} + \eta_3 = 0, \tag{4.17}$$

where

$$\eta_1 = \nu_1^2 + \frac{2\nu_1\nu_3\nu_6}{\nu_4} - 2\nu_2 - \nu_3^2,$$
$$\eta_2 = \frac{2\nu_6}{\nu_4}\{\nu_3(\nu_7 - \nu_9) + \nu_1\nu_8 - \nu_1\nu_5\} + 2\nu_1\nu_7 - (2\nu_1\nu_9 + \nu_4^2 + \nu_6^2 + 2\nu_3\nu_8 - \nu_2^2 - 2\nu_3\nu_5),$$
$$\eta_3 = \nu_9^2 + 2\nu_5\nu_8 - \nu_5^2 - \nu_7^2 - \nu_8^2 + \frac{2\nu_6}{\nu_4}(\nu_7 - \nu_9)(\nu_8 - \nu_5) + 2\nu_7(\nu_7 - \nu_9).$$

The roots of Eq. (4.17) are the six values of b^* such that the relation for the critical value of τ holds, i.e., $cos(b^*\tau_c) = 0$, which implies $(b^*\tau_c) = (2n+1)\frac{\pi}{2}$. For $n = 0$, the critical value τ_c can be calculated as $\tau_c = \frac{\pi}{2b^*}$, where the value of the required b^* can be calculated from Eq. (4.17). Note that one can obtain at most six different real values for b^*. Only one of these real roots provides us with our desired critical value of the delay parameter at the Hopf bifurcation.

4.3.3 Validation of analytical finding

In Fig. (4.3), we identify a classical signature of Hopf bifurcation: a qualitative transition in the system's dynamics where a stable equilibrium loses stability and a

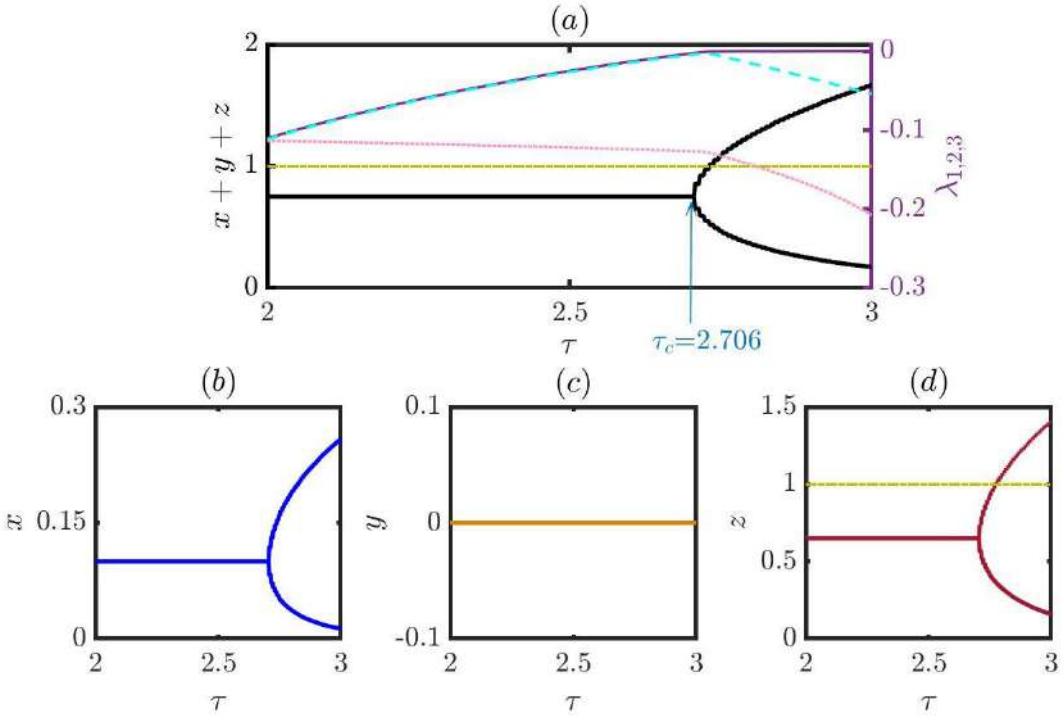

Figure 4.9: **Verification of the critical time delay** τ_c: (a) Bifurcation diagram and Lyapunov exponents of the delay model over $\tau \in [2, 3]$ confirm a Hopf bifurcation at $\tau_c = 2.706$, matching the analytical prediction. Parameters: $\xi = 0.40$, $\beta = 1.50$, $\delta = 0.56$, $\sigma_1 = 1.20$, $\sigma_2 = 1.70$, $\sigma_3 = 1.0$. The largest exponent λ_1 (solid purple) hits zero at τ_c and stays flat; λ_2 (cyan dashed) touches zero at τ_c but is negative elsewhere; λ_3 (pink dotted) remains negative. A green dash-dotted line separates bounded from overcrowded solutions where $x + y + z > 1$. (b-d) Show τ's effect on each species; punishers go extinct despite receiving highest free space benefits. Initial conditions: non-delayed $(0.1, 0.2, 0.5)$, delayed $(0.3, 0.3, 0.3)$.

stable limit cycle emerges. This bifurcation manifests precisely at the critical value $\tau = 8.98$, marking the onset of sustained periodic oscillations. The emergence of this limit cycle validates the presence of a non-trivial dynamical regime governed by time-delay, and importantly, this numerically observed critical point aligns perfectly with the analytically predicted threshold τ_c, thereby reinforcing the theoretical consistency of our model.

Extending our investigation further, Fig. (4.9) presents the bifurcation diagram of the delay-induced system (4.6), where the delay parameter τ is systematically varied within the interval $[2, 3]$. This high-resolution continuation is performed using a fine step size of 0.002 to capture subtle dynamical transitions, while keeping the parameters fixed at $\xi = 0.40$, $\beta = 1.50$, $\delta = 0.56$, $\sigma_1 = 1.20$, $\sigma_2 = 1.70$, and $\sigma_3 = 1.0$. Under these ecological conditions, the structure of free space naturally favors punishers, as implied by the hierarchy $\sigma_2 > \sigma_1 > \sigma_3$. Yet, in a counterintuitive outcome, the long-term dynamics reveal the extinction of punishers, as clearly evidenced in panel (c) of Fig. (4.9).

Interestingly, even though free space disadvantages defectors, they eventually

dominate over cooperators in the long-time limit, as illustrated in panels (b) and (d). This indicates that evolutionary stability in this system cannot be solely attributed to ecological favorability, but instead emerges from a complex interplay between delay-induced instability and strategic competition. Notably, as the delay parameter increases and crosses the threshold $\tau = 2.706$, the previously stable fixed point becomes unstable, giving rise to a limit cycle oscillation. This dynamical transition is again precisely in agreement with our analytically derived Hopf bifurcation point, $\tau_c = 2.706$, further substantiating the analytical insights.

To corroborate this bifurcation, we compute the maximum Lyapunov exponent λ_1, shown as the solid purple curve in Fig. (4.9) (a). It remains exactly zero beyond the critical point, a hallmark of sustained periodic behavior. Simultaneously, the second-largest Lyapunov exponent λ_2, plotted as a cyan dashed line, also reaches zero at $\tau = 2.706$, offering further dynamical evidence of the Hopf bifurcation. These Lyapunov-based validations provide robust numerical support for the analytical and qualitative findings.

However, as τ continues to increase, the system begins to exhibit biologically unrealistic behavior. Specifically, the total population size $(x+y+z)$ exceeds the upper bound of 1, leading to an overcrowded solution space that violates the ecological constraints of the model. To delineate the biologically admissible regime, we draw a horizontal dash-dotted line in subfigures (a) and (d) of Fig. (4.9), clearly marking the boundary beyond which ecological interpretations lose validity. Solutions lying beneath this threshold remain ecologically feasible and maintain interpretive relevance in the context of our strategic species model.

4.4 Conclusions

Eco-evolutionary dynamics represents a vital framework for understanding how ecological and evolutionary processes reciprocally influence each other over time. It reveals the complex feedback loops that shape population dynamics and community structures by linking ecological processes, such as competition, predation, and resource availability, with the evolution of traits within populations. Conversely, these evolved traits can, in turn, modulate ecological interactions, ultimately affecting the resilience and stability of ecosystems. Such insights are particularly pertinent for conservation biology, where environmental changes, such as habitat fragmentation or climate change, can alter selective pressures and evolutionary trajectories, thereby reshaping community composition and ecosystem functioning. Understanding the multifaceted interplay between ecological and evolutionary dynamics is thus critical for predicting and managing ecosystem responses to rapid environmental change.

In this chapter, we have examined the intertwined effects of ecological and evolutionary processes by focusing on the classical PD game. The PD remains a cornerstone in evolutionary game theory for modeling conflicts between cooperation and defection in both social and biological systems. By embedding the PD in an eco-evolutionary framework, we explored how strategic interactions, combined with ecological variables, shape evolutionary outcomes. Notably, we introduced free space as an ecological variable that contributes altruistically to the system. Here, free space acts analogously to an individual that sacrifices its fitness to benefit

others, embodying a key aspect of altruism observed across biological and social systems—from charity and volunteering in humans to self-sacrificing parental care in animals. Despite initial skepticism about the evolutionary stability of such altruistic behavior, empirical evidence highlights its widespread occurrence and evolutionary relevance, particularly in shaping cooperative dynamics.

Complementing altruism, we incorporated punishment as an evolutionary strategy to discourage defection. Punishment introduces a cost to non-cooperative behavior, effectively deterring defection by making it less profitable. This strategy, widely recognized in both human and non-human systems, promotes social norms, enhances group cohesion, and sustains cooperation. By integrating punishment into the classical PD framework alongside free space, our model captures the complex interplay of social and ecological factors that influence evolutionary dynamics. This enriched model reveals how eco-evolutionary feedback can foster or inhibit cooperation, depending on the ecological and strategic context.

Looking ahead, the next chapter of this thesis builds upon these insights by investigating evolutionary strategies in a cyclically dominant environment, where species interactions are characterized by dynamic cycles of dominance akin to the Rock-Paper-Scissors (RPS) game. Recent studies have underscored the importance of these cyclic dynamics in promoting biodiversity and maintaining ecosystem stability. In this expanded framework, we develop a model featuring three interconnected strategic species—prey, predator, and parasite—each adopting distinct evolutionary strategies that mirror RPS dynamics. These "strategic species" adhere to the principles of eco-evolutionary game dynamics, capturing the nuanced interactions between ecological factors and evolutionary responses. Furthermore, we incorporate a global sensitivity analysis using Sobol indices to systematically assess the influence of payoff parameter variations on system behavior. This comprehensive approach deepens our understanding of how eco-evolutionary processes operate in complex, multi-species systems and sets the stage for future investigations into higher-order interactions and ecosystem resilience.

Chapter 5

The eco-evolutionary dynamics of the strategic species, following Rock-Paper-Scissor (RPS) game dilemma [§]

Ecological factors profoundly shape the evolutionary adaptations of species across different environments. This reciprocal influence means that abundant species adapt to their environment while leaving ecological footprints that modify their habitats [186, 187]. A classic example is the industrial melanism of black moths in Manchester, UK, during the 19th century [188–192]. Other historical cases include the evolution of house mice on islands [193, 194], phenotypic plasticity in plants [195], and the rapid adaptation of house sparrows in North America [196].

In recent decades, research has shifted from viewing evolution as a slow process overshadowed by rapid ecological changes to recognizing that significant evolutionary changes can occur over just a few generations [197–203]. Ecologists and population biologists have increasingly focused on the dynamics of heterogeneous traits within habitats [204]. Mathematical models describing predator-prey-parasite interactions have been central to this chapter since the foundational studies of Lotka and Volterra [205, 206], later expanded by Rosenzweig and MacArthur [207].

Parasites, abundant in ecological systems, contribute substantially to global biomass [208–210]. They exist as endoparasites and ectoparasites, influencing host dynamics in diverse ways [211–217]. Parasites can even facilitate coexistence between dominant and subordinate species, enhancing biodiversity [218–220]. Examples include seabird ectoparasites in the Gulf of California islands shaping predator-prey dynamics [221–223].

In this chapter, we focus on a three-dimensional eco-evolutionary model featuring prey, predators, and parasites. In this model, predators consume prey biomass, parasites exploit predators by depleting their immunity, and prey can suppress par-

[§]A considerable part of this chapter has been published in **Proceedings of the Royal Society A**, Volume 480, Article ID: Roy, S., Ghosh, S., Saha, A., Chandra Mali, P., Perc, M. and Ghosh, D., 2024. The eco-evolutionary dynamics of strategic species. Proceedings of the Royal Society A, 480(2288), p.20240127.

asites by exploiting growth advantages, thereby promoting their own survival. This interaction forms a cyclic food chain reminiscent of the RPS game. We apply evolutionary game theory principles to these strategic species and incorporate ecological free space, which acts as an altruistic variable enhancing each species' fitness without expecting returns [224, 225]. This dynamic highlights how free space can shape evolutionary dynamics by contributing positively to reproductive opportunities [160, 163, 226, 44, 164, 227].

Our model also captures the fraction of each strategy and free space, maintaining a sum of unity. Each strategy's growth depends on game payoffs and benefits from free space, while extinction rates are constant—contrasting with earlier studies that assumed arbitrary extinction rates [228, 59].

Global sensitivity analysis is critical in ecology for quantifying uncertainties in model outputs [229–233]. Sensitivity analysis not only identifies key parameters but also guides model validation and refinement [234]. Here, we emphasize the Sobol index as a valuable tool to reveal the underlying features of our eco-evolutionary model.

We structure this chapter as follows: First, we present our three-dimensional eco-evolutionary model of strategic species—prey, predator, and parasite—mirroring RPS dynamics. We then analyze the model's stationary attractors and transitions between them, showing how frequencies of strategies shift under different ecological and evolutionary factors. We also identify oscillatory and unstable dynamics that manifest as cyclic behaviors (Hopf bifurcations). Next, we provide numerical simulations illustrating parameter interplays affecting both stable and unstable dynamics. Finally, we perform a global sensitivity analysis of the system's payoff parameters to evaluate their influence on evolutionary outcomes.

5.1 Mathematical model

The foundation of the theoretical framework in this article lies in a fundamental three-dimensional ecological configuration, comprising three primary species within an environment: prey, predator, and parasite. The essence of their existence revolves around mutual dependencies for sustenance and energy. The integration of evolutionary strategies into this ecological chain hinges on the patterns of interactions among these three types of species in an ecosystem. Thus, we present the ecological model as a means to explore these dynamics,

$$\begin{aligned}
\frac{dx}{dt'} &= rx - d_1x - d_4xy + e_1d_6xz, \\
\frac{dy}{dt'} &= -d_2y - d_5yz + e_2d_4xy, \\
\frac{dz}{dt'} &= -d_3z - d_6xz + e_3d_5yz,
\end{aligned} \tag{5.1}$$

where x, y, and z are the abundance of prey, predator and parasite species in the ecological habitat, with r is being considered to be the innate growth rate of the prey species, d_i $(i = 1, 2, 3)$ are the natural rates of extinction of prey, predator and parasite traits respectively, whereas, d_4 is the rate of predation taken by the

predators to hunt down the prey kinds, which, counter intuitively, contributes to the growth of the predator kinds. In addition to absorb food, predators consume a fixed amount of biomass e_2 from prey species. Moreover, d_5 is the rate, in which parasites consume their food living on the predators, along with consuming a biomass of quantity e_3. In the same way, prey takes energy from the plant parasites in the rate d_6, in the same manner how prey kinds get a fixed biomass e_1 from the parasites in terms of their own growth.
We now execute some of the following transformations to the model (5.1) as,
$t = rt'$, $u = \frac{e_1 d_4 x}{r}$, $v = \frac{e_2 d_5 y}{r}$ and $w = \frac{e_3 d_6 z}{r}$.
Using these transformations, we can reach up to the following results,

$$\begin{aligned} \frac{du}{dt} &= u[(1-\alpha) + (-\frac{d_4}{e_2 d_5})v + \frac{e_1}{e_3}w], \\ \frac{dv}{dt} &= v[-\beta + (-\frac{d_5}{e_3 d_6})w + \frac{e_2}{e_1}u], \\ \frac{dw}{dt} &= w[-\xi + (-\frac{d_6}{e_1 d_4})u + \frac{e_3}{e_2}v]. \end{aligned} \tag{5.2}$$

where $\alpha = \frac{d_1}{r}$, $\beta = \frac{d_2}{r}$ and $\xi = \frac{d_3}{r}$.
Now, looking at the system (5.2), and considering all the system parameters to be positive (> 0), we can observe the one-to-one interaction flow, which has being maintained in a cyclic way, among the three described species in all three equations of the system (5.2). If we represent these interactions among these three species in matrix form, we get,

$$\begin{array}{c} \\ \textbf{Prey} \\ \textbf{Predator} \\ \textbf{Parasite} \end{array} \begin{array}{c} \begin{array}{ccc} \textbf{Prey} & \textbf{Predator} & \textbf{Parasite} \end{array} \\ \begin{pmatrix} 0 & -\frac{d_4}{e_2 d_5} & \frac{e_1}{e_3} \\ \frac{e_2}{e_1} & 0 & -\frac{d_5}{e_3 d_6} \\ -\frac{d_6}{e_1 d_4} & \frac{e_3}{e_2} & 0 \end{pmatrix} \end{array}$$

Moreover, we get to observe no effect by the intra-species interaction (as in the above matrix, all the diagonal elements are 0) and there is a certain chain to dominate and being dominated by the other trait in a cyclic manner, in terms of inter-species collision, as all the ecological parameters are taken to be positive.
Nevertheless, if we pay our attention into the interaction mannerisms of the very well-known RPS game dilemma, we observe the same signature orders in the outcomes through the face-offs between the heterogeneous player species. To introduce the conflicts of the social dilemma in the species' evolutionary schemes, we present a payoff matrix that reflects the conflicts between heterogeneous strategies of the RPS game dilemma, which acts as the custom of interaction among different species in the ecological circumstances. For this we replace the interaction matrix obtained from the system (5.2) by a newly proposed payoff matrix depicting the RPS game dilemma. In our consideration of this game dilemma, if one particular strategy gets victory over the other and gains an amount p as payoff, the loser trait following

the trounced strategy gets the negation (-p) of the exact same payoff on it's defeat. Maintaining this rule, we introduce three payoffs' a, b and c (all are chosen to be positive, i.e., ≥ 0), treated as the interactive attributes of the species present in the ecological surrounding. The payoffs a, b, and c are used in such a manner that, in a one-to-one conflict, paper triumphs over rock by winning a payoff of fractional amount a, while rock has to lose the same amount at its defeat. The same phenomenon regarding the payoff value b is considered when the scissor strategy gets trounced by the action of rock. The players following rock as strategy secure the payoff amount b, while the scissor loses b by getting defeated. Similarly, during the face-off between paper and scissor moves, scissor earns the payoff amounting c, whereas paper loses the same aggregate proved to be a loser ($-c$). Thus, we can represent the payoff matrix of our consideration of the RPS game dilemma as follows,

$$\begin{array}{c} \\ \textbf{Rock} \\ \textbf{Paper} \\ \textbf{Scissor} \end{array} \begin{array}{c} \begin{array}{ccc} \textbf{Rock} & \textbf{Paper} & \textbf{Scissor} \end{array} \\ \begin{pmatrix} 0 & -a & b \\ a & 0 & -c \\ -b & c & 0 \end{pmatrix} \end{array}. \tag{5.3}$$

In addition to this game dilemma, we also treat the ecological free space to act as an altruistic strategy, which only showers reproductive benefits to these strategic species, those are being parts in the proposed game dilemma. These free space induced resources are considered to be, σ_R, σ_P and σ_S (all are taken to be positive) towards rock, paper and scissor respectively. As ecological free space only shows selfless behavior towards the traits, free space does not take any kind of benefit from any of these traits. After inducing free space as a independent attribute to this game, we can extend our three dimensional payoff matrix (5.3) into four dimensional one as follows,

$$\begin{array}{c} \\ \textbf{Rock} \\ \textbf{Paper} \\ \textbf{Scissor} \\ \textbf{Free space} \end{array} \begin{array}{c} \begin{array}{cccc} \textbf{Rock} & \textbf{Paper} & \textbf{Scissor} & \textbf{Free space} \end{array} \\ \begin{pmatrix} 0 & -a & b & \sigma_R \\ a & 0 & -c & \sigma_P \\ -b & c & 0 & \sigma_S \\ 0 & 0 & 0 & 0 \end{pmatrix} \end{array}. \tag{5.4}$$

From the above mentioned payoff matrix (5.4), we can deduce average fitness of each of the proposed strategies. We moreover consider the size of an entire ecological environment to be 1, among which $R+P+S$ is the total size of the strategic traits, where the fraction R represents the abundance of the species taking the strategy 'rock', namely the rock strategic species, or the rock species, P is the fractional quantity of the traits, choosing the strategy 'paper', referred as the paper strategic species, or the paper species and S is the frequency of traits following the strategy 'scissor', called out to be the scissor strategic species, or the scissor species present in any considered dilemma, which eventually portrays the evolutionary schemes of the prey, predator and parasite species described in any ecological perspective. Additionally, we introduce the fraction F, that quantifies the free space amount. Thus, we have the constraint in terms of boundary, that is, $R + P + S + F = 1$. From which, we treat the fraction of the free space as, $F = 1 - R - P - S$ in our

model formulation perspective.
We now propose mean fitness of rock, paper, scissor and free space as,

$$\begin{aligned} f_{\mathbf{R}} &= -aP + bS + \sigma_R F = -\sigma_R R - (a+\sigma_R)P + (b-\sigma_R)S + \sigma_R, \\ f_{\mathbf{P}} &= aR + -cS + \sigma_P F = (a-\sigma_P)R - \sigma_P P - (c+\sigma_P)S + \sigma_P, \\ f_{\mathbf{S}} &= -bR + cP + \sigma_S F = -(b+\sigma_S)R + (c-\sigma_S)R - \sigma_S S + \sigma_S, \\ f_{\mathbf{F}} &= 0. \end{aligned} \tag{5.5}$$

In our analysis, we evaluate the mean fitness denoted by f_R, f_P, and f_S corresponding to the strategies, viz.,'rock,' 'paper,' and 'scissors,' respectively. These fitness values are computed using the growth factors outlined in equation (5.5), representing the evolutionary advantages of each strategic species. Additionally, based on the ecological model expressed in equation (5.2), we assume that each strategy ('rock', 'paper', and 'scissor') has its own associated death rate: $(1-\alpha)$, β, and ξ, respectively. These death rates are derived from the transformed ecological system in equation (5.2). Utilizing the computed growth and death rates, we propose an eco-evolutionary dynamical system for the strategic species, where the actions 'rock (R),' 'paper (P),' and 'scissor (S)' represent the species' responses within the ecological dilemma. The formulation of this system is presented below,

$$\begin{aligned} \dot{R} &= R[-\sigma_R R - (a+\sigma_R)P + (b-\sigma_R)S + (\sigma_R + \alpha - 1)], \\ \dot{P} &= P[(a-\sigma_P)R - \sigma_P P - (c+\sigma_P)S + (\sigma_P - \beta)], \\ \dot{S} &= S[-(b+\sigma_S)R + (c-\sigma_S)P - \sigma_S S + (\sigma_S - \xi)]. \end{aligned} \tag{5.6}$$

We conduct an in-depth investigation of our proposed model (5.6) utilizing the Runge-Kutta-45 method to solve the system of differential equations. This examination aims to explore the outcomes of the model (5.6), representing the normalized frequency of strategic species in the ecological environment under consideration.
Throughout the study of our model (5.6) in this chapter, we maintain the initial quantities of the three state variables, R, P, and S, equal, reflecting their inherent influence on each other. These initial values are set to $(0.3, 0.3, 0.3)$. Each experiment consists of 10^7 iterations, with a time step length of 0.01.

5.2 The strategic attractors

Our proposed eco-evolutionary dynamical system of three strategic species (5.6) is constructed based on the theory of the RPS game dilemma, enhanced by incorporating ecological extinction factors and the replicatory effects arising from free space. This enriched framework reflects not only the classical competitive interactions seen in the RPS model but also ecological feedback that shape strategic survival. In accordance with the theoretical trajectory of the RPS dilemma, none of the strategies or actions in isolation can be considered an evolutionary stable strategy (ESS). However, due to the combined influence of multiple parameters and the broad range of possible ecological scenarios embedded in the structure of our model, the dynamical system governed by (5.6) exhibits multiple solutions that capture different long-term behaviors. These solutions describe various possible compositions where strategic species either coexist or one of them uniquely dominates in the environment.

These equilibrium solutions, when they display asymptotic stability, are referred to as the stable strategic attractors of the strategic species. Each attractor reflects a biologically meaningful outcome where one or more strategic populations persist in a dynamically stable configuration. To better conceptualize and visualize these attractors, we introduce the idea of a three-dimensional strategy space spanned by three mutually perpendicular axes—x, y, and z—each representing the population proportion of one strategic species: rock (R), paper (P), and scissor (S), respectively (Fig. 5.1). Within this space, the trajectories of the eco-evolutionary system evolve over time and ultimately converge toward specific attractors. Based on the nature of these attractors, we categorize them and analyze their respective mathematical structures and biological implications.

5.2.1 The null attractor

In our analysis of the strategic attractors in the system (5.6), we first observe the presence of the trivial stationary point $O(0, 0, 0)$, depicted in Fig. 5.1 (a). This point, referred to as the null strategic attractor (O), represents a state where none of the strategic species—regardless of their chosen evolutionary strategy—survives in the habitat. A compelling real-world analogy for this scenario is the Permian-Triassic extinction event, known as the "Great Dying," which occurred approximately 252 million years ago. During this catastrophic period, an estimated 96% of marine species and 70% of terrestrial vertebrates perished due to extreme volcanic activity, rapid climate changes, and disruptions in ocean chemistry.

Mathematically, the evolutionary stability of this seemingly simple yet devastating attractor depends on six key parameters in our eco-strategic system (5.6): α, β, ξ, σ_R, σ_P, and σ_S. Specifically, the null attractor $O(0, 0, 0)$ becomes asymptotically stable only when the following three inequalities are satisfied: $\sigma_R + \alpha < 1$, $\sigma_P < \beta$, and $\sigma_S < \xi$. Notably, the payoff values (a, b, and c) of the RPS game do not influence whether the system converges to this attractor, meaning that even with fixed payoffs, extinction can occur purely due to parametric instability.

To validate this, we conducted numerical simulations using the parameter set $a = 0.70$, $b = 0.25$, $c = 0.5$, $\sigma_R = 0.5$, $\sigma_P = 0.15$, $\sigma_S = 0.25$, $\alpha = 0.05$, $\beta = 0.2$, and $\xi = 0.30$. Under these conditions, we observe $\alpha + \sigma_R = 0.55 < 1$, $\sigma_P < \beta$, and $\sigma_S < \xi$, fulfilling all stability criteria. Consequently, all state variables R, P, and S in (5.6) decay to zero, confirming convergence to the null attractor O.

Conversely, any violation of these three inequalities destabilizes O, allowing the system to evolve toward non-trivial fixed points where at least one strategic species survives. These alternative equilibria represent scenarios where ecological balance is partially or fully restored, emphasizing the delicate parametric thresholds governing survival and extinction in our model.

5.2.2 The axial attractors, and the non-attractors

Within the complex evolutionary dynamics of our eco-strategic system (5.6), axial attractors represent fundamental equilibrium states where only one of the three competing strategies achieves long-term dominance, while the other two face inevitable

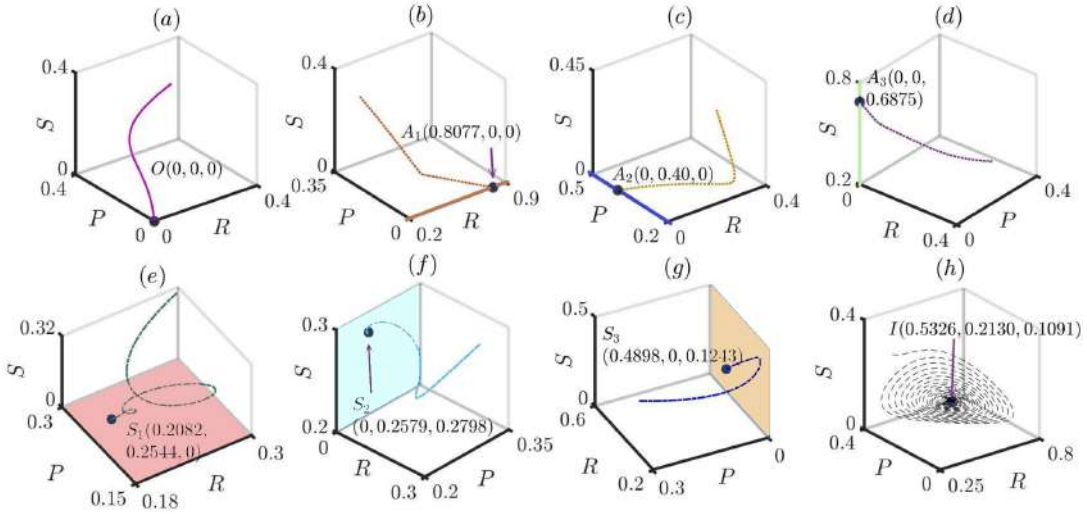

Figure 5.1: **Trajectories of different steady strategic attractors of the strategic species**: This figure portraits three dimensional phase diagrams of the state variables R (rock), P (paper), and S (scissor) of our system (5.6) starting from the same initial aggregate $(0.3, 0.3, 0.3)$. There are eight stationary attractors of the system, depicted in the eight consecutive subfigures. We obtain the presence of the null attractor $O(0,0,0)$ in subfigure (a), while subfigures $(b), (c)$, and (d) showcase the stable axial strategic attractors (I(A_1), II(A_2), and III(A_3) respectively), and the converged axes are being marked by brown, blue and light green colors accordingly in these sub-diagrams. We denote the path trajectories for the axial attractors by the dotted lines. In the subfigures $(e), (f)$, and (g), we observe that the paths produced by the state variables converge to the planar attractors (I(S_1), II(S_2), and III(S_3) respectively). We use dash-dotted lines to represent the trajectories of the variables for the planar attractors. The planes, in which the trajectories of the species converge are marked by salmon pink, cyan and yellow backgrounds respectively. Finally, we obtain a spirally stable spatial stable attractor (I), which preserves the presence of three strategies simultaneously. We mark this path by dashed line. The set of parameter values used to make these figures are described in the main text sections accordingly.

extinction. These attractors are termed "axial" due to their geometric positioning along the principal axes of our three-dimensional strategy space, reflecting the exclusive survival of either rock, paper, or scissor strategists. Their stability is governed by precise parametric conditions that determine which strategy prevails, offering a mathematical lens to study winner-takes-all ecological scenarios.

• Axial attractor-I $(A_1(\hat{R}, 0, 0))$: This equilibrium state emerges when the rock-strategic species dominates, driving both paper- and scissor-strategic populations to extinction. Mathematically, it is characterized by the fixed point $A_1(\hat{R}, 0, 0)$, where the surviving rock-strategist population $\hat{R}$ is explicitly given by $\hat{R} = \dfrac{\sigma_R + \alpha - 1}{\sigma_R}$. This expression reveals that the equilibrium abundance of rock strategists depends critically on the interplay between the strategy-specific weight α and the decay rate σ_R. To empirically validate this attractor, we simulate the system with parameters

$a = 0.11$, $b = 1.64$, $c = 0.55$, $\sigma_R = 0.52$, $\sigma_P = 0.72$, $\sigma_S = 0.60$, $\alpha = 0.9$, $\beta = 0.24$, and $\xi = 0.20$. These values satisfy the stability condition $\sigma_R + \alpha > 1$, leading to convergence at $\hat{R} = 0.8077$, as depicted in Fig. 5.1 (b). This outcome mirrors ecological systems where a single trait (e.g., aggression in rock strategists) becomes unbeatable due to environmental or competitive asymmetries.

• Axial attractor-II ($A_2(0, \hat{P}, 0)$): Here, the paper strategy prevails, outcompeting rock and scissor strategists through superior adaptive pressure. The equilibrium is quantified by $A_2(0, \hat{P}, 0)$, where $\hat{P} = \dfrac{\sigma_P - \beta}{\sigma_P}$ reflects the fraction of paper strategists at stability. The numerator $\sigma_P - \beta$ highlights that survival requires the decay rate σ_P to exceed the strategy-specific pressure β. For instance, with parameters $a = 0.30$, $b = 0.40$, $c = 0.15$, $\sigma_R = 0.35$, $\sigma_P = 0.40$, $\sigma_S = 0.28$, $\alpha = 0.9$, $\beta = 0.24$, and $\xi = 0.25$, the system stabilizes at $\hat{P} = 0.40$ (Fig. 5.1 (c)). This scenario models ecosystems where traits like resource efficiency (paper strategists) trump brute-force competition.

• Axial attractor-III ($A_3(0, 0, \hat{S})$): Dominance of scissor strategists defines this equilibrium, with $\hat{S} = \dfrac{\sigma_S - \xi}{\sigma_S}$ representing their equilibrium population. The stability condition $\sigma_S > \xi$ ensures that the decay rate σ_S outweighs the strategic cost ξ. Using parameters $a = 0.50$, $b = 0.03$, $c = 0.50$, $\sigma_R = 0.60$, $\sigma_P = 0.72$, $\sigma_S = 0.80$, $\alpha = 0.78$, $\beta = 0.24$, and $\xi = 0.25$, we observe $\hat{S} = 0.6875$ (Fig. 5.1 (d)). Such dynamics mimic systems where "specialist" traits (e.g., scissor-like precision) dominate due to high environmental specificity.

The non-attractors

Besides the asymptotic stability of these three single-strategic attractors of the system, we also observe a repulsive, kind of tug-of-war scenario, working cyclically among these three axial attractors, where each strategy tries to sustain the inherited species to let them evolutionary dominant over the other two. Eventually though, each of the strategies fails to make its respective species sustain over time by the overpowering domination of the preceding ability in a cyclic manner. As per the theory of the regular RPS dilemma, we observe a certain chain of domination among these three actions (Paper dominates rock, scissor dominates paper, and rock dominates scissor), this phenomenon also reflects the same way of the repulsive nature among these three axial attractors of the strategic species present in the ecosystem.

To overview this repulsive dynamical phenomenon among these three axial attractors, we carry out another experiment by fixing the parameter values at $a = 0.40$, $b = 0.25$, $c = 0.55$, $\sigma_R = 0.52$, $\sigma_P = 0.72$, $\sigma_S = 0.60$, $\alpha = 0.9$, $\beta = 0.24$, and $\xi = 0.20$ (showing in Fig. 5.2), which yields our model (5.6) out as,

$$\begin{aligned} \dot{R} &= R(-0.52R - 0.92P - 0.27S + 0.42), \\ \dot{P} &= P(-0.32R - 0.72P - 1.27S + 0.48), \\ \dot{S} &= S(-0.85R - 0.05P - 0.60S + 0.40). \end{aligned} \tag{5.7}$$

The above three-dimensional system (5.7) produces three axial fixed points:

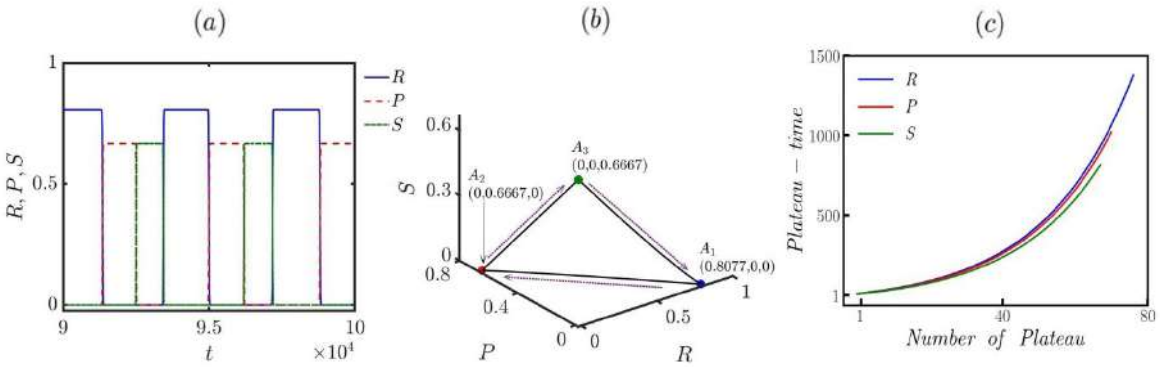

Figure 5.2: **Repulsion between the three axial strategies**: This diagram showcases an unstable dynamical portrait of the strategic species reduced from the system (5.7). Subfigure (a) portrays the oscillatory time series measures of R (rock),P (paper), and S (scissor), whereas subfigure (b) shows the three-dimensional phase diagram of the three kinds of species, showcasing sort of a tug of war kind of situation (the violet dotted arrows indicate the dominating chain of the three axial equilibrium points) among the three single-strategic unstable fixed points $(0.8077, 0, 0)$ (blue bubble), $(0, 0.6667, 0)$ (red bubble), and $(0, 0, 0.6667)$ (green bubble). These two subfigures experiments have been made with 10^7 number of iterations, extracting transient of initial 90×10^5 iterations. We in subfigure (c) mark the duration periods of these three axial non-attractors, seeming to act like the solo-dominant one, against the number of plateaus arises from the system deducing the initial 20,000 time iterations. Blue, red, and deep green lines are used to indicate rock, paper, and scissor strategic traits' increasing plateau times with respect to their number till 10^7 time iterations.

$(0.8077, 0, 0)$, $(0, 0.6667, 0)$, and $(0, 0, 0.6667)$. Analytical investigation reveals that all three of these points are unstable saddle points. Their respective eigenvalues are as follows: for $(0.8077, 0, 0)$, the eigenvalues are -0.4200, 0.2215, and -0.2865; for $(0, 0.6667, 0)$, they are -0.4800, -0.1933, and 0.3667; and for $(0, 0, 0.6667)$, the values are -0.4000, 0.2400, and -0.3667 (see Appendix 5.6.1 for detailed derivations).

Upon analyzing the time series behavior of system (5.7), we discover a remarkable phenomenon: during specific intervals of time, one of the strategic species momentarily dominates the ecosystem, effectively suppressing and eliminating the others. This species temporarily behaves as though it has achieved ecological supremacy, presenting itself as a stable axial attractor. However, over time, this apparent dominance is disrupted as another strategic species outcompetes the former, replacing its transient supremacy. This cyclical pattern of dominance is captured clearly in the time series trajectory illustrated in Fig. 5.2(a).

In the three-dimensional phase space constructed using the time series of the system (5.7), we observe a closed-loop trajectory representing the dynamic switching of dominance among species. Rather than forming a conventional limit cycle, the trajectory constructs a limit triangle, whose vertices correspond to the three axial fixed points of the system: $(0.8077, 0, 0)$ (blue solid dot), $(0, 0.6667, 0)$ (red solid dot), and $(0, 0, 0.6667)$ (green solid dot) as shown in Fig. 5.2(b). Despite being fixed

points, these vertices are not true attractors of the system (5.7) but serve instead as transitional pseudo-stable states in the dynamical cycle.

From the ecological perspective, we interpret this dynamical behavior as a form of rotating dominance among the 'rock', 'paper', and 'scissor' strategies. Notably, the rock species reaches a maximum abundance of 0.8077, while both the paper and scissor species peak at 0.6667, albeit over different temporal durations at their respective dominance phases.

To assess the persistence and sustainability of these pseudo-attractors, we conduct a long-run numerical experiment involving 10^7 iterations with a step size of 0.01, excluding the initial transients. The outcome of this test is presented in Fig. 5.2(c), where the duration of strategic dominance is traced over time. The three colored lines—blue for rock, red for paper, and green for scissor—show monotonic growth patterns, indicating that each strategic species sustains its dominance phase for progressively longer intervals as time evolves. Despite the stochastic-like fluctuations, this result underscores a subtle co-persistence mechanism, where no species is permanently excluded, and all maintain intermittent supremacy over sufficiently long timescales.

5.2.3 The planar attractors

The planar attractors in general signify the steady strategic outcomes of the system (5.6), those are propelled by particularly two strategies and their respective species in the habitat simultaneously, acting as the surviving species in the race of evolution. These dual strategic attractors locate on the coordinate planes of the considered three dimensional strategy space, which lead them to name as the planar attractor. Our system yields three planar attractors based on their convergence to any of the three considered planes of the strategy space.

• **Planar attractor-I ($S_1(\hat{R}, \hat{P}, 0)$):** Planar attractor-I sets a stage for an ecological scenario in which traits associated with evolutionary 'rock' (R) and 'paper'(P) strategies to dominate the entire environment, superseding the influence of the 'scissor'(S) strategy and leading to the defeat of its follower species. This strategic state is represented mathematically as $S_1(\hat{R}, \hat{P}, 0)$, where $\hat{R}$ and $\hat{P}$ denote the normalized frequency of species adopting the rock and paper strategies, respectively. Here, $\hat{R} = \dfrac{\beta(a+\sigma_R) - \sigma_P(a-\alpha+1)}{a(a+\sigma_R-\sigma_P)}$ and $\hat{P} = \dfrac{\sigma_R(a-\beta) + (a-\sigma_P)(\alpha-1)}{a(a+\sigma_R-\sigma_P)}$ are the parametric shapes of the frequency of rock and paper strategic species surviving in the dilemma accordingly. We execute an experiment taking parameter values $a = 2.5$, $b = 0.80$, $c = 0.45$, $\sigma_R = 1.37$, $\sigma_P = 0.52$, $\sigma_S = 0.80$, $\alpha = 0.90$, $\beta = 0.80$, and $\xi = 0.40$, to reach out the stable planar attractor-I $S_1(0.2082, 0.2544, 0)$ (see Fig. 5.1 (e)).

• **Planar attractor-II ($S_2(0, \hat{P}, \hat{S})$):** This planar attractor ensures durability of only those player species, whose action in evolution are 'paper' (P) and 'scissor' (S) respectively. We name this dual strategic attractor as planar attractor-II $S_2(0, \hat{P}, \hat{S})$, where $\hat{P} = \dfrac{\xi(c+\sigma_P) - \sigma_S(c+\beta)}{c(c+\sigma_P-\sigma_S)}$, and $\hat{S} = \dfrac{\beta(\sigma_S-c) - \sigma_P(\xi-c)}{c(c+\sigma_P-\sigma_S)}$ determine the frequency of these two strategic traits present in the habitat. For our experiment, we use the set of parameter values, $a = 0.60$, $b = 0.50$, $c = 0.56$, $\sigma_R = 0.49$, $\sigma_P = 0.75$,

$\sigma_S = 0.25$, $\alpha = 0.50$, $\beta = 0.19$, and $\xi = 0.26$, which enhance planar attractor-II $S_2(0, 0.2579, 0.2798)$ to become stable (Fig. 5.1 (f)), and the paper, and scissor strategic species to remain evolutionary surviving species in the race of evolution.

• **Planar attractor-III ($S_3(\hat{R}, 0, \hat{S})$):** Like the two previously discussed planar attractors, this dual strategic planar attractor-III represents an evolutionary stable abode of the combined strategies 'rock' (R) and 'scissor' (S), winning over the action of 'paper' (P) in this dilemma. Symbolically, we denote the planar attractor-III as $S_3(\hat{R}, 0, \hat{S})$, where $\hat{R} = \dfrac{\sigma_S(b+\alpha-1) - \xi(b-\sigma_R)}{b(b+\sigma_S-\sigma_R)}$, and $\hat{S} = \dfrac{(1-\alpha)(b+\sigma_S)}{b(b+\sigma_S-\sigma_R)}$ denote the parametric shapes of the species having 'rock' and 'scissor' strategies respectively surviving in this situation. We can visualize the consequent presence of these two species from our model (5.6) by using parameter values $a = 0.60$, $b = 0.12$, $c = 0.25$, $\sigma_R = 0.35$, $\sigma_P = 0.45$, $\sigma_S = 0.80$, $\alpha = 0.85$, $\beta = 0.70$, and $\xi = 0.25$, which leads the system to converge at planar attractor-III $S_3(0.4898, 0, 0.1243)$ (see Fig. 5.1 (g)).

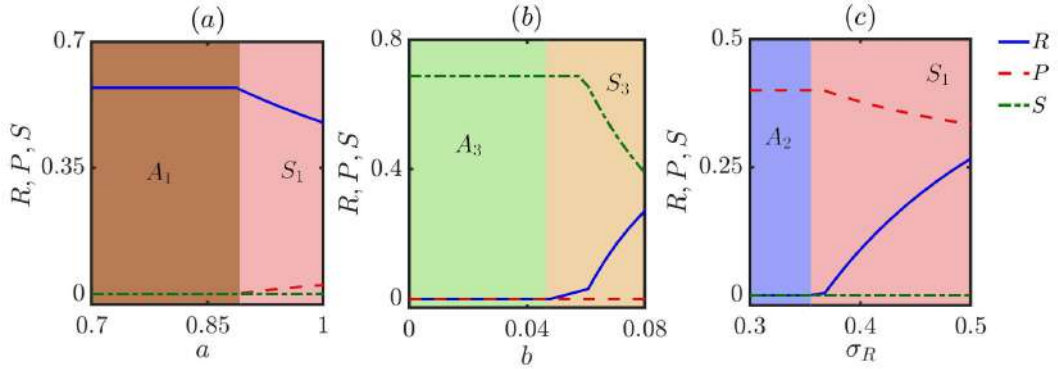

Figure 5.3: **Parametric routes, causing interchange of the strategic behaviors from axial to planar in the variation of the payoff amount parameters a, b, and the free space reduced contribution towards the rock strategic species σ_R:** These figure diagram showcases the variations of three parameters, a (subfigure (a)),b (subfigure (b)) and σ_R (subfigure (c)), which leads the system transform their stable strategic features. Subfigure (a) represents the transformation from of the axial attractor-I (A_1) into the planar attractor-I (S_1), with respect to the increment of the payoff parameter a. Subfigure (b) though indicates the change of the axial attractor-III (A_3) getting transformed into planar attractor-III(S_3) with the increasing frequency of the payoff value b. Lastly, subfigure (c) gives a view of how the axial attractor-II (A_2) gets transformed into planar attractor-I (S_1), jointly driven by strategies of 'rock' and 'scissors' as we increase the frequency of the free space induced resource σ_R. We take 10^7 numbers of iterations with step size 0.01, letting the initial 95×10^5 exclude from consideration. Brown colored background indicates the strategic axial attractor-I (A_1), blue colored region depicts the axial attractor-II (A_2), light green colored region indicates the axial attractor-III (A_3), salmon pink colored region identifies the planar attractor-I (S_1), and cream colored region is the planar attractor-III (S_3).

Change of system parameters interchanging the modes of stability of the strategic attractors from axial to planar

In this segment, we essentially examine the transition from a stable axial attractor to a stable planar attractor of our system (5.6) by observing the variation of one of the system parameters. For this, we carry out three experiments, of which firstly we use variation in the payoff size a from 0.7 to 1, keeping the other parameters fixed at, $b = 1.50$, $c = 0.25$, $\sigma_R = 0.35$, $\sigma_P = 0.45$, $\sigma_S = 0.80$, $\alpha = 0.85$, $\beta = 0.70$, and $\xi = 0.25$ (Fig. 5.3 (a)). Till $a = 0.8875$, we observe the player traits having the evolutionary sense 'rock' (axial attractor-I $A_1(0.5714, 0, 0)$ denoted by brown colored background in Fig. 5.3 (a)) to be taking the charge up for the entire game dilemma keeping all the other strategies to be subjugated by it. Since $a > 0.8875$, the strategic attractor takes different shape, as the sufficiently large amount a enhance the paper strategic traits to sustain their kinds along with the decreasing quantity of the rock traits, and making the axial attractor-I A_1 getting transformed into the planar attractor-I, with a-parametric shape $S_1\Big(\frac{100a+71}{40a(10a-1)}, \frac{80a-71}{40a(10a-1)}, 0\Big)$ (denoted by salmon pink region in Fig. 5.3 (a)). In the planar attractor-I S_1, we observe the frequency of the two present strategies to be in reversely varying with each other. In the Fig. 5.3 (b), we observe another transition in the nature of the attractors, as we keep increasing the second game payoff factor b keeping all other parameters to be fixed at $a = 1.5$, $c = 0.25$, $\sigma_R = 0.35$, $\sigma_P = 0.45$, $\sigma_S = 0.80$, $\alpha = 0.85$, $\beta = 0.70$, and $\xi = 0.25$. With this set of parameter values, our model (5.6) alleviates to,

$$\begin{aligned} \dot{R} &= R(-0.35R - 1.85P + (b - 0.35)S + 0.20), \\ \dot{P} &= R(1.05R - 0.45P - 0.70S - 0.25), \\ \dot{S} &= S(-(b + 0.80)R - 0.55P - 0.80S + 0.55). \end{aligned} \tag{5.8}$$

As per the Fig. 5.3 (b) portrays, we observe the solo dominance of the strategy 'scissor' (S) for the value of the payoff parameter b, being varied from 0 onwards. With the consideration of our chosen parameter attributes, we get the stable axial attractor-III taking the shape up as $A_3(0, 0, 0.6875)$ $(\frac{\sigma_S - \xi}{\sigma_S} = \frac{0.8 - 0.25}{0.8} = 0.6875)$ and denoted by light green background in Fig. 5.3 (b)). For such axial strategic attractor, we find the eigenvalues from the Jacobian matrix of the system 5.8 to be -0.73125 (< 0), $-0.55 (< 0)$, and $0.6875b - 0.040625$. Now, according to Sotomayor's theorem (the entire theoretical work is done at 5.6.1), on the note of the occurrence of Transcritical bifurcation causing the change in the nature of our model's attractors, one eigenvalue must be equal to 0. Based on this theory, we observe this occurrence to take place at $b = \frac{0.040625}{0.6875} \approx 0.0591$. At Fig. 5.3 (b), we find that the transition between these two strategic attractors stages exactly at the same parameter value $(b = 0.0591)$. Onwards, the axial attractor-III $A_3(0, 0, 0.6875)$ looses it's stability and the strategic planer attractor III $(S_3\Big(\frac{220b - 13}{20b(20b + 9)}, 0, \frac{13 - 80b}{20b(20b + 9)}\Big)$ and marked by cream colored background in Fig. 5.3 (b)) takes the charge of being the stable strategic attractor by assigning the rock and scissor strategic species to

govern the habitat in reciprocal frequency to each other. In the game theoretic sense, as the payoff value b increases, the chances of more survivability of the player kinds consuming the rock strategy increase. In similar way-out, Fig. 5.3 (c) illustrates identical transition scenario in the stability of the axial attractor-II. This transition is instigated by the sole strategy of 'paper' (A_2 $(0, 0.40, 0)$, marked with blue background in Fig. 5.3 (c)) being threatened by the planar attractor, jointly dominated by the strategies of 'rock' and 'paper' ($S_1\Big(\frac{4(30\sigma_R-11)}{5(30\sigma_R-3)}, \frac{6\sigma_R+1}{30\sigma_R-3}, 0\Big)$, indicated by a salmon pink background in Fig. 5.3 (c)). Clearly, σ_R is the free space induced reproductive resource parameter, providing direct benefit to the species consuming the 'rock' strategy. The other conditions those satisfy the conditions of Transcritical bifurcation are discussed in the Appendix section (5.6.3).

5.2.4 The interior spatial strategic attractor and the instances of Hopf bifurcations in it

The strategically most significant attractor, from both a biological and game theoretical perspectives, is the stable scenario involving all three evolutionary strategies: 'rock', 'paper', and 'scissor' - existing togetherly at a same time instance. Derived from our system (5.6), this fixed point, termed to be the interior spatial strategic attractor, represents a stable stationary state where all three species with their corresponding strategies persist together in the evolutionary dilemma. This evolutionary attractor situates within the strategy space reduced by the co-ordinate axes, along which, the three evolutionary actions 'rock', 'paper', and 'scissor' are being considered. We denote this spacial attractor as $I(\hat{R}, \hat{P}, \hat{S})$, where

$$\hat{R} = \frac{\psi_1(c\psi_4) + (a+\sigma_R)\psi_5 + (\sigma_R - b)\psi_{10}}{\Delta},$$
$$\hat{P} = \frac{\sigma_R\psi_2 + \psi_1\psi_6 - (b-\sigma_R)\psi_7}{\Delta},$$
$$\hat{S} = \frac{\sigma_R\psi_3 + (a+\sigma_R)\psi_9 + \psi_1\psi_8}{\Delta},$$

with $\psi_1 = (\sigma_R + \alpha - 1)$, $\psi_2 = \xi(c+\sigma_P) - \sigma_S(c+\beta)$, $\psi_3 = \sigma_P(c-\xi) + \beta(\sigma_S - c)$, $\psi_4 = c + \sigma_P - \sigma_S$ $\psi_5 = \sigma_S(c+\beta) - \xi(c+\sigma_P)$, $\psi_6 = \sigma_S(a+c) + b(\sigma_P + c)$, $\psi_7 = \xi(a-\sigma_P) - \sigma_S(a+\beta) + b(\beta - \sigma_P)$, $\psi_8 = a(c-\sigma_S) - \sigma_P(b+c)$, $\psi_9 = b(\sigma_P - \beta) - \sigma_S(\beta - a) + \xi(\sigma_P - a)$, $\psi_{10} = \beta(c-\sigma_S) - \sigma_P(c-\xi)$, and $\Delta = a^2\sigma_S + b^2\sigma_P + c^2\sigma_R) + ab(\sigma_P + \sigma_S) + bc(\sigma_R + \sigma_P) + ca(\sigma_R + \sigma_S$ representing the quantities of the strategic species in parametric shapes of the system, present in the terrain.

A real ecological instance involving three cyclically dominant species is observed in some of the aquatic ecosystems, particularly in phytoplankton dynamics. This phenomenon is often referred to as the"phytoplankton rock-paper-scissors" game, where three types of phytoplankton survive togetherly in a same habitat. We moreover execute an experiment by setting the system parameters at values, $a = 0.90$, $b = 0.75$ $c = 0.25$, $\sigma_R = 1.1$, $\sigma_P = 2.05$, $\sigma_S = 2.52$, $\alpha = 0.95$, $\beta = 0.75$, and $\xi = 0.02$, which emits the spirally steady interior stationary

point $I(0.5326, 0.2130, 0.1091)$ (portrayed in Fig. 5.1 (h)). Analytically, this stable stationary attractor $I(0.5326, 0.2130, 0.1091)$ proves out to be a spirally stable strategic state, as this setup of parameter values emerges eigenvalues as, $\lambda_1 = -1.2868$, and $\lambda_{2,3} = -0.0053 \pm 0.273i$.

This strategic configuration captures the transition in the steady coexistence of

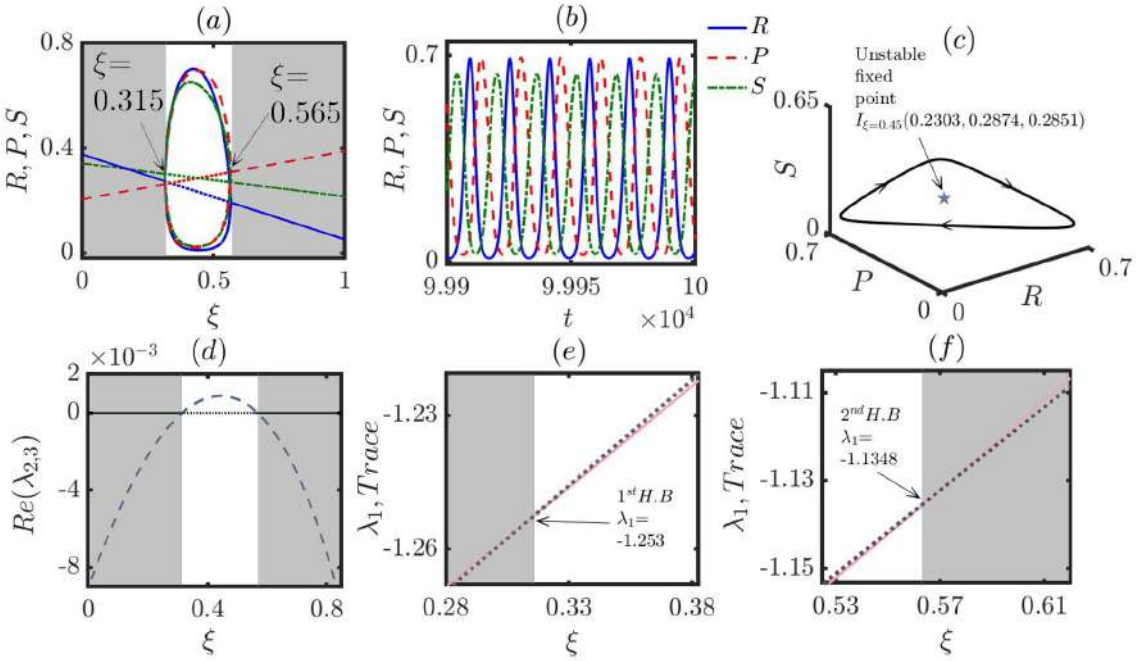

Figure 5.4: **Modulating the extinction rate of scissor species (ξ) induces successive Hopf bifurcations in the spatial strategic attractor:** This figure illustrates two consecutive Hopf bifurcations triggered by varying the extinction rate of the scissor species $\xi \in (0, 1]$, along with analytical validations. Light grey zones in subfigures $(a), (d), (e)$, and (f) denote stable coexistence; uncolored areas represent instability. subfigure (a) shows the bifurcation diagram with maximum and minimum trait frequencies over ξ, revealing oscillatory onset between $\xi = 0.315$ and 0.565. Rock, paper, and scissor strategies are marked by blue solid, red dashed, and green dash-dotted lines, respectively; dotted lines indicate unstable fixed points of system (5.6). subfigure (b) displays oscillations at $\xi = 0.45$, and (c) shows the 3D phase portrait with a closed trajectory and unstable fixed point (blue star). subfigure (d) plots $Re(\lambda_{2,3})$ (blue dashed) and zero-threshold (black) over ξ. subfigures (e) and (f) depict the trace (black dotted) and real eigenvalue λ_1 (pink) confirming super- and sub-critical Hopf bifurcations, respectively.

these species to let them oscillate in a sequence of events, responsive to variations in a specific system parameter. The oscillatory dynamics of these strategic species aptly illustrate the dilemmatic circumstances of the game dilemma in a cyclic manner, as illustrated in Fig. 5.4 (b). Notably, the oscillatory coexistence, caused by super-critical Hopf bifurcation and countermand sub-critical Hopf bifurcation, is uniquely observed in this coexisting representation of the strategic species.

We consider the set of parameters, $a = 1.5$, $b = 1$, $c = 1.2$, $\sigma_R = 1.5$, $\sigma_P = 1.25$, $\sigma_S = 1.7$, $\alpha = 0.85$, $\beta = 0.25$, and vary the ecological parameter ξ, the rate of

extinction of the evolutionary species having the strategy scissor within the range $(0, 1]$ to observe the variation in the interior spatial attractor $I(\hat{R}, \hat{P}, \hat{S})$. We also verify some of the analytical justification regarding these simultaneous events found from this experiment.
With all other parameters to be fixed at the above values, and with a variable ξ, our model reduces to the ξ-parametric shape as,

$$\begin{aligned} \dot{R} &= R(-1.5R - 3P - 0.5S + 1.35), \\ \dot{P} &= P(0.25R - 1.25P - 2.45S + 1), \\ \dot{S} &= S(-2.7R - 0.5P - 1.7S + (1.7 - \xi)). \end{aligned} \tag{5.9}$$

In order to vary the ecological extinction rate ξ, first we obtain our interior spatial attractor to be acquiring the parametric shape of $I_\xi(0.3763 - 0.3246\xi, 0.2048 + 0.1834\xi, 0.3421 - 0.1267\xi)$. The frequency of this strategic attractor gradually varies, as the parameter value ξ changes from 0 onwards. In the chain of RPS, rock-strategy grabs a clear win over the strategy scissor. Eventually, as the decaying rate starts increasing for the scissor species, interesting consequences of falling for both the strategies rock and scissor are observed (blue colored solid line, and green dash-dotted line in Fig. 5.4 (a)). Moreover, the decaying calamity of the rock species is found to be more redundant than that of the scissor kinds, even we observe the monotonically increasing decaying flow of the scissor traits only (green dash-dotted lines in the Fig. 5.4 (a)). This slower decaying cascade of the scissor strategy also seems worthwhile due to the even-handedly high contribution of the free space to this particular trait ($\sigma_S = 1.7 > \sigma_R$). Nevertheless, a complementary effect is seen for the paper strategic species because of the weakness of paper move against the ability of scissor. That works out well to the increasing flow of the paper strategic species (red dashed line in Fig. 5.4 (a)) in our dynamical framework. However, the analogy of the stable co-existence breaks at the value of ξ to reach at 0.315, where the first Hopf bifurcation (super-critical) occurs. After this critical value of ξ, the appearance of oscillatory presence is found among the player populations. After the super-critical Hopf bifurcation transpires, the stable mannered co-existence of the strategic species breaks into unstable oscillations, exhibiting cyclical dominating frequencies of the three species present in the habitat. The cycle formed by the oscillatory frequencies of the species remains well-justified to the analogy of strategies of the proposed game dilemma (see the oscillatory dynamics for $\xi = 0.45$ Fig. 5.4 (b)). With further increment of the extinction rate ξ, a sub-critical Hopf bifurcation is seen to occur at $\xi = 0.565$. Remarkably, surpassing the sub-critical Hopf bifurcation, we note a significant increase in the frequency of paper strategic traits, surpassing that of all others. Analytically, intriguing changes in the eigenvalues of the system become apparent at the critical values of the parameter ξ, resulting in consecutive Hopf bifurcations in our system. Specifically, upon reaching to the super-critical Hopf bifurcation at $\xi(= 0.315)$, our system (5.6) manifests eigenvalues as follows: $\lambda_1 = -1.253$, precisely the same to the trace of the Jacobian matrix (see section 5.6.1) derived from system (5.6), and calculated concerning the interior spatial fixed point formed at $\xi = 0.315$, and all other fixed values of parameters. Notably, the other two eigenvalues exclusively possess purely imaginary attributes,

namely $\lambda_{2,3} = \pm 0.5997i$ (equal to $\pm\kappa_2$ of (5.12) in section 5.6.1). However, the mathematical verification to this phenomenon are given through the Figs. 5.4 $(d), (e)$, and (f). In the portions exhibiting steady coexistence of the strategic species (marked by light grey backgrounds in Figs. 5.4$(a), (d), (e)$, and (f)), the complex conjugated eigenvalues attain a negative real part, and the real eigenvalue ensures of having a higher magnitude than that of trace of the Jacobian matrix of the system (real eigenvalues of the system are plotted with pink lines, and traces are marked with black dots in Figs. 5.4 (e), and (f)). Onwards with the occurrence of the super-critical Hopf bifurcation, we observe riveting changes. The real part of the complex conjugate eigenvalues turns out to be positive (real part of the complex conjugated eigenvalues is plotted with blue dashed curve in Figs. 5.4 (d)), while the value of trace exceeds the the value of the real eigenvalue of the system (see Fig. 5.4 $(e), (f)$). This phenomenon breaks its order when the sub-critical Hopf bifurcation appears at $\xi = 0.565$ and the oscillations turn into steady co-existence of the strategic species. Afterwards, the real parts of the complex conjugate eigenvalues turn down to be negative, whereas the real eigenvalues start exceeding over to the value of trace.

For an overview to see the unstable abundance of species, we consider the same set of parameter values as we considered in (5.9), but here we fix ξ at 0.45. With such consideration, our model reduces to,

$$\begin{aligned} \dot{R} &= R(-1.5R - 3P - 0.5S + 1.35), \\ \dot{P} &= P(0.25R - 1.25P - 2.45S + 1), \\ \dot{S} &= S(-2.7R - 0.5P - 1.7S + 1.25). \end{aligned} \tag{5.10}$$

System (5.10) yields an unstable interior fixed point as, $I(0.2303, 0.2874, 0.2851)$. Thus, due to emerging unstable features, our eco-evolutionary system (5.10) unveils oscillatory dynamics in such a manner that each of the three moves, viz., 'rock', 'paper', and 'scissor' is able to overpower the succeeding move, and also faces vanquish to the previous action. One real ecological instance that corresponds to the likely oscillatory cyclic behavior among three species is the prey-predator interaction involving hare, lynx, and their shared vegetation resources. This ecological dynamic is observed in the world's northernmost forest, the Boreal forests of North America. Nevertheless, we delineate the time series of our system's oscillatory dynamics, and three-dimensional phase plane portrait of the three strategies respectively in Figs. 5.4 (b), and (c). The oscillatory time series (Fig. 5.4 (b)) of the three corresponding strategic species exhibits a cyclic chain in frequencies preserving the game dilemmatic, and the ecological manners of food and energy in a well-justified way. Blue, red, and green colored lines (solid, dashed, and dash-dotted ways respectively) in the time series diagram represent the 'rock', 'paper', and 'scissor' strategic species respectively. A cyclic chain among the abilities of 'rock', 'paper', and 'scissor' is preserved, which resembles enough with the oscillatory cyclic behavior in this ecological scenario demonstrating a dynamic interplay among lynx, hares, and vegetation. In our case of depicting a three dimensional phase portrait, a stable limit cycle is found (Fig. 5.4 (c)), performing a closed trajectory surrounding the three dimensional space. The interior unstable equilibrium point $I(0.2303, 0.2874, 0.2851)$ reduced from this system is also marked by a shape as a

star in Fig. 5.4 (c). To view in corresponding analytical overview, the occurrence of Hopf bifurcation in the interior fixed strategic point with respect to varying a single parameter induced to the system follows the outline of the theory.
• Let our three-dimensional eco-evolutionary dynamical system reduce $I_\xi(\hat{R}, \hat{P}, \hat{S})$ as an interior equilibrium point reduced in terms of one of the variable parameters ξ induced to the system (5.6), and $J(\xi)$ is the Jacobian matrix of the system, corresponding to the equilibrium point $I_\xi(\hat{R}, \hat{P}, \hat{S})$. At $\xi = \xi_c$, the critical instance of ξ, where the occurrence of Hopf bifurcation is seen in the system, the trace and the three eigenvalues of the Jacobian matrix $(J(\xi_c))$ at the critical instance of ξ yield following behaviors:
(i) The real eigenvalue reduced from the system at ξ_c manifests as, $\lambda_1(\xi_c) = Trace(J(\xi_c)) < 0$, and
(ii) The complex-conjugated eigenvalues follow: $\lambda_{2,3}(\xi_c) = \pm i\sqrt{A_{11}(\xi_c) + A_{22}(\xi_c) + A_{33}(\xi_c)}$,
where $A_{11}(\xi_c) = a_{22}(\xi_c)a_{33}(\xi_c) - a_{23}(\xi_c)a_{32}(\xi_c)$, $A_{22}(\xi_c) = a_{11}(\xi_c)a_{33}(\xi_c) - a_{13}(\xi_c)a_{31}(\xi_c)$, $A_{33}(\xi_c) = a_{11}(\xi_c)a_{22}(\xi_c) - a_{12}(\xi_c)a_{21}(\xi_c)$, representing the co-factors of the diagonal elements of the Jacobian matrix $J(\xi_c)$. Moreover, the determinant of $J(\xi_c)$ can be found as, $det(J(\xi_c)) = Trace(J(\xi_c))(A_{11}(\xi_c) + A_{22}(\xi_c) + A_{33}(\xi_c)) < 0$ (for further calculation check section 5.6.1).

5.3 Single parameter bifurcation ripple: Evolutionary dynamics of strategic species

In this section, we vary four of the system parameters β, α, σ_R, and c (shown in Figs. 5.5 $(a), (b), (c)$, and (d) respectively) with all other parameters' values fixed. In our mathematical framework, β is considered to be the rate of extinction of the paper kinds in the cyclic chain of the strategic species. In the observation that varies this rate from 0 percent to 100 percent (thus from 0 to 1), the consideration of very low frequency of β, with fixed parameter values, $a = 1, b = 0.5, c = 0.25, \sigma_R = 0.35, \sigma_P = 0.95, \sigma_S = 0.8, \alpha = 0.85$, and $\xi = 0.25$, the situation yields a reciprocated coexistence of the species having strategies 'paper' and 'scissor' simultaneously (planar attractor II is marked by cyan background in Fig. 5.5 (a)) in the environment. This dual strategic evolutionary rhythm sustains until the value of β reaches up to 0.09. Afterwards, the evolutionary dynamics unfold as the extinct rock species resurges alongside the other two strategic species. The rise of the rock species triggers a growing decline in the scissor species, dropping from 0.5434. Subsequently, the paper species, though challenged by the scissor's defeat, experiences a slower rate of decay. Stability in the interior spatial attractor I is maintained (light grey background in Fig. 5.5 (a)) until the first (super-critical) Hopf bifurcation at $\beta = 0.38$. Coexistence stability gives way to oscillations, leading to cyclic dominance among the traits (uncolored/white background in Fig. 5.5 (a)). Following a sub-critical Hopf bifurcation at $\beta = 0.59$, stable coexistence of the strategic species resumes. The rock species surpasses the frequencies of paper and scissor, and after $\beta = 0.93$, the scissor species succumb to the high frequency of their opponent, rock. Subsequently, only rock and paper species persist in the ecological environment up

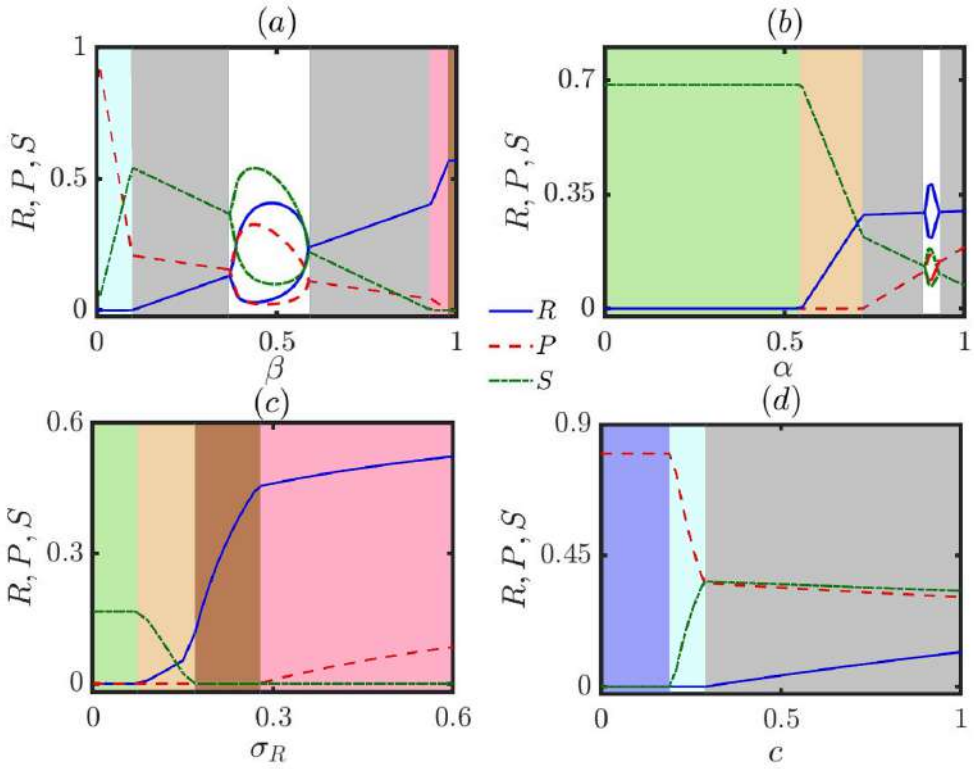

Figure 5.5: **Single parameter bifurcation diagrams:** These diagrams show how various dynamical features change with variations in the annihilation rate of paper traits (β), the reversed extinction frequency of rock species (α), the evolutionary contribution of free space to rock species (σ_R), and the game payoff amount (c). Blue solid, red dashed, and green dash-dotted lines represent the maximum and minimum frequencies of rock, paper, and scissor strategies, respectively. Background colors (explained in the main text) indicate different stable attractors, while uncolored areas denote unstable regions. Simulations are run for 10^7 iterations, with the first 95×10^5 treated as transient and excluded from analysis.

to $\beta = 0.97$ (planar attractor I identified by salmon pink background in Fig. 5.5 (a)). Beyond this point, the extinction rate of paper traits rises, leading to their extinction like the previously extincted scissor traits. From $\beta = 0.97$ to 1, we observe the asymptotic stability of axial attractor-I, where only the rock species remains, sustaining at a constant level (0.5714) in the environment (brown background in Fig. 5.5 (a)).

In following experiment (5.5 (b)), we vary the parameter α, representing the reversed rate of death for the rock species in the competitive environment. With a very low frequency of α (up to $\alpha = 0.54$), the rock species faces high extinction rates, leading to their absence in the ecological system. Since the paper strategy prevails over rock, there is no presence of paper kinds in this infertile region for the rock. Consequently, the frequency of the scissor species dominates the entire game, and the asymptotic stability of axial attractor-III is observed (light green background in Fig. 5.5 (b)). Upon crossing $\alpha = 0.54$, the extinction rate decreases, allowing the rock species to coexist with the scissor kinds. Rock starts dominating

over scissor, resulting in a stable planar attractor-III (cream background in Fig. 5.5 (b)) with reciprocated frequency changes between rock and scissor. Subsequently, as the rock species increases, the paper strategy gains an opportunity to survive along with rock and scissor species. After $\alpha = 0.72$, the planar attractor-III transitions to an interior spatial attractor (light grey background in Fig. 5.5 (b)). Notably, the rock species frequency increases slowly, while reciprocal behaviors between paper and scissor frequencies are observed. Consecutive Hopf bifurcations occur at $\alpha = 0.89$ and $\alpha = 0.93$, breaking the stability of the spatial attractor and introducing oscillations (uncolored region in Fig. 5.5 (b)). During this unstable period, no cyclic dominance is evident, as the amplitudes of rock remain extremely high compared to others. No other strategy prevails over the dominance of the rock strategy in this parameter range. The remaining fixed parameters for this experiment are $a = 1, b = 0.5, c = 0.25, \sigma_R = 0.35, \sigma_P = 0.95, \sigma_S = 0.8, \beta = 0.70$, and $\xi = 0.25$.
In the variation of the free space-produced replicative welfare parameter σ_R within the range of 0 to 1, consecutive evolutionary stable axial and planar attractors emerge. The constant values for other parameters are set at $a = 1, b = 0.5, c = 0.25, \sigma_P = 0.45, \sigma_S = 0.3, \alpha = 0.85, \beta = 0.70$, and $\xi = 0.25$. For small fractional values of σ_R (up to 0.07), the low sustainability of rock's action leads to the dominance of the scissor species, making axial attractor-III evolutionary stable (light green background in Fig. 5.5 (c)). Beyond 0.07, the rock species gains enough benefit to coexist with scissor, stabilizing planar attractor-III (cream background in Fig. 5.5 (c)) with oscillating frequencies between rock and scissor. As σ_R grows to 0.17, the presence of the rock species alone dominates, making axial attractor-I stable (brown background in Fig. 5.5 (c)) until $\sigma_R = 0.27$. In this stable region, the rock species frequency significantly increases with the gradual increment of σ_R up to 0.27. However, stability is lost as paper species, prevailing over rock, starts to grow, reducing the rock species' rate of growth. For the range where planar attractor-I is stable (salmon pink background in Fig. 5.5 (c)), both rock and paper species' frequencies gradually increase. The growth in rock's frequency is evident due to an increased intake from the ecological free space, while paper species also strengthen themselves by winning over rock's ability.
In the variation of the payoff amount c, derived from the interaction between species with paper and scissor strategies, a fascinating sequence of strategic attractors emerges. The fixed parameters are kept at $a = 2.3, b = 1.5, \sigma_R = 1.5, \sigma_P = 1.25, \sigma_S = 1.7, \alpha = 0.85, \beta = 0.25$, and $\xi = 0.30$, while c is varied from 0 to 1. For small values of c, the paper species dominates, with a high frequency (0.8) in a stable axial attractor-II (blue background in Fig. 5.5 (d)). The substantial payoff amount ($a = 2.3$) for defeating rock contributes to the stability of this attractor up to $c = 0.20$. Beyond this, as c increases, the scissor species' frequency grows reciprocally with a decay in paper species. This fast growth in scissor species is due to the higher free space-induced benefit for the scissor strategy. A reciprocated trend forms a stable planar attractor-II (cyan background in Fig. 5.5 (d)). The scenario shifts at $c = 0.29$, where paper and scissor frequencies become almost equal. Beyond this point, rock species start to expand along with the other two strategies. The interior spatial attractor becomes stable (light grey background in Fig. 5.5 (d)). As rock expands, scissor frequencies begin to decay, and due to the dominating nature of

rock over scissor, the decay of scissor slows down. Paper species also start to decline, but the slower decay of scissor leads to a more gradual decay in paper, resulting in a slower decay compared to the previous planar attractor.

5.4 Variations of different strategic extant in two dimensional parameter spans of the system

We execute a few more appraisals with the aim to understand the distribution of the several strategic attractors, and the unstable features of our proposed eco-evolutionary system of strategic species. For this experiment, we take parameter values, $a = 1, b = 0.5, c = 0.25, \sigma_R = 0.35, \sigma_P = 0.45, \sigma_S = 0.80, \alpha = 0.85, \beta = 0.70$, and $\xi = 0.25$. Holding all but two parameters fixed at these reference values, we systematically vary the remaining pair to observe how the resulting shifts reshape both the locations of strategic attractors and the qualitative nature of the dynamics.

The outcomes are summarized in Fig. 5.6, which is organized into six sub-panels, (a) through (f). Each panel isolates a different category of parameter variation—payoff magnitudes, ecological thresholds, or extinction pressure—and visualizes the consequent changes in species composition and attractor stability. Together, these six portraits offer a comparative lens on how specific parameter pairings modulate the phase landscape: they reveal where new coexistence equilibria emerge, where single-species dominance reappears, and where regions of transient or oscillatory behaviour expand or contract. In this way, Fig. 5.6 provides a concise yet comprehensive map of the strategic regimes accessible to the model under the chosen parameter framework.

The proposed distributions of parameters in the "rock-paper-scissors (RPS)" dilemma hold biological and evolutionary significance, providing grounds for the stability of strategic attractors from both analytical and game theoretic perspectives. The simultaneous distribution of payoff measures a and b reveals stability patterns in various spans of the payoff values. For sufficiently low values of payoff b (up to 0.05), the environment favors the scissor species, resulting in the stable axial attractor-III (light olive green region in Fig. 5.6 (a)). As b increases, the sustainability of rock species alongside scissor is ensured, leading to the stability of planar attractor-III (cream-colored region in Fig. 5.6 (a)). This coexistence gradually diminishes as a increases from 0.90. A notable increment in b (from 0.16 onwards) transforms the coexistence into the sole survival of rock species (axial attractor-I in maroon-colored region in Fig. 5.6 (a)) until a reaches 0.88. This stable environment breaks down as a exceeds 0.88. With higher values of a, paper traits start to survive alongside rock, leading to the presence of planar attractor-I (salmon pink region in Fig. 5.6 (a)) beside axial attractor-I. A significant portion indicates the simultaneous survival of all three strategic species (grey region in Fig. 5.6 (a)). The evolutionary stability of the interior spatial attractor follows an increasing sequence of b with the increment of a. For example, at $a = 0.9$, coexistence starts with $b = 0.16$, and at $a = 0.95$, the attractor stabilizes at $b = 0.25$. Analytical borders of the stable attractors are denoted by black lines in each subfigure of Figure 5.6.
The distributions of the strategic attractors varying the payoffs b and c remain a

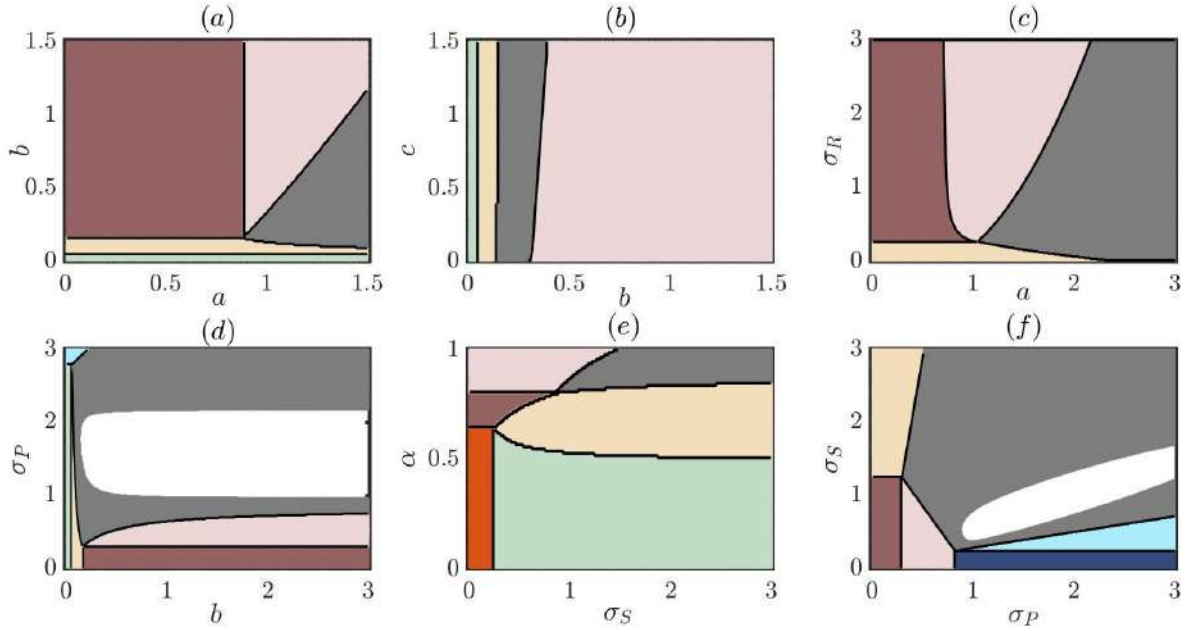

Figure 5.6: **Distributions of various evolutionary behaviors of the strategic species while two system parameters vary simultaneously:** These parameter-space diagrams (subfigures (a)–(f)) chart the strategic attractors of the model as two parameters change. Red in (e) marks the null attractor $(0, 0, 0)$. Maroon, deep blue, and olive green zones denote axial attractors I, II, and III—$(\hat{R}, 0, 0)$, $(0, \hat{P}, r)$, and $(0, 0, \hat{S})$—respectively. Salmon pink, cyan, and peach indicate planar attractors I, II, and III—$(\hat{R}, \hat{P}, 0)$, $(0, \hat{P}, \hat{S})$, and $(\hat{R}, 0, \hat{S})$. Grey regions show the interior mixed attractor $(\hat{R}, \hat{P}, \hat{S})$. Uncoloured areas in (d) and (f) are unstable, exhibiting oscillatory dynamics. Parameters: $a = 1$, $b = 0.5$, $c = 0.25$, $\sigma_R = 0.35$, $\sigma_P = 0.45$, $\sigma_S = 0.8$, $\alpha = 0.85$, $\beta = 0.70$, $\xi = 0.25$. Simulations run for 10^7 iterations, discarding the first 9.5×10^6 as transient. Black borders mark analytical state boundaries. Initial fractions are $(0.3, 0.3, 0.3)$.

bit simpler than the previous one. We observe simultaneous changes in the attractors while increasing the payoff value b, though c does not show much variations of dynamical schemes in order to increase them. Sufficiently tiny values of b, up to 0.05, showcases the exact same ambience where only the scissor strategic species remain existing in the race of evolution (olive green region in Fig. 5.6 (b)). That turns out to an obvious manner to the existence of the rock species along with the scissor kinds, making the planar attractor-III stable in the evolution (cream region in Fig. 5.6 (b)). Afterwards sufficient increment of b plays as an optimal way to sustain the paper kinds too, getting benefited by winning over rock along with the other two strategies, and making the interior spatial attractor to become stable for a fair portion (grey colored background) in the spans of these two parameters. After sufficiently enlarging the payoff value b, rock strategic species get quite a large payoff as evolutionary benefit, which let it's the vulnerable species scissor to get extinct, and eventually after a note, only two strategies, rock and paper (planar attractor-I, indicated by salmon pink region in Fig. 5.6 (b)) remain to sustain in the environ-

ment side by side steadily.
In the simultaneous fluctuation of two parameters, the payoff parameter a and the free space-contributed evolutionary parameter σ_R, various stable and unstable scenarios unfold (Figs. 5.6 (c) to (e)). The variation of a concerning σ_R shows the asymptotic stability of different strategic scenarios based on the parameters' significance to the system. With a small contribution of free space to the rock species, inferior species can survive alongside rocks (planar attractor-III in cream region in Fig. 5.6 (c)) up to $\sigma_R = 0.25$. This stability threshold reduces as a increases from 1.07. As a positively affects paper species, all three strategies get a fair chance to manifest their potential through their respective species (interior spatial strategic attractor I in light grey region in Fig. 5.6 (c)). With higher values of σ_R, the existence of scissor species becomes compromised, leading the planar attractor to converge to axial attractor-I (maroon region in Fig. 5.6 (c)), where only rock species sustain for an extended parameter space. As a increases, allowing paper to survive with rock, axial attractor-I transforms into planar attractor-I (salmon pink region in Fig. 5.6 (c)), where rock and paper coexist. With even higher frequencies of a, the paper species become dominant, providing benefits to the scissor kinds alongside the surviving rock and paper strategic species.
Diverse steady dynamical distributions of strategic attractors, along with a segment where the asymptotic stability of attractors fails, emerge in the parameter span of b and σ_P. For initial values of b up to 0.05, a narrow region (axial attractor-III in olive green region in Fig. 5.6 (d)) appears where only scissor strategic species survive. This is due to high mortality rate induced on paper strategic traits, restricting rock species from coexisting with scissor. As b increases, the survivability of traits with rock ability grows, leading to coexistence with scissor kinds (cream region in Fig. 5.6 (d) indicates planar attractor-III). This stable portion diminishes with the increasing value of σ_P. With a further increment in payoff b, planar attractor-III diminishes the frequency of scissor species, allowing only rock to dominate the game entirely (axial attractor-I in maroon color in Fig. 5.6 (d)) until σ_P reaches 0.29. Beyond that, σ_P produces sufficient benefit to the paper strategy, leading to coexistence with rock in the environment (planar attractor-I in salmon pink region in Fig. 5.6 (d)). Further increase in σ_P allows paper traits to sustain and contribute to the coexistence of the species with scissor strategy in the interior spatial strategic attractor (grey region in Fig. 5.6 (d)) for a large parameter space. This coexistence breaks as Hopf bifurcation occurs with an increase in σ_P, leading to cyclically dominating species (uncolored region in Fig. 5.6 (d)). The unstable situation transitions back into coexisting stability with the reverse Hopf bifurcation at higher values of σ_P. Another intriguing feature occurs at the end of planar attractor-III, where, for a small span, with sufficiently low values of b, both scissor and paper strategic species survive together, forming planar attractor-II (cyan region in Fig. 5.6 (d)).
The variation the parameter σ_S with respect to the reversed extinction rate parameter of rock strategic species α, capitulate such a situation, where no strategic species gets a chance to survive in the environment. This situation depicts the existence and stability of the null attractor (orange region in Fig. 5.6 (e)), up to α to become 0.64 $(1 - \sigma_R = 0.65)$, and σ_S to reach up to 0.24 $(< \xi = 0.25)$. On growing both the reserved mortality rate parameter α from 0.64 onwards, the rate of extinction

of the rock species reduces enough, and endorses a fair portion where only the rock strategic species are able to sustain in the environment (axial attractor-I identified by maroon region in Fig. 5.6 (e)). The size of the stable portion of this strategic scene enlarges with growing α in very obvious manner, and on reaching up to the value 0.80, the growing quantity of rock species ensures the existence of the dominating strategy for rock, viz., the paper to sustain and survive it's kind species side by side with the rock strategic species till the extinction rate of rock becomes 0. Meanwhile, the growing attribute of the free space produced benefit to the scissor kinds σ_S results the axial attractor-III (marked by olive green region in Fig. 5.6 (e)) to become stable on up to a certain increment of α, making the scissor strategic species to sustain over the others in the environment. On increasing the fractional quantity of α from the axial attractor-III, the decaying mortality rate provides the rock species to survive along with the scissor strategic species ensuring the existence of a fair portion containing the planar attractor-III (cream colored region in Fig. 5.6 (e)) up on the stable axial attractor-III. On further growth of α, the survival instinct of the paper strategic species also enlarges alongside the two evolutionary traits, rock and scissor, resulting a steady portion for the interior spatial attractor (marked by light grey portion in Fig. 5.6 (e)) to appear in the parameter space.
In the final experiment, we explore the two-dimensional parameter space by varying σ_P and σ_S simultaneously, which dictate the replicatory benefit provided to paper and scissor strategic species, respectively, from the ecological free space. Starting from 0 to $\sigma_P = 0.29$ and $\sigma_S = 1.25$, a region emerges where only the influence of the rock strategy is observed (axial attractor-I denoted by maroon region in Fig. 5.6 (f)). However, increasing σ_S reduces the sole dominance of the rock strategy, leading to a combined effect of rock and scissor strategies, represented by planar attractor-III (cream colored region in Fig. 5.6 (f)). As σ_P increases beyond 0.29, providing paper strategic traits fair evolutionary opportunities, a region emerges where both rock and paper species dominate, forming planar attractor-I (salmon pink region in Fig. 5.6 (f)). This stable region gradually diminishes with increasing σ_P relative to σ_S, transitioning planar attractor-I into the interior spatial attractor (grey region in Fig. 5.6 (f)), where all three strategies coexist. However, for $\sigma_S \leq 0.24$ and $\sigma_P \geq 0.83$, only paper strategic species exist in the environment due to high evolutionary benefit, forming stable axial attractor-II (blue region in Fig. 5.6 (f)). With an increase in σ_S, scissor species begin to survive alongside paper strategic species (cyan region indicates planar attractor-II in Fig. 5.6 (f)), expanding as σ_P increases. With further enhancement of scissor species, rock species also thrive, leading to the simultaneous existence of all three species. The interior spatial attractor occupies the maximum portion of this parameter space, exhibiting stability failures in some regions, resulting in oscillatory behaviors (uncolored/white portion in Fig. 5.6 (f)).

5.5 Sensitivity analysis of parameters in the system

Sensitivity analysis is a vital tool across disciplines, quantifying uncertainties in model predictions due to factors like measurement errors and incomplete understanding. While input uncertainties are quantifiable, output uncertainties can be challenging due to model complexities. In such cases, sensitivity analysis estimates uncertainties and confidence intervals for model outputs, finding applications in diverse studies and aiding model development. Methodologically, it is classified into local (efficient but limited to linear aspects) and global methods (suitable for non-linear, multi-parameter models). The Sobol method, a global approach, systematically ranks parameters, optimizing computational resources by focusing on crucial ones and using variance decomposition for non-linear effect assessment.

In preceding sections, we delved into the diverse dynamical regimes of the eco-evolutionary model, pinpointing parameters leading to qualitative changes and unraveling their underlying mechanisms. This analysis offered intricate insights into local changes as parameters underwent gradual variations within specific ranges. This section shifts focus to probing global properties by addressing specific questions: (a) Can we characterize overall dynamics within high-dimensional subsections of the parameter space? (b) How does the effectiveness of each strategy respond to slight changes in the payoff matrix? (c) To what extent do uncertainties in certain pay-offs manifest in the model's output? To address these inquiries, we undertake a comprehensive sensitivity analysis, centering on computing Sobol indices, as originally conceptualized by I. M. Sobol [234]. The subsequent subsection outlines the method and software for calculating Sobol indices, followed by presenting the analysis results, with a keen focus on the aforementioned questions.

5.5.1 Computation of Sobol Indices

Let us consider a function, $y = \{y_1, y_2, \ldots, y_n\} = f(x; p) : \mathbb{R}^n \to \mathbb{R}^n$, with an n-dimensional state variable $x = \{x_1, x_2, \ldots, x_n\}$ and an m-dimensional parameter vector $p = \{p_1, p_2, \ldots, p_m\}$.

The variability of each scalar component $y_i \in y$ depends on the influence of each parameter $p_j \in p$. The sensitivity of y_i with respect to p_j is given by the first-order Sobol index,

$$S_{i,j} = \frac{V_{i,j}}{V_i} = \frac{V\left(E\left(y_i|p_j\right)\right)}{V(y_i)}. \tag{5.11}$$

Here, $V_{i,j} = V\left(E\left(y_i|p_j\right)\right)$ is the variance in the expected value of y_i when the parameter p_j is fixed and $V_i = V(y_i)$ is the variance in the value of y_i without any restrictions.

For the purposes of this chapter, y is the 3-dimensional solution vector of Eq. (5.6) and the parameter-space is given by the parameter vector $p = \{a, b, c, \sigma_R, \sigma_P, \sigma_S, \alpha, \beta, \xi\}$. While the Sobol indices may be computed with respect to any subset the parameters, we choose to compute them with respect to the game parameters $a, b,$ and c. This specific choice enables us to gain valuable qualitative

insights through sensitivity analysis, while also keeping the paper concise. Since the function y cannot be expressed in an analytically closed form, the computation of these indices requires the estimation of output variable variances. To address this, we employed stochastic collocation method [235] which involves discrete univariate point sampling within the parameter space, model evaluation at these points, and subsequent multivariate interpolant construction for approximating y_i in Eq. (5.11). The computational demands of the FACS simulations were met by leveraging ARCHER2's high-performance capabilities, spread across 5,860 nodes with an estimated peak performance of 28 Pflops per second. The efficient distribution of simulations across these nodes was facilitated using QCG-PilotJob. The sensitivity analysis, inclusive of Sobol index computation, is conducted using EasyVVUQ software. To streamline the integration and utilization of these diverse tools and HPC resources, FabSim3 is employed as a unifying interface.

Using the setup described above, we compute the Sobol index over time to find out the sensitivity of the parameters of the system. Keeping the values of the other parameters fixed, we computed the conditional and non-conditional variances of the output variables R, P, and S while varying the values of a, b, and c. This is done by repeatedly simulating the system for a time interval of 1000 units after transience and computing the variances as a function of time. Computing the ratios of these variances according to Eq. (5.11) gives us first-order Sobol indices for each point in time. Additionally, we analyze the temporal mean Sobol index and its variance for a range of ξ values, to understand how changes in ξ influence the system's sensitivity.

5.5.2 Analysing and interpreting the Sobol indices

Figures 5.7 illustrate both the temporal evolution of strategic species (2^{nd}, 3^{rd}, and 4^{th} columns of each row) over 1000 time instances and the corresponding temporal averages of the Sobol sensitivity indices (1^{st} column of each row). These indices are associated with the primary payoff parameters a, b, and c, which are visually distinguished using pink, orange, and purple color schemes, respectively. Throughout this experiment, all other system parameters are kept fixed at $\sigma_1 = 1.5$, $\sigma_2 = 1.25$, $\sigma_3 = 1.7$, $\alpha = 0.85$, and $\beta = 0.25$, in alignment with the conditions considered during the Hopf bifurcation investigation described in section 5.2.4. The three rows of Fig. 5.7 represent the behavior of each strategic species—rock (R), paper (P), and scissor (S)—as the extinction rate of the scissor species ξ is varied from 0 to 1 in increments of 0.1.

In the first row (A) of Fig. 5.7, corresponding to the rock (R) strategy, it becomes apparent that the influence of payoff parameter c (marked in purple) remains consistently dominant across the entire explored range of ξ. This persistent dominance is highlighted by the pronounced values of the Sobol index corresponding to c in each of the sub-diagrams. Furthermore, the second through fourth columns in row (A) reveal the dynamic trajectories of the R species for selected values of ξ (specifically $\xi = 0.1$, 0.4, and 0.8). Notably, for $\xi = 0.1$ and $\xi = 0.8$, the Sobol indices for all three payoffs (a, b, and c) exhibit non-oscillatory trends, which aligns with the observation that the dynamical system does not manifest oscillatory behavior in

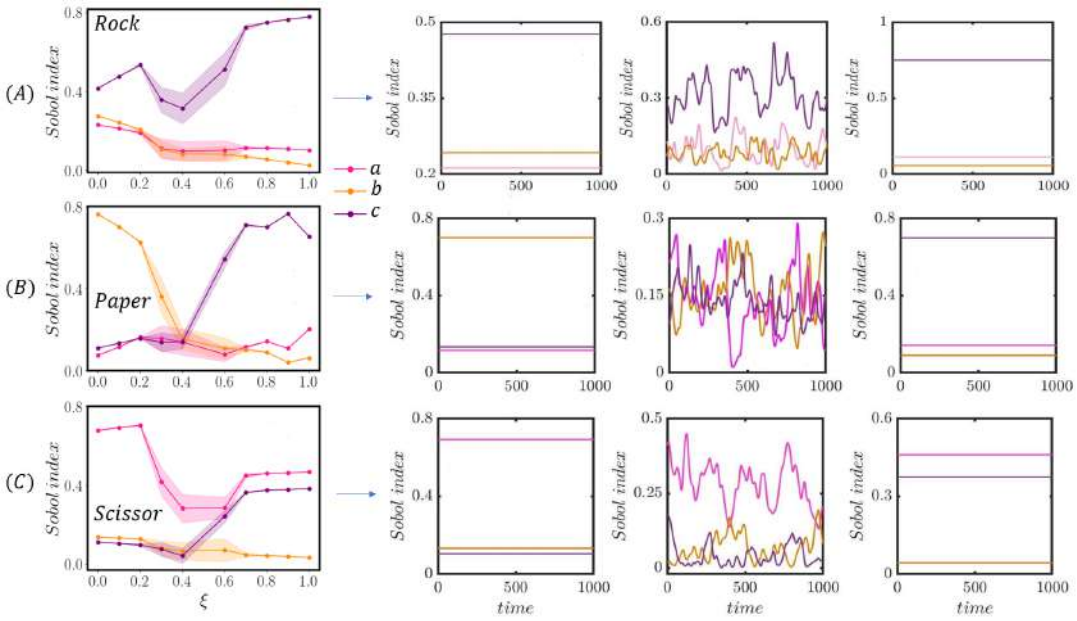

Figure 5.7: **Sensitivity analysis to the payoff parameters a, b, and c of the RPS game dilemma for three strategies: rock, paper, and scissor (R, P, and S presented in consecutive rows, namely $(A), (B)$, and (C):** There are 3 rows with 4 diagrams in each row depicting the natures of temporal average of the Sobol indices in order to vary the elimination rate of the scissor strategic species (ξ) from 0 to 1 taking 0.1 step length (1st column of each row) and the time series plots over 1000 times of those indices for particularly three values of $\xi = 0.1$, $\xi = 0.4$ and $\xi = 0.8$ in the 2nd, 3rd and 4th columns, respectively. The lightly shaded areas represent the range derived from the maximum and minimum variance values of Sobol indices computed over a significant number of iterations.

the strategic traits for these values of ξ, despite variations in the payoff parameters. This suggests a strong stabilizing influence of the ecological context at low and high ξ values.

In contrast, row (B) of Fig. 5.7, representing the paper (P) strategy, exhibits a notable shift in parameter influence as ξ increases. Up to the threshold value $\xi = 0.4$, the payoff parameter b (orange) dominates the dynamics, indicating its primary role in shaping the success of the paper strategy. However, beyond this threshold—particularly as the mortality of the scissor species escalates—payoff parameter c emerges as the dominant contributor to variability in P's dynamics. This shift indicates an ecological feedback mechanism, where the weakening of one competing species (scissor) alters the relative influence of interactions on another (paper).

The third row (C) of Fig. 5.7 focuses on the scissor (S) strategy. Here, payoff parameter a (pink) consistently exhibits the most significant impact across the entire spectrum of ξ. This suggests that the dynamics of the scissor species are strongly and persistently governed by the payoff arising from interactions with the rock strategy. The remaining payoff parameters (b and c) exert considerably lower influence on the behavior of S, a fact that holds true across the full ξ range. These findings underscore a degree of asymmetry in the ecological interactions, where one specific

payoff channel remains predominantly responsible for governing the species' fate.

To ensure robustness of these conclusions, confidence intervals for the Sobol indices are derived for each case, calculated as the range between maximum and minimum variance values across repeated iterations. These intervals are visualized in each subfigure of Fig. 5.7, adding a layer of statistical reliability to our sensitivity analysis.

Within the broader context of Hopf bifurcation analysis, our system reveals the occurrence of two successive Hopf bifurcations at $\xi = 0.315$ and $\xi = 0.565$, given fixed payoff values $a = 1.5$, $b = 1$, and $c = 1.2$. When examining the temporal evolution of Sobol indices and their averages across $\xi \in [0.2, 0.7]$, we observe a clear oscillatory pattern in the contribution of each payoff parameter. This oscillation in sensitivity confirms the dynamic instability emerging in this range, indicating the system's passage through bifurcation points. These oscillatory fluctuations in the Sobol indices are especially pronounced when the parameters a, b, and c are varied within the range $(0, 3]$, providing an additional validation for the bifurcation landscape identified through dynamical analysis. Thus, the Sobol-based sensitivity analysis not only elucidates the parameter dependencies across species and ecological states but also serves as a complementary tool to detect and characterize bifurcation phenomena in eco-evolutionary dynamics.

5.6 Mathematical analysis of the model

5.6.1 Stability analysis of the system

Our proposed system is given by

$$\begin{aligned}
\dot{R} &= R[-\sigma_R R - (a+\sigma_R)P + (b-\sigma_R)S + (\sigma_R + \alpha - 1)],\\
\dot{P} &= P[(a-\sigma_P)R - \sigma_P P - (c+\sigma_S)S + (\sigma_P - \beta)],\\
\dot{S} &= S[-(b+\sigma_S)R + (c-\sigma_S)P - \sigma_S S + (\sigma_S - \xi)].
\end{aligned}$$

This proposed mathematical model involves several categories of variable parameters, all of which are taken to be positive, and encapsulates their own game theoretic (a, b, and c) , evolutionary (σ_R, σ_P, and σ_S), and ecological (α, β, and ξ) signatures to construct the model.

In order to analyze linear stability of the equilibrium states of the system (5.6), we deduce the Jacobian matrix J of the three-dimensional system, with respect to any arbitrary strategic fixed point $\hat{X}(\hat{R}, \hat{P}, \hat{S})$ (see section 5.2 of the system (5.6)) and the corresponding characteristic equation becomes

$$\lambda^3 - \kappa_1\lambda^2 + \kappa_2\lambda - \kappa_3 = 0, \tag{5.12}$$

where,

$$\begin{aligned}
&\kappa_1 = Trace(J) = a_{11} + a_{22} + a_{33},\\
&\kappa_2 = A_{11} + A_{22} + A_{33} = a_{11}a_{22} + a_{22}a_{33} + a_{11}a_{33} - a_{23}a_{32} - a_{12}a_{21} - a_{13}a_{31},\\
&\kappa_3 = det(J) = a_{11}a_{23}a_{32} + a_{12}a_{21}a_{33} + a_{13}a_{31}a_{22} - a_{11}a_{22}a_{33} - a_{12}a_{23}a_{31} - a_{13}a_{32}a_{21},
\end{aligned}$$

with $a_{11} = -2\sigma_R\hat{R} - (a+\sigma_R)\hat{P} + (b-\sigma_R)\hat{S} + (\sigma_R + \alpha - 1), a_{12} = -(a+\sigma_R)\hat{R}, a_{13} = (b-\sigma_R)\hat{R}, a_{21} = (a-\sigma_P)\hat{P}, a_{22} = (a-\sigma_P)\hat{R} - 2\sigma_P\hat{P} - (c+\sigma_P)\hat{S} + (\sigma_P - \beta), a_{23} =$

$-(c+\sigma_P)\hat{P}, a_{31} = -(b+\sigma_S)\hat{S}, a_{32} = (c-\sigma_S)\hat{S}, a_{33} = -(b+\sigma_S)\hat{R}+(c-\sigma_S)\hat{P}-2\sigma_S\hat{S}+(\sigma_S-\xi)$. Now according to the Routh-Hurwitz criteria stability, the boundaries for asymptotic stability of the fix strategic state $\hat{X}(\hat{R},\hat{P},\hat{S})$ are as follows,

$$\begin{cases} a_{11}+a_{22}+a_{33}<0, \\ a_{11}a_{22}+a_{22}a_{33}+a_{33}a_{11}>a_{23}a_{32}+a_{12}a_{21}+a_{13}a_{31}, \\ a_{11}a_{23}a_{32}+a_{22}a_{13}a_{31}+a_{33}a_{12}a_{21}>a_{11}a_{22}a_{33}+a_{12}a_{23}a_{31}+a_{13}a_{32}a_{21}, \\ (a_{11}+a_{22}+a_{33})(a_{11}a_{22}+a_{22}a_{33}+a_{33}a_{11}-a_{23}a_{32}-a_{12}a_{21}-a_{13}a_{31}) \\ <(a_{11}a_{22}a_{33}+a_{12}a_{23}a_{31}+a_{13}a_{32}a_{21}-a_{11}a_{23}a_{32}-a_{22}a_{13}a_{31}-a_{33}a_{12}a_{21}). \end{cases} \tag{5.13}$$

5.6.2 Mathematical probity of the model

We examine some of the virtues in order to justify the mathematical features like existence, uniqueness, and the natures to the solution of our considered model (5.6). The functions in the right hand side of the system (5.6) are all taken to be real polynomial functions of highest degree to be 2. Thus, they all are continuously differentiable functions for all real values of the state variables R, P, and S, as well as, for all real and positive set of parameter values incorporated to it. In addition, the functions also satisfy to become locally Lipschitz in the domain $\mathbb{R}\times\mathbb{R}\times\mathbb{R}$, providing the affirmation that the solutions of the system (5.6) exist uniquely in the real ranges.
In order to check the positive invariance of the outcomes of the equations, we start with rewriting the system (5.6) as,

$$\frac{dR}{dt} = R\phi_1(R,P,S;a,b,c,\sigma_R,\sigma_P,\sigma_S,\alpha,\beta,\xi),$$

$$\frac{dP}{dt} = P\phi_2(R,P,S;a,b,c,\sigma_R,\sigma_P,\sigma_S,\alpha,\beta,\xi),$$

$$\frac{dS}{dt} = S\phi_3(R,P,S;a,b,c,\sigma_R,\sigma_P,\sigma_S,\alpha,\beta,\xi).$$

where, $\phi_1 = -\sigma_R R-(a+\sigma_R)P+(b-\sigma_R)S+(\sigma_R+\alpha-1)$, $\phi_2 = (a-\sigma_P)R-\sigma_P P-(c+\sigma_S)S+(\sigma_P-\beta)$, and $\phi_3 = -(b+\sigma_S)R+(c-\sigma_S)P-\sigma_S S+(\sigma_S-\xi)$, are three integrable functions in Riemannian sense, and by executing the integration, we obtain, Now, integrating both sides to above system both sides, we get the following relations,

$$\begin{aligned} R &= k_1\exp(\textstyle\int\phi_1(R,P,S;a,b,c,\sigma_R,\sigma_P,\sigma_S,\alpha,\beta,\xi)dt)\geq 0, \\ P &= k_2\exp(\textstyle\int\phi_2(R,P,S;a,b,c,\sigma_R,\sigma_P,\sigma_S,\alpha,\beta,\xi)dt)\geq 0, \\ S &= k_3\exp(\textstyle\int\phi_3(R,P,S;a,b,c,\sigma_R,\sigma_P,\sigma_S,\alpha,\beta,\xi)dt)\geq 0, \end{aligned} \tag{5.14}$$

where, k_1, k_2, and k_3 are the integrating constants depending up on the initial fractions of the state variables R, P, and S, which always keep their sign to be positive. The inequalities (5.14) conclude the positiveness of our desired results. The lower bound of the solutions, as well as the sum of the solutions are always greater than or equals to 0 $(R+P+S\geq 0)$.

5.6.3 Transcritical bifurcation analysis

In Fig. 5.3 (b), the Transcritical bifurcation is observed while we vary the value of parameter b from 0 to 0.08. The b-parametric model is given by the Eq. (5.8), which reduces a stable strategic fix point as, $A_3(0, 0, 0.6875)$. Concerning this stable attractor, its Jacobian matrix shapes up like follows:

$$J_1(A_3) = \begin{bmatrix} 0.6875b - 0.040625 & 0 & 0 \\ 0 & -0.73125 & 0 \\ -0.6875b - 0.55 & -0.378125 & -0.55 \end{bmatrix} \tag{5.15}$$

From the above Jacobian matrix J_1, the reduced eigenvalues are: $0.6875b-0.040625$, -0.73125 (< 0), and -0.55 (< 0) respectively, among which $0.6875b - 0.040625$ shapes up its magnitude to be negative till $b = \dfrac{0.040625}{0.6875} = 0.0591$. Resultantly, from our experimental perspective, we also find our fixed strategic attractor where the entire ecosystem is dominated by scissor strategic species with a constant frequency of 0.6875 getting into stake, with combined dominance of both rock and scissor strategic traits by transforming into a planar strategic attractor from $b = 0.0591$. We execute the suitability of the other criteria to observe the Transcritical bifurcation for the transition of attractors from axial (A_3) to the planar (S_3).

Now, to verify the occurrence of the Transcritical bifurcation at the point $b = 0.0591$, we proceed to the further verification schemes one by one. Firstly, assuming the eigen vector of the Jacobian matrix $J_1(A_3)$ corresponding to eigenvalue 0 (which occurs at $b = 0.0591$) to be, $\omega = (u_1, v_1, w_1)^T$ and satisfying the relation, $J_1(A_3)\omega = \mathcal{O}$, gives the following relations, $(0.6875b-0.040625)u_10$, $-0.73125v_1 = 0$, and $(-0.6875b - 0.55)u_1 - 0.378125v_1 - 0.55w_1 = 0$. This gives, $v_1 = 0$, and $w_1 = -(1 + 1.25b)u_1$.

Thus, our required eigen vector corresponding to the eigenvalue 0 (for the value of parameter $b = 0.0591$) is, $\omega = (1, 0, -1 - 1.25b)^T$. Afterwards, we execute the same procedure to find the eigenvector corresponding to eigenvalue 0 of the matrix $J_1(A_3)^T$, and name that eigenvector as $\bar{\omega}$, which is equal to $(1, 0, 0)^T$. The corresponding representation of the system (5.8) in a 3×1 vector format looks like, $U(R, P, S) = (U_1, U_2, U_3)^T = (-0.35R^2 - 1.85RP + (b - 0.35)RS + 0.2R, 1.05RP - 0.45P^2 - 0.7PS - 0.25P, -(b + 0.8)RS - 0.55PS - 0.8S^2 + 0.55S)^T$, and gives, $U_b(R, P, S) = (\dfrac{\partial}{\partial b}(U_1), \dfrac{\partial}{\partial b}(U_2), \dfrac{\partial}{\partial b}(U_3))^T = (U_{1,b}, U_{2,b}, U_{3,b})^T = (RS, 0, -RS)^T$. Thus, $U_b(0, 0, 0.6875) = (0, 0, 0)^T$. Hence, we can conclude to express that $\bar{\omega}^T U_b(0, 0, 0.6875) = 0$.

Next, we proceed to verify the next criteria of satisfying Transcritical bifurcation on the particular note, such that, $\bar{\omega}^T U_b'(0, 0, 0.6875)\omega = \begin{bmatrix} 1 & 0 & 0 \end{bmatrix} \begin{bmatrix} 0.6875 & 0 & 0 \\ 0 & 0 & 0 \\ -0.6875 & 0 & 0 \end{bmatrix} \begin{bmatrix} 1 \\ 0 \\ -1 - 1.25b \end{bmatrix} = 0.6875 \neq 0$, matches well to the third criteria of occurrence of Transcritical bifurcation at $b = 0.0591$.

Lastly, to verify the forth and the concluding criteria to make us sure the occurrence of the Transcritical bifurcation is, $\bar{\omega}^T U_b''(0, 0, 0.6875) < \omega, \omega > =$

$$\begin{bmatrix} 1 & 0 & 0 \end{bmatrix} \begin{bmatrix} \dfrac{\partial^2 U_1}{\partial R^2}(u_1^2) + 2\dfrac{\partial^2 U_2}{\partial R \partial P}(u_1 v_1) \\ \dfrac{\partial^2 U_2}{\partial R^2}(u_1^2) + 2\dfrac{\partial^2 U_2}{\partial R \partial P}(u_1 v_1) + \dfrac{\partial^2 U_2}{\partial P^2}(v_1^2) + 2\dfrac{\partial^2 U_2}{\partial P \partial S}(v_1 w_1) \\ \dfrac{\partial^2 U_3}{\partial P^2}(v_1^2) + 2\dfrac{\partial^2 U_3}{\partial P \partial S}(v_1 w_1) + \dfrac{\partial^2 U_3}{\partial S^2}(w_1^2) \end{bmatrix} = \text{-0.35} \neq 0.$$

With this fulfilling four simultaneous criteria of Sotomayor's theorem, we can conclude that there exists a Transcritical bifurcation in order to depict the transition of states (from A_3 to S_3) at the value of the parameter $b = 0.0591$. With the same mathematical procedure, all the other Transcritical bifurcation phenomenon (including those of Figs. 5.3 (a), and 5.3 (c)) describing the changes in strategic fix attractors can be shown.

5.6.4 Hopf bifurcation analysis

We execute a few analytical experiments in order to verify the occurrence of the stable Hopf bifurcation in the system (5.9) with respect to change of one of the system parameters ξ in the variation 0.2 to 0.7, as portrayed in Fig. 5.8. For this

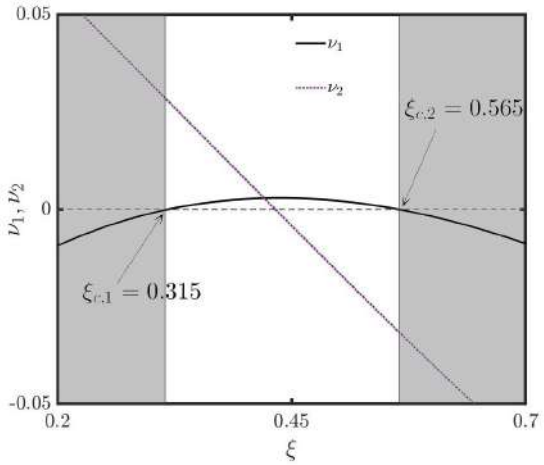

Figure 5.8: **Verification of two occurrences of Hopf bifurcations with respect to $\nu_1 = \kappa_1\kappa_2 - \kappa_3$, and $\nu_2 = \kappa_1\kappa_2' + \kappa_2\kappa_3' - \kappa_3'$ in order to vary the extinction rate of scissor kinds (ξ):** This figure diagram justifies analytically the simultaneous occurrence of Hopf bifurcations with increasing ξ in a proposed range. The values $\nu_1 = \kappa_1(\xi)\kappa_2(\xi) - \kappa_3(\xi)$ is denoted by black solid line, and the value $\nu_2 = \kappa_1(\xi)\kappa_2'(\xi) + \kappa_2(\xi)\kappa_3'(\xi) - \kappa_3'(\xi)$, which is denoted by the purple dotted line. The occurrence of Hopf bifurcation takes place at two consecutive values of ξ, and we denote them as $\xi_{c,i} = 0.315$, and 0.565 $(i = 1, 2)$. We also observe that the value ν_1 shapes up to be positive on the unstable phases of our eco-evolutionary system of strategic species.

we use the coefficient terms κ_1, κ_2, and κ_3 of the characteristic equation (5.12) of the Jacobian matrix at any interior strategic fix state $I(\hat{R}, \hat{P}, \hat{S})$ of our system.

Analysing the nature of these coefficients and their constraints for the stability of the strategic attractors of the system, we deduce and verify some of the criteria for which we observe the simultaneous occurrence of Hopf bifurcations on varying the parameter ξ within our desired range. With all parameters to be fixed at values, $a = 1.5, b = 1, c = 1.2, \sigma_R = 1.5, \sigma_P = 1.25, \sigma_3 = 1.7, \alpha = 0.85$, and $\beta = 0.25$, we acquire our trace, sum of the co-factors of diagonal elements and determinant of the Jacobian matrix taking up the shape with respect to the interior strategic fix point $I_\xi(0.3763 - 03246\xi, 0.2048 + 0.1834\xi, 0.3241 - 0.1267\xi)$ become: $\kappa_1(\xi) = Trace(J(I_\xi)) = 0.473\xi - 1.402$, $\kappa_2(\xi) =$ Sum of the co-factors of the matrix $J(I_\xi)$, and $\kappa_3(\xi) = det(J(I_\xi)) = -0.156194\xi^3 + 0.428609\xi^2 + 0.184509\xi - 0.546369$, that leads us to the following conclusions.

• The proposed eco-evolutionary dynamical system of strategic species (5.6) undergoes a stable Hopf bifurcation with respect to the variation of the extinction rate parameter ξ at $\xi_{c,i}$ $(i = 1, 2)$, under the conditions:

a. $\kappa_1(\xi_{c,i})\kappa_2(\xi_{c,i}) = \kappa_3(\xi_{c,i})$.

b. $\kappa_1(\xi_{c,i})\kappa_2'(\xi_{c,i}) + \kappa_2(\xi_{c,i})\kappa_3'(\xi_{c,i}) \neq \kappa_3'(\xi_{c,i})$.

Keeping instance with the above statement, we let $\nu_1 = \kappa_1(\xi)\kappa_2(\xi) - \kappa_3(\xi)$, and $\nu_2 = \kappa_1(\xi)\kappa_2'(\xi) + \kappa_2(\xi)\kappa_3'(\xi) - \kappa_3'(\xi)$, and vary these two considered variables ν_1, and ν_2 (black solid line and purple dotted line respectively in Fig. 5.8) within the range $\xi = 0.2$ to 0.7. As we obtained two consecutive Hopf bifurcations previously in main text (also see Fig. 5.4 of main text), this verification also goes with our numerical findings as $\nu_1 = 0$, and $\nu_2 \neq 0$ at $\xi = 0.315$, and 0.565, which makes complete verification for the values of the parameters ξ, where the system undergoes the stable Hopf bifurcations.

5.7 Conclusion

The eco-evolutionary game dynamics elaborated through the Rock-Paper-Scissors framework in this chapter has provided a profound exploration of the intricate interplay between evolutionary strategies and ecological interactions among three strategic species: prey, predators, and parasites. This model has revealed how the strategic interactions, coupled with ecological feedback mechanisms, can produce a remarkably rich tapestry of dynamic regimes, including stable coexistence, oscillatory behaviors, multi-stability, and even transitions toward chaotic or quasi-cyclic dynamics. These outcomes are heavily shaped by the interplay of key parameters that govern strategic rewards, mortality rates, mutation probabilities, and the availability of ecological resources.

Our analyses underscore that in such cyclically dominant systems, the evolutionary fate of each strategic species is inextricably linked to the adaptive strategies and population densities of its competitors. For instance, an increase in predator abundance may not only suppress prey densities but can also indirectly affect parasite populations through complex trophic interactions. This highlights the interconnectedness of all strategic species within an ecological network, demonstrating that the dynamics of no single species can be fully understood in isolation from the broader community. By capturing these feedback loops mathematically, the RPS game framework allows us to dissect how strategic decisions cascade through eco-

logical networks, reshaping evolutionary trajectories at the community level.

The RPS game model developed here captures not just the classical cyclic interactions, where each strategy dominates one and is dominated by another, but also reveals how nuanced ecological contexts, such as free space availability and environmental carrying capacity, influence the emergence, persistence, and extinction of particular strategies. These dynamics reflect real-world ecological phenomena: from microbial communities where antibiotic-producing strains interact with sensitive and resistant types, to predator-prey-parasite systems where disease and parasitism can shift competitive balances and alter food web stability. Furthermore, these insights extend even beyond ecology into socio-ecological systems, where strategic interactions among competing social behaviors, such as cooperation, defection, and enforcement- can also be analyzed through similar frameworks.

A particularly striking insight from this chapter is the role of ecological free space, modeled as an altruistic, non-strategic variable that contributes to the reproductive opportunities of all strategic species without demanding any return. This concept reinforces the idea that resources and environmental structure are not passive backdrops but are active players in shaping evolutionary dynamics. In this sense, free space acts as a facilitator of biodiversity and community resilience, allowing cooperative or less competitive strategies to persist even under strong selection pressures. This finding aligns with recent advances in eco-evolutionary theory, which emphasize that environmental structure and resource availability are critical determinants of evolutionary stability and the maintenance of strategic diversity.

Collectively, the insights gained from this chapter contribute to a deeper and more holistic understanding of the eco-evolutionary dynamics that govern complex biological communities. By integrating game-theoretic approaches with ecological feedbacks and environmental constraints, this chapter illuminates how strategic species co-evolve and adapt in a shared habitat, shedding light on the mechanisms that sustain biodiversity and shape community-level patterns. These findings lay the groundwork for applying the strategic species framework to a wider range of ecological and socio-ecological systems, where understanding the interplay between individual strategies, environmental resources, and evolutionary feedbacks is crucial for predicting and managing the dynamics of complex adaptive systems.

As we transition to the next chapter of this thesis, we will delve deeper into how the mechanisms developed here for generating strategic species dynamics can be applied to shape other perspectives of ecosystem interactions and extend our understanding to socially relevant phenomena such as rumor spreading. By distilling the complex dynamics of strategic species interactions, we aim to bridge the ecological and social domains, highlighting how principles from eco-evolutionary game theory can inform our understanding of cooperation, competition, and the emergence of complex behaviors in both biological and human systems. This integrative approach not only reinforces the foundational role of eco-evolutionary dynamics but also sets the stage for exploring the universality of these mechanisms across diverse domains.

Chapter 6

Other applications of eco-evolutionary dynamics of the strategic species, from predator-prey interaction to rumor spreading phenomenon ¶

Building upon the insights gained from the previous chapter, where the complex cyclic dominance (RPS) dynamics between prey, predator, and parasite species illuminated the interplay of eco-evolutionary dynamics, this chapter broadens the scope by examining how the two-species model can be reduced from the RPS system and subsequently applied to more general ecological and even social contexts. While RPS dynamics highlight cyclic interactions and symmetric competition, many real-world ecosystems exhibit asymmetric interactions that cannot be captured by strict cyclic models alone. For example, predator-prey systems often exhibit hierarchical structures where one species consistently dominates the other. Furthermore, extending eco-evolutionary modeling to social systems—such as rumor spreading—provides a bridge between ecological and societal dynamics, illustrating the universality of strategic interactions.

In this chapter, we develop a two-strategic-species model rooted in the classical prisoner's dilemma game, capturing key aspects of competitive and cooperative dynamics. This model is first applied to a predator-prey system, showing how eco-evolutionary feedback can shape population dynamics, including extinction thresholds and coexistence scenarios. We then apply the same model to the rumor spreading phenomenon, demonstrating the versatility of this eco-evolutionary approach in analyzing social dilemmas and highlighting the factors that promote or hinder cooperation.

¶A considerable part of this chapter has been published in **Journal of Theoretical Biology**, Volume 595, Article ID: Ghosh, S., Roy, S., Perc, M. and Ghosh, D., 2024. The eco-evolutionary dynamics of two strategic species: From the predator-prey to the innocent-spreader rumor model. Journal of Theoretical Biology, 595, p.111955.

6.1 Mathematical model from cyclic dominance to hierarchical interactions

In the previous chapter, we examined a three-species cyclic dominance framework (RPS model) that captures dynamic competition among prey, predator, and parasite in a closed loop. These interactions produce oscillatory patterns, reflecting the hallmark cyclic rhythms of rock–paper–scissors dynamics and ensuring that each trait periodically regains dominance—a compelling demonstration of how biodiversity can be maintained through strategic non-transitive interactions.

However, many real-world ecological systems can be effectively modeled by pairwise interactions, involving only two strategic species, such as a classic predator–prey system. Within these, one species often displays cooperative or mutualistic behavior, while the other exhibits defector-like, exploitative characteristics, dominating the interaction. Such pairwise systems can be viewed as a reduced form of more complex RPS dynamics, arising naturally when one species becomes competitively weak or effectively extinct. Mathematically, this corresponds to projecting the dynamics onto a lower-dimensional subspace by assuming negligible abundance of one species.

Crucially, despite the reduction in species number, this simplified system retains the strategic complexity of the original game—particularly when modeled using the PD payoff structure. In this framework, defection yields short-term individual gains, whereas cooperation leads to greater long-term communal benefits. This structure has been used extensively to study cooperation in evolutionary biology, sociology, and economics. For instance, Axelrod and Hamilton (1981) demonstrated that reciprocal strategies like "tit-for-tat" could emerge as evolutionarily stable in iterated PD tournaments, highlighting how cooperative behavior can persist even under defection-favoring conditions.

Within ecological contexts, introducing PD dynamics into predator–prey models has revealed rich outcomes. A recent eco-evolutionary model combining PD strategy interactions with prey–predator dynamics confirms multiple stable equilibria—including cooperator-only, defector-only, and coexistence states, modulated by payoff and ecological parameters . Furthermore, ecological mechanisms such as density dependence and assortative interactions (e.g., habitat fragmentation, settlement in empty habitats) can shift the balance in favor of cooperation, even under PD conditions [236].

This two-species PD-based model thus offers a powerful and broadly applicable framework. It synthesizes ecological processes—such as mortality, density, habitat structure—with the evolutionary game dynamics of cooperation vs. defection. This unification allows us to analyze both ecological and social dilemmas under a coherent eco-evolutionary lens, offering deep insights into the conditions that sustain cooperation, deter defection, or promote coexistence.

The two-species eco-evolutionary model begins with the Lotka-Volterra-inspired predator-prey system, but incorporates payoff parameters directly derived from Prisoner's Dilemma game theory. Let x and y denote the abundances of prey (cooperators) and predators (defectors), respectively. The baseline ecological dynamics can be expressed as:

$$\frac{dx}{dt'} = r_1 x - p_1 xy - m_1 x,$$

$$\frac{dy}{dt'} = ep_1 xy - m_2 y^2 - m_3 y.$$

Here, r_1 is the prey growth rate, p_1 is the predation rate, e is the efficiency of converting prey biomass into predator biomass, m_1 and m_3 are natural death rates, and m_2 captures intra-species cannibalism among predators.

By non-dimensionalizing the system (setting $t = r_1 t'$) and transforming variables, the system can be written in terms of dimensionless variables u (prey) and v (predator) as:

$$\begin{aligned} \frac{du}{dt} &= (1 - \tfrac{m_1}{r_1})u - \tfrac{p_1}{em_3}uv, \\ \frac{dv}{dt} &= -\tfrac{m_3}{r_1}v + euv - \tfrac{m_2}{em_3}v^2. \end{aligned} \tag{6.1}$$

This formulation of Eq. (6.1) allows direct mapping to the payoffs of PD, with R (reward), S (sucker), T (temptation), and P (punishment) extracted from the interaction matrix:

$$\begin{pmatrix} 0 & -\frac{p_1}{em_3} \\ e & -\frac{m_2}{em_3} \end{pmatrix}.$$

The key inequality $T > R > P > S$ ensures that defection is the dominant strategy in the one-shot game, while mutual cooperation yields moderate benefits.

To realistically model eco-evolutionary dynamics, we extend the model by introducing strategic species fractions: cooperators p, defectors q, and altruistic free space s. Free space represents ecological opportunities that facilitate reproduction but do not engage in strategic interactions, mirroring ecological niches like open habitats or unclaimed resources.

The evolutionary payoff matrix is given by:

$$\begin{pmatrix} R & S & \sigma_c \\ T & P & \sigma_d \\ 0 & 0 & 0 \end{pmatrix},$$

where σ_c and σ_d represent the free space benefits to cooperators and defectors, respectively.

The eco-evolutionary dynamics then become:

$$\begin{aligned} \tfrac{dp}{dt} &= p\left[(R - \sigma_c)p + (S - \sigma_c)q + (\sigma_c + \alpha - 1)\right], \\ \tfrac{dq}{dt} &= q\left[(T - \sigma_d)p + (P - \sigma_d)q + (\sigma_d - \beta)\right]. \end{aligned} \tag{6.2}$$

In Eq. (6.1), $\alpha = \dfrac{m_1}{r_1}$ and $\beta = \dfrac{m_3}{r_1}$ represent the mortality rates for cooperation driven species and defection driven species, respectively, calculated similarly to how we encapsulated the intrinsic mortality factors in our previous chapter, Eq. (5.1). These equations allow us to explore various strategic equilibria (extinct, defector-free, cooperator-free, and co-existence), depending on parameter values.

6.2 Strategic stability of the model

In this section, we discuss the biological essence of the stable strategic states arising in our eco-evolutionary model (6.1). Each state is described mathematically with references to real-world ecological systems where similar dynamics manifest.

6.2.1 The extinct strategic state (E_0)

At the trivial equilibrium point $E_0(0, 0)$, neither strategic species survives in the evolutionary race. This scenario emerges when the following inequalities are satisfied:

$$\sigma_c + \alpha < 1 \quad \text{and} \quad \sigma_d < \beta.$$

Biologically, this state represents mutual extinction, analogous to the well-documented population collapses in predator-prey systems such as the snowshoe hare (*Lepus americanus*) and the Canada lynx (*Lynx canadensis*) in the boreal forests of North America [237]. Historical data from the Hudson's Bay Company reveal dramatic population crashes that reflect the delicate balance in these interactions.

6.2.2 Defector species-free strategic State (E_1)

The second strategic state $E_1(p^*, 0)$ captures an environment where only the cooperative trait survives:

$$p^* = \frac{\sigma_c + \alpha - 1}{\sigma_c - R}.$$

The stability of this state requires:

$$\sigma_c + \alpha > 1 \quad \text{and} \quad T(\sigma_c + \alpha - 1) + \beta(R - \sigma_c) < \sigma_d(\alpha + R - 1).$$

Ecologically, this scenario mirrors the case of Antarctic krill (*Euphausia superba*) populations in the Southern Ocean. Despite heavy predation by baleen whales, krill thrive due to high reproductive rates and nutrient-rich waters that sustain them as a key prey species in the ecosystem [238].

6.2.3 Cooperator species-free strategic state (E_2)

The third strategic state $E_2(0, q^*)$ represents a setting where the defector trait dominates:

$$q^* = \frac{\sigma_d - \beta}{\sigma_d - P}.$$

Its stability depends on:

$$\sigma_d > \beta \quad \text{and} \quad S(\sigma_d - \beta) + \sigma_c(\beta - P) < (P - \sigma_d)(\alpha - 1).$$

A classic example of defector species flourishing in the absence of competition is the invasive kudzu vine (*Pueraria montana*) in the southeastern United States. Kudzu spreads rapidly, outcompetes native species, and overwhelms ecosystems by forming dense mats that suppress other plant growth [239].

6.2.4 The coexisting state of strategies (E_3)

The fourth strategic state $E_3(p^*, q^*)$ is the most biologically significant, where both strategic species coexist:

$$p^* = \frac{(S-\sigma_c)(\sigma_d-\beta)-(\alpha+\sigma_c-1)(P-\sigma_d)}{(R-\sigma_c)(P-\sigma_d)-(S-\sigma_c)(T-\sigma_d)},$$
$$q^* = \frac{(\alpha+\sigma_c-1)(T-\sigma_d)-(R-\sigma_c)(\sigma_d-\beta)}{(R-\sigma_c)(P-\sigma_d)-(S-\sigma_c)(T-\sigma_d)}.$$

The local stability of this state is determined by:

$$a_{11}+a_{22}<0 \quad \text{and} \quad a_{11}a_{22}-a_{12}a_{21}>0,$$

where:

$$a_{11} = 2p^*(R-\sigma_c)+q^*(S-\sigma_c)+(\sigma_c+\alpha-1),$$
$$a_{12} = (S-\sigma_c)p^*,$$
$$a_{21} = (T-\sigma_d)q^*,$$
$$a_{22} = (T-\sigma_d)p^*+2q^*(P-\sigma_d)+(\sigma_d-\beta).$$

Biologically, this state parallels the coexistence of cooperative and cheating strains in microbial biofilms, where enzyme-producing cooperators and non-producing cheaters coexist on surfaces, forming complex communities that balance community benefits and individual strategies [240, 241].

6.2.5 Ecological summary of strategic states

Table 6.1: Summary of ecological analogues for each strategic state.

State	Equilibrium	Ecological Analogue	Key Biological Insight
E_0	$(0,0)$	Snowshoe hare and lynx	System collapse when survival and reproduction rates are insufficient
E_1	$(p^*,0)$	Antarctic krill	Cooperators thrive alone in resource-rich environments
E_2	$(0,q^*)$	Kudzu invasion	Defectors dominate in the absence of competitors
E_3	(p^*,q^*)	Microbial biofilms	Cooperator-defector coexistence via spatial structure and community benefits

6.2.6 Distribution of different stationary strategic states with varying system parameters

This chapter aims to examine the persistence and conservation of cooperative traits among biological strategic species in their environment. We incorporate a reward

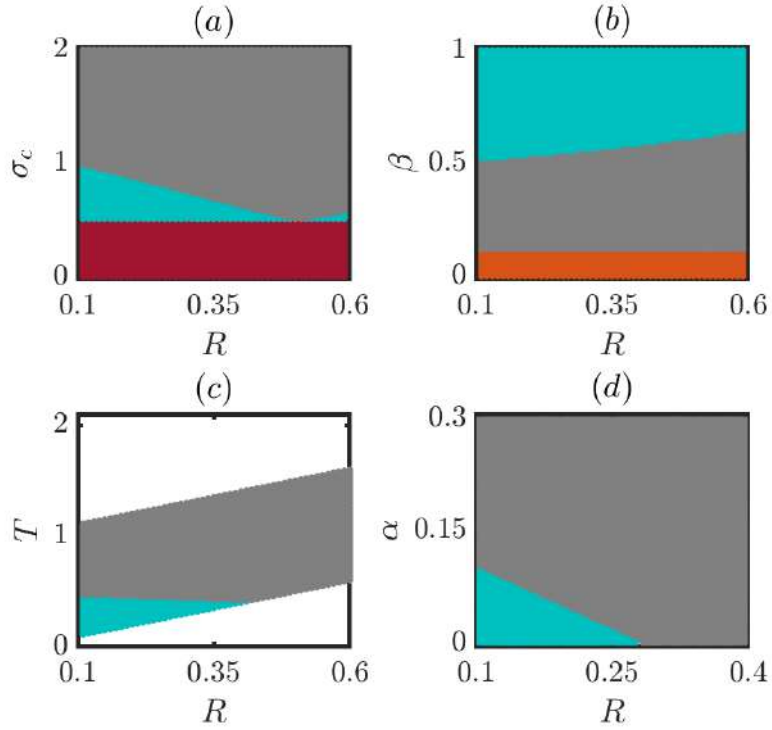

Figure 6.1: **Distribution of different strategic zones of species by tuning different system parameters concerning the increasing trend of the reward payoff R:** This figure diagram depicts the strategic distribution of stable strategic states of our model (6.1) by varying four different system parameters σ_c, β, T, and α respectively in sub-figures $(a), (b), (c)$, and (d), computed along with the varying frequency of R, the payoff value on both ways cooperation. Four distinct colors have been used to portray four different strategic states of the species, viz. deep red (E_0), sea blue (E_1), orange (E_2), and grey (E_3). We set the other parameters' value at $S = 0.08, T = 0.6, P = 0.1, \sigma_c = 1.9, \sigma_d = 0.15, \alpha = 0.5$, and $\beta = 0.4$.

payoff (R) for mutual cooperation between species (players) acting as cooperators. Such ecological interactions, like group defense strategies, collective foraging, or alarm signals to evade predators, often enhance cooperation between prey and predators. In populations comprising both cooperators and defectors, cooperative prey may evolve strategies that become evolutionarily stable, particularly if prey-prey interactions improve survival or reproductive success. The ecological framework given by Eq. (6.1) initially excludes intra-species benefits among prey in the considered environment. Hence, introducing the reward payoff (R) acts as a tuning parameter in our analysis of the strategic species dynamics in Eq. (6.1), allowing us to investigate how cooperation among prey species can be sustained and enhanced through R within the evolutionary context.

The evolutionary dynamics of these strategic traits also depend on other system parameters in addition to the reward reward. The payoff R from interactions between cooperators plays a critical role in shaping dynamical outcomes, particularly when varied alongside other parameters. To explore this, we conducted several

numerical experiments, as shown in Fig. 6.1, illustrating the effects of varying system parameters together with the reward payoff frequency (R). Fixed parameter values in these experiments were set as $S = 0.08$, $T = 0.6$, $P = 0.1$, $\sigma_c = 1.9$, $\sigma_d = 0.15$, $\alpha = 0.50$, and $\beta = 0.40$. We used the Runge-Kutta-45 method with 10^7 time iterations and initial species frequencies of $(0.35, 0.35)$.

We varied four key system parameters—σ_c, β, T, and α—while maintaining the standard inequality of the prisoner's dilemma game ($T > R > P > S$). When varying the replicator factor for cooperators (σ_c) from 0 to 2 while increasing R from $P = 0.1$ to $T = 0.6$, we identified three distinct strategic zones. For $\sigma_c < 0.49$, no strategy could support the survival of either species (extinct state $E_0(0, 0)$, marked deep red in Fig. 6.1(a)), consistent with the condition $\sigma_c + \alpha < 1$ while keeping $\sigma_d < \beta$. As σ_c increased to 0.50, cooperative species found opportunities to persist (sea blue region in Fig. 6.1(a)). The defector-free region diminished as R increased up to 0.49. Beyond this, the defector-free margin began to expand again with increasing R. At even higher σ_c, both cooperative and defector strategies could coexist (grey region in Fig. 6.1(a)), showing that higher replication potential also allows defectors to thrive alongside cooperators.

Next, varying the defector annihilation rate β against R revealed different strategic distributions. For β from 0 to 0.11, only defectors survived (orange region in Fig. 6.1(b)). Increasing β slightly allowed cooperators to coexist with defectors (grey region, state E_3). The upper boundary of this coexistence zone expanded with increasing R from 0.1 to 0.6. Further increases in β ultimately suppressed defectors entirely, leaving only cooperators (sea blue region in Fig. 6.1(b)).

A third experiment simultaneously varied T and R, maintaining the inequality $T > R$. Starting from $R = 0.1$ and increasing R, we examined outcomes at each corresponding $T > R$. Initially, a defector-free zone appeared (sea blue region, state E_1, Fig. 6.1(c)). Up to $R = 0.41$, only cooperators persisted. Beyond this, coexistence between cooperators and defectors emerged (grey region, E_3). Biologically, sufficient intra-species benefits to prey and inter-species costs to predators can thus promote stable coexistence.

Finally, varying the decay rate of cooperators (α) against R revealed that lower decay rates (i.e. higher α) support cooperative persistence (sea blue region, E_1, Fig. 6.1(d)). As R increased, the threshold α for cooperative-only survival shifted downward. At higher α values, both strategies coexisted (grey region, E_3), suggesting that cooperative survival is enhanced both by higher rewards and by lower extinction rates for cooperators.

6.3 Rumor spreading phenomenon

Rumor spreading within a society [242–244] can be conceptualized through a framework that categorizes individuals into two primary groups: susceptible or non-spreaders (S) and spreaders (I). Susceptible non-spreaders are those who are exposed to rumors but choose not to propagate them, while spreaders actively disseminate rumors among society. This dynamic significantly impacts societal trust and the quality of information flow. When spreaders are abundantly expanded, misinformation spreads rapidly, eroding trust and causing potential harm. Conversely, a

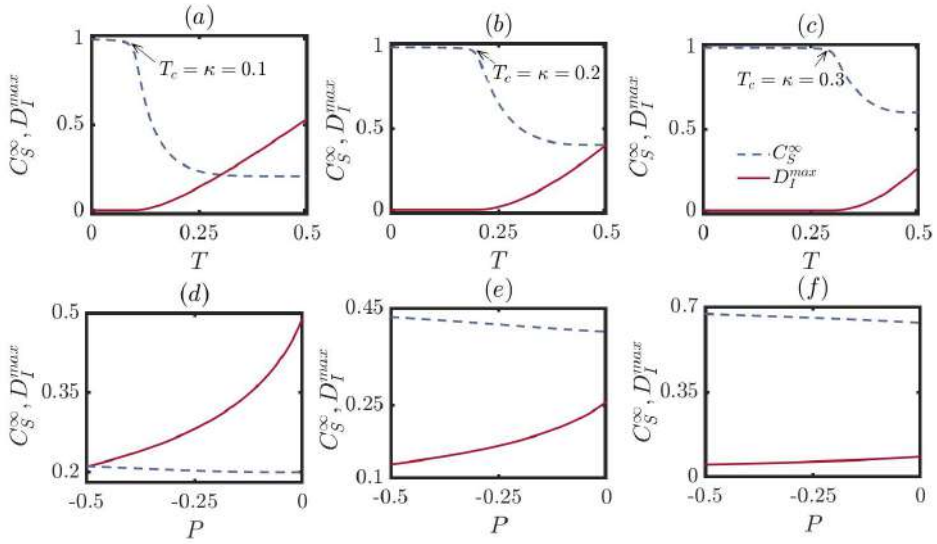

Figure 6.2: **Effect of increasing κ on the long-term frequency of cooperative susceptible individuals under varying payoff parameters T and P in rumor spreading:** These plots show how the long-term frequency of cooperative susceptibles and the peak frequency of defector spreaders change with $T = \theta\mu$ (sub-figures (a) for $\kappa = 0.1$, (b) for 0.2, (c) for 0.3) and $P = -\delta$ (sub-figures (d)–(f) for the same κ values). Yale blue dashed lines represent cooperative susceptibles; deep red solid lines show peak defector frequencies. As κ increases, cooperative individuals maintain higher frequencies over spreaders. Initial fractions are 0.999 (cooperators) and 0.001 (spreaders), with fixed parameters $\theta = 0.8$, $\mu = 0.5$, giving $T = 0.4$ in (d)–(f) and $P = -0.1$ in (a)–(c). Each case uses 3×10^5 iterations.

higher proportion of susceptible non-spreaders helps maintain the integrity of information and societal cohesion. Understanding this chassis highlights the importance of promoting behaviors that curb the spread of rumors to foster a more informed and resilient society. Rumor spreading in society can be effectively modeled using the principles of PD game theory, which illustrate the conflict between individual incentives and collective welfare. The dynamics of rumor spreading align with the prisoner's dilemma framework, where each individual's decision to spread or not spread a rumor mirrors the choice between cooperation and defection. Spreader individuals face the temptation of becoming the spreaders due to the perceived immediate benefits, such as social attention or the thrill of sharing new information. However, as more individuals choose to spread the rumor (defect), the overall trust and information quality within the society diminish, negatively impacting everyone, including the spreaders.

Conversely, if individuals choose not to spread the rumor (cooperate), society benefits from higher trust and accurate information dissemination, even though cooperators might feel disadvantaged when they resist the urge to share potentially enticing information. This situation reflects the essence of PD, where the optimal collective outcome is achieved through cooperation, but individual incentives can lead to widespread defection and societal harm.

We thus aim to establish a link between two strategic species models and their practical implications in the context of rumor spreading [242–244]. This connection can be achieved using a basic rumor model that comprises two population compartments, suspicious individuals and spreaders. The suspicious individuals (S) basically are the innocent population kinds, those having hardly any responsibility in the spreading of any sort of furphy in the society, whereas the spreaders (I) perform their job by spreading the hearsay and spread among the innocent populations as well. In this context of spreading the rumor in the society, susceptible individuals can be viewed as the cooperator kinds, and be represented as C_S, while spreader individuals can be seen as the defectors, and we denote their fraction to be D_I. The transition of the population's state from innocence to becoming a spreader, and conversely, is influenced by various factors, such as contact, forgetfulness, and doubts. Based on all these factors, we propose the time evolution dynamics of these two compartments as follows,

$$\begin{aligned} \frac{dC_S}{dt} &= -\mu C_S D_I + \kappa D_I, \\ \frac{dD_I}{dt} &= \theta\mu C_S D_I - \delta D_I^2 - \kappa D_I, \end{aligned} \tag{6.3}$$

where the expression μ signifies the rate in which individuals of two different types

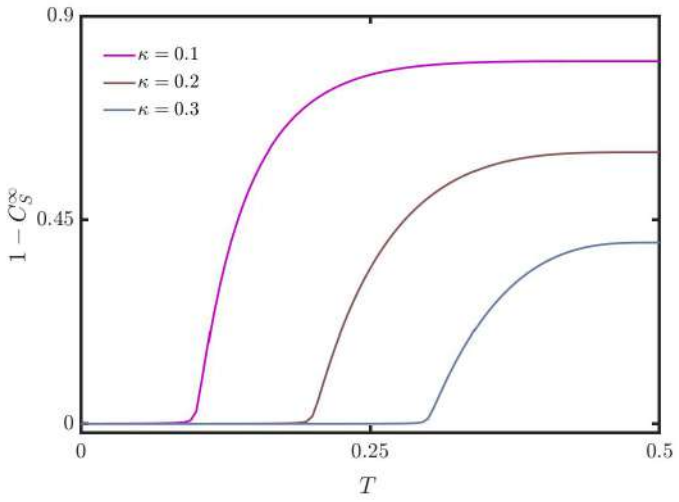

Figure 6.3: **The recovered population vs. T:** The variation in the fraction of recovered individuals ($1 - C_S^\infty$), particularly concerning the payoff $T = \theta\mu$, is examined in relation to different frequencies of $\kappa = (0.1,0.2,0.3)$. The curves indicate a critical threshold value of $T_c = \kappa$ in the smooth transition from a non-recovered to a recovered state.

interact among each other, and $\mu C_S D_I$ indicates the amount of the innocent population, who have been influenced by the contact with the spreaders and by the hearing of rumors. μ is rumor transmission rate. $\theta\mu C_S D_I$ is the proportion of the susceptible population that becomes affected and turn into spreader with a probability $\theta\mu$, where $(1-\theta)\mu C_S D_I$ is the proportion of susceptible individuals contact

with spreader but exhibiting hesitancy. The expression δD_I^2 signifies the spreader individuals interacting with each other, assessing the validity of the rumor, and rejecting the information with a probability of δ or an another interpretation can be an active "spreader" stops spreading the rumor after encountering another spreader and realizing that it has lost its "news value" [242]. The term κD_I indicates the spreader individuals who gradually forget the rumor and transition back into the state of suspicion with a probability denoted by κ. In this model, there are four key parameters: μ, κ, θ, and δ, representing the interaction strength, forgetting rate, transmission rate, and correction rate, respectively. The correction rate (δ) acts as a form of punishment (P) payoff in PD that is applied only when two individuals interact, exhibiting defection. Moreover, this correction attribute (δ) becomes relevant when two spreader individuals encounter each other, leading to the correction of the rumor, and eventually rumor-spreading resulting in their decline; the negative sign in the term $-\delta D_I^2$ indicates to this phenomenon. In contrast, the interaction rate (μ) reflects when a cooperator-minded non-spreader faces off the spreader, suffering from a sucker's payoff (S), which in turn performs as $-\mu$ to the cooperative non-spreader individuals in the entire phenomenon of this spreading. Due to this interaction, the population of innocents decreases, bearing the cost of interaction paying the sucker's payoff of $S = -\mu$. In the case of the transmission rate θ, the spreader population grows, making it analogous to the gains from the transmission of rumors, thus experiencing the temptation of amount $T = \theta\mu$. This reflects the incentive for defectors to continue spreading rumors, as the transmission of rumors leads to an increase in the defector-minded spreader population. The payoff matrix represents the rewards or outcomes that two species or individuals receive based on the strategies they choose. When a player cooperates with a spreader partner, the player bears a cost of $S = -\mu$, while the partner gains a benefit of $T = \theta\mu$. Further, when innocent individuals cooperate with any partner who is a spreader (defector) and help spread the rumor, the innocent person incurs a cost of $-\mu$ (where $\mu > 0$), while the spreader population gains a benefit of $\theta\mu$ (where $\theta > 0$). Therefore, spreaders consistently act as defectors, while the innocent non-spreaders behave as cooperators by facing direct loss in their interactions with any other kinds. In connection with the two systems, we can represent the interaction matrix, reflecting the exact same scenario in terms of the payoffs obtained by the prisoner's game dilemma for the strategic species in our rumor spreading model as,

$$\begin{array}{c} \\ C_S \\ D_I \end{array} \begin{array}{c} \begin{array}{cc} C_S & D_I \end{array} \\ \begin{pmatrix} R = 0 & S = -\mu \\ T = \theta\mu & P = -\delta \end{pmatrix} \end{array}. \tag{6.4}$$

These four parameters follow the inequality condition $T > R > P > S$ as in this model, $\theta\mu > 0 > -\delta > -\mu$, and $2R = 0 > \theta\mu - \mu = T + S$, following the exact trend of inequality in the payoffs' quantities that in general, Prisoner's dilemma portrays. Here, we investigate how the parameters $T = \theta\mu$ and $P = -\delta$ influence two significant observable: the maximum number of spreader individuals, denoted by D_I^{max} (red solid lines in Fig. 6.2), also acting as the defection strategic population in our consideration of the spreading chain of rumors and secondly, the long-term population size of susceptible individuals, treated as non-spreading cooperative behaved

individuals in the society at a long-term limit, as time conceptually approaches infinity. We denote this abundance as C_S^{∞} (blue dashed lines in Fig. 6.2). The variation of D_I^{max} and C_S^{∞} as a function of T for $P = -0.1$, i.e., $\delta = 0.1$ and for three different values of κ= 0.1, 0.2, and 0.3 is shown in Figs. 6.2 $(a) - (c)$, which suggests that, after a certain critical value of T denoted as T_c, D_I^{max} value will increase and C_S^{∞} will decrease. To derive the condition for rumor spread, it must hold the inequality: $\theta\mu C_S D_I - \delta D_I^2 - \kappa D_I > 0$. Taking into account the initial stage of infection, taking $C_S \approx 1$ and $\delta D_I^2 \approx 0$, we can write $\theta\mu D_I - \kappa D_I > 0$. Now, we can obtain the condition for rumor spread $T = \theta\mu > \kappa$. Thus, we reach up to the observation that the critical value of the temptation payoff value (T_c) is equal to the frequency κ, viz., $T_c = \kappa$. The critical value is $T_c = \kappa$, which fits perfectly with our numerical findings, as shown in Figs. 6.2 $(a) - (c)$ tested for different values of the parameter κ. Based on the values of these parameters, the system can maintain a higher population of the cooperative susceptible or innocent individuals over an extended period, as we increase the value of κ. To promote a greater number of stable cooperators within the system, it is necessary to increase the value of κ and reduce the value of T. In Figs. 6.2 $(d) - (f)$, we plot the change of D_I^{max} and C_S^{∞} in relation with $P = -\delta$ for constant value of $T = \theta\mu = 0.4$ and $\kappa = 0.1, 0.2$, and 0.3, respectively. These two figures indicate that an increasing trend in P from -0.5 $(= S)$ to 0 $(= R)$ leads to a reduction in the susceptible population while concurrently increasing the spreader population within the system. But with increasing magnitude of κ, the frequency of the cooperative susceptible population increases and eventually onwards $\kappa = 0.2$, in spite of the decaying flow of the cooperative individuals with increasing P, C_S^{∞} never let the defector strategic spreaders (D_I^{max}) to exceed their highest magnitude over their quantity in the society. The fraction of recovered individuals, comprising hesitant individuals and spreaders who opted not to propagate the rumor, identified as $1 - C_S^{\infty}$, is depicted as a function of the game parameter T in Fig. 6.3 for three different values of κ, i.e., 0.1, 0.2, 0.3.

6.4 Conclusion

This chapter has illustrated the remarkable versatility and depth of the eco-evolutionary framework developed throughout this thesis. Starting from the foundational three-species cyclic dynamics explored in earlier chapters, where prey, predator, and parasite species engaged in strategic interactions akin to the RPS game dilemma, we demonstrated how this framework can be systematically generalized to capture hierarchical two-species interactions. Such reductions allow us to model both ecological systems, such as predator-prey dynamics, and complex social processes, including rumor spreading phenomena.

By grounding our models in the well-established structure of the Prisoner's Dilemma payoff matrix, we seamlessly transitioned from ecological scenarios to broader social dilemmas. This unifying strategic species approach allowed us to explore the emergence and persistence of cooperation, the conditions that favor defection, and the role of altruistic free space as an ecological variable that supports population growth and stability. Through a careful adjustment of key parameters—including payoff values, mortality rates, ecological constraints, and behavioral

mutation—we uncovered a rich tapestry of dynamical outcomes ranging from stable coexistence to oscillatory regimes and even chaotic dynamics.

A key highlight of this chapter has been the extension of our eco-evolutionary models to the rumor spreading phenomenon, a process of profound relevance in human societies. By mapping the dynamics of rumor spreaders and non-spreaders onto the strategic species framework, we revealed how the same fundamental principles governing predator-prey interactions can illuminate the mechanisms of information diffusion, trust erosion, and social stabilization. Parameters such as interaction rates, forgetting mechanisms, and correction processes emerged as crucial levers in controlling the spread and persistence of rumors, thereby linking ecological insights with strategies for managing misinformation and promoting collective well-being.

Altogether, this chapter exemplifies the generality and adaptability of the eco-evolutionary game-theoretic framework developed in this thesis. From microbial communities to vertebrate populations and from ecological interactions to human social dilemmas, the models presented here capture the interplay of individual strategies, ecological constraints, and evolutionary feedbacks. This integrative approach highlights the interconnectedness of natural and social systems, providing a robust theoretical foundation for understanding and managing complex adaptive systems.

In the following and final chapter of this thesis, we synthesize the insights gained from the entire body of research, drawing overarching conclusions about the eco-evolutionary dynamics of strategic species. We reflect on the implications for both fundamental science and applied management, discuss the limitations of the current approaches, and propose future directions for research in this rapidly evolving field. Through this concluding synthesis, we aim to provide a coherent narrative that unites the diverse threads explored in this work, underscoring the profound impact of eco-evolutionary dynamics on our understanding of the natural and human worlds alike.

Chapter 7

Conclusion and future directions

The journey undertaken in this thesis has traversed the rich and complex landscape where evolutionary game theory and ecological dynamics intersect, revealing profound insights into how cooperation emerges, persists, and transforms within biological and social systems. By constructing and analyzing mathematical models that incorporate multigame interactions, ecological feedback through free space, time delays, mutation, and cyclic dominance, we have uncovered mechanisms that challenge classical assumptions about the inevitability of defection in social dilemmas. The findings collectively paint a picture of cooperation not as a fragile anomaly but as a robust outcome of dynamic systems shaped by reciprocal interactions between individual strategies and their environments. The implications of this work extend far beyond theoretical biology, offering potential applications in conservation science, public policy, the social sciences, and even the design of artificial intelligence systems where cooperative strategies are essential for long–term performance and resilience.

One of the most striking revelations has been the role of ecological variables—particularly free space—in mediating evolutionary outcomes. By acting as an altruistic enabler of reproduction, free space introduces a critical feedback loop that can stabilize cooperation even in the absence of classical enforcement mechanisms such as punishment, policing, or reputation systems. In doing so, it re-frames our understanding of ecological constraints from passive background conditions to active, strategy–mediating forces. The multi-game framework developed here further enriches this perspective by demonstrating how the coexistence of distinct strategic contexts, such as simultaneous Prisoner's Dilemma, Snowdrift, and Public Goods interactions, creates dynamic niches where cooperation, defection, and hybrid strategies can coexist in shifting mosaics. Within this mosaic, mutation functions as a vital source of innovation, repeatedly restoring lost strategies and preventing the collapse of diversity. These insights collectively redefine cooperation as an emergent, self–structured property of eco-evolutionary feedback rather than a static equilibrium sustained solely by extrinsic incentives.

Time delays, a second critical dimension explored in this work, revealed how temporal lags in feedback mechanisms fundamentally restructure evolutionary trajectories. When reproduction, information flow, or environmental feedback is delayed, strategy dynamics can depart radically from the equilibria predicted by instanta-

neous models. In moderate regimes, delays introduce stable limit cycles that preserve cooperation through rhythmic fluctuations in abundance and resource levels; in more extreme regimes, complex quasi-periodic or chaotic oscillations can emerge, sustaining diversity by continually reshaping the fitness landscape. These findings underscore that temporal structure is not a peripheral technicality but a primary driver of long–term stability, mirroring empirical phenomena ranging from seasonal breeding cycles in ecological communities to delayed social sanctioning in human societies. In particular, the discovery that cyclic dominance can arise endogenously through delayed feedback highlights a plausible route by which ecosystems and social systems maintain coexistence without centralized regulation.

Extending these ideas to multi-species interactions, especially the canonical rock–paper–scissors motif, underscored the importance of cyclic dominance in preserving biodiversity. By embedding RPS dynamics in an eco-evolutionary framework, we demonstrated that environmental fluctuations, asymmetric interactions, and adaptive behavior can together sustain a tangled web of transient advantages, preventing any single species from achieving permanent dominance. Empirical analogues abound—from toxin–producing bacteria and competing strains of lizards to social conventions in primate groups, affirming the biological relevance of these theoretical structures. Sensitivity analyzes within this framework revealed tipping points where small parameter perturbations precipitate dramatic phase shifts, emphasizing both the fragility and the resilience of cooperative networks in the face of environmental change.

Looking ahead, the work undertaken here generates a broad horizon of open questions and emerging research directions. First, spatial structure remains a frontier of considerable promise. Real–world populations rarely resemble well–mixed systems; instead, they occupy fragmented landscapes with patchy resources, directional migration, and heterogeneous interaction networks. Incorporating explicit space, whether through cellular automata, reaction–diffusion partial differential equations, or adaptive graph frameworks, would illuminate how local clustering, dispersal corridors, and habitat fragmentation reinforce or erode cooperative behavior. Such efforts could bridge eco–evolutionary theory with landscape ecology, shedding light on range expansions, biological invasions, and the design of wildlife corridors.

Second, stochasticity warrants deeper exploration. Small populations and rare events both amplify the role of demographic noise, while environmental variability introduces extrinsic fluctuations that can synchronize or destabilize population cycles. Stochastic dynamical systems and agent–based models would provide a more faithful representation of natural processes, revealing mechanisms such as noise–induced stabilization, stochastic resonance, and random switching between attractors. Understanding how drift, selection, and noise interact could refine conservation strategies for endangered species and inform interventions in threatened ecosystems.

Third, the study of adaptive networks—wherein the architecture of interactions co–evolves with individual strategies—offers a powerful framework for capturing the reciprocal shaping of behavior and connectivity. In microbial communities, cells modulate chemical signaling pathways; in social networks, humans break or reinforce ties based on reciprocity and trust. Modeling the co–evolution of network topology

and strategy could reveal whether cooperation is more likely to emerge in fluid or rigid structures, and under what conditions social institutions spontaneously arise to enforce collective norms.

Fourth, richer payoff structures remain underexplored. Games with asymmetric, context–dependent, or temporally varying payoffs reflect the complex incentives faced by organisms in real environments. Incorporating such heterogeneity could account for phenomena such as resource pulses, seasonality, and interspecific facilitation. Moreover, higher–order interactions—where payoffs depend on the combined state of three or more individuals—are biologically realistic in group hunting, microbial public goods production, and human collaboration, yet pose substantial analytical challenges. Advances in hypergraph theory and simplicial complexes promise to unlock these systems, potentially revealing new cooperative phases inaccessible to pairwise models.

Beyond theoretical expansions, this body of work holds significant practical relevance. In conservation biology, understanding how cooperation and mutualistic interactions respond to habitat loss, climate change, and species introductions is essential for designing resilient ecosystems. Our findings on free space dynamics suggest that restoring ecological niches, rather than directly manipulating species abundances, may be a more effective strategy for promoting coexistence and recovery. Policy makers could use these insights to prioritize habitat heterogeneity and connectivity in restoration efforts.

In social systems, the models herein provide a framework for designing institutions that harness ecological feedback to foster compliance and public goods provision. For instance, dynamic taxation schemes that adjust in response to resource depletion parallel the adaptive reproduction penalties imposed by free space scarcity, suggesting novel approaches to managing common–pool resources such as fisheries or climate.

In artificial intelligence and robotics, the principles of eco–evolutionary dynamics can inform decentralized control algorithms. By embedding feedback mechanisms analogous to free space or delayed information, multi–agent systems can achieve robust cooperation without centralized oversight. Applications range from swarm robotics and distributed sensor networks to traffic coordination among autonomous vehicles. The study of time–delay effects is particularly relevant in scenarios where communication latency or processing constraints are unavoidable, enabling agents to maintain coordinated behavior despite imperfect information.

At a philosophical level, this thesis highlights the porous boundary between ecological context and evolutionary strategy, underscoring that neither side alone can fully explain the richness of biological and social organization. Cooperation emerges not despite conflict but through it, sculpted by the flows of energy, information, and matter that sustain living systems. The models developed here, while idealized, capture essential truths about the principles of self-organization: the inexorable coupling of feedback loops, the creative tension between selection and randomness, and the layered temporalities that weave short–term adaptation into long–term persistence.

Nonetheless, limitations remain. Deterministic models gloss over genetic, environmental, and behavioral noise; homogeneous mixing assumptions neglect spatial

heterogeneity; and simplified payoff matrices abstract away the genealogies of real interactions. Future work must calibrate these models with empirical data, leverage high–throughput experiments, and engage with emerging techniques in comparative genomics and environmental metagenomics. Ultimately, theory and data must converge to refine predictions, guide field studies, and inspire new mathematical structures.

In closing, this thesis seeks to illuminate the dance between ecology and evolution, revealing several new steps in their intricate choreography. The insights gained—that cooperation is as much a product of environment as of strategy; that delays, space, and stochasticity sculpt evolutionary outcomes; and that diversity thrives in dynamic tension—stand as guiding principles for the next generation of research. The road ahead is rich with possibilities, from mapping the adaptive landscapes of microbial consortia to designing resilient socio–technological systems. As new questions arise and old answers are refined, the enduring lesson remains: life is not a set of isolated equilibria, but a restless, creative dialogue among strategies, environments, and the ever-shifting canvas of time.

Bibliography

[1] Ernst Mayr. Cause and effect in biology: kinds of causes, predictability, and teleology are viewed by a practicing biologist. *Science*, 134(3489):1501–1506, 1961.

[2] Charles Darwin. *On the origin of species: A facsimile of the first edition*. Harvard University Press, 1964.

[3] E Warning. Ecology of plant. an introduction to the study of communities, 1909.

[4] Frederic Edward Clements. *Plant succession: an analysis of the development of vegetation*. Number 242. Carnegie institution of Washington, 1916.

[5] Marc Swetlitz. Julian huxley and the end of evolution. *Journal of the History of Biology*, pages 181–217, 1995.

[6] Julian S Huxley. Guest editorial: Evolution, cultural and biological. *Yearbook of Anthropology*, pages 2–25, 1955.

[7] Alfred James Lotka. *Elements of physical biology*. Williams & Wilkins, 1925.

[8] V. Volterra. *Variazioni e fluttuazioni del numero d'individui in specie animali conviventi, memoria del socio Vito Volterra*. Società anonima tipografica" Leonardo da Vinci, 1926.

[9] Ronald Aylmer Fisher. *The genetical theory of natural selection: a complete variorum edition*. Oxford University Press, 1999.

[10] Sewall Wright. Evolution in mendelian populations. *Genetics*, 16(2):97, 1931.

[11] G Evelyn Hutchinson. The ecological theater and the evolutionary play. *(No Title)*, 1965.

[12] G Evelyn Hutchinson. Homage to santa rosalia or why are there so many kinds of animals? *The American Naturalist*, 93(870):145–159, 1959.

[13] Robert H MacArthur. *Geographical ecology: patterns in the distribution of species*. Princeton University Press, 1984.

[14] Peter R Grant and B Rosemary Grant. Unpredictable evolution in a 30-year study of darwin's finches. *Science*, 296(5568):707–711, 2002.

[15] Barbara Rosemary Grant and Peter Raymond Grant. Evolution of darwin's finches caused by a rare climatic event. *Proceedings of the Royal Society of London. Series B: Biological Sciences*, 251(1331):111–117, 1993.

[16] Richard Levins. *Evolution in changing environments: some theoretical explorations*. Number 2. Princeton University Press, 1968.

[17] Daniel H Janzen. When is it coevolution? 1980.

[18] Nelson G Hairston Jr, Stephen P Ellner, Monica A Geber, Takehito Yoshida, and Jennifer A Fox. Rapid evolution and the convergence of ecological and evolutionary time. *Ecology Letters*, 8(10):1114–1127, 2005.

[19] David M Post and Eric P Palkovacs. Eco-evolutionary feedbacks in community and ecosystem ecology: interactions between the ecological theatre and the evolutionary play. *Philosophical Transactions of the Royal Society B: Biological Sciences*, 364(1523):1629–1640, 2009.

[20] Richard L Thompson, Roger Edwards, John A Hart, Kimberly L Elmore, and Paul Markowski. Close proximity soundings within supercell environments obtained from the rapid update cycle. *Weather and Forecasting*, 18(6):1243–1261, 2003.

[21] Takehito Yoshida, Laura E Jones, Stephen P Ellner, Gregor F Fussmann, and Nelson G Hairston Jr. Rapid evolution drives ecological dynamics in a predator–prey system. *Nature*, 424(6946):303–306, 2003.

[22] David Reznick and John A Endler. The impact of predation on life history evolution in trinidadian guppies (poecilia reticulata). *Evolution*, pages 160–177, 1982.

[23] Eric P Palkovacs and David M Post. Experimental evidence that phenotypic divergence in predators drives community divergence in prey. *Ecology*, 90(2):300–305, 2009.

[24] Anurag A Agrawal, Amy P Hastings, Marc TJ Johnson, John L Maron, and Juha-Pekka Salminen. Insect herbivores drive real-time ecological and evolutionary change in plant populations. *Science*, 338(6103):113–116, 2012.

[25] Jeffrey Podos and Paige S Warren. The evolution of geographic variation in birdsong. *Advances in the Study of Behavior*, 37:403–458, 2007.

[26] Michael D Greenfield. Mechanisms and evolution of communal sexual displays in arthropods and anurans. *Advances in the Study of Behavior*, 35:1–62, 2005.

[27] Henrik Brumm and Hans Slabbekoorn. Acoustic communication in noise. *Advances in the Study of Behavior*, 35:151–209, 2005.

[28] Hans Slabbekoorn. Songs of the city: noise-dependent spectral plasticity in the acoustic phenotype of urban birds. *Animal Behaviour*, 85(5):1089–1099, 2013.

[29] George P Georghiou. Overview of insecticide resistance. ACS Publications, 1990.

[30] Paul Schliekelman and Fred Gould. Pest control by the release of insects carrying a female-killing allele on multiple loci. *Journal of Economic Entomology*, 93(6):1566–1579, 2000.

[31] David O Conover, Stephen A Arnott, Matthew R Walsh, and Stephan B Munch. Darwinian fishery science: lessons from the atlantic silverside (menidia menidia). *Canadian Journal of Fisheries and Aquatic Sciences*, 62(4):730–737, 2005.

[32] Mikko Heino, Beatriz Díaz Pauli, and Ulf Dieckmann. Fisheries-induced evolution. *Annual Review of Ecology, Evolution, and Systematics*, 46(1):461–480, 2015.

[33] Andrew P Hendry, Kiyoko M Gotanda, and Erik I Svensson. Human influences on evolution, and the ecological and societal consequences, 2017.

[34] Josef Hofbauer and Karl Sigmund. *Evolutionary games and population dynamics*. Cambridge university press, 1998.

[35] Barry Sinervo, Erik Svensson, and Tosha Comendant. Density cycles and an offspring quantity and quality game driven by natural selection. *Nature*, 406(6799):985–988, 2000.

[36] Sebastien Lion, Vincent AA Jansen, and Troy Day. Evolution in structured populations: beyond the kin versus group debate. *Trends in Ecology & Evolution*, 26(4):193–201, 2011.

[37] Vítor V Vasconcelos, Francisco C Santos, Jorge M Pacheco, and Simon A Levin. Climate policies under wealth inequality. *Proceedings of the National Academy of Sciences*, 111(6):2212–2216, 2014.

[38] Peter Ashcroft, Arne Traulsen, and Tobias Galla. When the mean is not enough: Calculating fixation time distributions in birth-death processes. *Physical Review E*, 92(4):042154, 2015.

[39] David Tilman. Competition and biodiversity in spatially structured habitats. *Ecology*, 75(1):2–16, 1994.

[40] David Reznick and Joseph Travis. The empirical study of adaptation in natural populations. *Adaptation*, 243:289, 1996.

[41] Peter M Visscher. Whole genome approaches to quantitative genetics. *Genetica*, 136(2):351–358, 2009.

[42] John N Thompson. Rapid evolution as an ecological process. *Trends in Ecology & Evolution*, 13(8):329–332, 1998.

[43] Theodosius Dobzhansky. Nothing in biology makes sense except in the light of evolution. *The American Biology Teacher*, 75(2):87–91, 2013.

[44] Gregor F Fussmann, Michel Loreau, and Peter A Abrams. Eco-evolutionary dynamics of communities and ecosystems. *Functional Ecology*, pages 465–477, 2007.

[45] David Lack. *Darwin's finches*. Cambridge University Press, 1983.

[46] David N Reznick, Frank H Shaw, F Helen Rodd, and Ruth G Shaw. Evaluation of the rate of evolution in natural populations of guppies (poecilia reticulata). *Science*, 275(5308):1934–1937, 1997.

[47] Jan D Van Der Laan and Pauline Hogeweg. Predator—prey coevolution: interactions across different timescales. *Proceedings of the Royal Society of London. Series B: Biological Sciences*, 259(1354):35–42, 1995.

[48] Martin A Nowak. Five rules for the evolution of cooperation. *Science*, 314(5805):1560–1563, 2006.

[49] Kerry B Marchinko. Predation's role in repeated phenotypic and genetic divergence of armor in threespine stickleback. *Evolution*, 63(1):127–138, 2009.

[50] Jeffery A Thompson. Proactive personality and job performance: a social capital perspective. *Journal of Applied psychology*, 90(5):1011, 2005.

[51] Barry Sinervo, Colin Bleay, and Chloe Adamopoulou. Social causes of correlational selection and the resolution of a heritable throat color polymorphism in a lizard. *Evolution*, 55(10):2040–2052, 2001.

[52] Stephen P Ellner, Monica A Geber, and Nelson G Hairston Jr. Does rapid evolution matter? measuring the rate of contemporary evolution and its impacts on ecological dynamics. *Ecology Letters*, 14(6):603–614, 2011.

[53] Andrew P Hendry. *Eco-evolutionary dynamics*. Princeton university press, 2017.

[54] Stuart A West, Ashleigh S Griffin, and Andy Gardner. Social semantics: altruism, cooperation, mutualism, strong reciprocity and group selection. *Journal of Evolutionary Biology*, 20(2):415–432, 2007.

[55] Babak Fotouhi, Naghmeh Momeni, Benjamin Allen, and Martin A Nowak. Evolution of cooperation on large networks with community structure. *Journal of the Royal Society Interface*, 16(152):20180677, 2019.

[56] David N Reznick, Jonathan Losos, and Joseph Travis. From low to high gear: there has been a paradigm shift in our understanding of evolution. *Ecology Letters*, 22(2):233–244, 2019.

[57] Greg Dwyer, Joseph R Mihaljevic, and Vanja Dukic. Can eco-evo theory explain population cycles in the field? *The American Naturalist*, 199(1):108–125, 2022.

[58] Marta D Santos, Sergey N Dorogovtsev, and José FF Mendes. Biased imitation in coupled evolutionary games in interdependent networks. *Scientific Reports*, 4(1):1–6, 2014.

[59] Sayantan Nag Chowdhury, Srilena Kundu, Matjaž Perc, and Dibakar Ghosh. Complex evolutionary dynamics due to punishment and free space in ecological multigames. *Proceedings of the Royal Society A*, 477(2252):20210397, 2021.

[60] Christoph Hauert, Miranda Holmes, and Michael Doebeli. Evolutionary games and population dynamics: maintenance of cooperation in public goods games. *Proceedings of the Royal Society B: Biological Sciences*, 273(1600):2565–2571, 2006.

[61] Karl Sigmund. *The calculus of selfishness*. Princeton University Press, 2010.

[62] TH Clutton-Brock, PNM Brotherton, MJ O'riain, AS Griffin, D Gaynor, R Kansky, L Sharpe, and GM McIlrath. Contributions to cooperative rearing in meerkats. *Animal Behaviour*, 61(4):705–710, 2001.

[63] Carey D Nadell, Joao B Xavier, and Kevin R Foster. The sociobiology of biofilms. *FEMS Microbiology Reviews*, 33(1):206–224, 2008.

[64] Sourav Roy, Sayantan Nag Chowdhury, Prakash Chandra Mali, Matjaž Perc, and Dibakar Ghosh. Eco-evolutionary dynamics of multigames with mutations. *PLoS one*, 17(8):e0272719, 2022.

[65] Sourav Roy, Sayantan Nag Chowdhury, Srilena Kundu, Gourab Kumar Sar, Jeet Banerjee, Biswambhar Rakshit, Prakash Chandra Mali, Matjaž Perc, and Dibakar Ghosh. Time delays shape the eco-evolutionary dynamics of cooperation. *Scientific Reports*, 13(1):14331, 2023.

[66] Sourav Roy, Subrata Ghosh, Arindam Saha, Prakash Chandra Mali, Matjaž Perc, and Dibakar Ghosh. The eco-evolutionary dynamics of strategic species. *Proceedings of the Royal Society A*, 480(2288):20240127, 2024.

[67] Subrata Ghosh, Sourav Roy, Matjaž Perc, and Dibakar Ghosh. The eco-evolutionary dynamics of two strategic species: From the predator-prey to the innocent-spreader rumor model. *Journal of Theoretical Biology*, 595:111955, 2024.

[68] John Von Neumann and Oskar Morgenstern. Theory of games and economic behavior, 2nd rev. 1947.

[69] J Maynard Smith. The theory of games and the evolution of animal conflicts. *Journal of Theoretical Biology*, 47(1):209–221, 1974.

[70] Peter D Taylor and Leo B Jonker. Evolutionary stable strategies and game dynamics. *Mathematical Biosciences*, 40(1-2):145–156, 1978.

[71] M Flood, M Dresher, A Tucker, and F Device. Prisoner's dilemma: game theory. *Experimental Economics*, 54:13, 1950.

[72] Robert Axelrod. Effective choice in the prisoner's dilemma. *Journal of Conflict Resolution*, 24(1):3–25, 1980.

[73] Michael Doebeli and Christoph Hauert. Models of cooperation based on the prisoner's dilemma and the snowdrift game. *Ecology Letters*, 8(7):748–766, 2005.

[74] Jiqi Shao, Nan Rong, Zhenchao Wu, Shaohua Gu, Beibei Liu, Ning Shen, and Zhiyuan Li. Siderophore-mediated iron partition promotes dynamical coexistence between cooperators and cheaters. *Iscience*, 26(9), 2023.

[75] Christian Hilbe, Maria Kleshnina, and Kateřina Staňková. Evolutionary games and applications: fifty years of 'the logic of animal conflict'. *Dynamic Games and Applications*, 13(4):1035–1048, 2023.

[76] Yigui Zhang, Qin Zhu, and Zhongqiu Li. The nature and motivation of human cooperation from variant public goods games. *Human Nature*, pages 1–19, 2024.

[77] Haozheng Xu, Yiwen Zhang, Xing Jin, Jingrui Wang, and Zhen Wang. The evolution of cooperation in multigames with uniform random hypergraphs. *Mathematics*, 11(11):2409, 2023.

[78] Zi-Xuan Guo, Tian-Jiao Feng, Yi Tao, Rui-Wu Wang, and Xiu-Deng Zheng. Evolutionary dynamics of cooperation coupled with ecological feedback compensation. *BioSystems*, 244:105282, 2024.

[79] Haowen Gong, Huijun Xiang, Yifei Wang, Huaijin Gao, and Xinzhu Meng. Strategy evolution of a novel cooperative game model induced by reward feedback and a time delay. *AIMS Mathematics*, 9(11):33161–33184, 2024.

[80] Tim H Clutton-Brock. *The evolution of parental care*, volume 10. Princeton University Press, 1991.

[81] Koh Hashimoto. Multigame effect in finite populations induces strategy linkage between two games. *Journal of Theoretical Biology*, 345:70–77, 2014.

[82] Santiago F Elena and Richard E Lenski. Evolution experiments with microorganisms: the dynamics and genetic bases of adaptation. *Nature Reviews Genetics*, 4(6):457–469, 2003.

[83] Kirill S Korolev, Mikkel Avlund, Oskar Hallatschek, and David R Nelson. Genetic demixing and evolution in linear stepping stone models. *Reviews of Modern Physics*, 82(2):1691–1718, 2010.

[84] Robert Boyd and Peter J Richerson. *Culture and the evolutionary process*. University of Chicago press, 1988.

[85] David G Rand and Martin A Nowak. Human cooperation. *Trends in Cognitive Sciences*, 17(8):413–425, 2013.

[86] György Szabó and Gabor Fath. Evolutionary games on graphs. *Physics Reports*, 446(4-6):97–216, 2007.

[87] Natalia L Komarova, Partha Niyogi, and Martin A Nowak. The evolutionary dynamics of grammar acquisition. *Journal of Theoretical Biology*, 209(1):43–59, 2001.

[88] Jörgen W Weibull. *Evolutionary game theory*. MIT press, 1997.

[89] Martin A Nowak. *Evolutionary dynamics: exploring the equations of life*. Harvard university press, 2006.

[90] Benjamin Allen, Gabor Lippner, Yu-Ting Chen, Babak Fotouhi, Naghmeh Momeni, Shing-Tung Yau, and Martin A Nowak. Evolutionary dynamics on any population structure. *Nature*, 544(7649):227–230, 2017.

[91] Sayantan Nag Chowdhury, Srilena Kundu, Jeet Banerjee, Matjaž Perc, and Dibakar Ghosh. Eco-evolutionary dynamics of cooperation in the presence of policing. *Journal of Theoretical Biology*, 518:110606, 2021.

[92] Elizabeth Pennisi. How did cooperative behavior evolve? *Science*, 309(5731):93–93, 2005.

[93] Matjaž Perc, Jillian J Jordan, David G Rand, Zhen Wang, Stefano Boccaletti, and Attila Szolnoki. Statistical physics of human cooperation. *Physics Reports*, 687:1–51, 2017.

[94] Zhen Wang, Satoshi Kokubo, Marko Jusup, and Jun Tanimoto. Universal scaling for the dilemma strength in evolutionary games. *Physics of Life Reviews*, 14:1–30, 2015.

[95] Francisco C Santos, Jorge M Pacheco, and Tom Lenaerts. Evolutionary dynamics of social dilemmas in structured heterogeneous populations. *Proceedings of the National Academy of Sciences*, 103(9):3490–3494, 2006.

[96] Koh Hashimoto. Unpredictability induced by unfocused games in evolutionary game dynamics. *Journal of Theoretical Biology*, 241(3):669–675, 2006.

[97] Chen Liu, Hao Guo, Zhibin Li, Xiaoyuan Gao, and Shudong Li. Coevolution of multi-game resolves social dilemma in network population. *Applied Mathematics and Computation*, 341:402–407, 2019.

[98] Yi Jie Huang, Zheng Hong Deng, Qun Song, Tao Wu, Zhi Long Deng, and Ming yu Gao. The evolution of cooperation in multi-games with aspiration-driven updating rule. *Chaos, Solitons & Fractals*, 128:313–317, 2019.

[99] Sayantan Nag Chowdhury, Srilena Kundu, Maja Duh, Matjaž Perc, and Dibakar Ghosh. Cooperation on interdependent networks by means of migration and stochastic imitation. *Entropy*, 22(4):485, 2020.

[100] Tian Guo, Mi Guo, Yan Zhang, and Shuanglu Liang. The effect of aspiration on the evolution of cooperation in spatial multigame. *Physica A: Statistical Mechanics and its Applications*, 525:27–32, 2019.

[101] Zheng-Hong Deng, Yi-Jie Huang, Zhi-Yang Gu, et al. Multigames with social punishment and the evolution of cooperation. *Physica A: Statistical Mechanics and its Applications*, 505:164–170, 2018.

[102] Ying Han, Zhao Song, Jialong Sun, Jiezhong Ma, Yangming Guo, and Peican Zhu. Investing the effect of age and cooperation in spatial multigame. *Physica A: Statistical Mechanics and its Applications*, 541:123269, 2020.

[103] Chen Chu, Simin Cui, Zheng Yuan, and Chunbin Yu. A win-stay-lose-learn mechanism based on aspiration can promote cooperation in a multigame. *Chaos, Solitons & Fractals*, 159:112125, 2022.

[104] Yujie Liu, Zemin Li, Xing Jin, Yuchen Tao, Hong Ding, and Zhen Wang. The effect of perceptions competition and learning costs on cooperation in spatial evolutionary multigames. *Chaos, Solitons & Fractals*, 157:111883, 2022.

[105] Zhen Wang, Attila Szolnoki, and Matjaž Perc. Different perceptions of social dilemmas: Evolutionary multigames in structured populations. *Physical Review E*, 90(3):032813, 2014.

[106] Jiahu Qin, Yaming Chen, Yu Kang, and Matjaž Perc. Social diversity promotes cooperation in spatial multigames. *EPL (Europhysics Letters)*, 118(1):18002, 2017.

[107] Robert Axelrod and William D Hamilton. The evolution of cooperation. *Science*, 211(4489):1390–1396, 1981.

[108] JMPGR Smith and George R Price. The logic of animal conflict. *Nature*, 246(5427):15–18, 1973.

[109] Anatol Rapoport. Two-person games: the essential ideas. *Ann Arbor, MI: University of Michigan Press*, 1966.

[110] Robert M May and Warren J Leonard. Nonlinear aspects of competition between three species. *SIAM Journal on Applied Mathematics*, 29(2):243–253, 1975.

[111] Tibor Antal, Martin A Nowak, and Arne Traulsen. Strategy abundance in $2\times$ 2 games for arbitrary mutation rates. *Journal of Theoretical Biology*, 257(2):340–344, 2009.

[112] Drew Fudenberg and Lorens A Imhof. Imitation processes with small mutations. *Journal of Economic Theory*, 131(1):251–262, 2006.

[113] Danielle FP Toupo, David G Rand, and Steven H Strogatz. Limit cycles sparked by mutation in the repeated prisoner's dilemma. *International Journal of Bifurcation and Chaos*, 24(12):1430035, 2014.

[114] Sourabh Mittal, Archan Mukhopadhyay, and Sagar Chakraborty. Evolutionary dynamics of the delayed replicator-mutator equation: Limit cycle and cooperation. *Physical Review E*, 101(4):042410, 2020.

[115] Michihiro Kandori, George J Mailath, and Rafael Rob. Learning, mutation, and long run equilibria in games. *Econometrica: Journal of the Econometric Society*, pages 29–56, 1993.

[116] Lorens A Imhof, Drew Fudenberg, and Martin A Nowak. Evolutionary cycles of cooperation and defection. *Proceedings of the National Academy of Sciences*, 102(31):10797–10800, 2005.

[117] Danielle FP Toupo and Steven H Strogatz. Nonlinear dynamics of the rock-paper-scissors game with mutations. *Physical Review E*, 91(5):052907, 2015.

[118] Mauro Mobilia. Oscillatory dynamics in rock–paper–scissors games with mutations. *Journal of Theoretical Biology*, 264(1):1–10, 2010.

[119] Mendeli H Vainstein, Ana TC Silva, and Jeferson J Arenzon. Does mobility decrease cooperation? *Journal of Theoretical Biology*, 244(4):722–728, 2007.

[120] Sayantan Nag Chowdhury, Soumen Majhi, Mahmut Ozer, Dibakar Ghosh, and Matjaž Perc. Synchronization to extreme events in moving agents. *New Journal of Physics*, 21(7):073048, 2019.

[121] Dirk Helbing and Wenjian Yu. The outbreak of cooperation among success-driven individuals under noisy conditions. *Proceedings of the National Academy of Sciences*, 106(10):3680–3685, 2009.

[122] Gourab K Sar, Sayantan Nag Chowdhury, Matjaž Perc, and Dibakar Ghosh. Swarmalators under competitive time-varying phase interactions. *New Journal of Physics*, 24(4):043004, apr 2022.

[123] Luo-Luo Jiang, Wen-Xu Wang, Ying-Cheng Lai, and Bing-Hong Wang. Role of adaptive migration in promoting cooperation in spatial games. *Physical Review E*, 81(3):036108, 2010.

[124] Sayantan Nag Chowdhury, Soumen Majhi, and Dibakar Ghosh. Distance dependent competitive interactions in a frustrated network of mobile agents. *IEEE Transactions on Network Science and Engineering*, 7(4):3159–3170, 2020.

[125] S Meloni, A Buscarino, L Fortuna, M Frasca, J Gómez-Gardeñes, V Latora, and Y Moreno. Effects of mobility in a population of prisoner's dilemma players. *Physical Review E*, 79(6):067101, 2009.

[126] Carey D Nadell, Kevin R Foster, and João B Xavier. Emergence of spatial structure in cell groups and the evolution of cooperation. *PLoS Computational Biology*, 6(3):e1000716, 2010.

[127] Robert D Holt. Bringing the hutchinsonian niche into the 21st century: ecological and evolutionary perspectives. *Proceedings of the National Academy of Sciences*, 106(supplement_2):19659–19665, 2009.

[128] Lawrence B Slobodkin. Growth and regulation of animal populations. Technical report, Holt, Rinehart and Winston,, 1961.

[129] Juan Wang, Wenwen Lu, Lina Liu, Li Li, and Chengyi Xia. Utility evaluation based on one-to-n mapping in the prisoner's dilemma game for interdependent networks. *PloS one*, 11(12):e0167083, 2016.

[130] David Angeli, James E Ferrell, and Eduardo D Sontag. Detection of multistability, bifurcations, and hysteresis in a large class of biological positive-feedback systems. *Proceedings of the National Academy of Sciences*, 101(7):1822–1827, 2004.

[131] Jean-Luc Schwartz, Nicolas Grimault, Jean-Michel Hupé, Brian CJ Moore, and Daniel Pressnitzer. Multistability in perception: binding sensory modalities, an overview. *Philosophical Transactions of the Royal Society B: Biological Sciences*, 367(1591):896–905, 2012.

[132] Sui Huang. Multistability and multicellularity: cell fates as high-dimensional attractors of gene regulatory networks. In *Computational Systems Biology*, pages 293–326. Elsevier, 2006.

[133] JA Scott Kelso. Multistability and metastability: understanding dynamic coordination in the brain. *Philosophical Transactions of the Royal Society B: Biological Sciences*, 367(1591):906–918, 2012.

[134] Shiva Dixit, Sayantan Nag Chowdhury, Awadhesh Prasad, Dibakar Ghosh, and Manish Dev Shrimali. Emergent rhythms in coupled nonlinear oscillators due to dynamic interactions. *Chaos: An Interdisciplinary Journal of Nonlinear Science*, 31(1):011105, 2021.

[135] Sayantan Nag Chowdhury, Dibakar Ghosh, and Chittaranjan Hens. Effect of repulsive links on frustration in attractively coupled networks. *Physical Review E*, 101(2):022310, 2020.

[136] Shiva Dixit, Sayantan Nag Chowdhury, Dibakar Ghosh, and Manish Dev Shrimali. Dynamic interaction induced explosive death. *EPL (Europhysics Letters)*, 133(4):40003, 2021.

[137] Robert Axelrod. An evolutionary approach to norms. *American Political Science Review*, 80(4):1095–1111, 1986.

[138] Garrett Hardin. The tragedy of the commons. In *Classic Papers in Natural Resource Economics Revisited*, pages 145–156. Routledge, 2018.

[139] Alexander F Skutch. Helpers among birds. *The Condor*, 63(3):198–226, 1961.

[140] Martin A Nowak and Robert M May. Evolutionary games and spatial chaos. *Nature*, 359(6398):826–829, 1992.

[141] Christoph Hauert and Michael Doebeli. Spatial structure often inhibits the evolution of cooperation in the snowdrift game. *Nature*, 428(6983):643–646, 2004.

[142] György Szabó and Csaba Tőke. Evolutionary prisoner's dilemma game on a square lattice. *Physical Review E*, 58(1):69, 1998.

[143] Attila Szolnoki and Matjaž Perc. Emergence of multilevel selection in the prisoner's dilemma game on coevolving random networks. *New Journal of Physics*, 11(9):093033, 2009.

[144] Francisco C Santos and Jorge M Pacheco. Scale-free networks provide a unifying framework for the emergence of cooperation. *Physical Review Letters*, 95(9):098104, 2005.

[145] Hisashi Ohtsuki, Martin A Nowak, and Jorge M Pacheco. Breaking the symmetry between interaction and replacement¡? format?¿ in evolutionary dynamics on graphs. *Physical Review Letters*, 98(10):108106, 2007.

[146] William D Hamilton. The genetical evolution of social behaviour. ii. *Journal of Theoretical Biology*, 7(1):17–52, 1964.

[147] Matjaž Perc and Attila Szolnoki. Social diversity and promotion of cooperation in the spatial prisoner's dilemma game. *Physical Review E—Statistical, Nonlinear, and Soft Matter Physics*, 77(1):011904, 2008.

[148] Attila Szolnoki, Matjaž Perc, and György Szabó. Topology-independent impact of noise on cooperation in spatial public goods games. *Physical Review E—Statistical, Nonlinear, and Soft Matter Physics*, 80(5):056109, 2009.

[149] Ernst Fehr and Simon Gächter. Altruistic punishment in humans. *Nature*, 415(6868):137–140, 2002.

[150] Matjaž Perc. Sustainable institutionalized punishment requires elimination of second-order free-riders. *Scientific Reports*, 2(1):344, 2012.

[151] Shadrielle Melijah G Espiritu, Lydia Y Liu, Yulia Rubanova, Vinayak Bhandari, Erle M Holgersen, Lesia M Szyca, Natalie S Fox, Melvin LK Chua, Takafumi N Yamaguchi, Lawrence E Heisler, et al. The evolutionary landscape of localized prostate cancers drives clinical aggression. *Cell*, 173(4):1003–1013, 2018.

[152] Hisashi Ohtsuki, Yoh Iwasa, and Martin A Nowak. Indirect reciprocity provides only a narrow margin of efficiency for costly punishment. *Nature*, 457(7225):79–82, 2009.

[153] Martijn Egas and Arno Riedl. The economics of altruistic punishment and the maintenance of cooperation. *Proceedings of the Royal Society B: Biological Sciences*, 275(1637):871–878, 2008.

[154] Anna Dreber, David G Rand, Drew Fudenberg, and Martin A Nowak. Winners don't punish. *Nature*, 452(7185):348–351, 2008.

[155] Peter Brandt, Andreas Funk, Verena Hormann, Marcus Dengler, Richard J Greatbatch, and John M Toole. Interannual atmospheric variability forced by the deep equatorial atlantic ocean. *Nature*, 473(7348):497–500, 2011.

[156] Jeet Banerjee, Sourav Kumar Sasmal, and Ritwik Kumar Layek. Supercritical and subcritical hopf-bifurcations in a two-delayed prey–predator system with density-dependent mortality of predator and strong allee effect in prey. *BioSystems*, 180:19–37, 2019.

[157] Dirk Helbing, Attila Szolnoki, Matjaž Perc, and György Szabó. Defector-accelerated cooperativeness and punishment in public goods games with mutations. *Physical Review E—Statistical, Nonlinear, and Soft Matter Physics*, 81(5):057104, 2010.

[158] Dashun Wang, Chaoming Song, and Albert-László Barabási. Quantifying long-term scientific impact. *Science*, 342(6154):127–132, 2013.

[159] Lev R Ginzburg, Lawrence B Slobodkin, Keith Johnson, and Andrew G Bindman. Quasiextinction probabilities as a measure of impact on population growth. *Risk Analysis*, 2(3):171–181, 1982.

[160] Fanie Pelletier, Dany Garant, and Andrew P Hendry. Eco-evolutionary dynamics, 2009.

[161] P Garred, M Harboe, T Oettinger, C Koch, and A Svejgaard. Dual role of mannan-binding protein in infections: another case of heterosis? *International Journal of Immunogenetics*, 21(2):125–131, 1994.

[162] Elizabeth A Law, Brett A Bryan, Erik Meijaard, Thilak Mallawaarachchi, Matthew J Struebig, Matthew E Watts, and Kerrie A Wilson. Mixed policies give more options in multifunctional tropical forest landscapes. *Journal of Applied Ecology*, 54(1):51–60, 2017.

[163] Xin Wang, Zhiming Zheng, and Feng Fu. Steering eco-evolutionary game dynamics with manifold control. *Proceedings of the Royal Society A*, 476(2233):20190643, 2020.

[164] Andrew P Hendry. A critique for eco-evolutionary dynamics. *Functional Ecology*, 33(1):84–94, 2019.

[165] Franziska S Brunner, Jacques A Deere, Martijn Egas, Christophe Eizaguirre, and Joost AM Raeymaekers. The diversity of eco-evolutionary dynamics: Comparing the feedbacks between ecology and evolution across scales. *Functional Ecology*, 33(1):7–12, 2019.

[166] Chaitanya S Gokhale and Christoph Hauert. Eco-evolutionary dynamics of social dilemmas. *Theoretical Population Biology*, 111:28–42, 2016.

[167] Muthusamy Lakshmanan and Dharmapuri Vijayan Senthilkumar. *Dynamics of nonlinear time-delay systems*. Springer Science & Business Media, 2011.

[168] MK Stephen Yeung and Steven H Strogatz. Time delay in the kuramoto model of coupled oscillators. *Physical Review Letters*, 82(3):648, 1999.

[169] Mukeshwar Dhamala, Viktor K Jirsa, and Mingzhou Ding. Enhancement of neural synchrony by time delay. *Physical Review Letters*, 92(7):074104, 2004.

[170] Xueting Wang, Jun Cheng, and Lei Wang. A reinforcement learning-based predator-prey model. *Ecological Complexity*, 42:100815, 2020.

[171] Srilena Kundu, Soumen Majhi, and Dibakar Ghosh. Resumption of dynamism in damaged networks of coupled oscillators. *Physical Review E*, 97(5):052313, 2018.

[172] Dibakar Ghosh, Santo Banerjee, and A Roy Chowdhury. Synchronization between variable time-delayed systems and cryptography. *Europhysics Letters*, 80(3):30006, 2007.

[173] Dibakar Ghosh. Projective-dual synchronization in delay dynamical systems with time-varying coupling delay. *Nonlinear Dynamics*, 66:717–730, 2011.

[174] Dibakar Ghosh and A Roy Chowdhury. Dual-anticipating, dual and dual-lag synchronization in modulated time-delayed systems. *Physics Letters A*, 374(34):3425–3436, 2010.

[175] Terry W Du Clos. Pentraxins: structure, function, and role in inflammation. *International Scholarly Research Notices*, 2013(1):379040, 2013.

[176] Dibakar Ghosh, Santo Banerjee, and A Roy Chowdhury. Generalized and projective synchronization in modulated time-delayed systems. *Physics Letters A*, 374(21):2143–2149, 2010.

[177] Debashis Ghosh, Jessica Lo, Daniel Morton, Damien Valette, Jingle Xi, Jennifer Griswold, Susan Hubbell, Chinaza Egbuta, Wenhua Jiang, Jing An, et al. Novel aromatase inhibitors by structure-guided design. *Journal of Medicinal Chemistry*, 55(19):8464–8476, 2012.

[178] Fatihcan M Atay, Jürgen Jost, and Andreas Wende. Delays, connection topology, and synchronization of coupled chaotic maps. *Physical Review Letters*, 92(14):144101, 2004.

[179] Lulan Wang, Jingzhe Shang, Shenghui Weng, Saba R Aliyari, Chengyang Ji, Genhong Cheng, and Aiping Wu. Genomic annotation and molecular evolution of monkeypox virus outbreak in 2022. *Journal of Medical Virology*, 95(1):e28036, 2023.

[180] Attila Szolnoki and Matjaž Perc. Decelerated invasion and waning-moon patterns in public goods games with delayed distribution. *Physical Review E—Statistical, Nonlinear, and Soft Matter Physics*, 87(5):054801, 2013.

[181] Bo Li, Houjun Liang, and Qizhi He. Multiple and generic bifurcation analysis of a discrete hindmarsh-rose model. *Chaos, Solitons & Fractals*, 146:110856, 2021.

[182] Blake M Rankin, Dor Ben-Amotz, Sietse T van der Post, and Huib J Bakker. Contacts between alcohols in water are random rather than hydrophobic. *The Journal of Physical Chemistry Letters*, 6(4):688–692, 2015.

[183] Yisi Hu, Wenliang Zhou, Yibo Hu, and Fuwen Wei. Conservation evolutionary biology: a unified framework connecting the past, present, and future of biodiversity conservation. *Molecular Biology and Evolution*, page msaf122, 2025.

[184] Wilhelm Kutta. *Beitrag zur näherungsweisen Integration totaler Differentialgleichungen*. Teubner, 1901.

[185] Attila Szolnoki, Mauro Mobilia, Luo-Luo Jiang, Bartosz Szczesny, Alastair M Rucklidge, and Matjaž Perc. Cyclic dominance in evolutionary games: a review. *Journal of the Royal Society Interface*, 11(100):20140735, 2014.

[186] Charles Darwin. On the origin of species, 1859, 2016.

[187] Charles Darwin. On the origins of species by means of natural selection. *London: Murray*, 247:1859, 1859.

[188] James William Tutt. *British moths*. G. Routledge, 1896.

[189] Michael EN Majerus. Industrial melanism in the peppered moth, biston betularia: an excellent teaching example of darwinian evolution in action. *Evolution: Education and Outreach*, 2(1):63–74, 2009.

[190] Bernard Kettlewell. Evolution of melanism: The study of a recurring necessity. 1973.

[191] Henry Bernard D Kettlewell. The phenomenon of industrial melanism in lepidoptera. *Annual Review of Entomology*, 6(1):245–262, 1961.

[192] HBD Kettlewell and DLT Conn. Further background-choice experiments on cryptic lepidoptera. *Journal of Zoology*, 181(3):371–376, 1977.

[193] Brian JL Berry. Cities as systems within systems of cities. *Papers in Regional Science*, 13(1):147–163, 1964.

[194] RJ Berry. The evolution of an island population of the house mouse. *Evolution*, pages 468–483, 1964.

[195] Anthony D Bradshaw. Evolutionary significance of phenotypic plasticity in plants. *Advances in Genetics*, 13:115–155, 1965.

[196] Richard F Johnston and Robert K Selander. House sparrows: rapid evolution of races in north america. *Science*, 144(3618):548–550, 1964.

[197] Andrew P Hendry and Michael T Kinnison. Perspective: the pace of modern life: measuring rates of contemporary microevolution. *Evolution*, 53(6):1637–1653, 1999.

[198] David N Reznick and Cameron K Ghalambor. The population ecology of contemporary adaptations: what empirical studies reveal about the conditions that promote adaptive evolution. *Microevolution Rate, Pattern, Process*, 112:183–198, 2001.

[199] Scott P Carroll, Andrew P Hendry, David N Reznick, and Charles W Fox. Evolution on ecological time-scales, 2007.

[200] J. Gómez-Gardeñes, M. Campillo, L. M. Floría, and Y. Moreno. Dynamical organization of cooperation in complex topologies. *Physical Review Letters*, 98:108103, Mar 2007.

[201] Zhen Wang, Marko Jusup, Rui-Wu Wang, Lei Shi, Yoh Iwasa, Yamir Moreno, and Jürgen Kurths. Onymity promotes cooperation in social dilemma experiments. *Science Advances*, 3(3):e1601444, 2017.

[202] Marco Alberto Javarone. *Statistical physics and computational methods for evolutionary game theory*. Springer, 2018.

[203] Marco Alberto Javarone. Solving optimization problems by the public goods game. *The European Physical Journal B*, 90:171, Sep 2017.

[204] Joel S Brown and Noel B Pavlovic. Evolution in heterogeneous environments: effects of migration on habitat specialization. *Evolutionary Ecology*, 6:360–382, 1992.

[205] Alfred J Lotka. Analytical note on certain rhythmic relations in organic systems. *Proceedings of the National Academy of Sciences*, 6(7):410–415, 1920.

[206] Vito Volterra. Fluctuations in the abundance of a species considered mathematically. *Nature*, 118(2972):558–560, 1926.

[207] Michael L Rosenzweig and Robert H MacArthur. Graphical representation and stability conditions of predator-prey interactions. *The American Naturalist*, 97(895):209–223, 1963.

[208] Elizabeth Nichols and Andrés Gómez. Conservation education needs more parasites. *Biological Conservation*, 144(2):937–941, 2011.

[209] Robert Poulin and Serge Morand. The diversity of parasites. *The Quarterly Review of Biology*, 75(3):277–293, 2000.

[210] Hamish McCallum and Andy Dobson. Detecting disease and parasite threats to endangered species and ecosystems. *Trends in Ecology & Evolution*, 10(5):190–194, 1995.

[211] John E Ubelaker, Robert D Specian, and Donald W Duszynski. Endoparasites. 1979.

[212] SN Thompson. Biochemical and physiological effects of metazoan endoparasites on their host species. *Comparative Biochemistry and Physiology Part B: Comparative Biochemistry*, 74(2):183–211, 1983.

[213] Jörg Heukelbach and Hermann Feldmeier. Ectoparasites—the underestimated realm. *The Lancet*, 363(9412):889–891, 2004.

[214] Carl W Dick. High host specificity of obligate ectoparasites. *Ecological Entomology*, 32(5):446–450, 2007.

[215] Per R Holmstad, Knut H Jensen, and Arne Skorping. Ectoparasite intensities are correlated with endoparasite infection loads in willow ptarmigan. *Oikos*, 117(4):515–520, 2008.

[216] Robert Poulin. Macroecological patterns of species richness in parasite assemblages. *Basic and Applied Ecology*, 5(5):423–434, 2004.

[217] Shai Pilosof, Carl W Dick, Carmi Korine, Bruce D Patterson, and Boris R Krasnov. Effects of anthropogenic disturbance and climate on patterns of bat fly parasitism. *PloS one*, 7(7)(7):e41487, 2012.

[218] Pieter TJ Johnson, Andrew Dobson, Kevin D Lafferty, David J Marcogliese, Jane Memmott, Sarah A Orlofske, Robert Poulin, and David W Thieltges. When parasites become prey: ecological and epidemiological significance of eating parasites. *Trends in Ecology & Evolution*, 25(6)(6):362–371, 2010.

[219] Melanie J Hatcher, Jaimie TA Dick, and Alison M Dunn. How parasites affect interactions between competitors and predators. *Ecology Letters*, 9(11):1253–1271, 2006.

[220] Michael P Hassell and RM May. Aggregation of predators and insect parasites and its effect on stability. *The Journal of Animal Ecology*, pages 567–594, 1974.

[221] D Preston and P Johnson. Ecological consequences of parasitism. *Nature Education Knowledge*, 3(10), 2010.

[222] Gary A Polis and Stephen D Hurd. Linking marine and terrestrial food webs: allochthonous input from the ocean supports high secondary productivity on small islands and coastal land communities. *The American Naturalist*, 147(3):396–423, 1996.

[223] Gary A Polis and Stephen D Hurd. Allochthonous input across habitats, subsidized consumers, and apparent trophic cascades: examples from the ocean-land interface. In *Food webs: integration of patterns & dynamics*, pages 275–285. Springer, 1996.

[224] Sayantan Nag Chowdhury, Jeet Banerjee, Matjaž Perc, and Dibakar Ghosh. Eco-evolutionary cyclic dominance among predators, prey, and parasites. *Journal of Theoretical Biology*, 564:111446, 2023.

[225] Sayantan Nag Chowdhury, Srilena Kundu, Jeet Banerjee, Matjaž Perc, and Dibakar Ghosh. Eco-evolutionary dynamics of cooperation in the presence of policing. *Journal of Theoretical Biology*, 518:110606, 2021.

[226] Xin Wang and Feng Fu. Eco-evolutionary dynamics with environmental feedback: Cooperation in a changing world. *Europhysics Letters*, 132(1):10001, 2020.

[227] Ilkka Hanski. Eco-evolutionary dynamics in a changing world. *Annals of the New York Academy of Sciences*, 1249(1):1–17, 2012.

[228] Sourav Roy, Sayantan Nag Chowdhury, Prakash Chandra Mali, Matjaž Perc, and Dibakar Ghosh. Eco-evolutionary dynamics of multigames with mutations. *PLOS ONE*, 17(8):1–26, 08 2022.

[229] Andrea Saltelli, Gabriele Bammer, Isabelle Bruno, Erica Charters, Monica Di Fiore, Emmanuel Didier, Wendy Nelson Espeland, John Kay, Samuele Lo Piano, Deborah Mayo, et al. Five ways to ensure that models serve society: a manifesto. *Nature*, 582(7813):482–484, 2020.

[230] Adrienn Gelesz, Elena Catto Lucchino, Francesco Goia, Valentina Serra, and András Reith. Characteristics that matter in a climate façade: A sensitivity analysis with building energy simulation tools. *Energy and Buildings*, 229:110467, 2020.

[231] Tamas Turanyi. Applications of sensitivity analysis to combustion chemistry. *Reliability Engineering & System Safety*, 57(1):41–48, 1997.

[232] Per Heiselberg, Henrik Brohus, Allan Hesselholt, Henrik Rasmussen, Erkki Seinre, and Sara Thomas. Application of sensitivity analysis in design of sustainable buildings. *Renewable Energy*, 34(9):2030–2036, 2009.

[233] Diana Suleimenova, David Bell, and Derek Groen. A generalized simulation development approach for predicting refugee destinations. *Scientific Reports*, 7(1):13377, 2017.

[234] Ilya M Sobol. Global sensitivity indices for nonlinear mathematical models and their monte carlo estimates. *Mathematics and Computers in Simulation*, 55(1-3):271–280, 2001.

[235] Yi-Yuan Tang, Qilin Lu, Xiujuan Geng, Elliot A Stein, Yihong Yang, and Michael I Posner. Short-term meditation induces white matter changes in the anterior cingulate. *Proceedings of the National Academy of Sciences*, 107(35):15649–15652, 2010.

[236] Feng Zhang and Cang Hui. Eco-evolutionary feedback and the invasion of cooperation in prisoner's dilemma games. *PLOS one*, 6(11):e27523, 2011.

[237] Charles S Elton. *The ecology of invasions by animals and plants*. Springer Nature, 2020.

[238] Rowland Atkinson. The evidence on the impact of gentrification: new lessons for the urban renaissance? *European Journal of Housing Policy*, 4(1):107–131, 2004.

[239] Torbjörn Forseth, Stefan Larsson, Arne J Jensen, Bror Jonsson, I Näslund, and Ingemar Berglund. Thermal growth performance of juvenile brown trout salmo trutta: no support for thermal adaptation hypotheses. *Journal of Fish Biology*, 74(1):133–149, 2009.

[240] Martha Jane Nadell. Portraits of the new negro woman: Visual and literary culture in the harlem renaissance, 2009.

[241] Bernard J Crespi. The evolution of social behavior in microorganisms. *Trends in Ecology & Evolution*, 16(4):178–183, 2001.

[242] Daryl J Daley and David G Kendall. Epidemics and rumours. *Nature*, 204(4963):1118–1118, 1964.

[243] Le He, Linhe Zhu, and Zhengdi Zhang. Turing instability induced by complex networks in a reaction–diffusion information propagation model. *Information Sciences*, 578:762–794, 2021.

[244] Yuxuan Tang, Shuling Shen, and Linhe Zhu. Study of turing patterns in a si reaction-diffusion propagation system based on network and non-network environments. *International Journal of Biomathematics*, 17(01):2350009, 2024.